Electron Propagator Theory: Fourth Order Diagrams, Composite Approach and Application to Anions, Superhalides and Double–Rydberg Anions

by

Manuel A. Díaz-Tinoco

A dissertation submitted to the Graduate Faculty of
Auburn University
in partial fulfillment of the
requirements for the Degree of
Doctor of Philosophy

Auburn, Alabama
August 3, 2019

Keywords: Electron Propagator, Green's Functions, Double–Rydberg Anions, High-order Correlation Diagrams, Ionization Energies, Electron Affinities

Approved by

J. V. Ortiz, Chair, Ruth W. Molette Professor of Chemistry and Biochemistry
Filip Pawłowski, Assistant Research Professor of Chemistry and Biochemistry
Konrad Patkowski, Associate Professor of Chemistry and Biochemistry
German Mills, Professor of Chemistry and Biochemistry
Hans Werner Van Wyk, Assistant Professor of Mathematics and Statistics

Abstract

The Electron Propagator Theory is useful for calculating vertical electron detachment energies and Dyson orbitals of neutral molecules and anions. The Electron Propagator Theory is a second quantization method that can be improved systematically by increasing the Super–Operator space or improving the order of couplings. In this work, a software (DROGON.D4) is used to obtain expressions, plots and program 316 fourth–order Brandow–type diagrams.

The combination of high correlation methods with complete basis sets is usually unfeasible for moderate–large molecular systems. For this reason, composite approaches are common for the high accuracy prediction of molecular and thermochemical properties. In this work, the exploration of the composite approach begins with an Electron Propagator Benchmark of methods for neutral molecules and anions in addition to the statistical study of additive properties of basis sets and high correlation effects. Then, composite electron propagator methods are defined and tested: CP3+/34, CN/34 are good approximations for neutral molecules with mean unsigned errors of 0.08 and 0.14 eV, respectively. For anions, CP3+/a23, CP3+/a34, CNR2/a23 and CNR2/a34 yield mean unsigned errors of 0.11, 0.12, 0.15 and 0.12 eV, respectively.

Case studies of several anions of interest are analyzed: $P_2N_3^-$ is a pentagonal ring with several accessible electronic states for its neutral form. The first vertical electron detachment energy is 4.41 eV and corresponds to a $^2A_1$ state. Its lower energy isomer, N_2PNP^- is also a pentagonal ring with a lower vertical electron detachment energy of 3.73 eV corresponding to a $^2B_2$ final state. In addition, vertical electron detachment energies for superhalides have been studied for $Al(BO_2)_4^-$, $Mg_2(CN)_5^-$, $CHB_{11}H_{11}^-$, $CHB_{11}F_{11}^-$ and $CHB_{11}Cl_{11}^-$.

Acknowledgments

I thank J.V. Ortiz for being an impeccable advisor and mentor always available for guidance, advice and interesting ideas to explore.

I thank my committee members for corrections and comments. I also thank Professors Michael McKee and Rik Blumenthal for their questions and comments during my oral examination for PhD candidacy.

I acknowledge the help and guidance from group members. Special thanks to Dr. Héctor Corzo for being an outstanding graduate student, close friend and competitor during graduate school.

To my family and friends who supported me during this process, specially to Dr. Maya West for taking care of me when I was having back and knee problems.

And finally, I'm eternally grateful to AA. not only for keeping me sober but more importantly for giving me a sense of purpose and belonging in my darkest days.

Table of Contents

List of Figures

List of Tables

List of abbreviations

3+	Renormalized third order
ADC(3)	Third–order Algebraic, Diagrammatic Construction
AIE	Adiabatic Ionization Energy
BDT1	Brueckner-doubles triple field operator
CBS	Complete Basis Set limit
CCSD	Coupled–Cluster Singles and Doubles
CCSD(T)	Coupled–Cluster Singles and Doubles plus approximate Triples
CEP	Composite Electron Propagator
CN	Composite Outer Valence Green's Function
CNR2	Composite Non-diagonal Renormalized second order
CP3	Composite Partial third order
D2	Diagonal second order
D3	Diagonal third order
EA	Electron Affinity
EBE	Electron Binding Energy
EE	Excitation Energy
EP	Electron Propagator
EPT	Electron Propagator Theory
HOMO	Highest Occupied Molecular Orbital
IE	Ionization Energy
KT	Koopmans's theorem
LUMO	Lowest Unoccupied Molecular Orbital

MUE	Mean Unsigned Error
MP2	Møller–Plezzet Perturbation Theory second order
NR2	Non-diagonal Renormalized second order
OVGF	Outer Valence Green’s Function
OVGF-A	Outer Valence Green’s Function-Version A
OVGF-B	Outer Valence Green’s Function-Version B
OVGF-C	Outer Valence Green’s Function-Version C
OVGF-N	Outer Valence Green’s Function-Recommended value
P3	Partial third order
P3+	Renormalized partial third order
PES	Photoelectron Spectroscopy
TDA	Two–particle–one–hole Tamm-Dancoff Approximation
VEAE	Vertical Electron Attachment Energy
VEDE	Vertical Electron Detachment Energy
VIE	Vertical Ionization Energy
ZPE	Zero Point Energy
μ	Mean Signed Error
σ	Standard Deviation

Chapter 1

Introduction

1.1 Ionization energies and electron affinities

The ionization energy (IE) is the energy needed to remove an electron from a molecule and the electron affinity (EA) is the energy released when adding an electron to a molecule. In addition, solving for the wavefunction of this molecule provides both occupied and unoccupied molecular spin–orbitals and their eigenvalues. A simple way of calculating the lower IEs and EAs for a molecule is by using the Koopmans's theorem (KT) in which the IE and EA are equal to the negative eigenvalue of the highest occupied molecular orbital (HOMO) and lowest unoccupied molecular orbital (LUMO), respectively.

Photoelectron spectroscopy (PES) is an experimental technique in which a high energy photon hits a molecule with enough energy to eject an electron from its spin–orbital. The binding energy of the electron can be obtained using the Einstein's photoelectric equation,

$$E_k = h\nu - \phi_0, \tag{1.1}$$

where E_k is the kinetic energy of the electron, $h\nu$ is the energy of the photon and ϕ_0 is the binding energy of the electron. Then, the lowest binding energy of a neutral molecule is the IE and the lowest binding energy of an anion is the EA (when the anionic and neutral geometries are similar).

When the neutral high correlation effects coming from localized lone pairs or excess of π electrons are present, the lowest IE might not come from the HOMO but instead the HOMO-1. This is called a Koopmans's defect and it occurs in the N_2 molecule. One can obtain orbital relaxation and correlation effects in the calculation of both the neutral and cation total energies by using ΔE methods. Then, there will be an IE for each molecular orbital related to each electronic final state (in the cation). ΔE methods have been used to assign peaks in PES providing an electronic structure detail of the valence molecular orbitals of neutral molecules.[2]

1.2 Electron Propagator Theory

Electron Propagator Theory (EPT) provides the theoretical background for the high accuracy prediction of vertical electron detachment energies (VEDEs) and vertical electron attachment energies (VEAEs).[3–5] Among the best properties of EPT or Green's function methods is that we can obtain several binding energies for the respective electronic state using a single reference determinant. In comparison, a ΔE method will need one calculation for the reference state and another calculation for each electronic final state. In addition, EPT provides Dyson orbitals which give a physical description of the ionization process and are useful when compared with spin–density contours of final electronic states when starting from a closed shell state.[6]

Solving for eigenvalues and eigenvectors of the superoperator Hamiltonian,

$$\hat{\mathbf{H}}\mathbf{C} = \mathbf{C}\omega, \tag{1.2}$$

yields all the binding energies and Dyson orbitals for a particular operator manifold. For example, we can have operators for ionization and electron affinity transitions involving two–occupied and one–virtual orbitals (2hp for the hole and particle analogy to occupied and virtual, respectively) and two–virtual and one–occupied (2ph) obtaining a super Hamiltonian with dimensions equal to (h+p+h^2p+p^2h). This matrix is extremely large to store and diagonalize. In addition, not all ionization and electron affinities are chemically important and their computation can be omitted by using the Davidson algorithm in the valence transitions.[7]

The superoperator problem can be simplified using the inverse form of the Dyson equation and finding poles of the electron propagator where

$$[\mathbf{F} + \mathbf{\Sigma}(E)]\mathbf{C} = E\mathbf{C}, \tag{1.3}$$

where **F** includes coulombic and exchange interactions at the canonical Hartree–Fock reference state and is equal to $F_{rs} = \delta_{rs}\epsilon_r$, E is the binding energy for the particular Dyson orbital **C** and $\mathbf{\Sigma}(E)$ is the self–energy operator.

1.3 Composite Methods

Thermochemical data of high accuracy can be approximated with composite methods by using the additivity of the basis set and high correlation effects. In other words, using high–order correlation methods at a small basis–set, to obtain the correlation effect, in combination with second–order correlation methods at the complete basis set limit (CBS), to obtain the basis–set effect. The addition of these two effects attains high accuracy electronic energy.[8–17]

Basis–set extrapolations have been successfully applied in quantum chemistry calculations of Hartree–Fock total energy, correlation energy and electron propagator methods.[18–21] These results show a saturation in the basis effect and allow the CBS limit prediction by using either a cubic or exponential extrapolation. In Chapter 4, a composite approach for EPT is proposed and tested using the G2-IP test–set.[11,21]

A CBS limitation is the need for correlation–consistent basis–sets which are quite demanding and not adequate for diffuse Rydberg–like anions. However, previous EPT studies have also shown good cancelation of errors when using Pople basis sets, compared with experimental results.[20,21] In addition, adding extra diffuse functions while retaining the highest angular momentum constant has been quite successful at obtaining binding energies of Rydberg–like diffuse electrons.[22–24] Therefore, CBS effects might not always be the best approach for EPT methods but are quite accurate and successful in the case of valence bound electrons.

1.4 Anions

A popular way of discovering new molecules and anions with subtle chemical bonding is through photoelectron spectroscopy and computational quantum chemistry. Photoelectron spectroscopy provides a fingerprint characteristic of the molecular ion. In addition, theoretical calculations assign the signals to particular electronic transitions of new molecular structures. For example, anionic photoelectron spectroscopy, structure search algorithms, electron affinities and excitation energies calculations have enabled the discovery of boron clusters with quite interesting structures and chemical bonding.[25]

Another successful story of excellent agreement between experiment and theory is the discovery of double–Rydberg anions, *e.g.* $(NH_4^+)^{2-}$, in which photoelectron spectra have a low energy sharp peak that agrees with the VEDE of the tetrahedral anionic structure EPT results.[26,27] The discovery of double–Rydberg anions changes the perspective of transference of electrons in solvated media with the possibility of outer–sphere–electron mechanisms.

In Chapter 5, a benchmark for prediction of VEDEs of closed shell anions with EPT has been performed and several recommendations are provided.[28] The golden standard ΔCCSD(T)/CBS for theoretical chemistry calculations was used to provide a high accuracy benchmark of VEDEs and compared against EPT approximations. The best EPT approximations were OVGF-A, P3+ and NR2 using either CBS or composite approaches (CP3+, for example) giving mean unsigned errors and error standard deviations below 0.15 eV. However, a problematic case study is the F^-–H_2O complex in which the OVGF-A approximation has a considerable error of 0.4 eV while P3+ and NR2 are within 0.15 eV from the computed standard.

The Outer Valence Green's Function (OVGF) approximation provides a selection algorithm between the A, B and C versions which is quite accurate for closed shell neutral small to medium molecules.[21] However, in the case of anions this selection algorithm usually selects the OVGF-B approximation which gives larger errors than OVGF-A. For this reason, it is suggested to use the OVGF-A version or P3+ (which is faster and easier to calculate than OVGF) for VEDE calculations in anions.

The extremely useful and accurate results obtained with NR2 can be obtained with the Gaussian 16 quantum chemistry package.[29] However in order to use this approximation, a thorough understanding of Dyson orbitals, KT and Davidson's diagonalization algorithm is required. For this reason, the Ortiz research group is working to provide a thorough documentation for the calculation and performance of Non–diagonal EPT methods. On the other hand, diagonal EPT calculations can be quickly achieved and are a good entry point for the understanding of Dyson orbitals and KT. In addition, Chapters 4 and 6 will provide examples of CBS extrapolations, composite additions, applications and exceptions KT and Dyson orbitals usefulness.

1.5 Super Halogens

Superhalogens are clusters with central atoms and highly electronegative ligands that have electron affinities higher than 3.6 eV, the electron affinity of Chlorine and the highest electron affinity in the periodic table. Superhalides are the corresponding anions and are usually closed shell anions with high symmetrical features and valence bound electrons.[6,30–33] A simple superhalogen is the combination of a metal with valence X with X+1 halogen atoms, for example MgF_3, where two of the halogen ligands take an electron from the metal and the remaining neutral ligand has a strong potential to fill its valence shell.

There can be composite superhalogens where a ligand is substituted with an organic group, like ethylene. These systems have higher electron affinities than their organic parents and might be used in synthesis and chemical bond activations. In addition, superhalides tend to be extremely stable basic systems and their conjugated Brønsted–Lowry acids have super acidic properties. Therefore, superhalogens can be used in two of the most important types of basic chemistry, acid–base and redox chemistry.

In Chapter 6, EPT approximations show good agreement when compared against the CCSD(T) method for several superhalogens.[6,28,30,31] For example, electron affinities of composite superhalogens were calculated with OVGF and accurate predictions of the vertical transitions and final electronic states were provided.[30] Accurate prediction of superhalogens electron affinities is not trivial due to high correlation effects, spin–contamination and close electronic excited states. A simple solution to these problems is to obtain VEDEs from the anionic reference state, which is a closed shell singlet, using an EPT approximation. In this way we can elude the spin–contamination and use Dyson orbitals to predict the ground state for the neutral species and its excitation energies to nearby electronic states, where the excitation energies are equal to the differences of vertical electron detachment energies.

1.6 Carboranes

Boranes are clusters composed of boron and hydrogen atoms; they can be neutral or anionic. For example, B_2H_6 is a diborane and its chemistry is interesting because of the formation of three–center two–electrons (3c-2e) bonds. This phenomenon is due to the electron deficiency of Boron and when more boron atoms are present in the borane highly symmetric cage–like (*closo*) dianions are formed.

The *closo*–$B_{12}H_{12}^{2-}$ borane cluster point group is I_h with a boron atom occupying each icosahedron vertex. Each boron is bonded to a hydrogen atom. This borane, is quite an stable dianion and a boron atom can be substituted with a carbon atom to obtain a carborane, $CHB_{11}H_{11}^{-}$. Protonated carboranes are superacidic and their conjugated basis are superhalides which are interesting properties for a cluster with no highly electronegative atoms or ligands. If the hydrogen atoms connected to boron atoms are substituted with fluorine or chlorine atoms halogenated carboranes are obtained, $CHB_{11}X_{11}^{-}$ for X = F or Cl.

In Chapter 4, the electronic structure of the neutral carboranes is explored and found o be quite interesting because of their high electron affinities (>6 eV) and the highly delocalized frontier orbitals.[34] In addition, the anionic carboranes have a delocalized negative charge that mainly accumulates on the side opposite to the carbon atom. Therefore, the protonated carboranes will have the acidic proton on the same side. In the case of X = H, the proton is bound to three boron atoms, pushing three hydrogens aside. For X = F and Cl, the proton binds between two halogen atoms, closer to the one that is opposite to carbon.

No correlation was found between the proton binding energies and the VEDEs for the HOMO and this might be due to the nodal structure of the Dyson orbital at the protonation side. However, for the HOMO-2 Dyson orbital (HOMO-1 and HOMO are degenerate) there are amplitudes available at the protonation side and, therefore, increasing the VEDE of this orbital will increase the superacidity of the protonated carborane.

1.7 Double–Rydberg Anions

Binding an extra electron to a closed–shell saturated cation is not a typical process. The electron tends to occupy a highly diffuse orbital with a small binding energy and is known as a molecular Rydberg radical. For example, the neutral NH_4 has a diffuse electron in the periphery of the NH_4^+ cation, $(NH_4^+)^-$. The addition of an extra electron forms a double–Rydberg anion ($(NH_4^+)^{2-}$) in which there is a doubly occupied orbital in the periphery of the NH_4^+ cation.[26,27] All three structures are tetrahedrals with similar bond lengths and vibronic structures accounting for sharp peaks and high Franck–Condon overlap.

Research in solvated double–Rydberg anionic clusters has been performed and diverse chemical interactions between the anions and the ammonia molecules have been discovered.[35,36]

In Chapter 7, double–Rydberg anions with more nitrogen atoms have been found thanks to the formation of strong hydrogen–bonding interactions, $(N_2H_7^+)^{2-}$, $(N_3H_{10}^+)^{2-}$, $(N_4H_{13}^+)^{2-}$ and $(N_5H_{16}^+)^{2-}$. In addition, ion–dipole interactions with ammonia monomers and dimers have also been encountered, where the anion is more stable, increasing the VEDE by 0.1 and 0.2 eV for the monomer and dimer, respectively.

Other interesting possibilities explored are protonated amines, singly protonated diamines and protonated aminoacids due to their importance in chemical reactivity, pH regulation and biochemistry. When having two sites that can allocate Rydberg–like orbitals the presence of excited triplets for double–Rydberg anions is possible. Therefore, open–shell Rydberg anions could initiate radical chemistry like polymerization or halogenation reactions at low temperatures.

1.8 Electron Propagator Diagrams

The description of correlation and relaxation effects in the electron propagator can be described in an efficient and graphical way by using Feynman–type diagrams. The second and third order electron propagator diagrams provide the terms belonging to the self–energy operator and represent the advanced mathematics and linear algebra corresponding to the EPT in graphical and condensed way.[4]

In Chapter 3, a vectorial representation is proposed for each Brandow's electron propagator diagram for third and fourth order. A computer algorithm named DROGON.D4 has been developed within the research leading to this dissertation and generated all possible vectors and combined them to obtain their corresponding diagrams. There are two types of diagrams that can be obtained: The Goldstone–type diagrams have all the information needed to obtain the self–energy term. The Hugenholtz diagrams are useful for discarding duplicated Goldstone diagrams. For this reason, both Goldstone and Hugenholtz vectorial representations are generated and compared.

Previously, Schirmer *et al*[37] obtained 228 fourth–order diagrams that are labeled in Appendix A as type–U, type–V and type–W diagrams. In agreement with Schirmer, DROGON.D4 obtained all these 228 diagrams plus 72 constant diagrams. However, DROGON.D4 also obtained 16 new diagrams, which 8 of them can be reduced to 2ph–2hp terms.

Chapter 2

Theory

In order to give a background for Electron Propagator Theory (EPT), we will discuss the following concepts in this chapter:

- Schrödinger equation
- Born–Oppenheimer approximation
- Variational principle
- Hartree products
- Slater determinants
- Hartree–Fock method
- Second quantization
- Electron propagator theory

2.1 The Schrödinger equation

The time–independent non-relativistic Schrödinger equation reads,

$$\hat{H}\psi = E\psi, \tag{2.1}$$

where ψ is the system's wavefunction, E is the system's energy and $\hat{H}$ is the Hamiltonian operator. The Hamiltonian operator is defined as,

$$\hat{H} = -\frac{\hbar^2}{2}\sum_{n=1}^{N}\frac{1}{m_n}\nabla_n^2 + V(\mathbf{r}_1, \mathbf{r}_2, ..., \mathbf{r}_N), \tag{2.2}$$

where $\hbar$ is Planck's constant divided by 2π $\left(\hbar = \frac{h}{2\pi}\right)$, n is the particle index, m_n is the mass for particle n, N is the total number of particles, V is the potential energy operator, $\mathbf{r}_n$ is the position vector for particle n and ∇^2 is the laplacian operator,

$$\nabla_n^2 = \frac{\partial^2}{\partial x_n^2} + \frac{\partial^2}{\partial y_n^2} + \frac{\partial^2}{\partial z_n^2}. \tag{2.3}$$

The Schrödinger equation can be solved exactly for some special cases:[38]

- Particle in a box
- Harmonic oscillator
- Rigid rotor
- Hydrogen atom

However, for the helium atom as well as H_2^+ cation it cannot be solved exactly. Let us suppose the general problem of two nuclei and one electron (A and B are nuclei, e is electron)

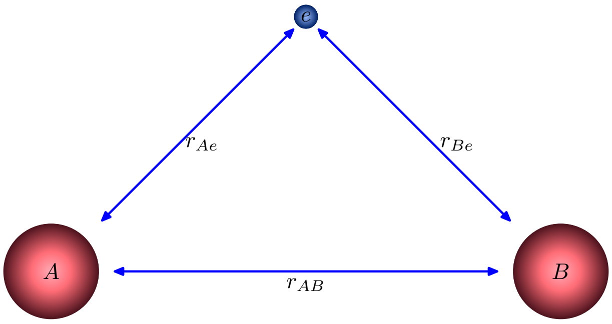

Figure 2.1: AB^+ cation, we can have A as hydrogen 1, B as hydrogen 2, e as an electron to have H_2^+.

Then, the Schrödinger equation for this system reads,

$$
\begin{aligned}
\hat{H}\psi(\mathbf{A},\mathbf{B},\mathbf{e}) &= -\frac{\hbar^2}{2m_A}\left(\frac{\partial^2}{\partial A_x^2}+\frac{\partial^2}{\partial A_y^2}+\frac{\partial^2}{\partial A_z^2}\right)\psi(\mathbf{A},\mathbf{B},\mathbf{e}) \\
&\quad -\frac{\hbar^2}{2m_B}\left(\frac{\partial^2}{\partial B_x^2}+\frac{\partial^2}{\partial B_y^2}+\frac{\partial^2}{\partial B_z^2}\right)\psi(\mathbf{A},\mathbf{B},\mathbf{e}) \\
&\quad -\frac{\hbar^2}{2m_e}\left(\frac{\partial^2}{\partial e_x^2}+\frac{\partial^2}{\partial e_y^2}+\frac{\partial^2}{\partial e_z^2}\right)\psi(\mathbf{A},\mathbf{B},\mathbf{e}) \\
&\quad +\left(-\frac{e^2}{4\pi\epsilon_0|\mathbf{A}-\mathbf{e}|}-\frac{e^2}{4\pi\epsilon_0|\mathbf{B}-\mathbf{e}|}+\frac{e^2}{4\pi\epsilon_0|\mathbf{A}-\mathbf{B}|}\right)\psi(\mathbf{A},\mathbf{B},\mathbf{e}) \\
&= E\psi(\mathbf{A},\mathbf{B},\mathbf{e}) \qquad (2.4)
\end{aligned}
$$

where $\mathbf{A}$, $\mathbf{B}$ and $\mathbf{e}$ are space vectors for particles A, B and e, respectively. A_x, A_y and A_z are cartesian components of $\mathbf{A}$; B_x, B_y and B_z are cartesian components of $\mathbf{B}$; e_x, e_y and e_z are cartesian components of $\mathbf{e}$. Eq. (2.4) can't be separated due to its dependency on coordinates $|\mathbf{A}-\mathbf{B}|$, $|\mathbf{A}-\mathbf{e}|$ and $|\mathbf{B}-\mathbf{e}|$. For this reason, the Born-Oppenheimer approximation is quite popular in order to solve the Schrödinger equation.

2.2 The Born–Oppenheimer approximation

The Born-Oppenheimer approximation consists in separating the system's molecular coordinates in fixed coordinates for the nuclei and moving coordinates for the electrons. This approximation is based in the fact that nuclei are thousands of times more massive than electrons and therefore their moving time-scale is slower.

In a molecular system, the Hamiltonian operator can be separated in five terms:

$$
\hat{H} = -\frac{\hbar^2}{2m}\sum_i \nabla_i^2 - \sum_A \frac{\hbar^2}{2M_A}\nabla_A^2 - \sum_{A,i}\frac{Z_A e^2}{4\pi\epsilon_0 r_{Ai}} + \sum_{A>B}\frac{Z_A Z_B e^2}{4\pi\epsilon_0 R_{AB}} + \sum_{i>j}\frac{e^2}{4\pi\epsilon_0 r_{ij}}, \qquad (2.5)
$$

where i, j are electron indexes, A, B are nuclear indexes.[39] Eq. (2.5) in atomic units is simpler,

$$
\hat{H} = -\frac{1}{2}\sum_i \nabla_i^2 - \sum_A \frac{1}{2M_A}\nabla_A^2 - \sum_{A,i}\frac{Z_A}{r_{Ai}} + \sum_{A>B}\frac{Z_A Z_B}{R_{AB}} + \sum_{i>j}\frac{1}{r_{ij}}. \qquad (2.6)
$$

We can have the Hamiltonian operator as a function of operators,

$$
\hat{H} = \hat{T}_N(\mathbf{R}) + \hat{T}_e(\mathbf{r}) + \hat{V}_{eN}(\mathbf{r},\mathbf{R}) + \hat{V}_{NN}(\mathbf{R}) + \hat{V}_{ee}(\mathbf{r}), \qquad (2.7)
$$

where **R** is the set of nuclei coordinates and **r** is the set of electronic coordinates. $\hat{T}_N$ is the nuclear kinetic energy operator, $\hat{T}_e$ is the electronic kinetic operator, $\hat{V}_{eN}$ is the potential energy operator between nuclei and electrons, $\hat{V}_{NN}$ is the potential energy operator between nuclei and $\hat{V}_{ee}$ is the potential energy operator between electrons.

Unfortunately, $\hat{V}_{eN}(\mathbf{r},\mathbf{R})$ operator does not allow a separation of nuclei and electron contributions, in which case we could write the wavefunction as the product of the nuclear and electronic terms $\psi(\mathbf{r},\mathbf{R}) = \psi(\mathbf{r})\chi(\mathbf{R})$. The Born–Oppenheimer approximation consists in changing the dependency of **R** to a parametric dependency. In this way the wavefunction is given by, $\psi(\mathbf{r},\mathbf{R}) \approx \psi(\mathbf{r};\mathbf{R})\chi(\mathbf{R})$.[39] Then, fixing the nuclei coordinates **R** to a parameter value, $\mathbf{R_a}$, we can solve for the electronic wavefunction $\psi(\mathbf{r};\mathbf{R_a})$, which now depends on **R** as a parameter. If this is solved for different **R** values we obtain a potential energy curve or hypersurface with respect to the nuclei movement.

Then, we can define the electronic Hamiltonian operator $\hat{H}_e$,

$$\hat{H}_e = \hat{T}_e(\mathbf{r}) + \hat{V}_{eN}(\mathbf{r};\mathbf{R}) + \hat{V}_{ee}(\mathbf{r}) \tag{2.8}$$

and the Schrödinger equation for the electronic contribution is:[39]

$$\hat{H}_e\psi(\mathbf{r};\mathbf{R}) = E_e\psi(\mathbf{r};\mathbf{R}). \tag{2.9}$$

2.3 Variational principle

The variational principle reads,[40]

$$E_\phi \geq E_0. \tag{2.10}$$

where E_ϕ is the energy of a guess wavefunction ϕ and E_0 is the energy of the ground–state wavefunction ψ_0. E_0 and E_ϕ can be obtained with the following equations,

$$E_0 = \frac{\int \psi_0^* \hat{H}_e \psi_0 d\tau}{\int \psi_0^* \psi_0 d\tau}, \tag{2.11}$$

$$E_\phi = \frac{\int \phi^* \hat{H}_e \phi d\tau}{\int \phi^* \phi d\tau}. \tag{2.12}$$

Then, using the variational principle we can use trial functions as approximations to the ground–state wavefunction. These trial functions will have parameters that can be optimized with respect to the energy in order to obtain the lowest energy possible.

Trial function $\quad$ Wavefunction

$$\psi(\mathbf{r},\beta) = \sqrt{\frac{3\beta^3}{\pi^3}}\,\mathrm{sech}(\beta\mathbf{r}) \qquad S(\mathbf{r}) = \frac{1}{\sqrt{\pi}}e^{-\mathbf{r}}$$

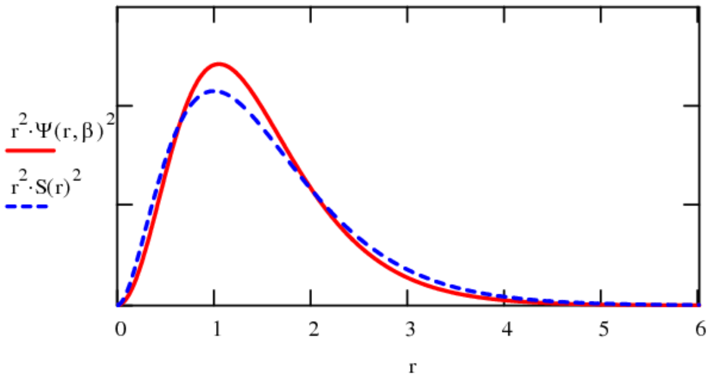

Figure 2.2: Trial function ($\psi(\mathbf{r},\beta)$) and ground–state wavefunction ($S(\mathbf{r})$) for the hydrogen atom.

As shown in Figure 2.2, the trial function ($\psi(\mathbf{r},\beta)$) reproduces the shape and values of the ground–state wavefunction ($S(\mathbf{r})$) to a certain level.

The trial function can also be chosen in the form of a linear combination of simpler basis functions,[38] such that each coefficient in each function can be optimized with respect to the energy in order to provide a better approximation to the ground–state wavefunction,

$$\phi = \sum_{j=1}^{N} c_j f_j = \sum_{j=1}^{N} c_j e^{-\alpha_j r^2}. \tag{2.13}$$

Then, the trial function becomes a linear combination of basis functions (basis set) in which each one of these functions has a parameter α_j and a coefficient c_j. Using the variational principle, the coefficients are optimized by minimizing the energy and Table 2.1 shows that the more complete the basis set is the more exact the trial function becomes. This applies to every method based on the variational principle, such as the Hartree–Fock approximation.

Table 2.1: Trial function (optimizing c_j and α_j for Eq. 2.13) energy as a function of the number of basis functions for the ground state energy of the hydrogen atom, the exact value is -0.50000 au.

N	$E_{min}/(m_e e^4/16\pi^2\epsilon_0^2\hbar)$
1	-0.42441
2	-0.48581
3	-0.49697
4	-0.49928
5	-0.49976
6	-0.49988
8	-0.49992
16	-0.49998

2.4 Hartree products

The Hartree products method consists of approximating the wavefunction as a product of N functions,

$$\psi^{HP}(\mathbf{x}_1,\mathbf{x}_2,\ldots,\mathbf{x}_N) = \chi_i(\mathbf{x}_1)\chi_j(\mathbf{x}_2)\ldots\chi_k(\mathbf{x}_N), \tag{2.14}$$

where N is the number of electrons in the system, ψ^{HP} is the Hartree product (HP) wavefunction, $\mathbf{x}_1,\mathbf{x}_2,\ldots,\mathbf{x}_N$ are the coordinates for electron 1, 2, …, N, respectively, $\chi_i(\mathbf{x}_1),\chi_j(\mathbf{x}_2),\ldots,\chi_k(\mathbf{x}_N)$, are the occupied spin–orbitals $i,j,\ldots,k$ by electrons $1,2,\ldots,N$, respectively.

Without electron–electron interaction, the simpler hamiltonian operator $\hat{H}$ reads

$$\hat{H} = \sum_{i=1}^{N} h^{HP}(i), \tag{2.15}$$

where $h^{HP}(i)$ is a monoelectronic operator which describes the kinetic and potential energy of electron i. The potential energy in $h^{HP}(i)$ can have an average way of including nuclear attraction and electron–electron repulsion.[41–43]

This operator has eigenvalues and eigenfunctions,

$$h^{HP}(i)\chi_j(\mathbf{x}_i) = \epsilon_j\chi_j(\mathbf{x}_i), \tag{2.16}$$

$$\hat{H}\psi^{HP} = E\psi^{HP}, \tag{2.17}$$

where the energy is the summation of all eigenvalues,

$$E = \sum_{i}^{k} \epsilon_i. \tag{2.18}$$

2.5 Slater Determinants

Fermions are indistinguishable particles with antisymmetric wavefunctions, such that when two fermions exchange their positions in direct spin space the wavefunction is the same but with the opposite sign. Electrons are fermions and the Slater determinants are useful at antisymmetrizing Hartree wavefunctions:[40]

$$|\psi(\mathbf{x}_1, \mathbf{x}_2, \ldots, \mathbf{x}_N)\rangle = (N!)^{-\frac{1}{2}} \begin{vmatrix} \chi_i(\mathbf{x}_1) & \chi_j(\mathbf{x}_1) & \cdots & \chi_k(\mathbf{x}_1) \\ \chi_i(\mathbf{x}_2) & \chi_j(\mathbf{x}_2) & \cdots & \chi_k(\mathbf{x}_2) \\ \vdots & \vdots & & \vdots \\ \chi_i(\mathbf{x}_N) & \chi_j(\mathbf{x}_N) & \cdots & \chi_k(\mathbf{x}_N) \end{vmatrix},$$

where $|\psi(\mathbf{x}_1, \mathbf{x}_2, \ldots, \mathbf{x}_N)\rangle$ is the antisymmetric wavefunction of N electrons called Slater determinant, $(N!)^{-\frac{1}{2}}$ is a normalization constant, columns contain spin–orbitals $\chi_i, \chi_j, \ldots, \chi_k$ and rows occupy the spin–orbitals with electrons at coordinates $\mathbf{x}_1, \mathbf{x}_2, \ldots, \mathbf{x}_N$. If two electrons are exchanged, the Slater determinant will change sign. Slater determinants can be represented as a vector composed of the diagonal elements in the determinant ($|\chi_i \chi_j \cdots \chi_k\rangle$). Using this notation, the wavefunction of N electrons reads,

$$|\psi(\mathbf{x}_1, \mathbf{x}_2, \ldots, \mathbf{x}_N)\rangle = |\chi_i \chi_j \cdots \chi_k\rangle, \tag{2.19}$$

where it is implicit that spin-orbitals $\chi_i, \chi_j, \ldots, \chi_k$ are occupied with electrons at the coordinates $\mathbf{x}_1, \mathbf{x}_2, \ldots, \mathbf{x}_N$, respectively.

2.6 Hartree–Fock method

Using the Born–Oppenheimer approximation and the Slater determinants we can separate the problem of many electrons into many problems of one electron, where electron–electron repulsion is treated in an average way.[40] This will be the Hartree–Fock method and the average field is represented by the electronic density, the square of the wavefunction. The Slater determinant is composed of trial functions that are optimized using the variational principle.

The ground–state energy in the Hartree–Fock method is:

$$E_0 = \langle \psi_0 | H | \psi_0 \rangle \tag{2.20}$$

where E_0 is the ground–state energy, $\langle \psi_0 | H | \psi_0 \rangle$ is the integral over all space of the ground–state wavefunction multiplying the Hamiltonian operator operating the ground–state wavefunction, known as the energy expectation value. This is for a real wavefunction. In the case of a complex wavefunction, the complex conjugate must be multiplying the Hamiltonian operator.

Then, the Hartree–Fock energy can be obtained using the Slater determinant:[40,44]

$$E_0 = \sum_{a}^{N} \langle a | h | a \rangle + \frac{1}{2} \sum_{ab}^{N} \langle ab || ab \rangle, \tag{2.21}$$

where a and b are indexes for occupied spin–orbitals, $\langle a|h|a\rangle$ is the integral over all space of spin–orbital a multiplying the monoelectronic operator h which operates on spin–orbital a and the term $\langle ab||ab\rangle$ is the antisymmetrized two electron repulsion integral, which contains the coulombic and exchange interactions between electrons occupying the spin–orbitals a and b.

The antisymmetrized two electron repulsion integral can be separated in two coulombic integrals,

$$\langle ij || kl \rangle = \langle ij | kl \rangle - \langle ij | lk \rangle, \tag{2.22}$$

where $i,\ j,\ k$ and l are spin–orbitals from the Slater determinant, these spin–orbitals can be occupied or unoccupied (called virtual). The coulombic integral, $\langle ij|kl\rangle$, reads,[40]

$$\langle ij | kl \rangle = \int d\mathbf{x}_1 d\mathbf{x}_2 \chi_i^*(\mathbf{x}_1) \chi_j^*(\mathbf{x}_2) r_{12}^{-1} \chi_k(\mathbf{x}_1) \chi_l(\mathbf{x}_2), \tag{2.23}$$

where r_{12}^{-1} is the distance between the coordinates of electrons ($\mathbf{x}_1$ and $\mathbf{x}_2$), χ_i^* and χ_j^* are the complex conjugates of spin–orbitals χ_i and χ_j, respectively.

Then, eigenvalues and eigenfunctions read,

$$f(i)\chi_a(\mathbf{x}_i) = \epsilon_a \chi_a(\mathbf{x}_i), \tag{2.24}$$

where $f(i)$ is the Fock operator for electron i, $\chi_a(\mathbf{x}_i)$ is the occupied spin–orbital a by electron i and ϵ_a is its eigenvalue.

The Fock operator is defined as:

$$f(i) = h(i) + \sum_{b}^{N} [J_b(i) - K_b(i)], \tag{2.25}$$

where $J_b(i)$ is the coulomb operator and $K_b(i)$ is the exchange operator and these are the interactions between spin–orbital a (occupied with electron i) and spin–orbital b (occupied with electron j).

The monoelectronic operator h reads,

$$h(i) = -\frac{1}{2}\nabla_i^2 - \sum_A \frac{Z_A}{r_{iA}}, \tag{2.26}$$

where A is the index for the nuclei in the system, Z_A is the nuclear charge for nuclei A and r_{iA} is the distance between electron i and nuclei A

The coulomb operator, J_b is defined as:

$$J_b(i)\chi_a(\mathbf{x}_i) = \left[\int d\mathbf{x}_j \chi_b^*(\mathbf{x}_j) r_{12}^{-1} \chi_b(\mathbf{x}_j)\right] \chi_a(\mathbf{x}_i). \tag{2.27}$$

The exchange operator, K_b, reads,

$$K_b(i)\chi_a(\mathbf{x}_i) = \left[\int d\mathbf{x}_j \chi_b^*(\mathbf{x}_j) r_{12}^{-1} \chi_a(\mathbf{x}_j)\right] \chi_b(\mathbf{x}_i). \tag{2.28}$$

The Hartree–Fock energy can be shown to contain the terms mentioned in Section 2.2. The operator $h(i)$ includes kinetic energy ($\hat{T}_e$) for electrons and potential energy between nuclei and electrons ($\hat{V}_{eN}$). In addition, the coulombic ($J_b(i)$) and exchange ($K_b(i)$) operators are consequences of coulombic repulsions between electrons operator ($\hat{V}_{ee}$).

2.7 Second quantization

The antisymmetry principle and the Schrödinger equations are axioms of quantum mechanics. Slater determinants assure that the wavefunction will be antisymmetric. Second quantization is a formalism in which antisymmetry is assured using algebraic operators. In this way, second quantization is another way of treating many electron systems in an elegant and sophisticated way.

This formalism has been used extensively in the many electron problems literature. In addition, electron propagator theory can be elegantly described using second quantization.

Creation and annihilation operators

Second quantization formalism is built by showing that Slater determinants' properties can be transferred to algebraic operators. For example, the creation operator $a_i^\dagger$ creates an electron in the occupied spin-orbital χ_i and is defined by its action on a general Slater determinant $|\chi_k \ldots \chi_l\rangle$ such that:[40]

$$a_i^\dagger|\chi_k \cdots \chi_l\rangle = |\chi_i\chi_k \cdots \chi_l\rangle, \tag{2.29}$$

where $a_i^\dagger$ occupies the spin–orbital χ_i with an electron. The order of creation operators is key, for example:

$$\begin{aligned} a_i^\dagger a_j^\dagger|\chi_k \cdots \chi_l\rangle = a_i^\dagger|\chi_j\chi_k \cdots \chi_l\rangle &= |\chi_i\chi_j\chi_k \cdots \chi_l\rangle & (2.30)\\ a_j^\dagger a_i^\dagger|\chi_k \cdots \chi_l\rangle = a_j^\dagger|\chi_i\chi_k \cdots \chi_l\rangle &= |\chi_j\chi_i\chi_k \cdots \chi_l\rangle & (2.31)\\ &= -|\chi_i\chi_j\chi_k \cdots \chi_l\rangle. & (2.32) \end{aligned}$$

Then the following anticommutation relation has been proved,

$$[a_i^\dagger, a_j^\dagger]_+ = a_i^\dagger a_j^\dagger + a_j^\dagger a_i^\dagger = 0. \tag{2.33}$$

This shows that two electrons cannot be created in the same spin–orbital, in accordance with the Pauli exclusion principle.

The annihilation operator, a_i, is the Hermitian conjugate (adjoint operator) of the creation operator, $a_i^\dagger$ (i.e., $(a_i^\dagger)^\dagger = a_i$), and it operates in a general Slater determinant such that:

$$a_i|\chi_i\chi_k \cdots \chi_l\rangle = |\chi_k \cdots \chi_l\rangle, \tag{2.34}$$

Note that in second quantization operators have no accent. This will be relevant when introducing superoperator notation for second quantization.

Therefore, a_i annihilates or destroys an electron in the spin–orbital χ_i. The annihilation operator can only operate on a determinant if the spin–orbital which is going to be operated upon is at the left of the determinant. If not, the determinant must exchange columns, changing the sign in the process. Specifically,

$$a_i|\chi_k\chi_l\chi_i\rangle = -a_i|\chi_i\chi_l\chi_k\rangle = -|\chi_l\chi_k\rangle = |\chi_k\chi_l\rangle. \tag{2.35}$$

The annihilation operator anticommutation relation is similar to Eq. (2.33),

$$[a_i, a_j]_+ = a_i a_j + a_j a_i = 0. \tag{2.36}$$

Ensuring that an electron not present cannot be annihilated,

$$a_i|\chi_k\chi_l\rangle = 0. \tag{2.37}$$

The last anticommutation relation is about both annihilation and creation operators,

$$[a_i, a_j^\dagger]_+ = a_i a_j^\dagger + a_j^\dagger a_i = \delta_{ij}, \tag{2.38}$$

where δ_{ij} is a Kronecker delta and is equal to 1 when $i = j$ or 0 when $i \neq j$.

The second quantization Hamiltonian is given by:

$$H = \sum_{p,q} h_{pq} a_p^\dagger a_q + \frac{1}{4} \sum_{p,q,r,s} \langle pq \| rs \rangle a_p^\dagger a_q^\dagger a_s a_r, \tag{2.39}$$

where h_{pq} is the monoelectronic term that includes kinetic energy and the nuclei–electron potential energy.

2.8 Electron Propagator Theory

The Electron Propagator Theory[3–5,45–53] is one of the most powerful tools for *ab initio* calculations of electron binding energies (EBEs). This theory is equivalent to other formulations like one electron Green's functions or equation of motion and provides interpretation to EBEs with Dyson orbitals in a direct and straightforward way.

The EBEs and Dyson orbitals are eigenvalues and eigenfunctions of one electron equations that include their potential, which is known as the self–energy. The Dyson orbitals are related with transition amplitudes of addition or removal of one electron. In addition, the sum of EBEs and their corresponding

Dyson orbitals are related to the one electron properties or total energies. Electron propagator methods can be improved systematically by improving the approximation operator–space or by increasing the basis–set. The one electron operator equations in EPT are similar to KT[5] and provide correlation expressions for the one electron transitions. Finally, there are diagrammatic expressions for the self–energy operator relating the many body theory with the sum of several correlation and relaxation terms. Electron propagator methods are derived from generalizations of multiple times and density matrices.

A summary of electron propagator basic concepts follows, discussing poles, residues and their physical meaning in terms of EBEs and Dyson orbitals. Approximations are obtained by coupling of the propagator to higher propagators and using the superoperator notation. Then, the electron propagator matrix is obtained by using partition techniques. Reference states and transition properties are related with the inverse form of the Dyson equation which provides a correlated generalization and self–consistent field.

Spectral Form: Electronic binding energies and Dyson orbitals

The electron propagator can be expressed in terms of field operators that annihilate or create electrons in a finite set of spin–orbitals, orthonormal among them, with indexes r, s, t, … such that the spectral form for the electron propagator matrix element r, s is:

$$G_{rs}(E) = \sum_{n} U^{*}_{nr} U_{ns} (E - D_n)^{-1} + \sum_{m} V^{*}_{ms} V_{mr} (E - A_m)^{-1}, \tag{2.40}$$

Where $U_{ns} = \langle N-1, n|a_s|N, 0\rangle$ and $V_{mr} = \langle N+1, m|a_r^{\dagger}|N, 0\rangle$ are residues in the electron propagator matrix,[5] indexes n and m run over states with $N-1$ or $N+1$ electrons, respectively. The reference state, $|N, 0\rangle$, is the ground state of the system with N electrons and has energy $E_0(N)$, ionization energies (IEs), $D_n = E_0(N) - E_n(N-1)$, and electron affinities (EAs), $A_m = E_m(N+1) - E_0(N)$. Poles occur when $E = D_n$ or when $E = A_m$, obtaining IEs or electron affinities EAs, respectively.

Dyson orbitals for ionization energies are defined as follows:

$$\varphi_n^{\text{Dyson}}(\mathbf{x_1}) = N^{\frac{1}{2}} \int \psi_N(\mathbf{x_1}, \mathbf{x_2}, \mathbf{x_3}, \ldots, \mathbf{x_N}) \psi^{*}_{n,N-1}(\mathbf{x_2}, \mathbf{x_3}, \mathbf{x_4}, \ldots, \mathbf{x_N}) d\mathbf{x_2} d\mathbf{x_3} d\mathbf{x_4} \ldots d\mathbf{x_N}. \tag{2.41}$$

Also, we can define the Dyson orbitals for electron affinities:

$$\varphi_m^{\text{Dyson}}(\mathbf{x_1}) = (N+1)^{\frac{1}{2}} \int \psi_{m,N+1}(\mathbf{x_1}, \mathbf{x_2}, \mathbf{x_3}, \ldots, \mathbf{x_N}, \mathbf{x_{N+1}}) \psi_N^*(\mathbf{x_2}, \mathbf{x_3}, \mathbf{x_4}, \ldots, \mathbf{x_N}, \mathbf{x_{N+1}}) d\mathbf{x_2} d\mathbf{x_3} d\mathbf{x_4} \ldots d\mathbf{x_N} d\mathbf{x_{N+1}}. \tag{2.42}$$

Superoperator notation

The electron propagator can be expressed as a series,

$$\begin{aligned} \langle\langle a_r^\dagger; a_s \rangle\rangle &= E^{-1} \langle N,0| \left[a_r^\dagger, a_s\right]_+ |N,0\rangle \\ &+ E^{-2} \langle N,0| \left[a_r^\dagger, [a_s, H]\right]_+ |N,0\rangle \\ &+ E^{-3} \langle N,0| \left[a_r^\dagger, [[a_s, H], H]\right]_+ |N,0\rangle \\ &+ E^{-4} \langle N,0| \left[a_r^\dagger, [[[a_s, H], H], H]\right]_+ |N,0\rangle \\ &+ \ldots \end{aligned} \tag{2.43}$$

where we can use the following notation, which highlights the role of field operators ($G_{rs}(E) \equiv \langle\langle a_r^\dagger; a_s \rangle\rangle$):

$$G_{rs}(E) \equiv \langle\langle a_r^\dagger; a_s \rangle\rangle. \tag{2.44}$$

A concise expression of Eq. (2.43) can be obtained by defining the superoperator vectorial space.[5,53,54] First, we define the inner product between two operators μ and ν,

$$(\mu|\nu) = \langle N,0|[\mu^\dagger, \nu]_+|N,0\rangle. \tag{2.45}$$

Then, for every operator A, including the Hamiltonian operator, we define a superoperator $\hat{A}$ whose action reads,

$$\hat{A}\mu = [\mu, A] = \mu A - A\mu. \tag{2.46}$$

To complete the vectorial linear space, it is necessary to define the identity superoperator $\hat{I}$ as follows,

$$\hat{I}\mu = \mu, \tag{2.47}$$

and the Hamiltonian superoperator

$$\hat{H}\mu = [\mu, H] = \mu H - H\mu. \tag{2.48}$$

Therefore, the electron propagator matrix can be expressed in superoperator notation,

$$\langle\!\langle a_r^\dagger; a_s \rangle\!\rangle = E^{-1}(a_r|a_s) + E^{-2}(a_r|\hat{H}a_s) + E^{-3}(a_r|\hat{H}^2 a_s) + E^{-4}(a_r|\hat{H}^3 a_s) + \ldots \tag{2.49}$$

By separating a E^{-1} term the $\hat{H}$ superoperator powers and E are related as follows,

$$\langle\!\langle a_r^\dagger; a_s \rangle\!\rangle = E^{-1}\left[(a_r|a_s) + E^{-1}(a_r|\hat{H}a_s) + E^{-2}(a_r|\hat{H}^2 a_s) + E^{-3}(a_r|\hat{H}^3 a_s) + \ldots\right], \tag{2.50}$$

which is similar to the geometric series:

$$\frac{1}{1-x} = 1 + x + x^2 + x^3 + \ldots \tag{2.51}$$

where $x = \hat{H}/E$ and its superoperator notation becomes,

$$\langle\!\langle a_r^\dagger; a_s \rangle\!\rangle = \frac{1}{E}\left(a_r \middle| \frac{1}{\hat{I} - \hat{H}/E} a_s\right). \tag{2.52}$$

Then, multiplying the $\frac{1}{E}$ and the inner product we obtain

$$\langle\!\langle a_r^\dagger; a_s \rangle\!\rangle = (a_r|(E\hat{I} - \hat{H})^{-1} a_s) = G_{rs}(E). \tag{2.53}$$

Operator space partitioning

A vector of creation operators, with range R equal to the spin–orbital basis, is defined as follows,

$$\mathbf{a}^\dagger = \left[a_1^\dagger a_2^\dagger a_3^\dagger \ldots a_R^\dagger\right]. \tag{2.54}$$

Then the electron propagator matrix reads,

$$\mathbf{G}(E) = (\mathbf{a}|(E\hat{I} - \hat{H})^{-1}\mathbf{a}). \tag{2.55}$$

The inversion of a superoperator can be avoided by having a matrix inversion instead performing an inner projection. This set of field operators product includes $\mathbf{a}$ elements (simple annihilators), as well as products of $\tilde{n}$ creators and $\tilde{n}+1$ annihilators for $\tilde{n}=1,\ 2,\ 3,\dots$ and is arranged in the vector $\mathbf{w}$,

$$\mathbf{G}(E)=(\mathbf{a}|\mathbf{w})(\mathbf{w}|(E\hat{I}-\hat{H})\mathbf{w})^{-1}(\mathbf{w}|\mathbf{a}). \tag{2.56}$$

The inner projection space can be partitioned into primary and secondary space, which is orthogonal to the primary space and contains triples, quintuples and higher annihilation and creation operators products.[55]

$$\mathbf{G}(E)=(\mathbf{a}|\mathbf{a};\mathbf{f})(\mathbf{a};\mathbf{f}|(E\hat{I}-\hat{H})\mathbf{a};\mathbf{f})^{-1}(\mathbf{a};\mathbf{f}|\mathbf{a}). \tag{2.57}$$

Separating the matrix in primary, secondary and mixed blocks gives,

$$(\mathbf{a}|\mathbf{a}) = \mathbf{1}_a \tag{2.58}$$

$$(\mathbf{f}|\mathbf{f}) = \mathbf{1}_f \tag{2.59}$$

$$(\mathbf{a}|\mathbf{f}) = \mathbf{0}_{a\times f} \tag{2.60}$$

$$(\mathbf{f}|\mathbf{a}) = \mathbf{0}_{f\times a}. \tag{2.61}$$

Eq (2.57) can be simplified as follows,

$$\mathbf{G}(E)=[\mathbf{1}_a\mathbf{0}_{a\times f}](\mathbf{a};\mathbf{f}|(E\hat{I}-\hat{H})\mathbf{a};\mathbf{f})^{-1}[\mathbf{1}_a\mathbf{0}_{a\times f}]^{\dagger}\ , \tag{2.62}$$

where the electron propagator matrix structure implies that the left superior block from the central unit $((\mathbf{a};\mathbf{f}|(E\hat{I}-\hat{H})\mathbf{a};\mathbf{f})^{-1})$ of the inverse matrix is identical to $\mathbf{G}(E)$. This can be proved by solving the following two equations simultaneously:[5]

$$(\mathbf{a}|(E\hat{I}-\hat{H})\mathbf{a})\mathbf{G}(E)+(\mathbf{a}|(E\hat{I}-\hat{H})\mathbf{f})\mathbf{g}_{fa}(E)=\mathbf{1}_a, \tag{2.63}$$

$$(\mathbf{f}|(E\hat{I}-\hat{H})\mathbf{a})\mathbf{G}(E)+(\mathbf{f}|(E\hat{I}-\hat{H})\mathbf{f})\mathbf{g}_{fa}(E)=\mathbf{0}_{f\times a}. \tag{2.64}$$

Solving for the term $\mathbf{g}_{fa}(E)$ in Eq. (2.64),

$$(\mathbf{f}|(E\hat{I}-\hat{H})\mathbf{f})\mathbf{g}_{fa}(E)=-(\mathbf{f}|(E\hat{I}-\hat{H})\mathbf{a})\mathbf{G}(E) \tag{2.65}$$

$$\mathbf{g}_{fa}(E) = -(\mathbf{f}|(E\hat{I} - \hat{H})\mathbf{f})^{-1}(\mathbf{f}|(E\hat{I} - \hat{H})\mathbf{a})\mathbf{G}(E) \tag{2.66}$$

and inserting this into Eq. (2.63) we obtain,

$$(\mathbf{a}|(E\hat{I} - \hat{H})\mathbf{a})\mathbf{G}(E) - (\mathbf{a}|(E\hat{I} - \hat{H})\mathbf{f})(\mathbf{f}|(E\hat{I} - \hat{H})\mathbf{f})^{-1}(\mathbf{f}|(E\hat{I} - \hat{H})\mathbf{a})\mathbf{G}(E) = \mathbf{1}_a, \tag{2.67}$$

We then factorize $\mathbf{G}(E)$,

$$[(\mathbf{a}|(E\hat{I} - \hat{H})\mathbf{a}) - (\mathbf{a}|(E\hat{I} - \hat{H})\mathbf{f})(\mathbf{f}|(E\hat{I} - \hat{H})\mathbf{f})^{-1}(\mathbf{f}|(E\hat{I} - \hat{H})\mathbf{a})]\mathbf{G}(E) = \mathbf{1}_a, \tag{2.68}$$

and simplify the following terms according to Eq. (2.58), Eq. (2.59), Eq. (2.60) and Eq. (2.61)

$$\begin{aligned}
(\mathbf{a}|(E\hat{I} - \hat{H})\mathbf{f}) &= E(\mathbf{a}|\hat{I}\mathbf{f}) - (\mathbf{a}|\hat{H}\mathbf{f}) = E(\mathbf{a}|\mathbf{f}) - (\mathbf{a}|\hat{H}\mathbf{f}) = -(\mathbf{a}|\hat{H}\mathbf{f}) && (2.69)\\
(\mathbf{f}|(E\hat{I} - \hat{H})\mathbf{a}) &= E(\mathbf{f}|\hat{I}\mathbf{a}) - (\mathbf{f}|\hat{H}\mathbf{a}) = E(\mathbf{f}|\mathbf{a}) - (\mathbf{f}|\hat{H}\mathbf{a}) = -(\mathbf{f}|\hat{H}\mathbf{a}). && (2.70)
\end{aligned}$$

Then, Eq. (2.68) is multiplied at the right by the electron propagator matrix, ($\mathbf{G}^{-1}(E)$) and we obtain the following:

$$\mathbf{G}^{-1}(E) = (\mathbf{a}|(E\hat{I} - \hat{H})\mathbf{a}) - (\mathbf{a}|\hat{H}\mathbf{f})(\mathbf{f}|(E\hat{I} - \hat{H})\mathbf{f})^{-1}(\mathbf{f}|\hat{H}\mathbf{a}). \tag{2.71}$$

Dyson equation

Partitioning the operator space can bring about efficient procedures to find poles and residues. One of these procedures is using the electron propagator matrix inverse from Eq. (2.71),[3]

$$\mathbf{G}^{-1}(E) = E\mathbf{1} - (\mathbf{a}|\hat{H}\mathbf{a}) - (\mathbf{a}|\hat{H}\mathbf{f})[E\mathbf{1} - (\mathbf{f}|\hat{H}\mathbf{f})]^{-1}(\mathbf{f}|\hat{H}\mathbf{a}), \tag{2.72}$$

and separating the zeroth order terms,

$$\mathbf{G}_0^{-1}(E)_{rs} = \delta_{rs}(E - \epsilon_r), \tag{2.73}$$

where it can be seen that poles are equivalent to the results of KT.[40] Then, the electron propagator inverse matrix can be related to its zeroth order analog,

$$\mathbf{G}^{-1}(E) = \mathbf{G}_0^{-1}(E) - \mathbf{\Sigma}(E), \tag{2.74}$$

leading to the Dyson equation (Eq. (2.74)) and the correction to the zeroth order electron propagator matrix, $\mathbf{\Sigma}(E)$, is the self–energy.

The self–energy is then separated in terms that depend on E and independent terms,

$$\mathbf{\Sigma}(E) = \boldsymbol{\sigma}(E) + \mathbf{\Sigma}(\infty), \tag{2.75}$$

when E tends to infinity only $\mathbf{\Sigma}(\infty)$ survives and is equal to:

$$\sum_{rs}(\infty) = \sum_{tu}\langle rt||su\rangle\rho_{tu}^{corr}, \tag{2.76}$$

where ρ_{tu}^{corr} is the tu element of the correlation density matrix, $\boldsymbol{\rho}^{corr}$ which includes the correlation contribution to the one electron density matrix.[5]

On the other hand, terms that depend on E are:

$$\boldsymbol{\sigma}(E) = (\mathbf{a}|\hat{H}\mathbf{f})[E\mathbf{1} - (\mathbf{f}|\hat{H}\mathbf{f})]^{-1}(\mathbf{f}|\hat{H}\mathbf{a}). \tag{2.77}$$

In order to solve the Dyson equation, the self–energy matrix can be approximated to a perturbation order using the Møller–Plesset partitioning of the Hamiltonian ($H = H_0 + V$).[3,56] For first order, the self–energy has no additional corrections to the zeroth order self–energy matrix.[4] For second order, we obtain the following:[3]

$$\mathbf{\Sigma}^{(2)}(E) = (\mathbf{a}|\hat{H}\mathbf{f})^{(1)}[E\mathbf{1} - (\mathbf{f}|\hat{H}\mathbf{f})^{(0)}]^{-1}(\mathbf{f}|\hat{H}\mathbf{a})^{(1)}, \tag{2.78}$$

where the order is in the superscripts of the matrix elements.

The matrix elements from the inner products needed for second order are:[3]

$$\begin{aligned}
(a_p|\hat{H}a_a^{\dagger}a_ia_j)^{(1)} &= \langle pa||ij\rangle && (2.79)\\
(a_q|\hat{H}a_i^{\dagger}a_aa_b)^{(1)} &= \langle qi||ab\rangle && (2.80)\\
(a_a^{\dagger}a_ia_j|\hat{H}a_b^{\dagger}a_ka_l)^{(0)} &= \delta_{ab}\delta_{ik}\delta_{jl}[\epsilon_i + \epsilon_j - \epsilon_a] && (2.81)\\
(a_i^{\dagger}a_aa_b|\hat{H}a_j^{\dagger}a_ca_d)^{(0)} &= \delta_{ij}\delta_{ac}\delta_{bd}[\epsilon_a + \epsilon_b - \epsilon_i], && (2.82)
\end{aligned}$$

where Eq. (2.81) requires that $i < j$ and $k < l$, and Eq. (2.82) requires that $a < b$ and $c < d$.

Using the previous matrix elements we can combine them in order to obtain the second order self–energy:[4,5]

$$\Sigma_{pq}^{(2)}(E) = \frac{1}{2}\sum_{aij}\frac{\langle pa||ij\rangle\langle ij||qa\rangle}{E + \epsilon_a - \epsilon_i - \epsilon_j} + \frac{1}{2}\sum_{iab}\frac{\langle pi||ab\rangle\langle ab||qi\rangle}{E + \epsilon_i - \epsilon_a - \epsilon_b}, \tag{2.83}$$

where i and j (a and b) are occupied spin–orbitals (virtuals), ϵ_a, ϵ_b, ϵ_i and ϵ_j are the Hartree–Fock eigenvalues for a, b, i and j spin–orbitals, respectively.

Pole search

Searching for poles from the Dyson equation leads to ionization energies and electron affinities for occupied and virtual orbitals, respectively. To find poles in the second order electron propagator one can use the diagonal approximation, also called the quasiparticle approximation. This approximation consists in making zero all the non–diagonal elements in the self–energy matrix. Then, the element pp of the self–energy matrix belongs to either an occupied (ionization energy) or virtual (electron affinity) spin–orbital,

$$\Sigma_{pp}^{2}(E) = \frac{1}{2}\sum_{aij}\frac{\langle pa||ij\rangle\langle ij||pa\rangle}{E + \epsilon_a - \epsilon_i - \epsilon_j} + \frac{1}{2}\sum_{iab}\frac{\langle pi||ab\rangle\langle ab||pi\rangle}{E + \epsilon_i - \epsilon_a - \epsilon_b}. \tag{2.84}$$

A simple way of solving for E is to guess the first value equal to ϵ_p, obtaining the first self–energy from this guess. Then solving for E again in the following equation (Eq. (2.85)),

$$E = \epsilon_p + \Sigma_{pp}(E). \tag{2.85}$$

In addition, using the Newton–Raphson method to find poles is suggested,[3] and it usually takes 3 to 4 iterations to reach a convergence value with a threshold of 10^{-5} hartree. Residues for poles obtained with the quasiparticle approximation are known as pole strengths and are calculated as follows:

$$\pi_p = \left(1 - \frac{d\Sigma_{pp}(E)}{dE}\right)^{-1}, \tag{2.86}$$

where $0 < \pi_p \leq 1$ and the approximation is correct when $\pi_p \geq 0.85$ because the pole consists mainly of one single determinant.

Chapter 3

Electron propagator Brandow (Feynman) diagrams.

Electron propagator diagrams are graphic tools that simplify the description of quantum correlation. Second and third order electron propagator diagrams are quite useful in building the self-energy operator. In addition, they efficiently represent advanced mathematics and linear algebra. In this work, we propose a vectorial representation for each diagram, and using computer software to create all possible vectors, plot diagrams, obtain self-energy expressions and program the expressions for fourth order electron propagator diagrams.

3.1 Introduction

The Brueckner-Goldstone many-body perturbation theory,[57,58] with perturbation corrections expressed in terms of Feynman-like diagrams,[59] has found widespread application in many fields. It was first applied to atomic systems by Kelly[60] and has since been successfully used to calculate a variety of atomic and molecular properties. An extension of the method to systems with degenerate or nearly degenerate unperturbed states was put forward by Bloch and Horowitz,[61] and recast in a connected-diagram, energy-independent form by Brandow.[62] Brandow's diagrams are used as graphic tools in electron propagator theory;[4] this is because they simplify the quantum correlation description avoiding the employment of long algebraic treatments and obtaining the expression of the self-energy matrix elements in a graphic way.

This work focuses on the automatic generation of Brandow's electron propagator diagrams, for third and fourth order. In order to obtain an automatic generation of the diagrams we first need to represent them as vectors. Then, we can link the diagram vectors with a graphic tool and a script to obtain third and fourth order diagrams, self-energy expressions and to compute the diagrams.

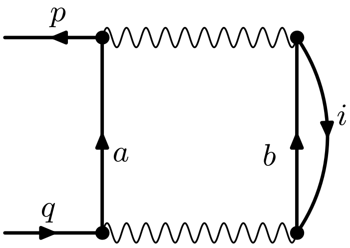

Figure 3.1: Fig. : 2ph second order diagram.

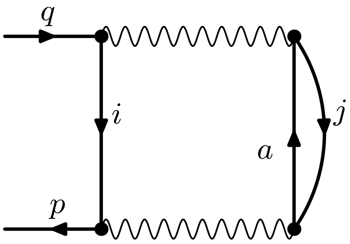

Figure 3.2: Fig. : 2hp second order diagram.

Brandow diagram construction

Brandow's electron propagator diagrams are a graphical representation of the self-energy matrix elements. In order to construct them, some rules must be followed. Each perturbation is represented by a horizontal wavy line, there are as many perturbation lines as the diagram order, and each perturbation line must be drawn at a different height or level. Each of these perturbation lines links two dots called nodes, the node in the left side is for the electron *1* and the node in the right side for the electron *2*. Every dot has two propagation lines with two arrows: one arrow enters and the other leaves the node. The propagation lines connect nodes in the same electron at different levels, except for two horizontal arrows of electron *1* which are disconnected such that one that enters and the other leaves the diagram. When the propagation lines are going up, they represent particles or unoccupied orbitals (a,b,c,d). Holes or occupied orbitals are present when the arrows are going down (i,j,k,l) and the general indexes (p,q) are used in the horizontal arrows.

Following these rules we can obtain the two Brandow second–order, electron propagator diagrams of Fig. 3.1 and Fig. 3.2.

Obtaining self-energy terms from diagrams

In order to solve for the Green's function poles, we need to calculate the self-energy expressions. Each self-energy expression is a summation of a product of electron repulsion integrals in the molecular–orbital basis and inverses of molecular–orbital energy differences. We can separate each self energy expression in these parts:

- Sign.
- Factor.
- Numerator.
- Denominator.
- Summation.

Sign

The sign of the diagram is defined as $Sign = (-1)^{h+l}$, where l is the number of closed loops and h the number of lines which represent spin-orbital occupied, arrows pointing down. The diagram in Fig. 3.1 has one loop formed by b and i ($l = 1$) and one propagation line going down, i ($h = 1$). Thus $Sign = +1$

Factor

A factor of $\left(\frac{1}{2}\right)^n$ is included, where n is the number of pairs of equivalent lines. Two lines are considered equivalent if both come from and finish in the same perturbation line. The diagram in Fig. 3.1 has a $n = 1$ and a $\frac{1}{2}$ factor, because the propagator lines a and b are equivalent.

Numerator

The numerator is a product of antisymmetrized two electron repulsion integrals; for each perturbation line, there is an integral. The integral, in Dirac notation has the form: $\langle pq \| rs \rangle$, where each index is chosen according to the label of the propagation lines entering the nodes on the perturbation lines.

1. p = electron 1 (left), leaving arrow.
2. q = electron 2 (right), leaving arrow.
3. r = electron 1 (left), entering arrow.
4. s = electron 2 (right), entering arrow.

Then, the numerator obtained for Fig. 3.1 is $\langle pi \| ab\rangle\langle ab \| qi\rangle$.

Denominator

The denominator is a sum of the spin-orbital energies. In order to get these terms, an imaginary horizontal line is drawn in the middle of two consecutive perturbation lines and a positive eigenvalue is added for each propagation line that crosses the imaginary line going down (a negative eigenvalue is added for each propagation arrow that crosses upward). There is another E term using an imaginary arrow going from q to p. For example, the diagram in Fig. 3.1 has the denominator $E + \epsilon_i - \epsilon_a - \epsilon_b$.

Summation

The summation runs over the orbitals present in the diagram, which are the indices in the propagation lines. The diagram in Fig. 3.1, runs over the orbitals *i, a, b.*

Finally, we obtain the following self–energy expression for the diagram in Fig. 3.1:

$$\frac{1}{2}\sum_{i,a,b}\frac{\langle pi \| ab\rangle\langle ab \| qi\rangle}{E + \epsilon_i - \epsilon_a - \epsilon_b} \tag{3.1}$$

3.2 Methodology

Brandow's propagator diagrams in vectorial representation

In order to represent Brandow's electron propagator diagrams as vectors we follow the next procedure:

1. Select order of diagram: second, third or fourth.
2. If diagram is second order separate the diagram in two electrons.
3. If diagram is third order separate the diagram in two or three electrons.
4. If diagram is fourth order separate the diagram in two, three or four electrons.
5. Build path vector for each electron.

Consider the diagram on the left side of Fig. 3.1. For electron one, we ignore the perturbation lines uniting the nodes and describe the electron route beginning with the level at which the orbital *q* enters at level one. Then, orbital *a* leaves level one and enters level two. Finally, orbital *p* leaves level two. We have defined the electron route (see matrix in Table 3.1). The right side is a loop and we define the beginning from level one to level two (*b*) and close the loop with *i*.

0	1	1	2
1	2	2	1
2	0		

Table 3.1: 2ph second order diagram vectorial representation.

Using this representation we can now generate Brandow's third order propagator diagrams. Then, we use the vectors to generate self–energy terms, both dependent and independent of E, and plot the generated diagrams.

The program DROGON.D4 has been created for generation of Brandow's electron propagator diagrams. The first part of the algorithm uses FORTRAN 90 and defines the diagram's order and structure. It generates all possible vectors for electrons one, two and three and then combines these individual vectors to obtain the vectorial representation of the diagram. The second part of the algorithm uses a bash script to plot the diagram via METAPOST. The third part of the algorithm uses FORTRAN 90 for the creation of the self-energy expressions in LATEX.

3.3 D3 Brandow's diagrams

We can define the structure of a diagram by how many levels and electrons are present. For example, a second order diagram will be 2-22 where the first number is the diagram level and the other two numbers are the number of nodes in electron one and two, respectively. For third order, we will have more possible structures: 3-330, 3-132 and 3-222. Drogon.D4 generates 12 diagrams for structure 3-330 (see type-A diagrams in Fig. 3.3), 6 diagrams for structure 3-132 (see type-B diagrams in Fig. 3.4) and 6 diagrams for structure 3-222 (see type-C diagrams in 3.5).

Using DROGON.D4 we can obtain all possible Brandow's diagrams. However, there are only 12 diagrams for third order electron propagator[4] and Drogon.D4 obtained 18, duplicating 6 type-A diagrams with type-C diagrams. For example, we can use in Fig. 3.6 a Hugenholtz diagram equivalent to both A2 and C2 diagrams.

A fourth–order Hugenholtz diagram has only one column, one arrow entering and another arrow leaving the diagram, each dot has two arrows entering and two arrows leaving, and the diagram can't be pulled apart. In addition, Hugenholtz diagrams for EPT should have at least two arrows between dots (a denominator with at least two eigenvalues). Collapsing a Brandow diagram into a Hugenholtz diagram

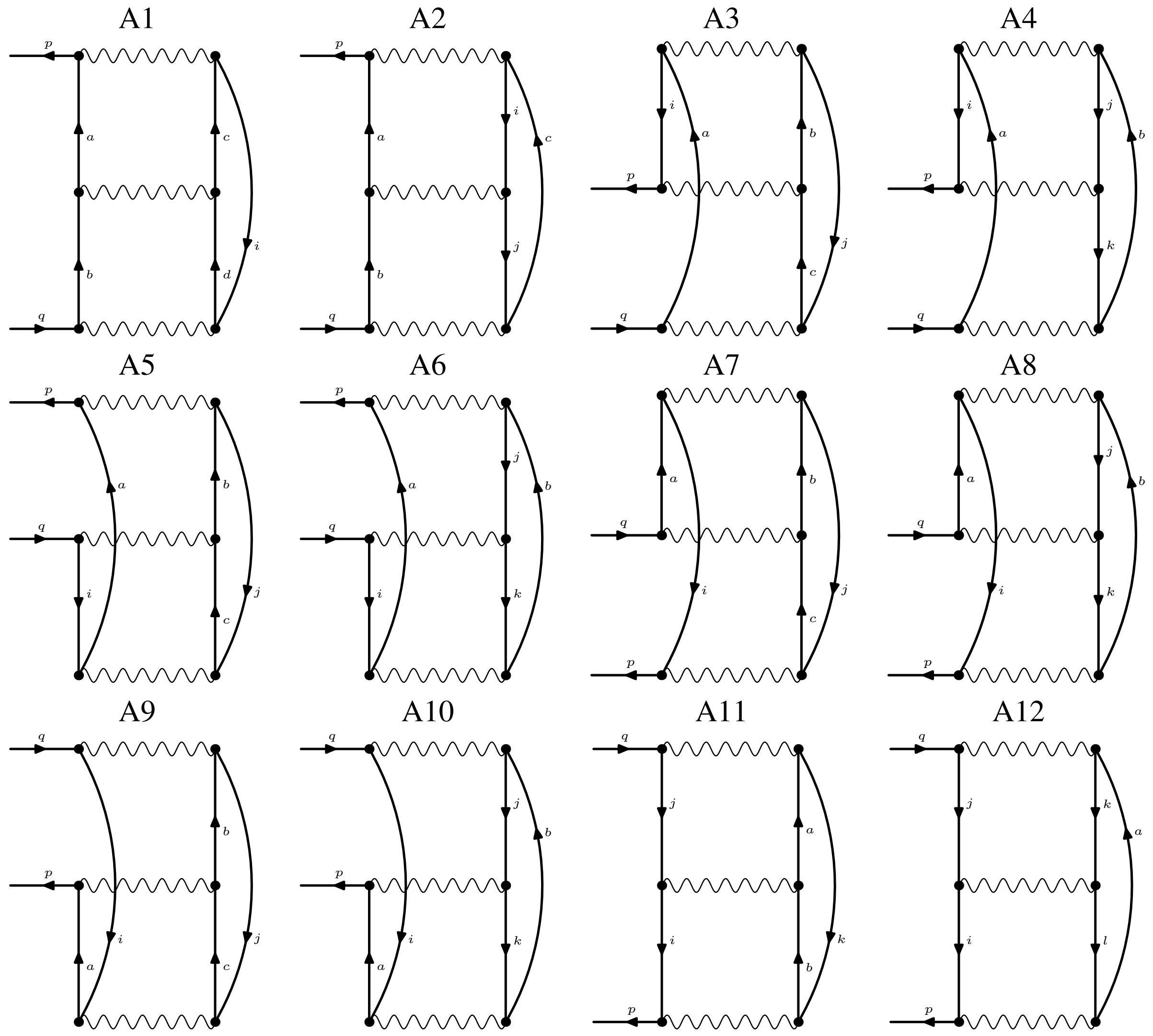

Figure 3.3: A-type third order diagrams

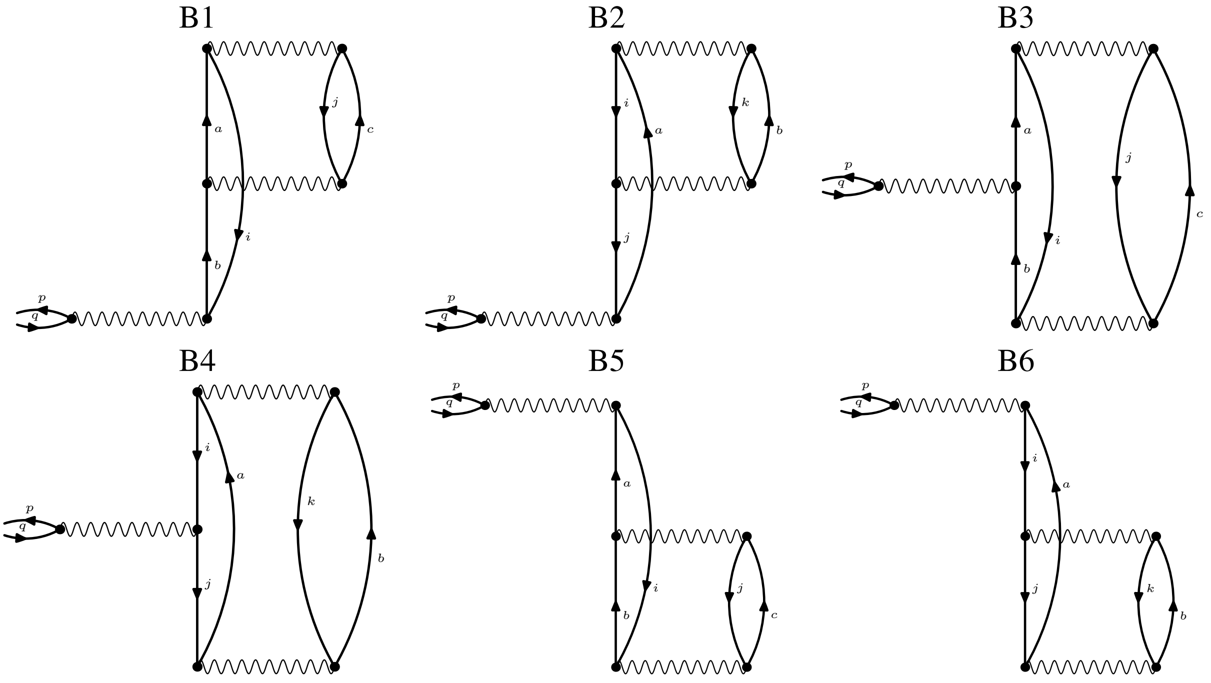

Figure 3.4: B-type third order diagrams

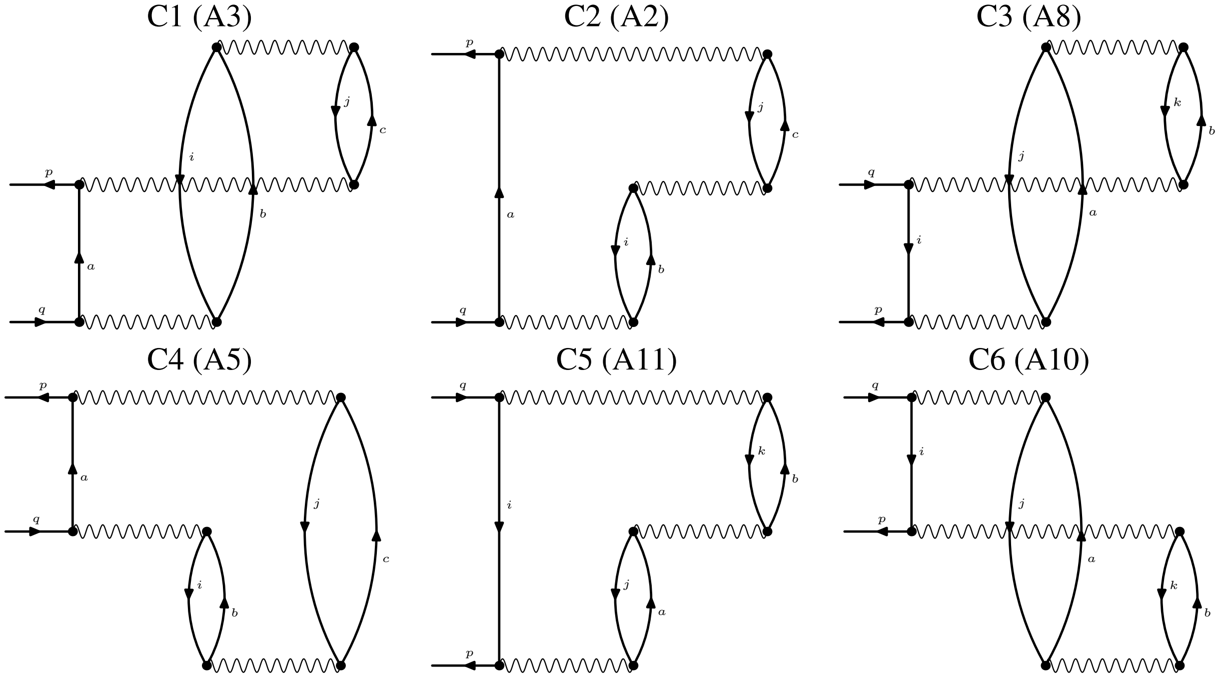

Figure 3.5: C-type third order diagrams

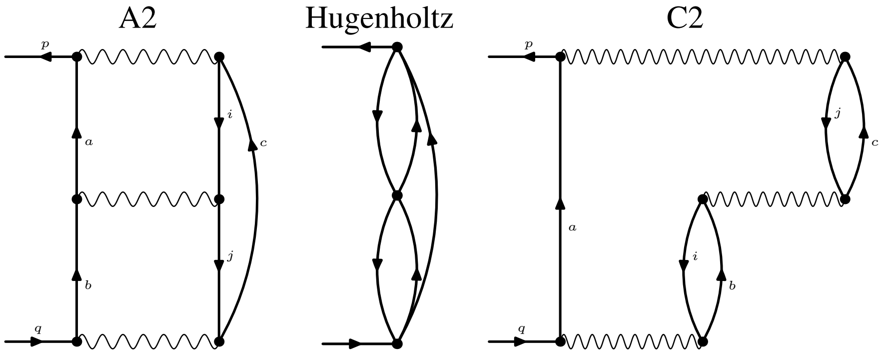

Figure 3.6: Equivalent third order diagrams

consist in converting the interaction lines into a single dots with two entering arrows and two leaving arrows.

Using the Hugenholtz diagrams, we can collapse all the type-C diagrams into type-A diagrams. This will be extremely helpful for selecting the unique diagrams at fourth order. Then, we will use DROGON.D4 to obtain both the LATEX expressions and METAPOST images. We will have twelve diagrams that are self-energy dependent (Eqns: 3.2–3.13) and six self-energy independent diagrams (Eqns: 3.14–3.19):

$$A1 = +\frac{1}{4}\sum_{i,a,b,c,d}\frac{\langle pi||ac\rangle\langle ac||bd\rangle\langle bd||qi\rangle}{(E+\epsilon_i-\epsilon_a-\epsilon_c)(E+\epsilon_i-\epsilon_b-\epsilon_d)} \tag{3.2}$$

$$A2 = -\sum_{i,j,a,b,c}\frac{\langle pi||ac\rangle\langle aj||bi\rangle\langle bc||qj\rangle}{(E+\epsilon_i-\epsilon_a-\epsilon_c)(E+\epsilon_j-\epsilon_b-\epsilon_c)} \tag{3.3}$$

$$A3 = -\sum_{i,j,a,b,c}\frac{\langle pb||ic\rangle\langle ij||ab\rangle\langle ac||qj\rangle}{(E+\epsilon_j-\epsilon_a-\epsilon_c)(\epsilon_i+\epsilon_j-\epsilon_a-\epsilon_b)} \tag{3.4}$$

$$A4 = +\frac{1}{4}\sum_{i,j,k,a,b}\frac{\langle pk||ij\rangle\langle ij||ab\rangle\langle ab||qk\rangle}{(E+\epsilon_k-\epsilon_a-\epsilon_b)(\epsilon_i+\epsilon_j-\epsilon_a-\epsilon_b)} \tag{3.5}$$

$$A5 = -\sum_{i,j,a,b,c}\frac{\langle pj||ab\rangle\langle ac||ij\rangle\langle ib||qc\rangle}{(E+\epsilon_j-\epsilon_a-\epsilon_b)(\epsilon_i+\epsilon_j-\epsilon_a-\epsilon_c)} \tag{3.6}$$

$$A6 = +\frac{1}{4}\sum_{i,j,k,a,b}\frac{\langle pj||ab\rangle\langle ab||ik\rangle\langle ik||qj\rangle}{(E+\epsilon_j-\epsilon_a-\epsilon_b)(\epsilon_i+\epsilon_k-\epsilon_a-\epsilon_b)} \tag{3.7}$$

$$A7 = -\frac{1}{4}\sum_{i,j,a,b,c}\frac{\langle pc||ij\rangle\langle ij||ab\rangle\langle ab||qc\rangle}{(\epsilon_i+\epsilon_j-E-\epsilon_c)(\epsilon_i+\epsilon_j-\epsilon_a-\epsilon_b)} \tag{3.8}$$

$$A8 = +\sum_{i,j,k,a,b}\frac{\langle pb||ik\rangle\langle ij||ab\rangle\langle ak||qj\rangle}{(\epsilon_i+\epsilon_k-E-\epsilon_b)(\epsilon_i+\epsilon_j-\epsilon_a-\epsilon_b)} \tag{3.9}$$

$$A9 = -\frac{1}{4} \sum_{i,j,a,b,c} \frac{\langle pb \| ac \rangle \langle ac \| ij \rangle \langle ij \| qb \rangle}{(\epsilon_i + \epsilon_j - E - \epsilon_b)(\epsilon_i + \epsilon_j - \epsilon_a - \epsilon_c)} \tag{3.10}$$

$$A10 = + \sum_{i,j,k,a,b} \frac{\langle pk \| aj \rangle \langle ab \| ik \rangle \langle ij \| qb \rangle}{(\epsilon_i + \epsilon_j - E - \epsilon_b)(\epsilon_i + \epsilon_k - \epsilon_a - \epsilon_b)} \tag{3.11}$$

$$A11 = + \sum_{i,j,k,a,b} \frac{\langle pb \| ik \rangle \langle ia \| jb \rangle \langle jk \| qa \rangle}{(\epsilon_j + \epsilon_k - E - \epsilon_a)(\epsilon_i + \epsilon_k - E - \epsilon_b)} \tag{3.12}$$

$$A12 = -\frac{1}{4} \sum_{i,j,k,l,a} \frac{\langle pa \| il \rangle \langle il \| jk \rangle \langle jk \| qa \rangle}{(\epsilon_j + \epsilon_k - E - \epsilon_a)(\epsilon_i + \epsilon_l - E - \epsilon_a)} \tag{3.13}$$

$$B1 = \frac{1}{2} \sum_{i,j,a,b,c} \frac{\langle pb \| qi \rangle \langle ij \| ac \rangle \langle ac \| bj \rangle}{(\epsilon_i - \epsilon_b)(\epsilon_i + \epsilon_j - \epsilon_a - \epsilon_c)} \tag{3.14}$$

$$B2 = -\frac{1}{2} \sum_{i,j,k,a,b} \frac{\langle pa \| qj \rangle \langle ik \| ab \rangle \langle jb \| ik \rangle}{(\epsilon_j - \epsilon_a)(\epsilon_i + \epsilon_k - \epsilon_a - \epsilon_b)} \tag{3.15}$$

$$B3 = \frac{1}{2} \sum_{i,j,a,b,c} \frac{\langle pa \| qb \rangle \langle ij \| ac \rangle \langle bc \| ij \rangle}{(\epsilon_i + \epsilon_j - \epsilon_a - \epsilon_c)(\epsilon_i + \epsilon_j - \epsilon_b - \epsilon_c)} \tag{3.16}$$

$$B4 = -\frac{1}{2} \sum_{i,j,k,a,b} \frac{\langle pj \| qi \rangle \langle ik \| ab \rangle \langle ab \| jk \rangle}{(\epsilon_j + \epsilon_k - \epsilon_a - \epsilon_b)(\epsilon_i + \epsilon_k - \epsilon_a - \epsilon_b)} \tag{3.17}$$

$$B5 = \frac{1}{2} \sum_{i,j,a,b,c} \frac{\langle pi \| qa \rangle \langle bc \| ij \rangle \langle aj \| bc \rangle}{(\epsilon_i + \epsilon_j - \epsilon_b - \epsilon_c)(\epsilon_i - \epsilon_a)} \tag{3.18}$$

$$B6 = -\frac{1}{2} \sum_{i,j,k,a,b} \frac{\langle pi \| qa \rangle \langle ab \| jk \rangle \langle jk \| ib \rangle}{(\epsilon_j + \epsilon_k - \epsilon_a - \epsilon_b)(\epsilon_i - \epsilon_a)} \tag{3.19}$$

3.4 D4 Brandow's diagrams

Appendix A has all the diagrams and equations obtained with DROGON.D4 for fourth–order electron propagator self–energy. Previously, Schirmer *et al*[37] obtained 228 fourth–order diagrams that are labeled in Appendix A as type–U, type–V and type–W diagrams. There are 16 type–U diagrams and 16 type–V diagrams which contain f_7 couplings $((E + \epsilon_i + \epsilon_j + \epsilon_k - \epsilon_a - \epsilon_b - \epsilon_c - \epsilon_d)^{-1})$. However, this terms can be reduced to f_3 terms by performing an algebraic reduction[37]. In addition, DROGON.D4 obtained more diagrams that appear to be pseudo–f_7 terms and diagrams that can be reduced to one diagram with 2ph–2hp terms.

Figure 3.7: Fourth order f7 diagrams

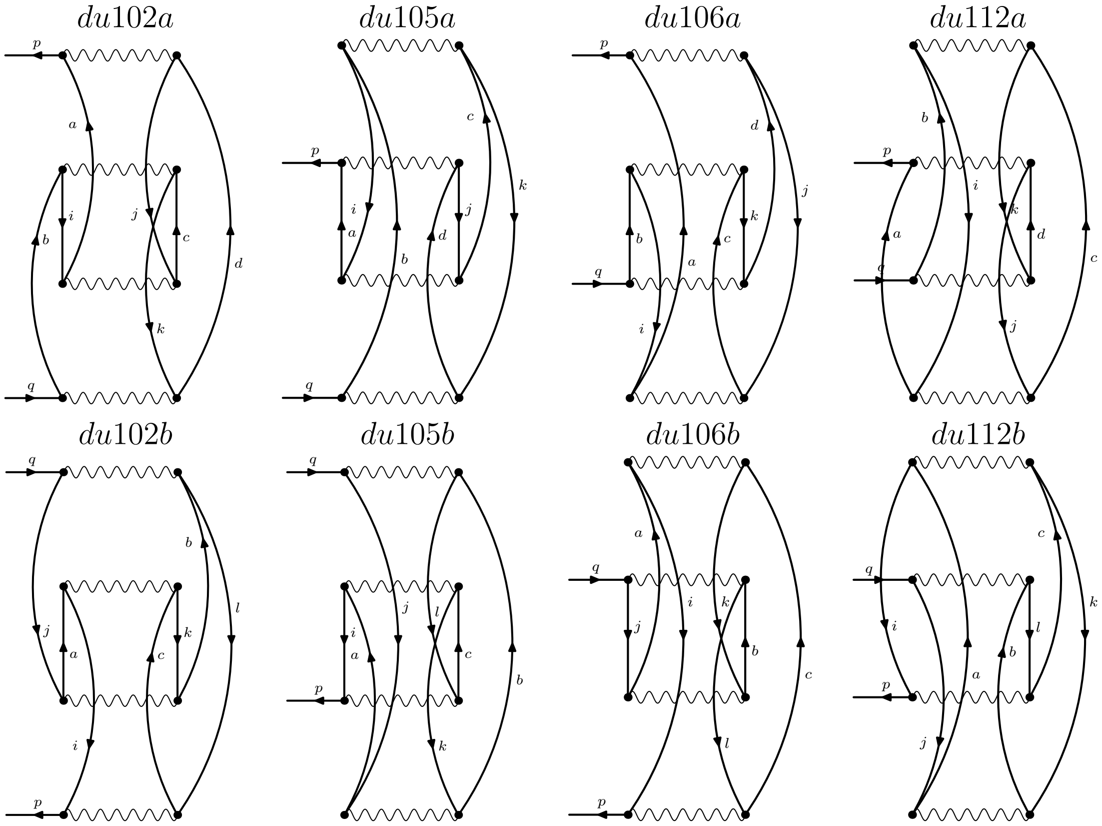

Algebraic reduction of pseudo–f_7 diagrams

Figure 3.7 shows diagrams corresponding to the U1 row for fourth–order EPT, and their mirror image. Each of these diagrams have pseudo–f_7 couplings. However as shown before,[37] these diagrams can be decomposed into simpler expressions.

$$du102a = \sum_{a,b,c,d,i,j,k} \frac{\langle pj||ad\rangle\langle ac||ij\rangle\langle ik||bc\rangle\langle bd||qk\rangle}{(E+\epsilon_k-\epsilon_b-\epsilon_d)(E+\epsilon_i+\epsilon_j+\epsilon_k-\epsilon_a-\epsilon_b-\epsilon_c-\epsilon_d)(E+\epsilon_j-\epsilon_a-\epsilon_d)} \tag{3.20}$$

$$du105a = \sum_{a,b,c,d,i,j,k} \frac{\langle pj||ad\rangle\langle ac||ij\rangle\langle ik||bc\rangle\langle bd||qk\rangle}{(E+\epsilon_k-\epsilon_b-\epsilon_d)(E+\epsilon_i+\epsilon_j+\epsilon_k-\epsilon_a-\epsilon_b-\epsilon_c-\epsilon_d)(\epsilon_i+\epsilon_k-\epsilon_b-\epsilon_c)} \tag{3.21}$$

$$du106a = \sum_{a,b,c,d,i,j,k} \frac{\langle pj||ad\rangle\langle ac||ij\rangle\langle ik||bc\rangle\langle bd||qk\rangle}{(\epsilon_i+\epsilon_j-\epsilon_a-\epsilon_c)(E+\epsilon_i+\epsilon_j+\epsilon_k-\epsilon_a-\epsilon_b-\epsilon_c-\epsilon_d)(E+\epsilon_j-\epsilon_a-\epsilon_d)} \tag{3.22}$$

$$du112a = \sum_{a,b,c,d,i,j,k} \frac{\langle pj||ad\rangle\langle ac||ij\rangle\langle ik||bc\rangle\langle bd||qk\rangle}{(\epsilon_i+\epsilon_j-\epsilon_a-\epsilon_c)(E+\epsilon_i+\epsilon_j+\epsilon_k-\epsilon_a-\epsilon_b-\epsilon_c-\epsilon_d)(\epsilon_i+\epsilon_k-\epsilon_b-\epsilon_c)} \tag{3.23}$$

$$du102b = -\sum_{a,b,c,i,j,k,l} \frac{\langle pc||il\rangle\langle ab||jk\rangle\langle ik||ac\rangle\langle jl||pb\rangle}{(\epsilon_i+\epsilon_l-E-\epsilon_c)(\epsilon_i+\epsilon_j+\epsilon_k+\epsilon_l-E-\epsilon_a-\epsilon_b-\epsilon_c)(\epsilon_j+\epsilon_l-E-\epsilon_b)} \tag{3.24}$$

$$du105b = -\sum_{a,b,c,i,j,k,l} \frac{\langle pc||il\rangle\langle ab||jk\rangle\langle ik||ac\rangle\langle jl||pb\rangle}{(\epsilon_j+\epsilon_k-\epsilon_a-\epsilon_b)(\epsilon_i+\epsilon_j+\epsilon_k+\epsilon_l-E-\epsilon_a-\epsilon_b-\epsilon_c)(\epsilon_j+\epsilon_l-E-\epsilon_b)} \tag{3.25}$$

$$du106b = -\sum_{a,b,c,i,j,k,l} \frac{\langle pc||il\rangle\langle ab||jk\rangle\langle ik||ac\rangle\langle jl||pb\rangle}{(\epsilon_i+\epsilon_l-E-\epsilon_c)(\epsilon_i+\epsilon_j+\epsilon_k+\epsilon_l-E-\epsilon_a-\epsilon_b-\epsilon_c)(\epsilon_i+\epsilon_k-\epsilon_a-\epsilon_c)} \tag{3.26}$$

$$du112b = -\sum_{a,b,c,i,j,k,l} \frac{\langle pc||il\rangle\langle ab||jk\rangle\langle ik||ac\rangle\langle jl||pb\rangle}{(\epsilon_j+\epsilon_k-\epsilon_a-\epsilon_b)(\epsilon_i+\epsilon_j+\epsilon_k+\epsilon_l-E-\epsilon_a-\epsilon_b-\epsilon_c)(\epsilon_i+\epsilon_k-\epsilon_a-\epsilon_c)} \tag{3.27}$$

Equations 3.20, 3.21, 3.22 and 3.23 can be added together,

$$\begin{aligned}
D &= du102a + du105a + du106a + du112a \\
D &= \sum_{a,b,c,d,i,j,k} \frac{\langle pj||ad\rangle\langle ac||ij\rangle\langle ik||bc\rangle\langle bd||qk\rangle}{E+\epsilon_i+\epsilon_j+\epsilon_k-\epsilon_a-\epsilon_b-\epsilon_c-\epsilon_d} \\
&\times \left[\frac{1}{(E+\epsilon_k-\epsilon_b-\epsilon_d)(E+\epsilon_j-\epsilon_a-\epsilon_d)} + \frac{1}{(E+\epsilon_k-\epsilon_b-\epsilon_d)(\epsilon_i+\epsilon_k-\epsilon_b-\epsilon_c)}\right. \\
&+ \left.\frac{1}{(\epsilon_i+\epsilon_j-\epsilon_a-\epsilon_c)(E+\epsilon_j-\epsilon_a-\epsilon_d)} + \frac{1}{(\epsilon_i+\epsilon_j-\epsilon_a-\epsilon_c)(\epsilon_i+\epsilon_k-\epsilon_b-\epsilon_c)}\right].
\end{aligned} \tag{3.28}$$

This, can be written in a simpler way

$$D = \sum_{a,b,c,d,i,j,k} \langle pj||ad\rangle\langle ac||ij\rangle\langle ik||bc\rangle\langle bd||qk\rangle d, \tag{3.29}$$

where

$$\begin{aligned}
d &= E_{12}^{-1}(E_1^{-1}E_2^{-1} + E_1^{-1}\epsilon_1^{-1} + E_2^{-1}\epsilon_2^{-1} + \epsilon_1^{-1}\epsilon_2^{-1}), \\
E_{12} &= E+\epsilon_i+\epsilon_j+\epsilon_k-\epsilon_a-\epsilon_b-\epsilon_c-\epsilon_d, \\
E_1 &= E+\epsilon_k-\epsilon_b-\epsilon_d, \\
E_2 &= E+\epsilon_j-\epsilon_a-\epsilon_d, \\
\epsilon_1 &= \epsilon_i+\epsilon_k-\epsilon_b-\epsilon_c, \\
\epsilon_2 &= \epsilon_i+\epsilon_j-\epsilon_a-\epsilon_c.
\end{aligned} \tag{3.30}$$

Now, d can be rearranged

$$d = E_{12}^{-1}E_1^{-1}E_2^{-1}\epsilon_1^{-1}\epsilon_2^{-1}(E_1E_2 + E_1\epsilon_1 + E_2\epsilon_2 + \epsilon_1\epsilon_2), \tag{3.31}$$

where the following can be proved

$$E_1E_2 + E_1\epsilon_1 + E_2\epsilon_2 + \epsilon_1\epsilon_2 = \frac{1}{2}E_{12}\left(E_1 + E_2 + \epsilon_1 + \epsilon_2\right), \tag{3.32}$$

First, we obtain all the terms for $E_1E_2 + E_1\epsilon_1 + E_2\epsilon_2 + \epsilon_1\epsilon_2$:

$$\begin{aligned}
E_1E_2 &= E^2+E\epsilon_j+E\epsilon_k-E\epsilon_a-E\epsilon_b-2E\epsilon_d+\epsilon_j\epsilon_k-\epsilon_j\epsilon_b-\epsilon_j\epsilon_d-\epsilon_k\epsilon_a-\epsilon_k\epsilon_d+\epsilon_a\epsilon_b+\epsilon_a\epsilon_d+\epsilon_b\epsilon_d+\epsilon_d^2,\\
E_1\epsilon_1 &= E\epsilon_i+E\epsilon_k-E\epsilon_b-E\epsilon_c+\epsilon_i\epsilon_k-\epsilon_k^2-\epsilon_i\epsilon_b-\epsilon_i\epsilon_d-2\epsilon_k\epsilon_b-\epsilon_k\epsilon_c-\epsilon_k\epsilon_d+\epsilon_b^2+\epsilon_b\epsilon_c+\epsilon_b\epsilon_d+\epsilon_c\epsilon_d,\\
E_2\epsilon_2 &= E\epsilon_i+E\epsilon_j-E\epsilon_a-E\epsilon_c+\epsilon_i\epsilon_j-\epsilon_j^2-\epsilon_i\epsilon_a-\epsilon_i\epsilon_d-2\epsilon_j\epsilon_a-\epsilon_j\epsilon_c-\epsilon_j\epsilon_d+\epsilon_a^2+\epsilon_a\epsilon_c+\epsilon_a\epsilon_d+\epsilon_c\epsilon_d,\\
\epsilon_1\epsilon_2 &= \epsilon_i^2+\epsilon_i\epsilon_j+\epsilon_i\epsilon_k+\epsilon_j\epsilon_k-\epsilon_i\epsilon_a-\epsilon_i\epsilon_b-2\epsilon_i\epsilon_c-\epsilon_j\epsilon_b-\epsilon_j\epsilon_c-\epsilon_k\epsilon_a-\epsilon_k\epsilon_c+\epsilon_a\epsilon_b+\epsilon_a\epsilon_c+\epsilon_b\epsilon_c+\epsilon_c^2,
\end{aligned} \tag{3.33}$$

where the total 64 terms are repeated in the following 128 terms:

$$\begin{aligned}
E_{12}E_1 &= E^2+E\epsilon_i+E\epsilon_j+2E\epsilon_k-E\epsilon_a-2E\epsilon_b-E\epsilon_c-2E\epsilon_d+\epsilon_i\epsilon_k+\epsilon_j\epsilon_k+\epsilon_k^2-\epsilon_i\epsilon_b-\epsilon_i\epsilon_d-\epsilon_j\epsilon_b-\epsilon_j\epsilon_d\\
&\quad -\epsilon_k\epsilon_a-2\epsilon_k\epsilon_b-\epsilon_k\epsilon_c-2\epsilon_k\epsilon_d+\epsilon_a\epsilon_b+\epsilon_a\epsilon_d+\epsilon_b^2+\epsilon_b\epsilon_c+2\epsilon_b\epsilon_d+\epsilon_c\epsilon_d+\epsilon_d^2,\\
E_{12}E_2 &= E^2+E\epsilon_i+2E\epsilon_j+E\epsilon_k-2E\epsilon_a-E\epsilon_b-E\epsilon_c-2E\epsilon_d+\epsilon_i\epsilon_j+\epsilon_j^2+\epsilon_j\epsilon_k-\epsilon_i\epsilon_a-\epsilon_i\epsilon_d-2\epsilon_j\epsilon_a-\epsilon_j\epsilon_b-\epsilon_j\epsilon_c-2\epsilon_j\epsilon_d\\
&\quad -\epsilon_k\epsilon_a-\epsilon_k\epsilon_d+\epsilon_a^2+\epsilon_a\epsilon_b+\epsilon_a\epsilon_c+2\epsilon_a\epsilon_d+\epsilon_b\epsilon_d+\epsilon_c\epsilon_d+\epsilon_d^2,\\
E_{12}\epsilon_1 &= E\epsilon_i+E\epsilon_k-E\epsilon_b-E\epsilon_c+\epsilon_i^2+\epsilon_i\epsilon_j+2\epsilon_i\epsilon_k+\epsilon_j\epsilon_k+\epsilon_k^2-\epsilon_i\epsilon_a-2\epsilon_i\epsilon_b-2\epsilon_i\epsilon_c-\epsilon_i\epsilon_d-\epsilon_j\epsilon_b-\epsilon_j\epsilon_c\\
&\quad -\epsilon_k\epsilon_a-2\epsilon_k\epsilon_b-2\epsilon_k\epsilon_c-\epsilon_k\epsilon_d+\epsilon_a\epsilon_b+\epsilon_a\epsilon_c+\epsilon_b^2+2\epsilon_b\epsilon_c+\epsilon_b\epsilon_d+\epsilon_c^2+\epsilon_c\epsilon_d,\\
E_{12}\epsilon_2 &= E\epsilon_i+E\epsilon_j-E\epsilon_a-E\epsilon_c+\epsilon_i^2+2\epsilon_i\epsilon_j+\epsilon_i\epsilon_k+\epsilon_j^2+\epsilon_j\epsilon_k-2\epsilon_i\epsilon_a-\epsilon_i\epsilon_b-2\epsilon_i\epsilon_c-\epsilon_i\epsilon_d-2\epsilon_j\epsilon_a-\epsilon_j\epsilon_b-2\epsilon_j\epsilon_c-\epsilon_j\epsilon_d\\
&\quad -\epsilon_k\epsilon_a-\epsilon_k\epsilon_c+\epsilon_a^2+\epsilon_a\epsilon_b+2\epsilon_a\epsilon_c+\epsilon_a\epsilon_d+\epsilon_b\epsilon_c+\epsilon_c^2+\epsilon_c\epsilon_d.
\end{aligned} \tag{3.34}$$

Then, using Eq. 3.32 in Eq. 3.31

$$d = \frac{1}{2}E_1^{-1}E_2^{-1}\epsilon_1^{-1}\epsilon_2^{-1}\left(E_1 + E_2 + \epsilon_1 + \epsilon_2\right), \tag{3.35}$$

Now, D has the form:

$$\begin{aligned}
D &= \frac{1}{2}\sum_{a,b,c,d,i,j,k}\frac{\langle pj||ad\rangle\langle ac||ij\rangle\langle ik||bc\rangle\langle bd||qk\rangle}{(E+\epsilon_k-\epsilon_b-\epsilon_d)(E+\epsilon_j-\epsilon_a-\epsilon_d)(\epsilon_i+\epsilon_k-\epsilon_b-\epsilon_c)(\epsilon_i+\epsilon_j-\epsilon_a-\epsilon_c)}\\
&\times \;[(E+\epsilon_k-\epsilon_b-\epsilon_d)+(E+\epsilon_j-\epsilon_a-\epsilon_d)+(\epsilon_i+\epsilon_k-\epsilon_b-\epsilon_c)+(\epsilon_i+\epsilon_j-\epsilon_a-\epsilon_c)]\\
D &= du102a'+du105a'+du106a'+du112a', \qquad (3.36)
\end{aligned}$$

where

$$\begin{aligned}
du102a' &= \frac{1}{2}\sum_{a,b,c,d,i,j,k}\frac{\langle pj||ad\rangle\langle ac||ij\rangle\langle ik||bc\rangle\langle bd||qk\rangle}{(E+\epsilon_k-\epsilon_b-\epsilon_d)(E+\epsilon_j-\epsilon_a-\epsilon_d)(\epsilon_i+\epsilon_k-\epsilon_b-\epsilon_c)}\\
du105a' &= \frac{1}{2}\sum_{a,b,c,d,i,j,k}\frac{\langle pj||ad\rangle\langle ac||ij\rangle\langle ik||bc\rangle\langle bd||qk\rangle}{(E+\epsilon_k-\epsilon_b-\epsilon_d)(\epsilon_i+\epsilon_k-\epsilon_b-\epsilon_c)(\epsilon_i+\epsilon_j-\epsilon_a-\epsilon_c)}\\
du106a' &= \frac{1}{2}\sum_{a,b,c,d,i,j,k}\frac{\langle pj||ad\rangle\langle ac||ij\rangle\langle ik||bc\rangle\langle bd||qk\rangle}{(E+\epsilon_k-\epsilon_b-\epsilon_d)(E+\epsilon_j-\epsilon_a-\epsilon_d)(\epsilon_i+\epsilon_j-\epsilon_a-\epsilon_c)}\\
du112a' &= \frac{1}{2}\sum_{a,b,c,d,i,j,k}\frac{\langle pj||ad\rangle\langle ac||ij\rangle\langle ik||bc\rangle\langle bd||qk\rangle}{(E+\epsilon_j-\epsilon_a-\epsilon_d)(\epsilon_i+\epsilon_k-\epsilon_b-\epsilon_c)(\epsilon_i+\epsilon_j-\epsilon_a-\epsilon_c)}. \qquad (3.37)
\end{aligned}$$

A similar approach can be used for all apparent f_7 diagrams. Note that for the diagonal case ($q = p$) we could exchange a for b and j for k for $du106a'$ resulting in an equivalent expression of $d102a'$ and similarly for $d112a'$. Then, the four diagrams ($du102a', du105a', du106a', du112a'$) are added in two diagrams labeled $du121a$ and $du123a$.

Algebraic reduction of pseudo–triple excitations

Figure 3.8 shows fourth-order EPT diagrams found with DROGON.D4 only and their mirror images. Each of these diagrams have apparent triple excitations that can be decomposed in simpler expressions, following an approach similar to that used previously.[37]

$$te(1)[a] = -0.250\sum_{a,b,c,d,i,j,k}\frac{\langle pc||ij\rangle\langle ak||bd\rangle\langle ij||ac\rangle\langle bd||qk\rangle}{(\epsilon_i+\epsilon_j-E-\epsilon_c)(\epsilon_i+\epsilon_j+\epsilon_k-\epsilon_b-\epsilon_c-\epsilon_d)(\epsilon_i+\epsilon_j-\epsilon_a-\epsilon_c)} \qquad (3.38)$$

$$te(2)[a] = -0.250\sum_{a,b,c,d,i,j,k}\frac{\langle ij||pc\rangle\langle bd||ak\rangle\langle ac||ij\rangle\langle qk||bd\rangle}{(\epsilon_i+\epsilon_j-\epsilon_a-\epsilon_c)(\epsilon_i+\epsilon_j+\epsilon_k-\epsilon_b-\epsilon_c-\epsilon_d)(E+\epsilon_k-\epsilon_b-\epsilon_d)} \qquad (3.39)$$

$$te(3)[a] = -0.250\sum_{a,b,c,d,i,j,k}\frac{\langle pc||ij\rangle\langle ak||bd\rangle\langle ij||ac\rangle\langle bd||qk\rangle}{(E+\epsilon_k-\epsilon_b-\epsilon_d)(\epsilon_i+\epsilon_j+\epsilon_k-\epsilon_b-\epsilon_c-\epsilon_d)(\epsilon_i+\epsilon_j-\epsilon_a-\epsilon_c)} \qquad (3.40)$$

Figure 3.8: Fourth order diagrams with apparent triple excitations

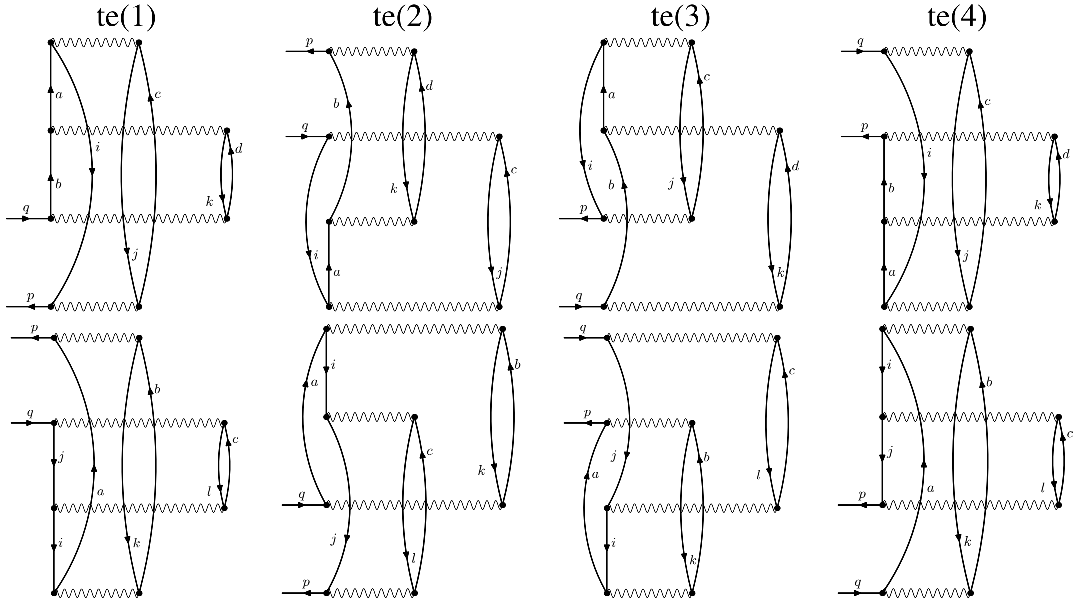

$$te(4)[a] = -0.250 \sum_{a,b,c,d,i,j,k} \frac{\langle ij||pc\rangle\langle bd||ak\rangle\langle ac||ij\rangle\langle qk||bd\rangle}{(\epsilon_i + \epsilon_j - \epsilon_a - \epsilon_c)(\epsilon_i + \epsilon_j + \epsilon_k - \epsilon_b - \epsilon_c - \epsilon_d)(\epsilon_i + \epsilon_j - E - \epsilon_c)} \tag{3.41}$$

$$te(1)[b] = 0.250 \sum_{a,b,c,i,j,k,l} \frac{\langle pk||ab\rangle\langle ab||ik\rangle\langle ic||jl\rangle\langle jl||qc\rangle}{(\epsilon_i + \epsilon_k - \epsilon_a - \epsilon_b)(\epsilon_j + \epsilon_k + \epsilon_l - \epsilon_a - \epsilon_b - \epsilon_c)(E + \epsilon_k - \epsilon_a - \epsilon_b)} \tag{3.42}$$

$$te(2)[b] = 0.250 \sum_{a,b,c,i,j,k,l} \frac{\langle ab||pk\rangle\langle ik||ab\rangle\langle jl||ic\rangle\langle qc||jl\rangle}{(\epsilon_j + \epsilon_l - E - \epsilon_c)(\epsilon_j + \epsilon_k + \epsilon_l - \epsilon_a - \epsilon_b - \epsilon_c)(\epsilon_i + \epsilon_k - \epsilon_a - \epsilon_b)} \tag{3.43}$$

$$te(3)[b] = 0.250 \sum_{a,b,c,i,j,k,l} \frac{\langle pk||ab\rangle\langle ab||ik\rangle\langle ic||jl\rangle\langle jl||qc\rangle}{(\epsilon_i + \epsilon_k - \epsilon_a - \epsilon_b)(\epsilon_j + \epsilon_k + \epsilon_l - \epsilon_a - \epsilon_b - \epsilon_c)(\epsilon_j + \epsilon_l - E - \epsilon_c)} \tag{3.44}$$

$$te(4)[b] = 0.250 \sum_{a,b,c,i,j,k,l} \frac{\langle ab||pk\rangle\langle ik||ab\rangle\langle jl||ic\rangle\langle qc||jl\rangle}{(E + \epsilon_k - \epsilon_a - \epsilon_b)(\epsilon_j + \epsilon_k + \epsilon_l - \epsilon_a - \epsilon_b - \epsilon_c)(\epsilon_i + \epsilon_k - \epsilon_a - \epsilon_b)} \tag{3.45}$$

Equations 3.38, 3.39, 3.40 and 3.41 can be added together, using the following rules $\langle pq||rs\rangle = \langle pq|rs\rangle - \langle pq|sr\rangle = -\langle pq||sr\rangle$

$$\begin{aligned}
D &= te(1)[a] + te(2)[a] + te(3)[a] + te(4)[a] \\
D &= -0.250 \sum_{a,b,c,d,i,j,k} \frac{\langle pc||ij\rangle\langle ak||bd\rangle\langle ij||ac\rangle\langle bd||qk\rangle}{\epsilon_i + \epsilon_j + \epsilon_k - \epsilon_b - \epsilon_c - \epsilon_d} \\
&\times \left[\frac{1}{(\epsilon_i + \epsilon_j - E - \epsilon_c)(\epsilon_i + \epsilon_j - \epsilon_a - \epsilon_c)} + \frac{1}{(\epsilon_i + \epsilon_j - \epsilon_a - \epsilon_c)(E + \epsilon_k - \epsilon_b - \epsilon_d)}\right. \\
&+ \left.\frac{1}{(E + \epsilon_k - \epsilon_b - \epsilon_d)(\epsilon_i + \epsilon_j - \epsilon_a - \epsilon_c)} + \frac{1}{(\epsilon_i + \epsilon_j - \epsilon_a - \epsilon_c)(\epsilon_i + \epsilon_j - E - \epsilon_c)}\right].
\end{aligned} \tag{3.46}$$

This, can be written in a simpler way

$$D = -0.250 \sum_{a,b,c,d,i,j,k} \langle pc||ij\rangle\langle ak||bd\rangle\langle ij||ac\rangle\langle bd||qk\rangle d, \tag{3.47}$$

where

$$\begin{aligned} d &= \epsilon_{12}^{-1}\epsilon_1^{-1}(2E_1^{-1}+2E_2^{-1}), \\ \epsilon_{12} &= \epsilon_i+\epsilon_j+\epsilon_k-\epsilon_b-\epsilon_c-\epsilon_d, \\ E_1 &= E+\epsilon_k-\epsilon_b-\epsilon_d, \\ E_2 &= \epsilon_i+\epsilon_j-E-\epsilon_c, \\ \epsilon_1 &= \epsilon_i+\epsilon_j-\epsilon_a-\epsilon_c. \end{aligned} \tag{3.48}$$

Now, d can be rearranged

$$d = 2\epsilon_{12}^{-1}\epsilon_1^{-1}E_1^{-1}E_2^{-1}(E_1+E_2), \tag{3.49}$$

where

$$E_1 + E_2 = \epsilon_{12} \tag{3.50}$$

Then, using Eq. 3.50 in Eq. 3.49

$$d = 2\epsilon_1^{-1}E_1^{-1}E_2^{-1}. \tag{3.51}$$

Now, D has the form:

$$\begin{aligned} D &= -\frac{1}{2}\sum_{a,b,c,d,i,j,k} \frac{\langle pc||ij\rangle\langle ak||bd\rangle\langle ij||ac\rangle\langle bd||qk\rangle}{(E+\epsilon_k-\epsilon_b-\epsilon_d)(\epsilon_i+\epsilon_j-E-\epsilon_c)(\epsilon_i+\epsilon_j-\epsilon_a-\epsilon_c)} \\ D &= te'[a]. \end{aligned} \tag{3.52}$$

The same can be done for the mirror image diagrams.

Total D4 Brandow's diagrams

Finally, fourth–order diagonal electron propagator is composed of 72 constant diagrams, 120 type–U diagrams, 48 type–V diagrams, 60 type–W diagrams and the following expressions, obtained only with DROGON.D4:

$$d47a21 = -0.25 \sum_{a,b,c,d,i,j,k} \frac{\langle pj||cb\rangle\langle ij||bc\rangle\langle ik||ad\rangle\langle da||pk\rangle}{(E+\epsilon_j-\epsilon_b-\epsilon_c)(E+\epsilon_k-\epsilon_a-\epsilon_d)(\epsilon_i+\epsilon_j-\epsilon_b-\epsilon_c)} \tag{3.53}$$

$$d47a22 = -0.25 \sum_{a,b,c,d,i,j,k} \frac{\langle pj||cb\rangle\langle ij||bc\rangle\langle ik||ad\rangle\langle da||pk\rangle}{(E+\epsilon_j-\epsilon_b-\epsilon_c)(\epsilon_i+\epsilon_j-\epsilon_b-\epsilon_c)(\epsilon_i+\epsilon_k-\epsilon_a-\epsilon_d)} \tag{3.54}$$

$$d47b21 = 0.25 \sum_{a,b,c,i,j,k,l} \frac{\langle pc||jl\rangle\langle ik||ab\rangle\langle jl||ac\rangle\langle ik||pb\rangle}{(E+\epsilon_b-\epsilon_i-\epsilon_k)(E+\epsilon_c-\epsilon_j-\epsilon_l)(\epsilon_i+\epsilon_k-\epsilon_a-\epsilon_b)} \tag{3.55}$$

$$d47b22 = -0.25 \sum_{a,b,c,i,j,k,l} \frac{\langle pc||jl\rangle\langle ik||ab\rangle\langle jl||ac\rangle\langle ik||pb\rangle}{(E+\epsilon_b-\epsilon_i-\epsilon_k)(\epsilon_j+\epsilon_l-\epsilon_a-\epsilon_c)(\epsilon_i+\epsilon_k-\epsilon_a-\epsilon_b)} \tag{3.56}$$

$$d46a21 = 0.5 \sum_{a,b,c,d,i,j,k} \frac{\langle pb||ij\rangle\langle ka||dc\rangle\langle ij||ab\rangle\langle dc||pk\rangle}{(E+\epsilon_k-\epsilon_c-\epsilon_d)(\epsilon_i+\epsilon_j-\epsilon_a-\epsilon_b)(\epsilon_i+\epsilon_j-E-\epsilon_b)} \tag{3.57}$$

$$d46b21 = -0.5 \sum_{a,b,c,i,j,k,l} \frac{\langle pj||ba\rangle\langle kl||ic\rangle\langle ij||ab\rangle\langle kl||pc\rangle}{(E+\epsilon_j-\epsilon_a-\epsilon_b)(\epsilon_i+\epsilon_j-\epsilon_a-\epsilon_b)(\epsilon_k+\epsilon_l-E-\epsilon_c)}. \tag{3.58}$$

3.5 Implementation of D4

All 306–D4 diagrams have been implemented in a modified version of Gaussian Development Version (GDV).[63] The following implementation procedure was followed:

1. A diagram or set of diagrams was programmed for an unrestricted Hartree–Fock determinant in a PYTHON using NUMPY libraries for the water molecule with the 6-31G(d) basis–set.
2. A diagram or set of diagrams was programmed for an unrestricted Hartree–Fock determinant in a GDV. Then, results were compared.
3. When all the diagrams were programmed, their derivatives with respect to E where programed analytically and numerically and compared. Now, there is a benchmark for each diagram and its derivative.
4. Some diagrams are equivalent when using the diagonal approximation. Numerical comparisons of both the diagram and its derivative helped identify these diagrams.
5. Linear algebra was used to diminish the N^7 scaling in the most demanding diagrams (ov^6, o^2v^5 and o^3v^4).
6. A comparison was performed with H_2O–H to test for errors when having a different number of electrons in the system.

The implementation was successful and the identical D4-diagrams are identified in Table 3.2.

Constant:	Type–U:	Type–V:	Type–W:
dc028=dc001	du104a=du103a	dv104a=dv103a	dw104a=dw103a
dc029=dc002	du104b=du103b	dv104b=dv103b	dw104b=dw103b
dc031=dc009	du106a=du105a	dv106a=dv105a	dw108a=dw107a
dc032=dc003	du106b=du105b	dv106b=dv105b	dw108b=dw107b
dc033=dc011	du108a=du107a	dv108a=dv107a	dw202a=dw201a
dc034=dc012	du108b=du107b	dv108b=dv107b	dw202b=dw201b
dc035=dc005	du110a=du109a	dv110a=dv109a	dw206a=dw203a
dc036=dc006	du110b=du109b	dv110b=dv109b	dw206b=dw203b
dc037=dc014	du204a=du203a	dv204a=dv203a	dw205a=dw204a
dc038=dc015	du204b=du203b	dv204b=dv203b	dw205b=dw204b
dc039=dc016	du206a=du205a	dv206a=dv205a	dw210a=dw207a
dc040=dc017	du206b=du205b	dv206b=dv205b	dw210b=dw207b
dc041=dc008	du208a=du207a	dv208a=dv207a	dw209a=dw208a
dc042=dc018	du208b=du207b	dv208b=dv207b	dw209b=dw208b
dc043=dc019	du210a=du209a	dv210a=dv209a	dw212a=dw211a
dc044=dc021	du210b=du209b	dv210b=dv209b	dw212b=dw211b
dc045=dc022	du401a=du301a		dw304a=dw303a
dc046=dc024	du401b=du301b		dw304b=dw303b
dc047=dc030	du402a=du302a		dw306a=dw305a
dc054=dc050	du402b=du302b		dw306b=dw305b
dc056=dc004	du404a=du303a		dw308a=dw307a
dc057=dc013	du404b=du303b		dw308b=dw307b
dc058=dc023	du403a=du304a		dw310a=dw309a
dc059=dc025	du403b=du304b		dw310b=dw309b
dc061=dc007	du406a=du305a		
dc062=dc010	du406b=du305b		
dc063=dc020	du405a=du306a		
dc064=dc026	du405b=du306b		
dc065=dc027	du408a=du307a		
dc066=dc048	du408b=du307b		
dc067=dc051	du407a=du308a		
dc068=dc052	du407b=du308b		
dc069=dc060	du410a=du309a		
dc070=dc049	du410b=du309b		
dc071=dc053	du409a=du310a		
dc072=dc055	du409b=du310b		
	du411a=du311a		
	du411b=du311b		
	du412a=du312a		
	du412b=du312b		
	du504a=du503a		
	du504b=du503b		
	du506a=du505a		
	du506b=du505b		
	du508a=du507a		
	du508b=du507b		
	du510a=du509a		
	du510b=du509b		

Table 3.2: Equivalent D4–diagrams for the diagonal case.

Chapter 4

Composite Electron Propagator Method for Calculating Ionization Energies and Electron Affinities

In this section we will summarize the most important findings and results for references 21,34, regarding the composite electron propagator method.

4.1 Composite Electron Propagator Method

High accuracy results for Hartree–Fock and correlation energies can be inferred with complete basis set limit (CBS) schemes.[18,19] In addition, previous works have shown that CBS extrapolations can be used with electron propagator methods.[20,21].

In order to predict Hartree–Fock energies at the CBS limit an exponential extrapolation is recommended,[18]

$$\mathrm{E}(X) = \mathrm{E}_{CBS} + Ae^{-BX}, \tag{4.1}$$

where X is the maximum angular momentum for a basis set, $\mathrm{E}(X)$ is the predicted energy with cc-pVXZ, E_{CBS} is the predicted energy for a complete basis set and A and B are fitting parameters. Therefore, at least three points are needed to extrapolate to CBS.

In order to predict correlation energies at the CBS limit, an inverse cubic function is recommended,[19]

$$\mathrm{E}(X) = \mathrm{E}_{CBS} + \frac{A}{X^3}, \tag{4.2}$$

where A is the only fitting parameter and the extrapolation is performed with two points. For example, aug-cc-pV(DT)Z will be the CBS limit when using the aug-cc-pVDZ and aug-cc-pVTZ results. Then, we define CBS1 and CBS2 as cc-pV(DT)Z and cc-pV(TQ)Z, respectively, while CBS3 is the exponential extrapolation using $X = 2, 3, 4$.

Previously, the validity of CBS extrapolations was tested with respect to EP/cc-pV5Z results.[21] Both extrapolations predicted results with mean unsigned errors (MUEs) ≤ 0.07 eV. The exponential extrapolation yields more accurate results than the inverse cubic ones with MUEs of 0.01 eV while CBS1 is the least accurate with MUEs of 0.03–0.07 eV. In general, for prediction and assignment of PES peaks, all three extrapolations are satisfactory and using augmented correlation consistent basis–sets shows no advantage for the prediction of IEs.

In addition to CBS effects, the composite approach assumes the separation of basis–set and correlation effects. For example, in the CEP method we first obtain poles with a relatively small basis,

$$E_i^M = \epsilon_i + \Sigma_{ii}^M(E_i^M), \tag{4.3}$$

where the M superscript designates the self–energy approximation. Then, diagonal second order electron propagator results, D2, are obtained with a larger basis set such that

$$\tilde{E}_i^{D2} = \tilde{\epsilon}_i + \tilde{\Sigma}_{ii}^{D2}(\tilde{E}_i^{D2}). \tag{4.4}$$

Finally, the CEP result for method M is:

$$E_i^{CM} = E_i^M + \tilde{E}_i^{D2} - E_i^{D2}. \tag{4.5}$$

A CEP approximation will consist of three selections: M which is the high order correlation method, X_M and X_{D2} are the basis–set at which M and D2 are calculated, respectively. The best options for X$_{D2}$ are CBS1 and CBS2 methods, where X_M is cc-pVDZ or cc-PVTZ for CBS1 or CBS2, respectively. See Table 4.1 for definitions of composite methods. Diagonal electron propagator methods include partial third order (P3), renormalized partial third order (P3+) and the Outer Valence Green's Function (OVGF).[5] Non–diagonal Renormalized second order (NR2) is one of the most efficient and accurate EP methods.[20]

Table 4.1: Composite methods

CEP	M	X_M	X_{D2}
CP3/23	P3	cc-pVDZ	CBS1
CP3+/23	P3+	cc-pVDZ	CBS1
CN/23	OVGF-N	cc-pVDZ	CBS1
CNR2/23	NR2	cc-pVDZ	CBS1
CP3/a23	P3	aug-cc-pVDZ	CBS1
CP3+/a23	P3+	aug-cc-pVDZ	CBS1
CN/a23	OVGF-N	aug-cc-pVDZ	CBS1
CNR2/a23	NR2	aug-cc-pVDZ	CBS1
CP3/34	P3	cc-pVTZ	CBS2
CP3+/34	P3+	cc-pVTZ	CBS2
CN/34	OVGF-N	cc-pVTZ	CBS2
CNR2/34	NR2	cc-pVTZ	CBS2

4.2 Application of Composite Electron Propagator Methods to Ionization Energies

In order to test the CEP methods, a test set was defined.[21] This test set consists of 52 closed shell molecules and atoms with different properties, both organic and inorganic. Standards were calculated with ΔCCSD(T)/CBS,

$$E = E_{\mathrm{HF}}/cc-pVQZ + E^{corr}_{\mathrm{MP2}}/cc-pV(TQ)Z + \delta^{\mathrm{CCSD(T)}}_{\mathrm{MP2}}/cc-pVTZ, \tag{4.6}$$

where E_{HF}/cc-pVQZ is the total energy at the Hartree-Fock/cc-pVQZ level, $E^{\mathrm{corr}}_{\mathrm{MP2}}$/cc-pV(TQ)Z is the correlation energy at the MP2/cc-pV(TQ)Z level and $\delta^{\mathrm{CCSD(T)}}_{\mathrm{MP2}}$/cc-pVTZ is the difference between CCSD(T)/cc-pVTZ[64] and MP2/cc-pVTZ correlation energies. Adiabatic corrections are obtained at the B3LYP/6-31G(2df,p) level including zero-point energies (ZPEs) for both the neutral and the cation.

Comparisons between the diagonal CEP methods and the CCSD(T) standards can be seen in Figure 4.1 for both vertical and adiabatic ionization energies. A vertical ionization energy is the difference between the minimum neutral energy and the cation energy at the neutral geometry. An adiabatic ionization energy consists of differences between the neutral and cation energy, including zero-point energy corrections, at their corresponding minimums. Mean unsigned errors (MUEs) and standard deviations (σ) of 0.1–0.2 eV are obtained for vertical ionization energies (VIEs). Improvements by using augmented basis sets are seen for composite methods based on P3 and P3+ but are not seen when based on

Table 4.2: Electron Propagator Methods

Acronym	Method	Arithmetic scaling$^{a)}$
KT	Koopmans's theorem	
D2	Diagonal Second Order	OV^2
D3	Diagonal Third Order	OV^4
OVGF-A	Outer Valence Green's Function-A	OV^4
OVGF-B	Outer Valence Green's Function-B	OV^4
OVGF-C	Outer Valence Green's Function-C	OV^4
OVGF-N	Outer Valence Green's Function-von Niessen	OV^4
P3	Partial Third Order	O^2V^3
P3+	Renormalized Partial Third Order	O^2V^3

$^{a)}O$ = number of occupied orbitals, V = number of virtual orbitals.

OVGF. The CN/34 model offers higher accuracy with a MUE of 0.08 eV but has larger arithmetic and storage requirements, see Table 4.2 for EPT requirements. For adiabatic ionization energies (AIEs), the error indices are slightly larger, but trends are similar to VIEs.

The histograms in Figure 4.2 display mean signed errors (μ), MUE and σ data for each Composite Electron Propagator method (CEP). It can be observed that as the basis set increases the absolute value of μ decreases for CP3 and CP3+ models. Use of aug–cc–pVDZ with CN yields larger errors than regular cc–pVDZ. The best statistics for these standards are CN/34 with MUE of 0.08 eV and σ of 0.10 eV in comparison with P3+/34 with MUE of 0.14 eV and σ of 0.17 eV.

4.3 Application of Composite Electron Propagator Methods to Electron Affinities of Carboranes

Shallow, uniform electrostatic potentials, large electron detachment energies and nodal structures in Dyson orbitals are properties of conjugate anions of superacidic protonated carboranes.[34]

This section presents *ab initio* composite electron propagator theory calculations (CEP) for vertical electron detachment energies (VEDEs) and Dyson orbitals of $CHB_{11}X_{11}^{-}$ (X = H, F, Cl) carboranes with final states, $^2E_2 < {}^2E_1$. Comparisons, between CEP methods (renormalized partial third order (CP3+) and non-diagonal, renormalized, second-order (CNR2)) and anion photoelectron spectra are in good agreement.[65]

Figure 4.1: Composite EP methods vs CCSD(T)$^{a,b)}$ (eV)

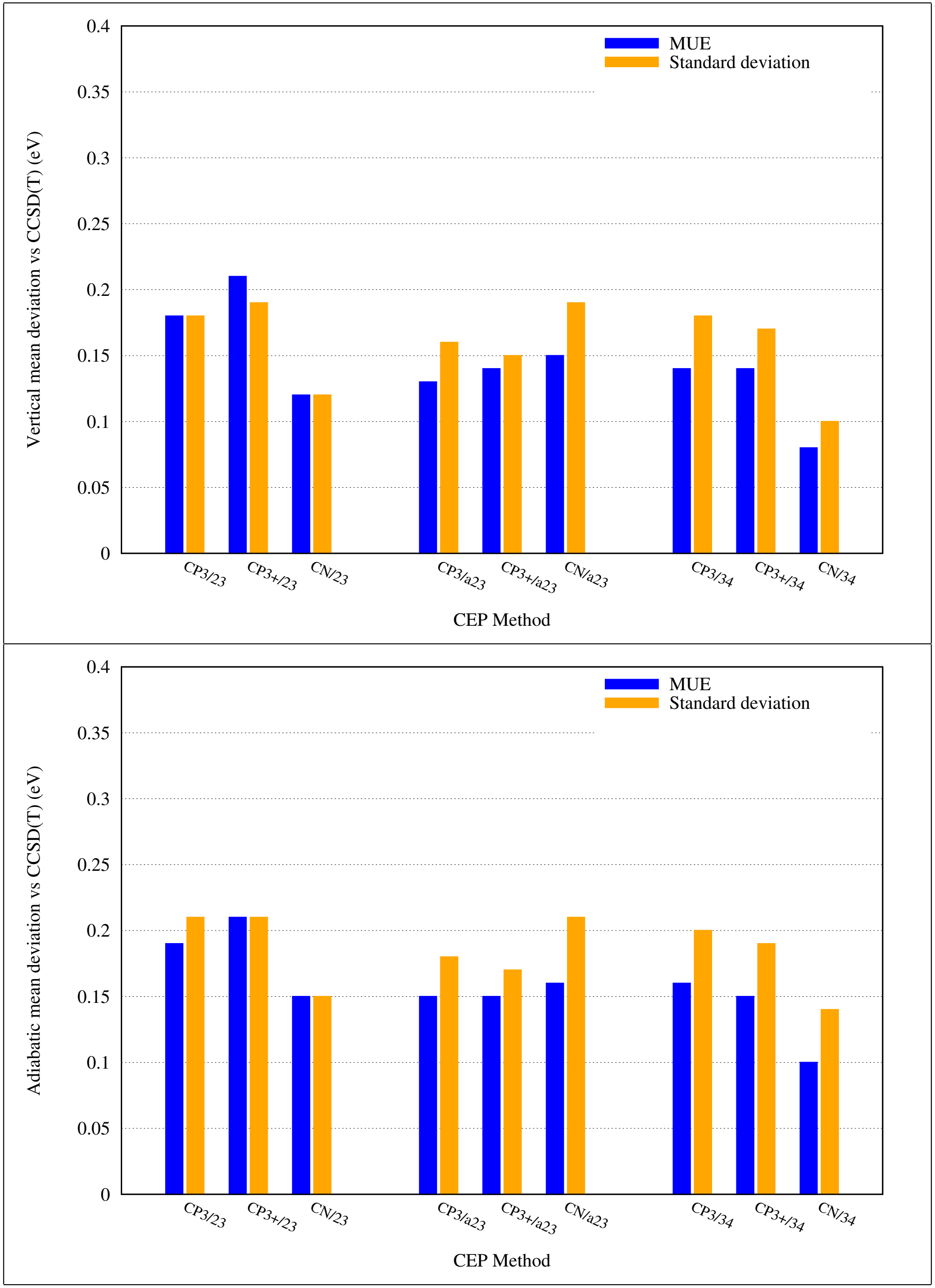

[a] Geometries were obtained with B3LYP/6-31G(2df,p).

[b] Values compared vs. ΔCCSD(T).

Figure 4.2: Vertical IE Error Distribution (eV, vs CCSD(T)): CEP Methods.[a)]

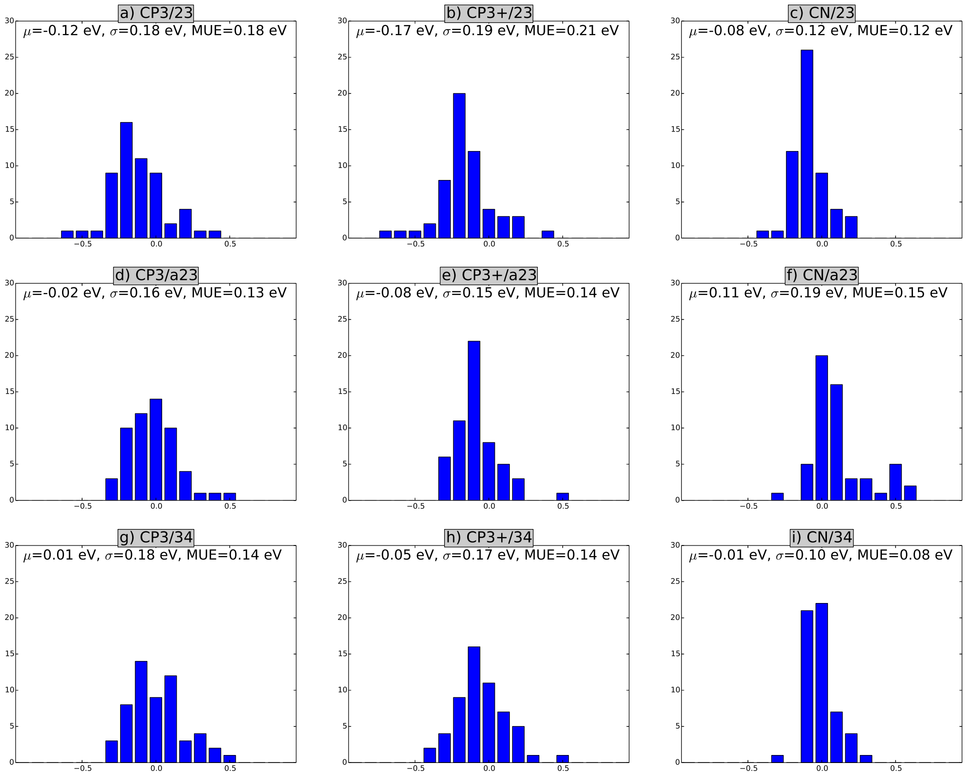

[a)] Geometries were obtained with B3LYP/6-31G(2df,p).

Table 4.3: Carborane VEDEs (eV) with composite EP methods

Anion	Final State	Basis set	CP3+	CNR2
$CHB_{11}H_{11}^-$	X $^2E_2$	a34	6.20	6.19
	A $^2E_1$	a34	6.38	6.33
	B $^2E_2$	a34	6.75	6.70
	C $^2A_1$	a34	6.89	6.83
	D $^2E_1$	a34	7.51	7.48
$CHB_{11}F_{11}^-$	X $^2E_2$	a23	6.95	6.85
	A $^2E_1$	a23	7.49	7.39
	B $^2A_1$	a23	9.88	9.76
	C $^2E_2$	a23	10.01	9.91
	D $^2E_1$	a23	10.71	10.59
$CHB_{11}Cl_{11}^-$	X $^2E_2$	a23	7.10	7.04
	A $^2E_1$	a23	7.39	7.33
	B $^2A_2$	a23	8.21	
	C $^2E_1$	a23	8.25	
	D $^2A_1$	a23	8.51	

Calculations yield a close correlation between the second VEDE of the anionic base (electron affinities of the neutral clusters) and acidity of the conjugated acid. In addition, the doublet neutral radicals are superhalogens due to their high electron affinities (>6 eV). Calculations were obtained using Gaussian 16 software.[29]

Table 4.3 contains VEDEs for the carborane anions calculated with the composite methods CP3+ and CNR2. For the $CHB_{11}H_{11}^-$ cluster, CP3+/a34 and CNR2/a34 results are available. For the $CHB_{11}F_{11}^-$ and $CHB_{11}Cl_{11}^-$ clusters, only CP3+/a23 and CNR2/a23 results are available. This is because the latter two clusters have more correlated electrons and basis functions than the first cluster.

The VEDE of $CHB_{11}Cl_{11}^-$ have been measured experimentally using photoelectron spectroscopy.[65] A VEDE of 7.0–7.1 eV was measured and is in good agreement with both CEP methods, 7.10 and 7.04 for CP3+ and CNR2, respectively.

Front and backs of Dyson orbitals for $CHB_{11}H_{11}^-$ are reported in Figure 4.3. The first electronic state is $^2E_2$ and it can be seen that all boron atoms that are neighbors to the boron atom in the back have nodal surfaces. The electronic density is localized in the boron atoms and there is no delocalization to the hydrogen atoms. The second electronic state is $^2E_1$ and there are some boron atoms in the back that have positive or negative contributions in them. Therefore, when protonating this cluster we can predict the addition to these boron atoms.

State	Dyson orbital		cP3+	cNR2
	Front	Back		
X $^2E_2$	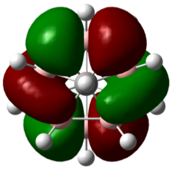	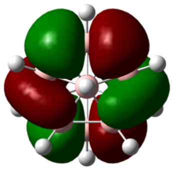	6.20	6.19
A $^2E_1$	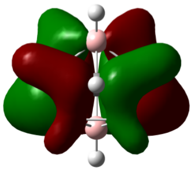	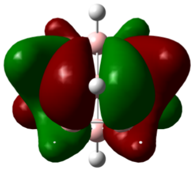	6.38	6.33
B $^2E_2$	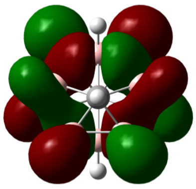	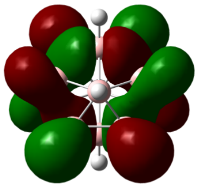	6.75	6.70
C $^2A_1$	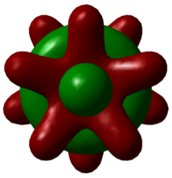	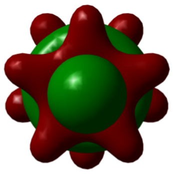	6.89	6.83
D $^2E_1$	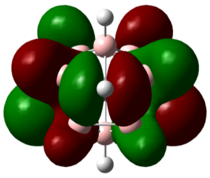	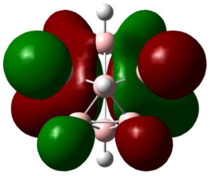	7.51	7.48

Figure 4.3: Dyson orbitals (isovalue = 0.02) and VEDEs (eV) for $CHB_{11}H_{11}^-$

Front and backs of Dyson orbitals for $CHB_{11}F_{11}^-$ are reported in Figure 4.4. The first two electronic states are $^2E_2$ and $^2E_1$, respectively. Boron atoms in the back of the cluster have nodal surfaces in the first electronic state. However, there are boron atoms that contain positive or negative amplitudes for the second electronic state. The electronic density is localized in the boron atoms and there is antibonding delocalization to the fluorine atoms in both electronic states. Protonation of this cluster will be close to a fluorine atom in the back of the cluster.

Similar to $CHB_{11}F_{11}^-$, front and backs of Dyson orbitals for $CHB_{11}Cl_{11}^-$ are reported in Figure 4.5. The first two electronic states are $^2E_2$ and $^2E_1$, respectively. Boron atoms in the back of the cluster have nodal surfaces in the first electronic state. However, there are boron atoms that contain positive or negative amplitudes for the second electronic state. The electronic density is localized in the boron atoms and there is antibonding delocalization to the chlorine atoms in both electronic states. Protonation of this cluster will be close to a chlorine atom in the back of the cluster.

The order of the electronic states varies between clusters: $^2E_2 <^2E_1 <^2E_2 <^2A_1 <^2E_1$ for $CHB_{11}H_{11}$, $^2E_2 <^2E_1 <^2A_1 <^2E_2 <^2E_1$ for $CHB_{11}F_{11}$ and $^2E_2 <^2E_1 <^2A_2 \approx^2E_1 <^2A_1$ for $CHB_{11}Cl_{11}$. However, all clusters have the $^2E_2 <^2E_1$ first two states and this work predicts the second state to be involved in the acidity of these clusters.

Figure 4.6 shows contours and electrostatic potential for all clusters. The more negative values are in red and they are in the back of the cluster. Distribution of the negative charge over these large volumes in combination with large VEDEs contribute to the strong acidity of their conjugated acids.

Optimized structures for the conjugate acids of the three anions can be seen in Figure 4.6 where the extra proton is in red color. The proton settles in the back of the clusters due to the antipodal effect.[66] For $CHB_{11}H_{11}$–H, the acidic proton is close to three boron atoms, ignoring the neighboring hydrogens. For both $CHB_{11}F_{11}$–H and $CHB_{11}Cl_{11}$–H, the acidic proton is coordinated to two halogen atoms, closer to one of them. These modes of bonding are in accord with both the most negative values of the electrostatic potentials and the non-nodal surfaces for the $^2E_1$ electronic state. Calculated protonation energies at the B3LYP/6-311++G(2df,p) level are 11.30, 9.69 and 10.34 eV for $CHB_{11}H_{11}^-$, $CHB_{11}F_{11}^-$ and $CHB_{11}Cl_{11}^-$, respectively. When compared with protonation energies of anionic carboxylates (14–15 eV) these values are too low and closer to protonation energies of neutral amines (9–10 eV).[67]

State	Dyson orbital Front	 Back	cP3+	cNR2
X $^2E_2$	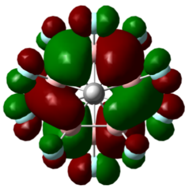	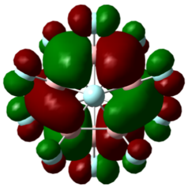	6.95	6.85
A $^2E_1$	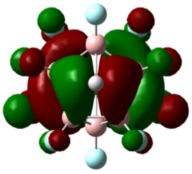	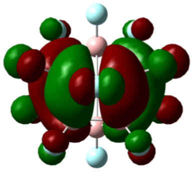	7.49	7.39
B $^2A_1$	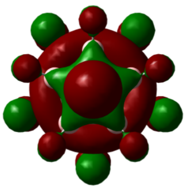	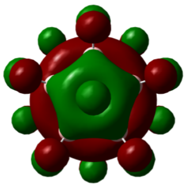	9.88	9.76
C $^2E_2$	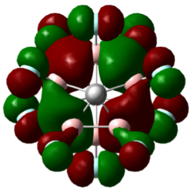	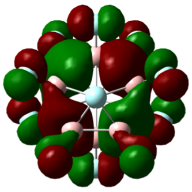	10.01	9.91
D $^2E_1$	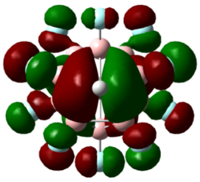	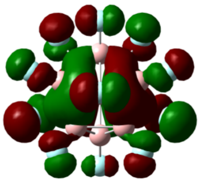	10.71	10.59

Figure 4.4: Dyson orbitals (isovalue = 0.02) and VEDEs (eV) for $CHB_{11}F_{11}^-$

State	Dyson orbital		cP3+	cNR2
	Front	Back		
X $^2E_2$	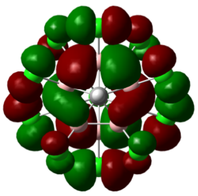	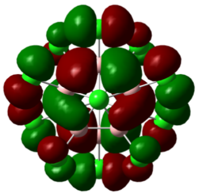	7.10	7.04
A $^2E_1$	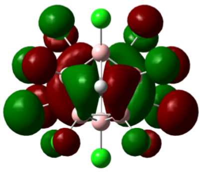	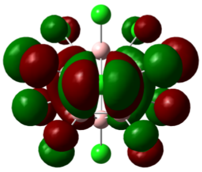	7.39	7.33
B $^2A_2$	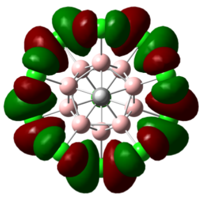	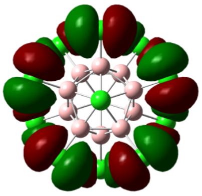	8.21	
C $^2E_1$	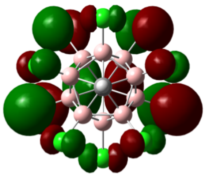	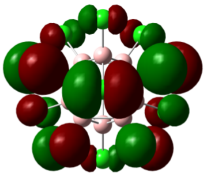	8.25	
D $^2A_1$	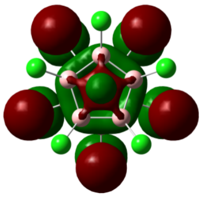	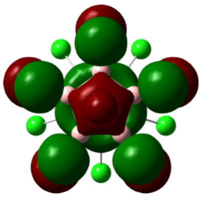	8.51	

Figure 4.5: Dyson orbitals (isovalue = 0.02) and VEDEs (eV) for $CHB_{11}Cl_{11}^-$

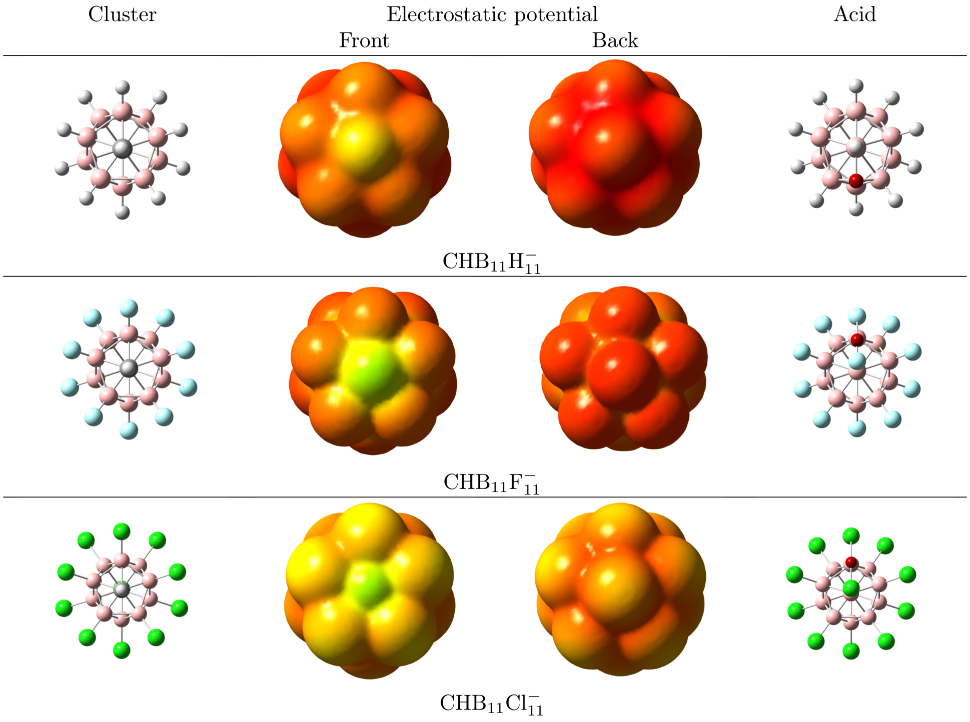

Figure 4.6: Electrostatic potential (isovalue = 0.0004 and a range of -0.147 to 0.147)

4.4 Conclusions

In this chapter the Composite Electron Propagator Methods have been defined and applied to the prediction of vertical and adiabatic ionization energies of neutral and closed–shell molecules. In addition, CEP methods have been applied to calculate the electron affinities of open–shell neutral doublets by calculating the vertical detachment energies of their corresponding closed–shell anions.

CN and CP3+ methods are recommended for neutral molecules with MUEs of 0.08 and 0.14 eV for CN/34 and CP3+/34, respectively. Similar results are obtained for adiabatic ionization energies.

CP3+ and CNR2 are excellent methods for the prediction of anionic VEDEs. Results from both of these methods are in excellent agreement with experimental photoelectron spectroscopy data. For anionic carboranes, the use of Dyson orbitals, VEDEs and protonation energies gives insight into the chemical bonding of their conjugated superacids.

Chapter 5

Electron–Propagator Methods for Vertical Electron–Detachment Energies of Anions: Benchmarks and Case Studies

In this chapter we will summarize the most important results obtained for reference 28, regarding benchmarks and case studies of EPT for VEDEs of anions.

A set of small, closed–shell, molecular anions of the first three periods is used as a benchmark for the accuracy of EP methods in the prediction of VEDEs of anions. First, a statistical analysis of this benchmark is produced and discussed. Then, case studies of the cyclopentadienyl anion, two pentagonal isomers $P_2N_3^-$ and N_2PNP^- and the $Al(BO_2)_4^-$ superhalide VEDEs were predicted with EP methods and compared to ΔCCSD(T) standards.

5.1 Small anions

First, the EP diagonal methods used in this chapter are: Koopmans theorem (KT), diagonal second order (D2), diagonal third order (D3), Outer Valence Green's Function version A (A), version B (B), version C (C), partial third order (P3) and renormalized partial third order (P3+). The EP non–diagonal methods used in this chapter are: two–particle–one–hole Tamm–Dancoff approximation (TDA), non-diagonal renormalized second order (NR2), third–order algebraic, diagrammatic construction (ADC(3)) and the renormalized third–order method (3+).[3,5]

Benchmark standards were generated using ΔCCSD(T)/CBS in a test–set consisting of 36 anions, see Table 5.1, and 55 VEDEs. Figures 5.1 and 5.2 show the error distributions of diagonal and non-diagonal EP methods, respectively. Each histogram show μ, MUE and σ.

Table 5.1: Point groups, bond lengths (Å) and angles (^{o}) of test anions

XY$^-$	PG	r_{XY}	XH$_x^-$	PG	r_{XH}	θ_{HXH}	HXY$^-$	PG	r_{HX}	θ_{HXY}	r_{XY}
BO$^-$	$C_{\infty v}$	1.24	F$^-$				HBN$^-$	$C_{\infty v}$	1.19	180.0	1.28
BS$^-$	$C_{\infty v}$	1.69	Cl$^-$				HBF$^-$	C_s	1.27	104.4	1.39
AlO$^-$	$C_{\infty v}$	1.65	OH$^-$	$C_{\infty v}$	0.96		HAlP$^-$	$C_{\infty v}$	1.61	180.0	2.12
AlS$^-$	$C_{\infty v}$	2.11	SH$^-$	$C_{\infty v}$	1.34		HAlCl$^-$	C_s	1.68	95.4	2.30
CN$^-$	$C_{\infty v}$	1.18	NH$_2^-$	C_{2v}	1.03	101.2	HCC$^-$	$C_{\infty v}$	1.07	180.0	1.25
CP$^-$	$C_{\infty v}$	1.61	PH$_2^-$	C_{2v}	1.43	91.7	HCO$^-$	C_s	1.22	109.7	1.24
SiN$^-$	$C_{\infty v}$	1.74	CH$_3^-$	C_{3v}	1.10	108.0	HSiSi$^-$	C_s	1.51	154.0	2.13
SiP$^-$	$C_{\infty v}$	2.13	SiH$_3^-$	C_{3v}	1.54	95.1	HSiS$^-$	C_s	1.56	102.9	2.06
OF$^-$	$C_{\infty v}$	1.52	BH$_4^-$	T_d	1.24		HNB$^-$	$C_{\infty v}$	1.00	180.0	1.29
OCl$^-$	$C_{\infty v}$	1.71	AlH$_4^-$	T_d	1.64		HNF$^-$	C_s	1.03	95.3	1.55
SF$^-$	$C_{\infty v}$	1.74					HPAl$^-$	C_s	1.45	72.5	2.24
SCl$^-$	$C_{\infty v}$	2.13					HPCl$^-$	C_s	1.43	92.9	2.21
							HOO$^-$	C_s	0.96	97.3	1.53
							HSS$^-$	C_s	1.35	101.3	2.12

Higher VEDEs and a shift to the right are observed in the histograms when the basis set is increased, similar to results obtained in Chapter 4. Error cancelation can provide small errors from calculations with aug–cc–pVDZ or aug-cc-pVTZ. The best results are obtained with OVGF-A and P3+, MUEs are 0.14 and 0.13 eV, respectively. The OVGF-N's selection procedure,[3,48] created for the accurate prediction of ionization energies of neutral molecules, usually recommends the OVGF-B function instead of OVGF-A. In addition, P3+/CBS results are in good agreement with CCSD(T) and they mostly overestimate VEDEs.

For non–diagonal methods, NR2 obtains the best results with MUE of 0.11 eV. Results obtained with other methods have either two maxima or cases with large errors, larger than 0.8 eV. The σ for NR2 is notably smaller and the histogram is more smooth and gaussian–like. Results for NR2/CBS have slightly better statistics than those of P3+/CBS.

5.2 Cyclopentadienyl anion

The cyclopentadienyl anion ($C_5H_5^-$) is a ligand with the capacity of binding with one, three or five atoms to atomic metal cations.[68] The first VEDE for $C_5H_5^-$ has been measured experimentally, 1.808 eV.[69] ΔCCSD(T)/CBS overestimates the VEDE value to 2.04 eV by little less than 0.2 eV, see Table 5.2. This is typical for VEDE predictions, when a high correlation method with a saturated basis set overestimates the experimental result by 0.1–0.2 eV. OVGF-A is in good agreement with experiment with a VEDE of

Figure 5.1: Error distributions (eV) for small anions: diagonal methods

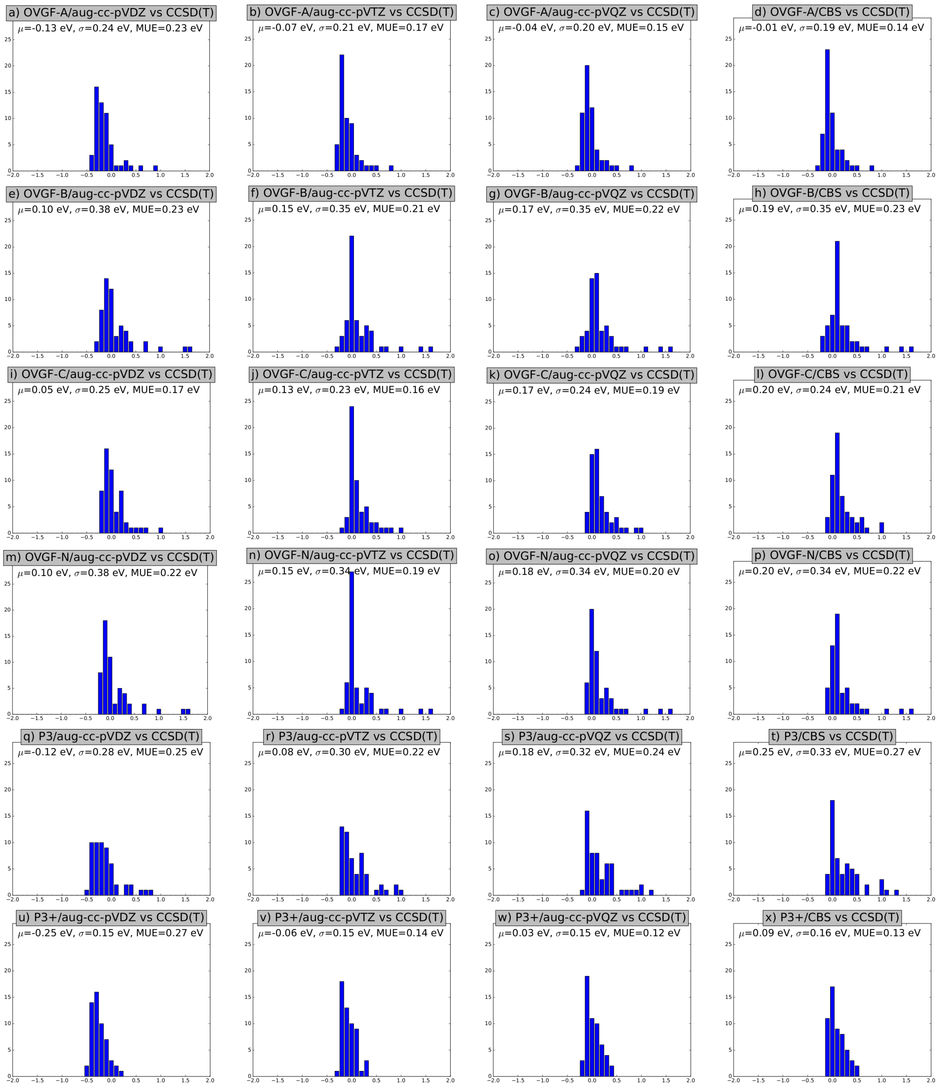

Figure 5.2: Error distributions (eV) for small anions: non–diagonal methods

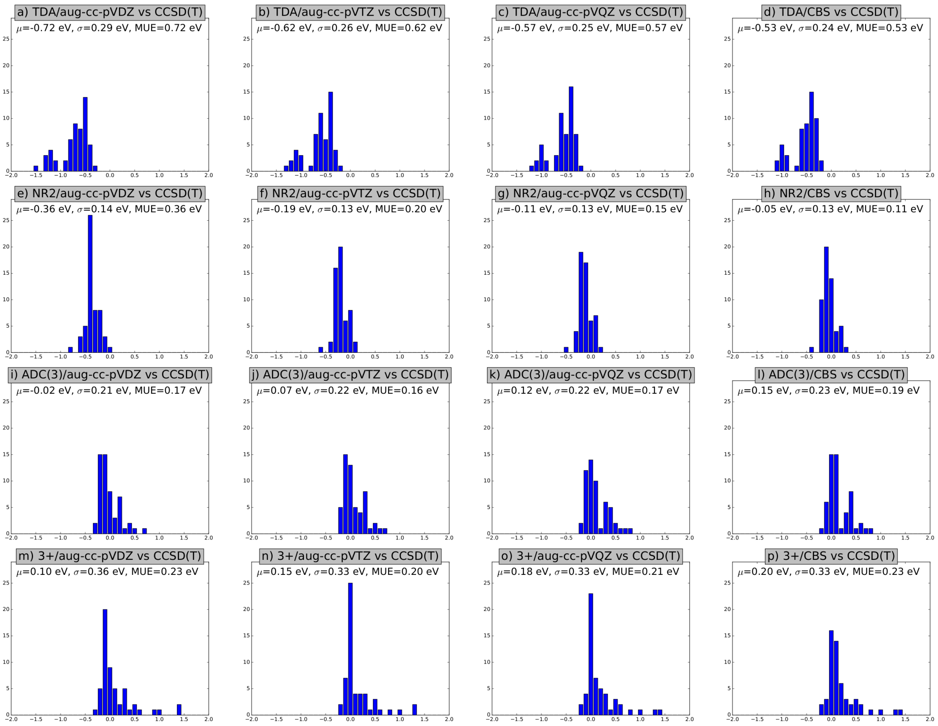

1.82 eV. OVGF-C is in excellent agreement with ΔCCSD(T) and P3+ overestimates by 0.16 eV. Results obtained with non–diagonal EP methods are also in good agreement with ΔCCSD(T) except for TDA, which drastically underestimates at 1.54 eV.

For the second VEDE, the experimental result is close to 6.1 eV.[69] and the ΔCCSD(T) value is in excellent agreement at 6.12 eV. EP methods are apparently in good agreement but the low pole strengths (0.66–0.69 for non–diagonal and 0.79–0.82 for diagonal methods) indicate that the Koopmans picture is not valid due to important shake–up character. Therefore, diagonal methods yield fortuitously good predictions but only the non-diagonal methods give accurate predictions and reasonable Dyson orbitals.

Figures 5.3 and 5.4 show relative times for the calculations of $C_5H_5^-$ with EP, MP2 and CCSD(T) methods as a function of augmented correlation consistent basis sets. First, Figure 5.3 shows relative times for the post Hartree-Fock calculations and it can be seen that CCSD(T) takes more time and is followed by D3, OVGF, TDA, ADC(3) and 3+. The fastest method is D2 and is followed by P3, P3+, NR2. When the time required for the integral transformation is included, it can be seen that this step governs diagonal EP methods and NR2 calculations, see Figure 5.4.

Table 5.2: $C_5H_5^-$ VEDEs, eV

Diagonal Methods$^{a)}$

State$^{b)}$	Basis$^{c)}$	KT	D2	D3	A	B	C	P3	P3+	ΔCCSD(T)
12 $^2E_1''$	aTZ	1.97	1.62	2.18	1.75	1.88	**2.01**	2.16	2.06	
12 $^2E_1''$	aQZ	1.98	1.69	2.18	1.79	1.88	**2.03**	2.24	2.14	
12 $^2E_1''$	CBS	1.98	1.74	2.18	1.82	1.88	**2.04**	2.30	2.20	2.04
11 $^2A_2''$	aTZ	7.66	5.57	6.71	6.14	**6.25**	6.36	6.22	6.06	
11 $^2A_2''$	aQZ	7.66	5.63	6.71	6.16	**6.24**	6.38	6.30	6.14	
11 $^2A_2''$	CBS	7.66	5.67	6.71	6.18	**6.24**	6.40	6.36	6.20	6.12

$^{a)}$A, B and C stand for OVGF-A, OVGF-B and OVGF-C, respectively. OVGF-N (recommended value) is shown in **bold** type.

$^{b)}$All pole strengths for the 11 $^2A_2''$ state are between 0.79-0.82.

$^{c)}$ aXZ = aug-cc-pVXZ. CBS = (4^3IE(aQZ)-3^3IE(aTZ))/(4^3-3^3)

Non-diagonal Methods$^{a)}$

State	Basis$^{b)}$	TDA	NR2	ADC(3)	3+	ΔCCSD(T)
12 $^2E_1''$	aTZ	1.45	1.95	2.02	1.95	
12 $^2E_1''$	aQZ	1.50	2.03	2.06	1.95	
12 $^2E_1''$	CBS	1.54	2.09	2.09	1.95	2.04
11 $^2A_2''$	aTZ	4.97(0.67)	5.71(0.66)	6.21(0.68)	6.17(0.68)	
11 $^2A_2''$	aQZ	5.00(0.67)	5.78(0.66)	6.25(0.68)	6.17(0.69)	
11 $^2A_2''$	CBS	5.02(0.67)	5.83(0.66)	6.28(0.68)	6.17(0.68)	6.12

$^{a)}$Pole strength in parentheses when lower than 0.85.

$^{b)}$aXZ = aug-cc-pVXZ. CBS = (4^3IE(aQZ)-3^3IE(aTZ))/(4^3-3^3)

Figure 5.3: Post Hartree-Fock relative time as a function of valence basis functions. Times are normalized to the maximum time overall.

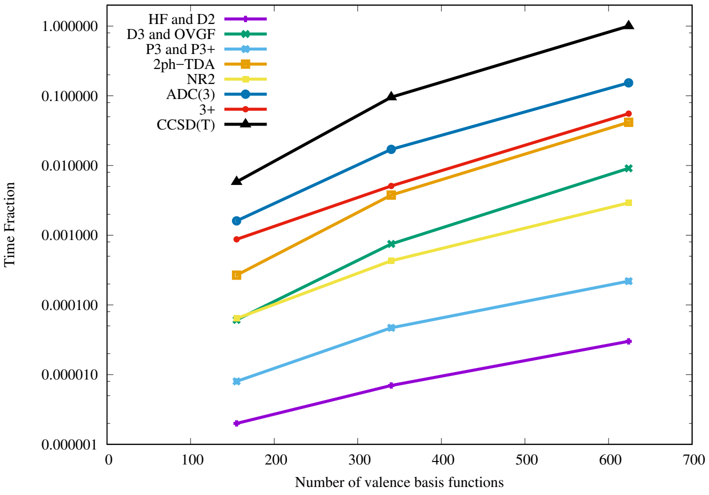

Figure 5.4: Post Hartree-Fock and integral transformation relative time as a function of valence basis functions. Times are normalized to the maximum time overall.

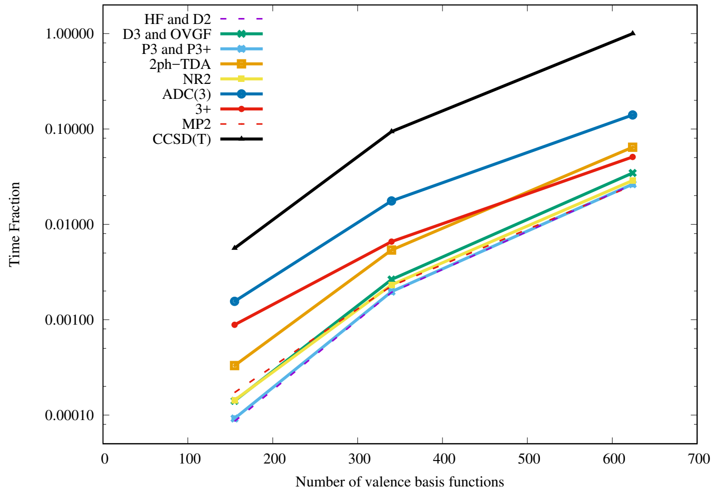

5.3 $P_2N_3^-$ Pentagons

Geometry optimizations for $P_2N_3^-$ and N_2PNP^- pentagonal rings are shown in Table 5.3. $P_2N_3^-$ has been synthesized by Velian *et al.*[70] However, this is not the most stable pentagonal isomer.[28]

The adiabatic electron detachment energy was measured experimentally to be 3.76 eV.[71] In addition, VEDEs have been predicted using ΔCCSD(T) and IP–EOM-CCSD to be 4.27 and 4.22 eV, respectively.[71,72] The large discrepancies between the adiabatic and vertical transitions are due to large, symmetry lowering, nuclear relaxation effects. Both calculations had a $^2A_1$ final state or a σ hole. In addition, IP–EOM-CCSD calculations accessed excited states and their VEDEs can be seen in Tables 5.4 and 5.5.

In this chapter, standards generated using ΔCCSD(T)/CBS are compared to previous IP–EOM–CCSD results and they agree in the order of the final states. However, the difference between the first two states is only 0.02 eV for CCSD(T) and is 0.16 eV for IP–EOM–CCSD. Figure 5.5 shows Dyson orbitals used to build reference UHF states for the CCSD(T) calculations on doublets. The large discrepancies between the spin densities of UHF and CCSD reveal important correlation effects and the order of the states is different from that of KT. Therefore, there is a Koopmans's defect in these anions and the Dyson orbital of the anionic HOMO does not correlate to the lowest electronic state of the neutral radical doublet.

Table 5.3: N_2PNP^- and $P_2N_3^-$ pentagonal structures and relative energies$^{a)}$

	N_2PNP^-		$P_2N_3^-$	
Relative Energy (eV)	0.00		0.77	
Adiabatic Detachment Energy (eV)	3.21 ($^2B_2$)		3.68 ($^2A_1$)	
Point Group	C_{2v}		C_{2v}	
Distance (Å)	P–N	1.675	P–P	2.100
Distance (Å)	P–N’	1.658	P–N	1.701
Distance (Å)	N–N	1.355	N–N	1.323
Angle (^{o})	P–N’–P	109.4	P–P–N	93.1
Angle (^{o})	N–N–P	113.8	N–N–N	119.4

$^{a)}$CCSD(T)/6-311+G(2df)

Results obtained with P3+/CBS reverse the order of the first two states but are in close numerical agreement to ΔCCSD(T)/CBS. The results for OVGF-N/CBS have VEDEs in reasonable agreement but the ordering of final states is different, $^2B_1$, $^2A_1$, $^2A_1$, $^2A_2$, $^2B_2$. NR2/CBS gives the best results for non-diagonal methods and its discrepancies with ΔCCSD(T) are of 0.15 eV or less.

The pentagonal N_2PNP^- isomer is lower in energy by 0.77 eV with respect to $P_2N_3^-$, see Table 5.3. The VEDE was predicted to be 3.73 eV (see Tables 5.6 and Tables 5.7) by calculations with ΔCCSD(T)/CBS. Strong correlation effects and large spin contamination of the UHF wavefunctions can be seen in Figure 5.6. However, the CCSD(T) method should be able to minimize these errors. Results obtained with P3+/CBS and OVGF-N/CBS are within 0.2 eV of CCSD(T) standards. In addition, NR2/CBS results are the best ones for non–diagonal methods. These results should be useful when the more stable isomer is synthesized or if both isomers are mixed in the experimental sample.

5.4 Superhalide $Al(BO_2)_4^-$

The anion $Al(BO_2)_4^-$ has a very large VEDE and the corresponding neutral molecule will have an electron affinity larger that 3.6 eV, the largest electron affinity of atoms which belongs to Cl. When a cluster has a higher electron affinity than chlorine, it is known as a superhalogen.[32,33,73] Therefore, $Al(BO_2)_4$ is a superhalogen and $Al(BO_2)_4^-$ is a superhalide.

Previous data from Gutsev *et al*,[74] show discrepancies between the ΔCCSD(T) and OVGF results of close to 0.4 eV. The findings listed on Table 5.8 agree with these results but it also shows good agreement between ΔCCSD(T) and P3+. In addition, the efficient non–diagonal method NR2 is able to predict the VEDEs of this large superhalogen, see Table 5.9. The agreement between ΔCCSD(T) and

Table 5.4: $P_2N_3^-$ VEDEs, eV, with Diagonal Methods$^{a)}$

State	Basis$^{b)}$	KT	D2$^{c)}$	D3	A	B	C	P3	P3+$^{c)}$	ΔCCSD(T)	EOM$^{d)}$
$13\,^2B_1$	aTZ	4.10	4.18	4.29	4.17	4.13	**4.26**	4.45	4.40	4.35	4.38
$13\,^2B_1$	aQZ	4.10	4.25	4.31	4.24	4.15	**4.30**	4.52	4.48	4.40	
$13\,^2B_1$	CBS	4.10	4.30	4.32	4.29	4.16	**4.33**	4.57	4.54	4.43	
$12\,^2A_1$	aTZ	5.19	4.20	4.87	4.48	**4.53**	4.67	4.76	4.65	4.50	4.70
$12\,^2A_1$	aQZ	5.19	4.28	4.91	4.52	**4.56**	4.73	4.85	4.73	4.59	
$12\,^2A_1$	CBS	5.19	4.34	4.94	4.55	**4.58**	4.77	4.92	4.79	4.65	
$11\,^2A_2$	aTZ	5.22	*4.39*	5.41	4.75	**4.90**	5.04	5.29	5.09	4.92	4.97
$11\,^2A_2$	aQZ	5.22	*4.47*	5.42	4.77	**4.90**	5.07	5.38	*5.18*	4.98	
$11\,^2A_2$	CBS	5.22	*4.53*	5.43	4.78	**4.90**	5.09	5.45	5.25	5.03	
$10\,^2A_1$	aTZ	5.76	*3.41*	5.46	4.36	**4.47**	4.67	4.89	4.51	4.30	4.22
$10\,^2A_1$	aQZ	5.76	*3.49*	5.49	4.39	**4.48**	4.71	5.00	4.60	4.36	
$10\,^2A_1$	CBS	5.76	*3.55*	5.51	4.41	**4.49**	4.74	5.08	4.67	4.41	
$9\,^2B_2$	aTZ	6.37	*3.56*	6.16	4.80	**4.97**	5.11	5.28	4.82	4.64	4.71
$9\,^2B_2$	aQZ	6.37	*3.65*	6.19	4.83	**4.98**	5.15	5.38	4.92	4.71	
$9\,^2B_2$	CBS	6.37	*3.72*	6.21	4.85	**4.99**	5.18	5.45	4.99	4.76	

$^{a)}$A, B and C stand for OVGF-A, OVGF-B and OVGF-C, respectively. OVGF-N (recommended value) is shown in **bold** type.

$^{b)}$aXZ = aug-cc-pVXZ. CBS = $(4^3\text{IE(aQZ)}-3^3\text{IE(aTZ)})/(4^3-3^3)$

$^{c)}$D2 values in italics have 0.80<PS<0.83. P3+ values in italics have PS = 0.84

$^{d)}$IP-EOM-CCSD/aug-cc-pVTZ//CCSD/aug-cc-pVTZ[72]

Table 5.5: $P_2N_3^-$ VEDEs, eV, with Non-diagonal Methods

State	Basis$^{a)}$	TDA	NR2	ADC(3)	3+	ΔCCSD(T)	EOM$^{b)}$
$13\,^2B_1$	aTZ	3.90	4.27	4.23	4.18	4.35	4.38
$13\,^2B_1$	aQZ	3.94	4.35	4.28	4.20	4.40	
$13\,^2B_1$	CBS	3.97	4.41	4.32	4.21	4.43	
$12\,^2A_1$	aTZ	4.07	4.60	4.64	4.63	4.50	4.70
$12\,^2A_1$	aQZ	4.12	4.68	4.70	4.66	4.59	
$12\,^2A_1$	CBS	4.16	4.74	4.74	4.68	4.65	
$11\,^2A_2$	aTZ	4.20	4.92	4.97	4.97	4.92	4.97
$11\,^2A_2$	aQZ	4.25	5.00	5.02	4.98	4.98	
$11\,^2A_2$	CBS	4.29	5.06	5.06	4.99	5.03	
$10\,^2A_1$	aTZ	3.41	4.40	4.78	4.77	4.30	4.22
$10\,^2A_1$	aQZ	3.46	4.49	4.83	4.79	4.36	
$10\,^2A_1$	CBS	3.50	4.56	4.87	4.80	4.41	
$9\,^2B_2$	aTZ	3.63	4.74	5.22	5.26	4.64	4.71
$9\,^2B_2$	aQZ	3.69	4.83	5.28	5.28	4.71	
$9\,^2B_2$	CBS	3.73	4.90	5.32	5.29	4.76	

$^{a)}$aXZ = aug-cc-pVXZ. CBS = $(4^3\text{IE(aQZ)}-3^3\text{IE(aTZ)})/(4^3-3^3)$

$^{b)}$IP-EOM-CCSD/aug-cc-pVTZ//CCSD/aug-cc-pVTZ[72]

Figure 5.5: Comparison between the spin density (isovalue = 0.02) and canonical molecular orbitals (isovalue = 0.05) for $P_2N_3^-$

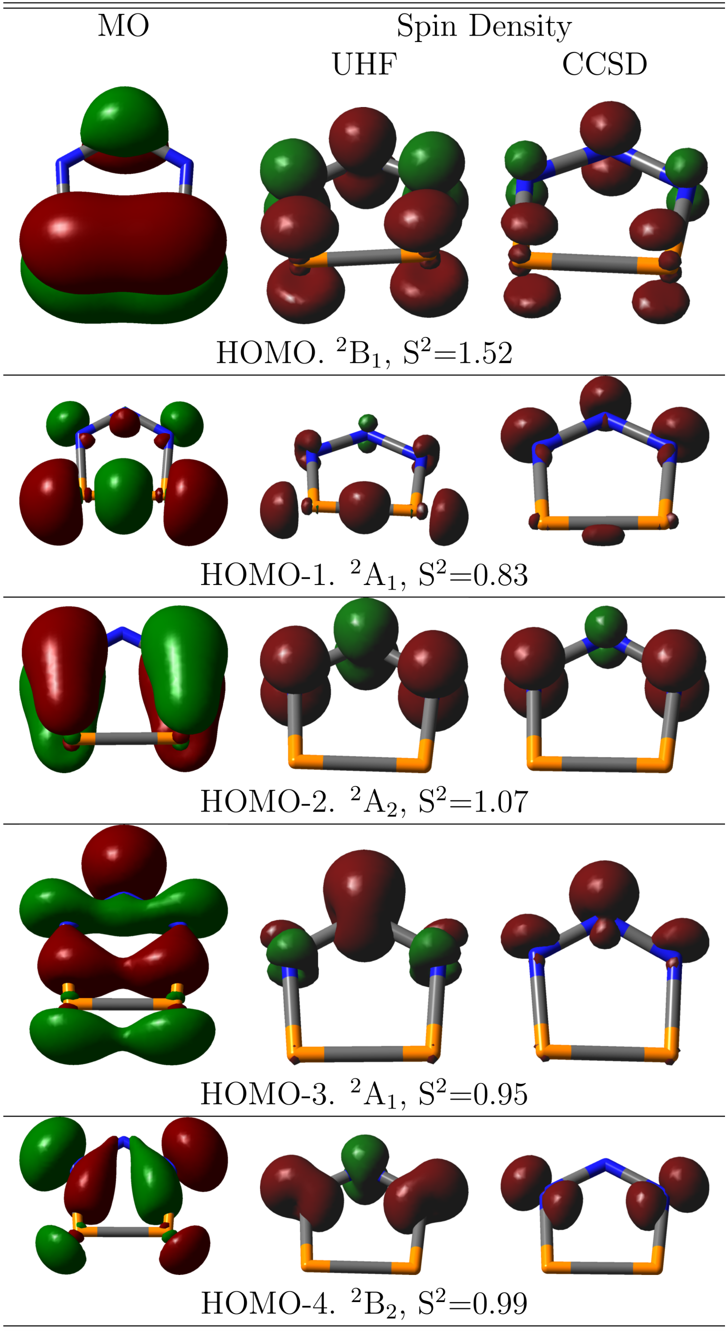

Table 5.6: N_2PNP^- VEDEs, eV, with Diagonal Methods[a)]

State	Basis[b)]	KT	D2[c)]	D3	A	B	C	P3	P3+[c)]	ΔCCSD(T)
$13\,^2A_2$	aTZ	3.44	3.56	3.84	3.52	3.64	**3.76**	3.95	3.89	3.79
$13\,^2A_2$	aQZ	3.44	3.63	3.86	3.57	3.64	**3.79**	4.02	3.96	3.83
$13\,^2A_2$	CBS	3.44	3.68	3.87	3.61	3.64	**3.81**	4.07	4.01	3.86
$12\,^2B_2$	aTZ	4.94	*2.82*	4.66	3.68	**3.80**	3.97	4.12	3.80	3.64
$12\,^2B_2$	aQZ	4.94	*2.90*	4.69	3.70	**3.81**	4.01	4.22	3.88	3.68
$12\,^2B_2$	CBS	4.94	*2.96*	4.71	3.71	**3.82**	4.04	4.29	3.94	3.73
$11\,^2B_1$	aTZ	6.16	*5.00*	6.21	5.49	**5.64**	5.77	5.99	*5.77*	5.64
$11\,^2B_1$	aQZ	6.17	*5.09*	6.23	5.52	**5.65**	5.81	6.09	*5.87*	5.70
$11\,^2B_1$	CBS	6.18	*5.16*	6.24	5.54	**5.66**	5.84	6.16	5.94	5.74
$10\,^2B_2$	aTZ	6.82	*4.76*	6.46	5.56	**5.70**	5.85	5.91	5.63	
$10\,^2B_2$	aQZ	6.82	*4.84*	6.50	5.60	**5.72**	5.89	6.01	5.72	
$10\,^2B_2$	CBS	6.82	*4.90*	6.53	5.63	**5.73**	5.92	6.08	5.79	
$9\,^2A_1$	aTZ	7.14	*4.06*	6.85	5.43	**5.59**	5.75	5.90	5.41	5.27
$9\,^2A_1$	aQZ	7.14	*4.17*	6.87	5.46	**5.60**	5.80	6.02	5.52	5.33
$9\,^2A_1$	CBS	7.14	*4.25*	6.88	5.48	**5.61**	5.84	6.11	5.60	5.38

[a)] A, B and C stand for OVGF-A, OVGF-B and OVGF-C, respectively. OVGF-N (recommended value) is shown in **bold** type.

[b)] aXZ = aug-cc-pVXZ. CBS = $(4^3$IE(aQZ)-3^3IE(aTZ))/$(4^3$-$3^3)$

[c)] D2 values in italics have 0.80<PS<0.83. P3+ values in italics have PS = 0.84

Table 5.7: N_2PNP^- VEDEs, eV, with Non-diagonal Methods

State	Basis[a)]	TDA	NR2	ADC(3)	3+	ΔCCSD(T)
$13\,^2A_2$	aTZ	3.38	3.77	3.70	3.70	3.79
$13\,^2A_2$	aQZ	2.74	3.84	3.74	3.72	3.83
$13\,^2A_2$	CBS	2.74	3.89	3.77	3.73	3.86
$12\,^2B_2$	aTZ	2.69	3.66	4.01	4.01	3.64
$12\,^2B_2$	aQZ	2.74	3.75	4.06	4.03	3.68
$12\,^2B_2$	CBS	2.78	3.82	4.10	4.04	3.73
$11\,^2B_1$	aTZ	4.78	5.53	5.66	5.64	5.64
$11\,^2B_1$	aQZ	4.84	5.62	5.72	5.67	5.70
$11\,^2B_1$	CBS	4.88	5.69	5.76	5.69	5.74
$10\,^2B_2$	aTZ	4.90	5.55	5.82	5.84	
$10\,^2B_2$	aQZ	4.94	5.62	5.88	5.87	
$10\,^2B_2$	CBS	4.97	5.67	5.92	5.89	
$9\,^2A_1$	aTZ	4.25	5.36	5.83	5.87	5.27
$9\,^2A_1$	aQZ	4.32	5.47	5.90	5.90	5.33
$9\,^2A_1$	CBS	4.37	5.55	5.95	5.92	5.38

[a)] aXZ = aug-cc-pVXZ. CBS = $(4^3$IE(aQZ)-3^3IE(aTZ))/$(4^3$-$3^3)$

Figure 5.6: Comparison between the spin density (isovalue = 0.02) and canonical molecular orbitals (isovalue = 0.05) for N_2PNP^-

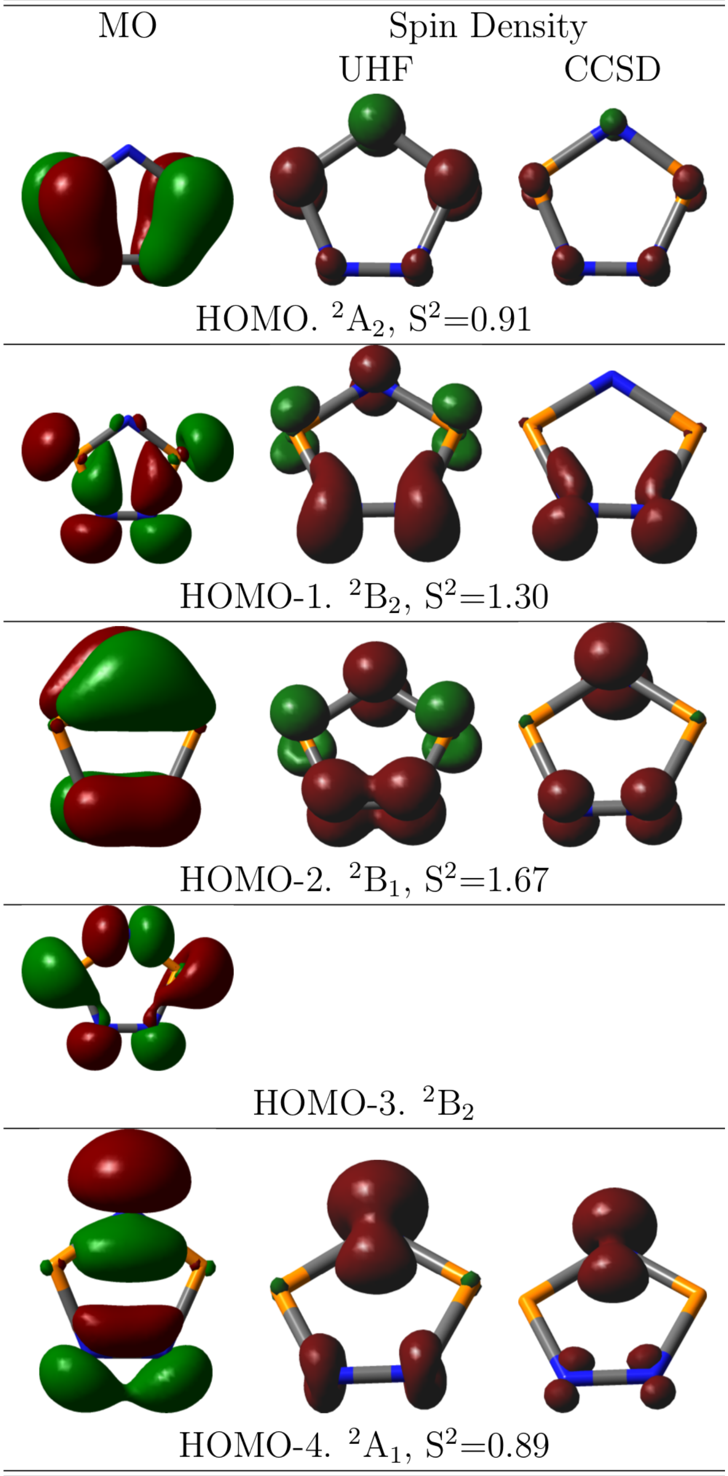

Table 5.8: Al(BO$_2$)$_4^-$ VEDEs, eV, with Diagonal Methods[a,b]

State	Basis[c]	KT	D2	D3	A	B	C	P3	P3+	ΔCCSD(T)[d]
30 $^2T_1$	TZ1	9.95	7.58	9.42	8.70	**8.90**[d]	8.88	8.75	8.55	8.36[e]
30 $^2T_1$	TZ2	9.93	7.79	9.62	8.83	**9.09**[d]	9.08	8.94	8.74	8.60
30 $^2T_1$	aTZ	9.92	7.79	9.64	8.85	**9.11**	9.10	8.95	8.75	8.62
30 $^2T_1$	aQZ	9.92	7.90	9.69	8.88	**9.15**	9.16	9.07	8.86	
30 $^2T_1$	CBS	9.92	7.98	9.73	8.90	**9.18**	9.20	9.16	8.94	8.76
28 ^2E	TZ1	10.16	7.88	9.73	8.99	**9.20**	9.18	9.03	8.82	8.69
28 ^2E	TZ2	10.14	8.05	9.91	9.10	**9.38**	9.36	9.20	9.00	8.91
28 ^2E	aTZ	10.13	8.06	9.94	9.12	**9.40**	9.38	9.21	9.01	8.93
28 ^2E	aQZ	10.13	8.16	9.98	9.15	**9.43**	9.44	9.33	9.12	
28 ^2E	CBS	10.13	8.23	10.01	9.17	**9.45**	9.48	9.42	9.20	9.06
25 $^2T_2$	TZ1	10.18	7.90	9.75	9.01	**9.23**	9.20	9.04	8.84	8.72
25 $^2T_2$	TZ2	10.15	8.07	9.93	9.12	**9.40**	9.38	9.22	9.02	8.94
25 $^2T_2$	aTZ	10.14	8.08	9.96	9.14	**9.42**	9.40	9.23	9.03	8.96
25 $^2T_2$	aQZ	10.14	8.18	10.00	9.17	**9.45**	9.46	9.35	9.14	
25 $^2T_2$	CBS	10.14	8.25	10.03	9.19	**9.47**	9.50	9.44	9.22	9.09

[a] Structure obtained from Ref.[74]

[b] A, B and C stand for OVGF-A, OVGF-B and OVGF-C, respectively. OVGF-N (recommended value) is shown in **bold** type.

[c] aXZ = aug-cc-pVXZ. CBS = (4^3IE(aQZ)-3^3IE(aTZ))/(4^3-3^3)

TZ1=6-311+G(d) and TZ2=6-311+G(3df)

[d] MP2/a(TQ)Z+$\delta_{MP2}^{CCSD(T)}$/a(DT)Z

[e] Values reported previously in Ref.[74]

NR2 is excellent and the predicted VEDE is 8.8 eV for the $^2T_1$ final state. Two excited states, ^2E and $^2T_2$, are 0.3 eV higher than the lowest final state. The order of these excited states remains uncertain due to how close in energy they are.

5.5 Composite Methods

In Chapter 4, the usefulness of CEP to predict high–accuracy VEDEs was discussed.[21] In addition, previous results within this chapter have shown the great accuracy of both P3+ and NR2 for the prediction of VEDEs for anions. For these reasons, the composite methods CP3+/a23, CNR2/a23, CP3+/a34 and CNR2/a34 will be compared against the generated ΔCCSD(T)/CBS standards. Figure 5.7 shows the error distributions for small anions with statistical measures below 0.15 eV for all four composite methods. These results are in excellent agreement with ΔCCSD(T) and when comparing with the VEDEs obtained for the case studies in previous sections of this chapter (see Figure 5.8), similar encouraging

Table 5.9: $Al(BO_2)_4^-$ VEDEs, eV, with Non-diagonal Methods[a)]

State	Basis[b)]	NR2	ΔCCSD(T)[c)]
30 $^2T_1$	TZ1	8.41	8.36[d)]
30 $^2T_1$	TZ2	8.60	8.60
30 $^2T_1$	aTZ	8.61	8.62
30 $^2T_1$	aQZ	8.72	
30 $^2T_1$	CBS	8.80	8.76
28 ^2E	TZ1	8.70	8.69
28 ^2E	TZ2	8.87	8.91
28 ^2E	aTZ	8.88	8.93
28 ^2E	aQZ	8.99	
28 ^2E	CBS	9.07	9.06
25 $^2T_2$	TZ1	8.72	8.72
25 $^2T_2$	TZ2	8.89	8.94
25 $^2T_2$	aTZ	8.90	8.96
25 $^2T_2$	aQZ	9.01	
25 $^2T_2$	CBS	9.09	9.09

[a)] Structure obtained from Ref.[74]

[b)] aXZ = aug-cc-pVXZ. CBS = (4^3IE(aQZ)-3^3IE(aTZ))/(4^3-3^3)

TZ1=6-311+G(d). TZ2=6-311+G(3df)

[c)] MP2/a(TQ)Z+$\delta_{MP2}^{CCSD(T)}$/a(DT)Z

[d)] Value reported previously in Ref.[74]

results are obtained. In general, CP3+ methods tend to overestimate whereas CNR2/a23 underestimate VEDE values. CNR2/a34 has a well behaved and symmetric gaussian curve.

5.6 Conclusions

In this chapter, VEDEs of closed–shell anions were accurately predicted with EP methods which have lower computational requirements than the ΔCCSD(T) standards. The best results for closed–shell small anions of the first three periods were obtained with OVGF-A, P3+ and NR2 EP methods. From these methods, P3+ has the lowest computational demands in addition to not having numerical parameters. For the non–diagonal EP methods, NR2 is both the more computationally efficient and accurate. OVGF methods require the four index virtual molecular two electron repulsion integrals and are more demanding than P3+ and NR2. In addition, the OVGF-N selection algorithm usually selects the OVGF-B method instead of the most accurate OVGF-A method.

The potential of electron propagator methods is displayed by accurate predictions of both organic and inorganic compounds in the case studies. For $C_5H_5^-$, the first VEDE is accurately predicted with

Figure 5.7: Error distributions (eV) for small anions: composite methods

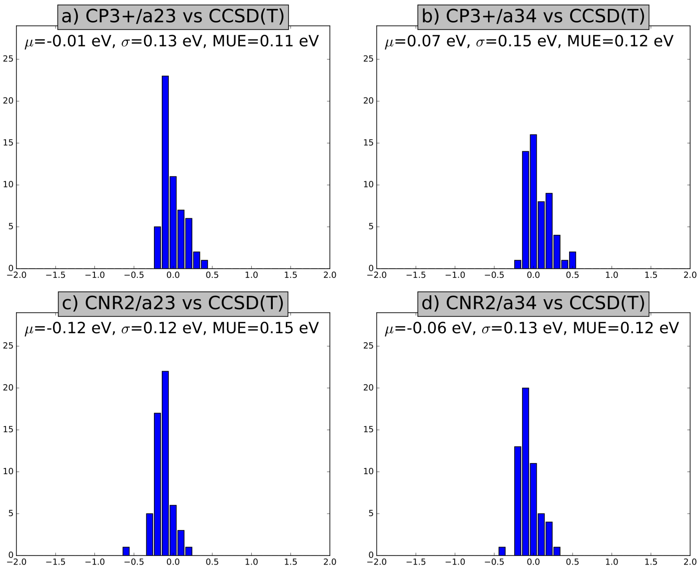

Figure 5.8: Error distributions (eV) for large anions: composite methods

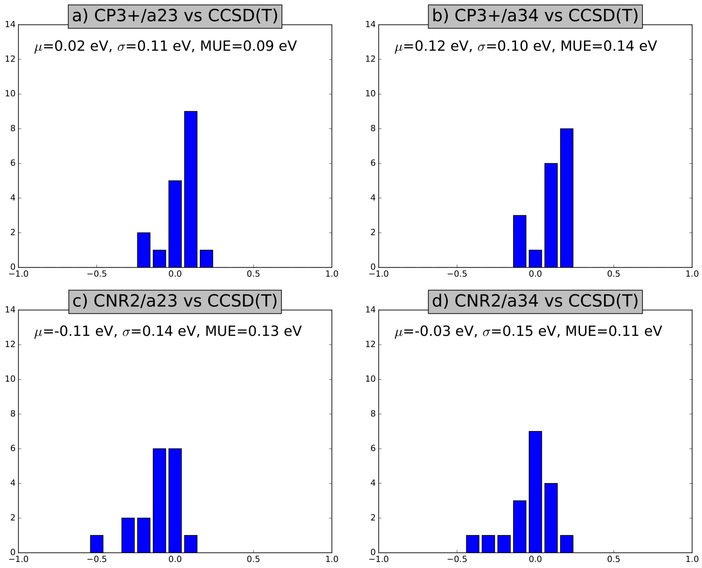

OVGF, P3+ and NR2 but the second VEDE has low pole strengths. For this reason, only results obtained with NR2 are accurate and yield correct Dyson orbitals. When dealing with the $P_2N_3^-$ and N_2PNP^- anions, high correlation effects are observed when comparing the Dyson orbitals to the spin densities obtained with the UHF and UCCSD methods. However, results obtained with both P3+ and NR2 are in good agreement with the ΔCCSD(T) and IP–EOM–CCSD methods. Finally, both P3+ and NR2 succeed in predicting with high accuracy VEDEs for the $Al(BO_2)_4^-$ superhalide, promising to be useful tools in the discovery of new superhalogens.

In addition, results obtained with CEP methods based on the P3+ and NR2 approximations are in excellent agreement with the ΔCCSD(T) standards. These composite methods were applied successfully to large carborane anions in Chapter 4. The accurate and balanced treatment of both initial–state correlation, final–state orbital relaxation and polarization effects by both P3+ and NR2 methods accounts for their accuracy and stability.

Chapter 6

Prediction of Vertical Electron Detachment Energies of Superhalides with Electron Propagator Methods

This chapter summarizes the most important findings of references 6,30,31 regarding the use of EPT to predict VEDEs of superhalides.

Halogens are elements in the periodic table that have large electron affinities and their anions or halides are closed–shell and valence bound electrons. The halogen with the highest electron affinity is chlorine with an electron affinity of 3.6 eV. Clusters with low electronegativity central atoms and highly electronegative ligands can have electron affinities higher than 3.6 and are known as superhalogens.[32,33] For example, MgF_3 will be a super halogen which consists of a metallic central atom with valence two and three fluorine ligands and the predicted EA is 7.66 eV.[75]

In addition, bridged superhalogens have two or more central atoms and electronegative ligands binding them together. These superhalogens can have larger EAs than their corresponding single superhalogens. When one of the ligands is substituted by an organic group, like ethylene, a composite superhalogen is formed. Composite superhalogens have larger electron affinities than their organic groups but lower than their respective superhalogen. Therefore, chemical synthesis and bond activations might be performed with these systems.

6.1 Prediction of VEDEs of Composite Superhalides with Electron Propagator Theory

Previous results by Li *et al* regarding the calculation of composite superhalides VEDEs[75] with the Outer Valence Green's Function[3,48,76] seem to be in disagreement with results obtained using ΔCCSD(T).[64]

Figure 6.1: Comparison between VEDE values at the OVGF and CCSD(T) levels; full and dashed lines are for ^{2}A" and ^{2}A' final states, respectively.

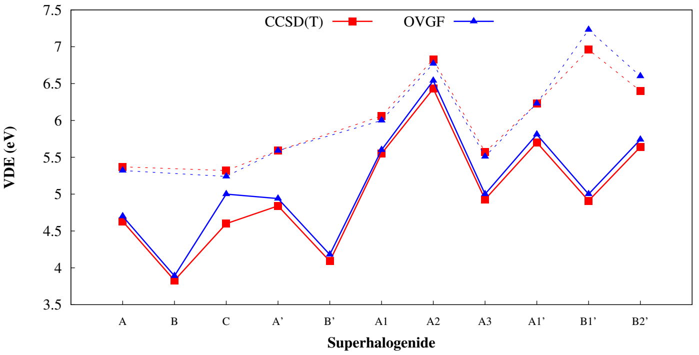

Unfortunately, Li *et al* failed to compare the right electronic states for these comparisons. For example, when a molecule has a plane of symmetry (C_s point group) there are two electronic states available, ^{2}A' and ^{2}A". This chapter shows that results obtained with both ΔCCSD(T) and OVGF are in excellent agreement when comparing the correct electronic transitions, see Table 6.1 and Figure 6.1. The composite superhalides considered can be seen in Figure 6.2 and the calculations were performed with Gaussian 09.[77] Results in bold type (see Table 6.1) are for final doublet states ignored by Li *et al*. Discrepancies between OVGF and ΔCCSD(T) have μ, MUE and σ of 0.07, 0.10 and 0.12 eV, respectively. In addition, OVGF is faster than CCSD(T) as has been demonstrated in Chapter 5.

Li *et al* fail to assign the correct Dyson orbital to the electronic final state by using the HOMO regardless of having different symmetry. When using EPT, the KT assigns the IE or EA to the negative of the HOMO or LUMO eigenvalue. This assumes that there are not strong correlation and orbital relaxation effects. When these effects are present, the lowest electronic state might have a different Dyson orbital than the HOMO and using the orbital symmetry can help to map the right vertical transitions. This is because the Dyson orbital should have the same irreducible representation as the doublet final state.

6.2 Prediction of VEDEs of doubly–bridged Superhalides with Electron Propagator Theory

Previous results obtained by Li *et al* claim large discrepancies between the OVGF and ΔCCSD(T) levels of theory for the prediction of doubly–bridged superhalide VEDEs.[1] In this section, calculations of VEDEs for six $Mg_2(CN)_5^-$ isomers have been performed with Gaussian 09 using the same methods

Table 6.1: Vertical Electron Detachment Energies (eV) of C_s Superhalides[a]

^{1}A’ Anion	State[b]	Orbital[c]	MP2	OVGF[d]	CCSD	CCSD(T)
A	^{2}A”	HOMO	**5.46**	5.32	**5.23**	**5.37**
A	^{2}A’	HOMO-1	5.05	**4.70**	4.61	4.63
B[e]	^{2}A’	HOMO	3.89	3.89	3.79	3.83
C	^{2}A’	HOMO	**4.91**	5.00	**4.61**	**4.60**
C	^{2}A”	HOMO-1	5.69	**5.24**	5.24	5.32
A’	^{2}A”	HOMO	**5.71**	5.59	**5.46**	**5.59**
A’	^{2}A’	HOMO-1	5.31	**4.94**	4.83	4.84
B’[e]	^{2}A’	HOMO	4.19	4.18	4.06	4.09
A1	^{2}A”	HOMO	**6.14**	6.00	**5.92**	**6.06**
A1	^{2}A’	HOMO-1	5.97	**5.60**	5.51	5.55
A2	^{2}A”	HOMO	**6.90**	6.77	**6.69**	**6.83**
A2	^{2}A’	HOMO-1	6.84	**6.54**	6.40	6.43
A3	^{2}A”	HOMO	**5.65**	5.51	**5.43**	**5.57**
A3	^{2}A’	HOMO-1	5.36	**5.00**	4.90	4.93
A1’	^{2}A”	HOMO	**6.34**	6.23	**6.10**	**6.23**
A1’	^{2}A’	HOMO-1	**6.16**	**5.81**	**5.68**	**5.70**
B1’	^{2}A’	HOMO	**4.99**	5.00	**4.87**	**4.91**
B1’	^{2}A”	HOMO-1	7.24	**7.23**	7.08	6.96
B2’	^{2}A’	HOMO	5.74	5.74	5.61	5.64
B2’	^{2}A”	HOMO-1	**6.59**	**6.60**	**6.48**	**6.40**

[a] Values in bold type pertain to final state doublets that were ignored by Li *et al*[75]

[b] Electronic state of superhalogen molecule

[c] Reference canonical Hartree–Fock orbital

[d] All Pole strengths are above 0.85

[e] This system has no Koopmans defect; only one VEDE is needed

Figure 6.2: Superhalogen composite structure anions.

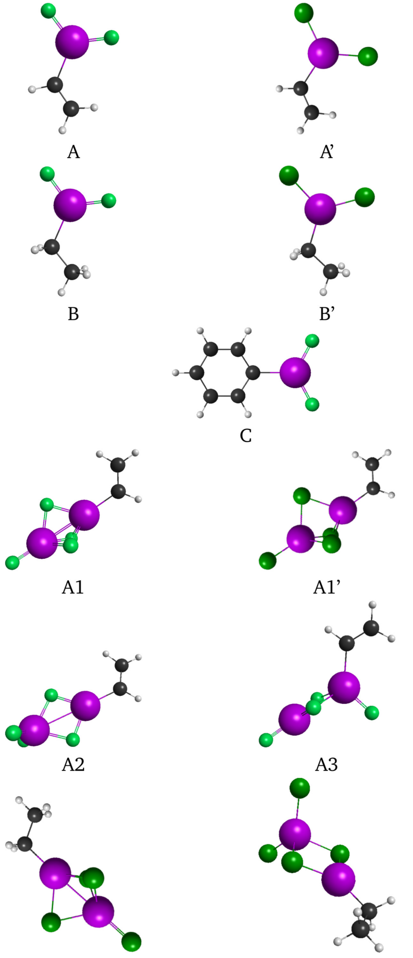

A A’

B B’

C

A1 A1’

A2 A3

B1’ B2’

H = light gray, C = black, F = light green, Cl = green, and Mg = purple.

Table 6.2: VEDEs of $Mg_2(CN)_5^-$ superhalides (eV).[a)]

Isomer	State[b)]	CMO[c]	OVGF[d]	CCSD(T)
A	^{2}A"	HOMO	7.14	6.90
B	^{2}A"	HOMO	7.13	6.89
C	^{2}A	HOMO-2	**6.99**	6.89
D	^{2}A'	HOMO-5	**8.15**	8.05
E	^{2}A	HOMO-2	**6.98**	6.87
F	^{2}A'	HOMO-2	**8.20**	8.10
1	$^2A_1$	HOMO-3	**8.25**	8.15
2	^{2}A'	HOMO-2	**7.01**	6.91
2	^{2}A"	HOMO-1	8.24	**8.17**
3	$^2A_1$	HOMO-4	**8.11**	8.00
4	$^2A_1$	HOMO-3	**8.19**	8.13
5	$^2B_2$	HOMO	7.14	6.93
6	^{2}A'	HOMO-2	**6.95**	6.82
6	^{2}A"	HOMO-1	8.20	**8.12**
7	^{2}A'	HOMO-2	**7.02**	6.92
7	^{2}A"	HOMO-1	8.24	**8.19**
8	$^2B_2$	HOMO	7.12	6.85
9	$^2B_2$	HOMO	7.15	6.94
10	$^2A_1$	HOMO-3	**8.19**	8.11
11	^{2}A'	HOMO-2	**6.96**	6.83
11	^{2}A"	HOMO-1	8.20	**8.13**
12	^{2}A'	HOMO-1	**7.07**	6.86

[a)] Values in bold type pertain to final–state doublets ignored by Li *et al.*

[b)] Electronic state of superhalogen molecule.

[c)] Reference canonical Hartree–Fock orbital.

[d)] All pole strengths are above 0.85.

and basis sets as Li *et al*, see Table 6.3 for basis set definitions. Table 6.2 and Figure 6.3 show results for the prediction of VEDEs with MUE and σ of 0.13 and 0.07, respectively. Optimized structures for the six superhalogens are reported in Figure 6.4.

Koopmans defects occur in species like N_2 with π bonds and σ lone pairs. In addition, OVGF calculations have been used to predict the correct ordering of final states obtained at the Koopmans level. However, this case is more subtle due to the final ordering of states with the same symmetry. In this case, comparisons between Dyson orbitals and final state spin densities are necessary to obtain the correct assignment of states, see Figure 6.5.

Table 6.3: Basis-set abbreviations.

Basis	C & N	Mg
TZ1	6-311+G*[78,79]	TZVP[80,81]
TZ2	6-311+G(3df)	TZVP
TZ3	TZVP+[a)]	Def2-TZVP[82]

[a)] Diffuse basis from 6-311+G.

Figure 6.3: Comparison between VEDEs predicted with OVGF and CCSD(T). Full lines are for ^{2}A' and ^{2}A final states. Dashed lines are for ^{2}A" final states. Previous OVGF results obtained by Li *et al*[1] with their TZ2 basis set are included for comparison.

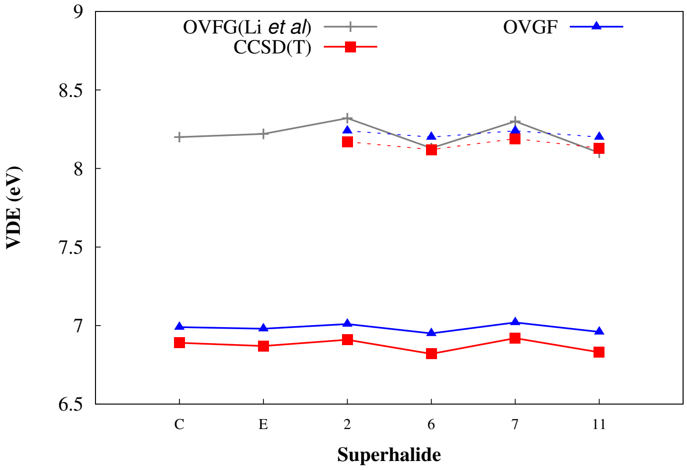

Figure 6.4: MP2/TZ1 structures of $[Mg_2(CN)_5]^-$ superhalides.

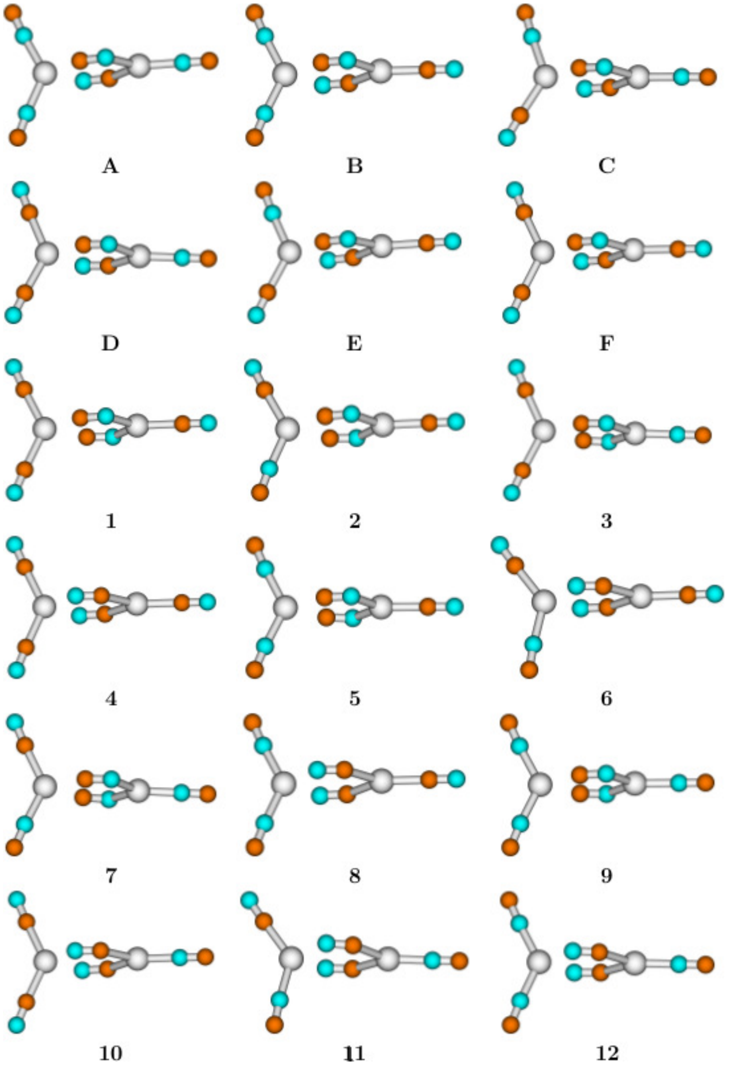

A B C

D E F

1 2 3

4 5 6

7 8 9

10 11 12

Figure 6.5: Unrestricted Hartree–Fock spin densities of ground–state superhalogens versus HOMO and HOMO-2 contours for superhalide anions with Koopmans defects.

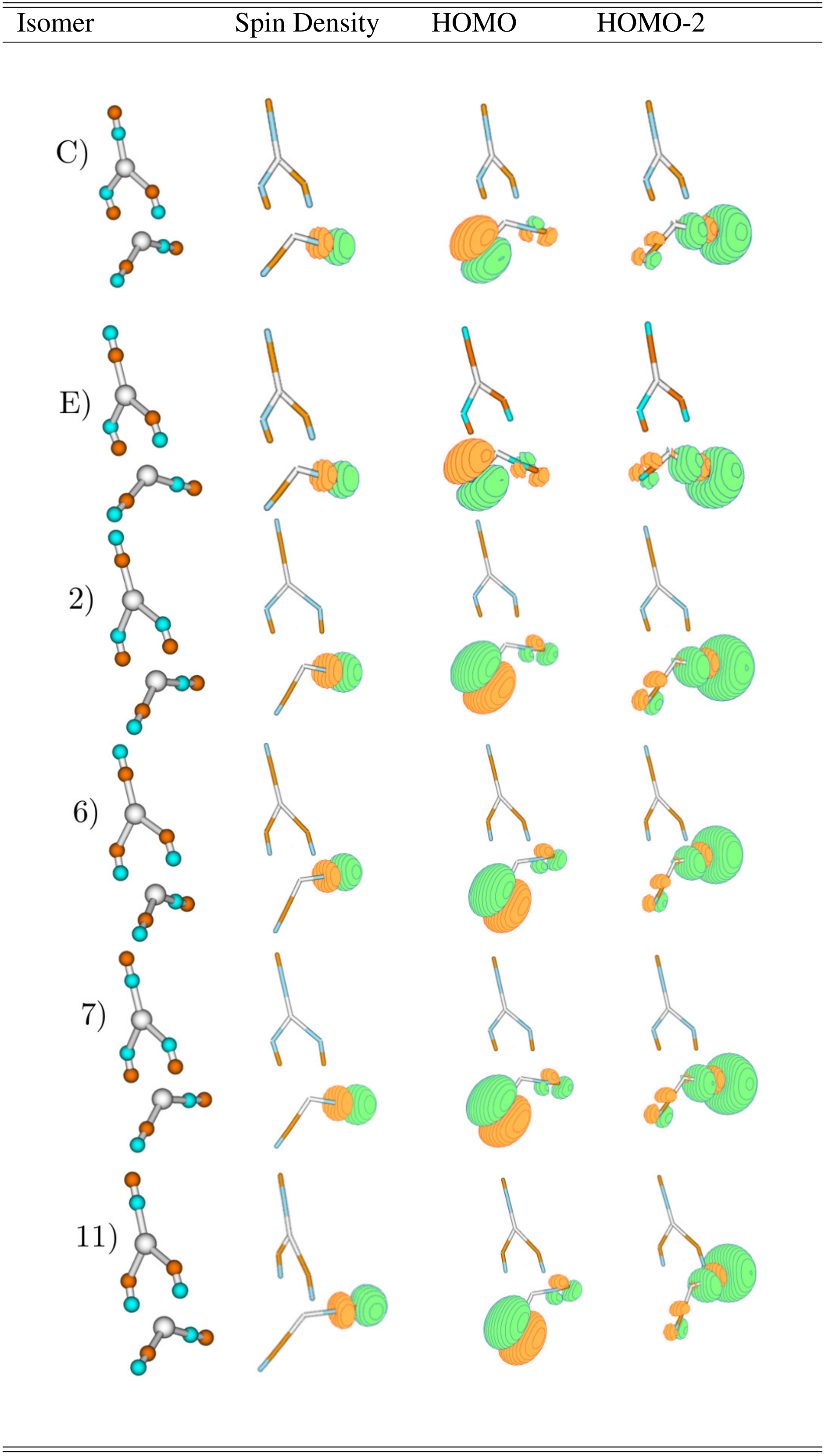

Table 6.4: Basis-set abbreviations.

Basis	C & N	Mg
TZ1	6-311+G*[78,79]	TZVP[80,81]
TZ2	6-311+G(3df)[85]	TZVP
TZ3	TZVP+[a)]	Def2-TZVP[82]

[a] Diffuse basis from 6-311+G.

6.3 Prediction of VEDEs of triply–bridged Superhalides with Electron Propagator Theory

OVGF Dyson orbitals provide reliable results for the calculation of VEDEs of superhalides. In addition, Dyson orbitals are useful for the mapping and prediction of VEDEs when using ΔE methods like ΔCCSD(T). Superhalogens have several high energy orbitals that compete through correlation and orbital relaxation effects to obtain the lowest energy doublet. In addition, spin contamination can add more difficulties to the calculation of VEDEs using Δ methods.

Previously, Yin *et al* claimed[83] that calculations on VEDEs of triply–bridged $Mg_2(CN)_5^-$ superhalides performed with the OVGF[3,48,76,84] method yield discrepancies of over 1 eV, for isomers D, E and F (see Figure 6.6) when comparing with the ΔCCSD(T) method.[64]

Unfortunately, using these methods as a black box can bring erroneous results and conclusions. Not only did Yin *et al* fail in making the right comparisons between Dyson orbitals and final doublet states, they also failed to obtain all the relevant vertical transitions for each isomer.[6]

This section involves results obtained for structures shown in Figure 6.6 using the same basis sets (see Table 6.4) as Yin *et al* for both OVGF and ΔCCSD(T) levels of theory using Gaussian 09.[77] Table 6.5 and Figure 6.7 show VEDEs for triply bridged superhalides with both OVGF and ΔCCSD(T). Excellent agreement between methods is seen with μ, MUE and σ of 0.09, 0.09 and 0.05 eV. In order to obtain the correct assignments, comparisons between Dyson orbitals and neutral state doublet's spin contamination contours are displayed in Figure 6.8.

6.4 Conclusions

The utility of OVGF in order to accurately predict VEDEs and Koopmans defects for superhalides has been proved in this chapter. OVGF is an EP method with an arithmetic scaling of ov^4 while the other

Table 6.5: Vertical Electron Detachment Energies of $Mg_2(CN)_5^-$ Isomers (eV)[a]

Isomer	State[b]	Orbital[c]	OVGF[d]	CCSD(T)	Isomer	State[b]	Orbital[c]	OVGF[d]	CCSD(T)
A	$^2A''$	HOMO	8.49	**8.41**	F	$^2A''$	HOMO	8.50	**8.42**
A	$^2A'$	HOMO-1	**8.49**	**8.41**	F	$^2A'$	HOMO-1	**8.49**	**8.42**
A	$^2A''$	HOMO-2	**8.57**	**8.49**	F[e]	$^2A'$	HOMO-2	**7.31**	7.23
A	$^2A'$	HOMO-3	**8.57**	**8.50**	F	$^2A''$	HOMO-3	**8.72**	**8.65**
B	^2E	HOMO	8.42	**8.32**	G[e]	$^2A_1$	HOMO	7.20	**7.07**
B	$^2A_2$	HOMO-4	**9.08**	**9.13**	G	^2E	HOMO-1	**8.69**	**8.50**
C[e]	$^2A_1$	HOMO	7.20	7.06	G[e]	$^2A_1$	HOMO-3	**7.37**	7.32
C	^2E	HOMO-1	**8.67**	**8.49**	G	^2E	HOMO-4	**8.77**	**8.74**
D	^2E	HOMO	8.42	**8.33**	H[e]	$^2A'$	HOMO	7.26	**7.15**
D[e]	$^2A_1$	HOMO-2	**7.36**	7.31	H	$^2A''$	HOMO-1	**8.71**	**8.59**
E	$^2A''$	HOMO	8.57	**8.51**	H[e]	$^2A'$	HOMO-2	**7.41**	7.24
E	$^2A'$	HOMO-1	**8.58**	**8.51**	H	$^2A'$	HOMO-3	**8.61**	**8.59**
E[e]	$^2A'$	HOMO-2	**7.25**	7.14	H	$^2A''$	HOMO-4	**8.74**	**8.71**
E	$^2A''$	HOMO-3	**8.70**	**8.58**					

[a] Bold type: doublets ignored in ref.[83]

[b] Electronic state of $Mg_2(CN)_5$

[c] Canonical Hartree–Fock orbital of $Mg_2(CN)_5^-$

[d] All pole strengths exceed 0.85

[e] States with $< S^2 >_{UHF}$ = 1.24–1.25 and T_1 diagnostic[86] = 0.037–0.038

Figure 6.6: MP2/TZ1 structures of $Mg_2(CN)_5^-$ triply–bridged superhalides. Mg: white, C: red, N: blue.

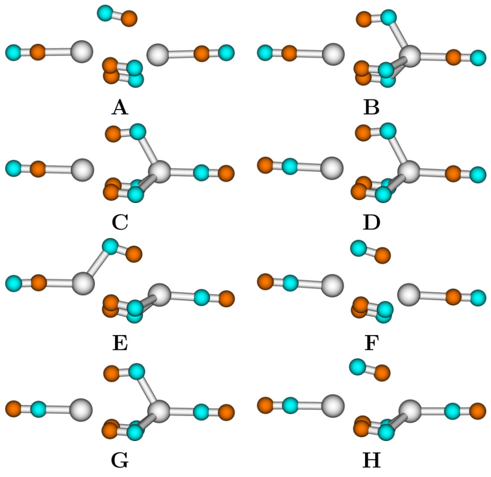

Figure 6.7: Comparison between first VEDEs predicted with OVGF and CCSD(T)

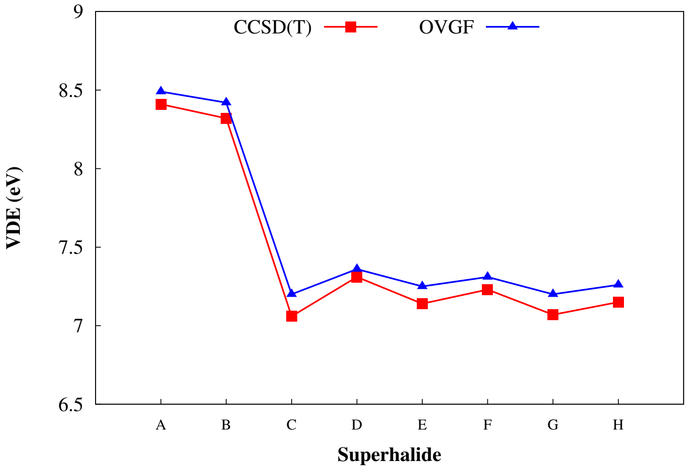

Figure 6.8: UHF spin densities for $Mg_2(CN)_5$ and canonical molecular orbitals (isovalue = 0.02 a.u.) for $Mg_2(CN)_5^-$

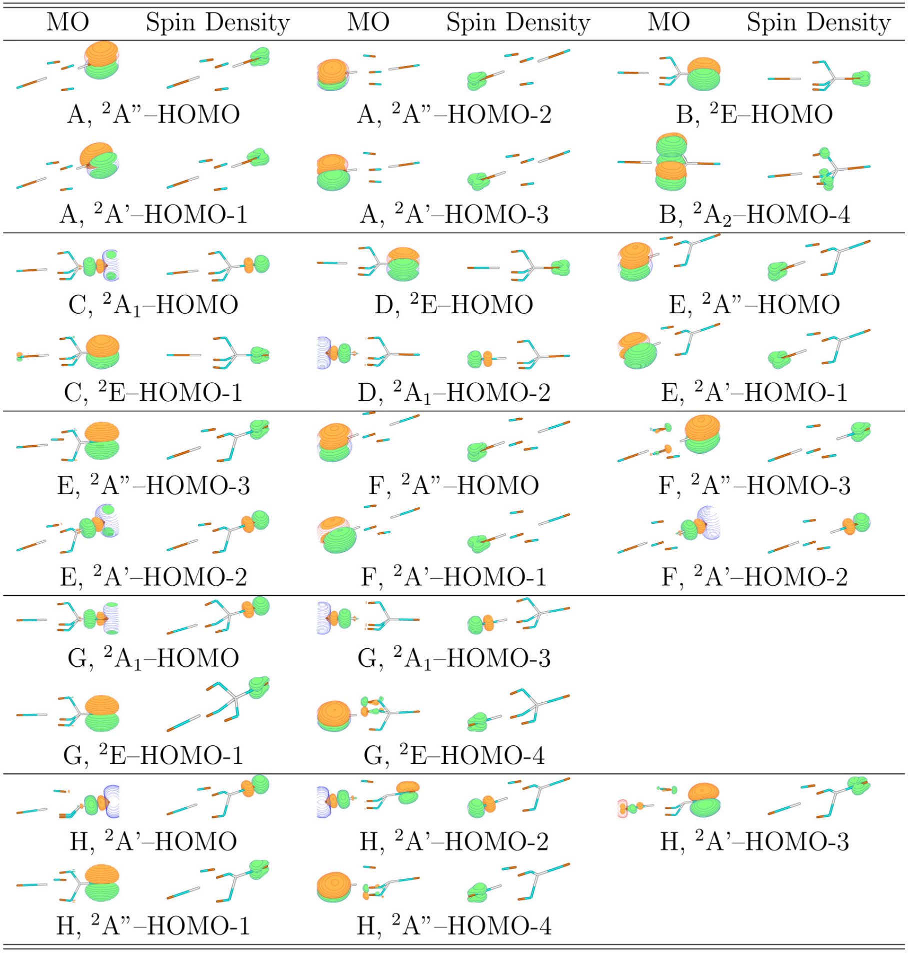

alternatives of CCSD and CCSD(T) have an arithmetic scaling of N^6 or N^7. In addition, one simple calculation of OVGF can produce several Dyson orbitals and their VEDEs whereas ΔE methods have to perform separate calculations for each electronic state. Several calculations in doublet states can also have large spin contamination or converge to excited states. Therefore, it is highly recommended that VEDEs predictions include EP methods such as OVGF.

Yin *et al* have claimed several times that OVGF fails to reproduce results obtained with ΔCCSD(T) for VEDEs of superhalides with Mg atoms. These claims have been refuted three times based on symmetry criteria and comparisons between Dyson orbitals and their corresponding doublet state's spin densities. Despite erroneous claims, OVGF is a great tool for predicting the right order of final states and Koopmans defects. In addition, OVGF predicts accurate VEDEs for superhalides based in cyano groups with MUEs below 0.1 eV.

Chapter 7

Double–Rydberg Anions: Using Electron Propagator Theory to find binding energies and Dyson orbitals

In this chapter, EPT will be used to obtain electron binding energies (EBEs) and Dyson orbitals of double–Rydberg Anions (DRAs). Predicted EBEs will be compared to experiment when available and when not these predictions will be useful for spectra assignment in future research.

7.1 Double–Rydberg anions based on ammonium–amines, $\mathbf{N}_n\mathbf{H}_{3n+1}^-$ for n = 1–5

Neutral cluster–like systems composed of a closed-shell cation and a hydrogenic electron are known as Rydberg radicals.[87] For example, NH_4 is a simple ammonium Rydberg radical $(NH_4^+)^-$. The Rydberg character in chemistry is important to predict intermediates in hydrogen atom transfer reactions and hydrated electrons.[88] When an extra electron is added to a Rydberg radical a DRA is synthesized, consisting of a closed-shell cationic core and two Rydberg–like electrons. For example, the DRA $(NH_4^+)^{2-}$ was discovered by Bowen's group[26] by its anion photoelectron spectrum and it was confirmed by theoretical studies.[27,89,90]

The tetrahedral anion has been found to be a stable species with vibrational frequencies and molecular structure similar to that of the NH_4 radical. Therefore, a fine sharp peak is observed in the photoelectron spectrum.[27,87] The HOMO orbital is diffuse and symmetric with two radial nodes, one of which occurs near the hydrogen atoms and the other around the nitrogen atom. The size and shape of this orbital has been related to Na^-.[91]

Other DRAs have been measured,[35,88] $(N_nH_{3n+1})^-$ for n = 2–5, through photoelectron spectra with dominating narrow peaks at low electron binding energies (0.4–0.5 eV). Besides the DRAs complexes between ammonia molecules and either hydride or a DRA are observed with the formulas $(H^-)(NH_3)_n$ or $(NH_4^+)^-(NH_3)_{n-1}$, respectively.

This work,[92] provides a confirmation of previous results by means of high quality theoretical predictions using CCSD[93] optimized structures and Brueckner-doubles triple field operator method (BDT1)[5,94–96] electron propagator binding energies. Agreement between experimental and calculated results are within 0.05 eV (on average the difference is only 0.02 eV) confirming the interpretation of vertical detachment energy peaks for DRAs and solvated anions.

Methodology

Structures of anions were optimized at the coupled–cluster singles and doubles (CCSD) level[93] with the 6-311++G(d,p) basis set[78,79,85] plus extra diffuse functions (exponents: H s 0.01080, N sp 0.01917) or 6-311+^{2}+^{2}G(d,p). All frequencies were real. Electron binding energies were predicted with BDT1 EPT[5,94–96] and the 6-311+^{2}+^{2}G(2df,2pd) basis set, where +^{2} stands for double diffuse functions. Brueckner–doubles coupled–cluster (BD)[97,98] calculations were performed with the oldfcbd and nosymm options. All pole strengths (norms of Dyson orbitals) were 0.85 or higher.

All calculations were executed with the GDV version of Gaussian.[63] Dyson orbitals of electron detachment from anions and electron attachment of cations were plotted using Gaussview[99] from a cube file generated with an enhanced edge size in Molden.[100] Isovalues in the orbital plots are equal to 0.02 for $n = 1, 2, 3$ and are equal to 0.012 for $n = 4, 5$.

Results

Tables 7.1–7.3 and Figures 7.1–7.7 display numerical and graphical results on various isomers of $N_nH_{3n+1}^-$.

For $n = 1$ (NH_4^-), the hydride–ammonia complex is considerably more stable than the tetrahedral DRA, NH_4^-. For the hydride complex, a single N–H bond in ammonia approaches the hydride in a C_s structure and increases the VEDE from 0.75 to 1.11 eV. The Dyson orbital can be seen in Figure 7.1 where the electrons are mainly in the hydride with some antibonding character in the approaching N–H bond. For the NH_4^- DRA, a symmetric Dyson orbital envelops the whole molecule like a membrane. In addition, the bond lengths are nearly unchanged with respect to the Rydberg radical or NH_4^+ confirming the unimportance of any antibonding character in the Dyson orbital. The low relative intensity of the

Table 7.1: $N_nH^-_{3n+1}$ isomerization and electron binding energies (eV)

n	Isomer	ΔE^{BD}_{isomer}	Theory	Expt.[35]
1	$H^-(NH_3)$	0	1.079	1.110
	NH_4^-	0.49	0.477	0.472
2	$H^-(NH_3)_2$	0	1.497	1.460
	$NH_4^-(NH_3)$	0.76	0.596	0.578
	$N_2H_7^-$	0.63	0.407	0.415
3	$H^-(NH_3)_3$	0	1.829	1.820
	$(NH_3)NH_4^-(NH_3)$	1.05	0.713	
	$NH_4^-[NH_3]_2$	0.96	0.679	0.660
	$N_2H_7^-(NH_3)$	0.93	0.498	0.495
	$N_3H_{10}^-$	0.73	0.398	0.424
4	$H^-(NH_3)_4$	0	2.159	2.111
	$(NH_3)_3NH_4^-$	1.08	0.743	
	$[NH_3]_2NH_4^-(NH_3)$	1.19	0.795	
	$NH_4^-[NH_3]_3$	1.27	0.919	
	$(NH_3)N_2H_7^-(NH_3)$	1.16	0.860	
	$N_2H_7^-[NH_3]_2$	1.07	0.564	
	$N_3H_{10}^-(NH_3)$	0.97	0.471	
	$N_4H_{13}^-$	0.72	0.398	0.427
5	$H^-(NH_3)_5$	0	2.420	2.360
	$N_5H_{16}^-$	0.71	0.389	0.434

peak observed in PES results from the relative instability of the DRA with respect to the hydride–ammonia complex.

For n = 2 ($N_2H_7^-$), three structures appear in the photoelectron spectrum.[35] A complex of hydride with two ammonia molecules in C_2 symmetry is the most stable structure (see Figure 7.2). The VEDE increases an additional 0.35 eV to a total value of 1.46 eV. There is a small delocalization onto the ammonia molecules but the Dyson Orbital remains localized in the hydride. The complex of $NH_4^-(NH_3)$ is also formed and the VEDE is about 0.1 eV larger than for the NH_4^- DRA. The coordinating ammonia molecule points the three hydrogen atoms towards the tetrahedral DRA and the Dyson orbital is mainly localized around the DRA. The remaining structure, resembles the cation $N_2H_7^+$ where there is a hydrogen bond between NH_4^+ and NH_3. Adding two electrons to this cation yields the $N_2H_7^-$ DRA with a C_{3v} structure. The binding energy is slightly lower than for NH_4^- (0.415 eV) and the Dyson orbital is mainly localized on the hydrogen atoms that are bound to the cationic nitrogen. Agreement between this work, previous calculations and experiment is excellent.[35,36,92]

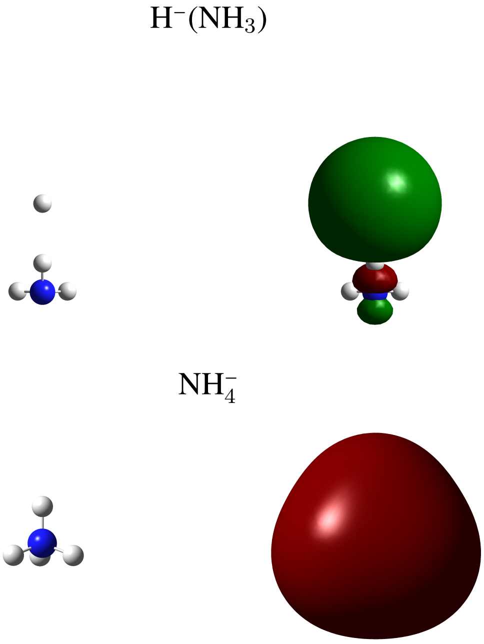

Figure 7.1: n = 1 structures and Dyson orbitals of electron detachment from anions

For n = 3 ($N_3H_{10}^-$), the spectrum is more complicated. First, the complex of hydride with three ammonia molecules in a C_3 structure (see Figure 7.3) has a binding energy about 0.35 eV higher (1.82 eV). Second, the DRA based on the $N_3H_{10}^+$ cationic C_{2v} structure is also observed at 0.424 eV. Then, combinations between DRAs and ammonia molecules can appear. However, not all of them are observed in the spectrum. This work, predicts VEDEs for $(NH_3)NH_4^-(NH_3)$, where both ammonia molecules coordinate from different angles, $NH_4^-[NH_3]_2$ where the DRA coordinates to an ammonia dimer (square brackets designate a hydrogen–bonded cluster) and to the $N_2H_7^-(NH_3)$ complex. The experimental spectrum has signals for $NH_4^-[NH_3]_2$ and $N_2H_7^-(NH_3)$ complexes but no signal for $(NH_3)NH_4^-(NH_3)$. This can be explained using the calculated relative energies, where the lowest structure is the hydride, then the relative energies for the DRA and DRA complexes are as follows: $N_3H_{10}^-$ 0.73 eV, $NH_4^-[NH_3]_2$ 0.96 eV, $N_2H_7^-(NH_3)$ 0.93 eV and $(NH_3)NH_4^-(NH_3)$ 1.05 eV. In addition, kinetic and orientation effects in the gas phase can also limit the formation of the last complex due to the need for a trimolecular interaction. Dyson orbitals appear in the DRA and VEDEs increase by about 0.1 eV when adding one ammonia molecule and about 0.2 eV when adding an ammonia hydrogen-bonded dimer. There is good agreement between this work and experiment.[35,92]

For n = 4 ($N_4H_{13}^-$), the spectrum is quite simple.[35] The hydride with four ammonia molecules arranges itself in a C_2 structure (see Figure 7.4) and has a binding energy about 0.3 eV higher for a total

$H^-(NH_3)_2$

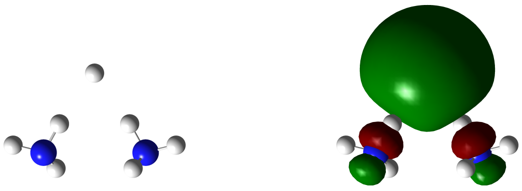

$NH_4^-(NH_3)$

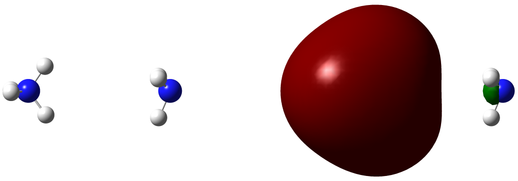

$N_2H_7^-$

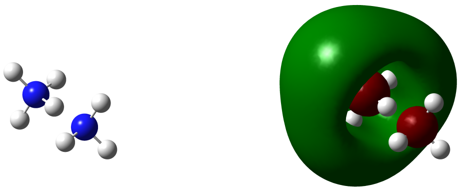

Figure 7.2: n = 2 structures and Dyson orbitals of electron detachment from anions

$H^-(NH_3)_3$

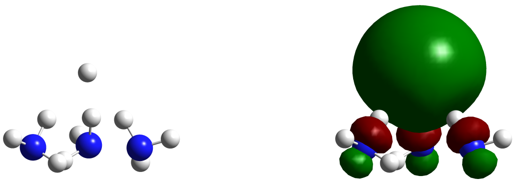

$NH_4^-(NH_3)_2$

$N_2H_7^-(NH_3)$

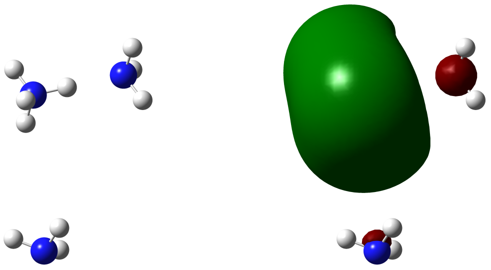

$N_3H_{10}^-$

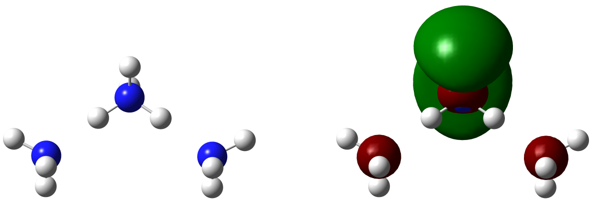

Figure 7.3: $n = 3$ structures and Dyson orbitals of electron detachment from anions

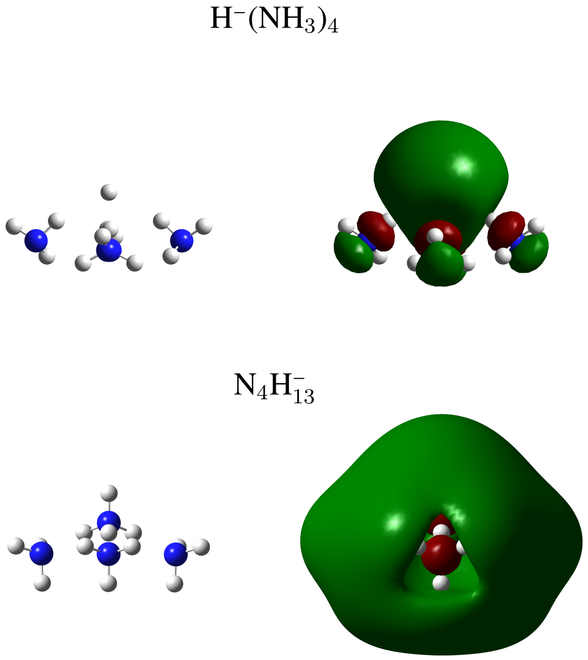

Figure 7.4: n = 4 structures and Dyson orbitals of electron detachment from anions

of 2.111 eV. The Dyson orbital is mainly localized in the hydride with some antibonding character in the N–H bonds. The DRA based on the $N_4H_{13}^+$ cation where an ammonium is hydrogen bound to three ammonia molecules in a C_{3v} structure has a VEDE of 0.427 eV. The Dyson orbital is delocalized around the hydrogen atoms of the neighboring amines and completely envelops the DRA. Agreement between experiment and this work is excellent.[35,92] In addition, this work predicts VEDEs and Dyson orbitals for DRAs complexes with ammonia molecules. (see Table 7.1 and Figure 7.4 for VEDEs and figures, respectively.) However, they are not observed in the spectrum. The relative energies between the DRAs complexes with ammonia for n = 3 and n = 4 are similar and the predicted complexes for n = 4 could be synthesized and studied spectroscopically.

For n = 5 ($N_5H_{16}^-$), the spectrum is also quite simple.[35] The hydride with five ammonia molecules arranges itself in a structure without symmetry (see Figure 7.5) where four ammonia molecules coordinate to the hydride in the first solvation shell and the remaining ammonia is hydrogen–bound to two ammonia units. The VEDE increases by 0.25 eV to a total of 2.36 eV and the Dyson orbital is dominated by the hydride orbital and antibonding character between the N–H bonds in the first solvation shell. The DRA corresponding to the $N_5H_{16}^+$ cation has completed the first solvation sphere in a tetrahedral structure. The Dyson orbital is symmetric around the tetrahedral structure and envelops the twelve

$H^-(NH_3)_5$

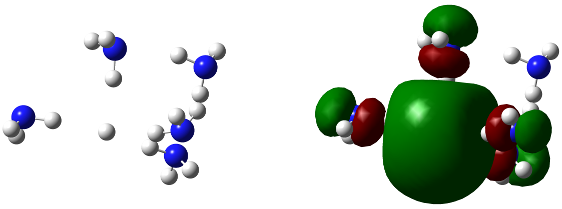

$N_5H_{16}^-$

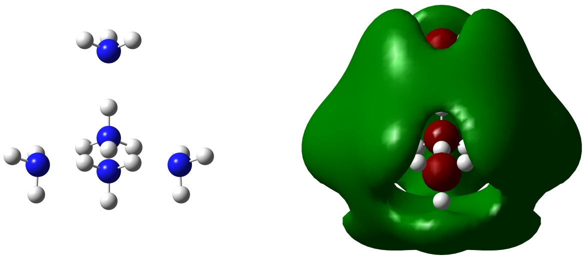

Figure 7.5: n = 5 structures and Dyson orbitals of electron detachment from anions

outer hydrogen atoms at an isovalue of 0.012. Computational predictions for $n = 2, 3, 4, 5$ for DRAs are between 0.39 and 0.41 eV while the experimental results are within 0.415 and 0.43 eV. Therefore, agreement between experiment and theory is excellent.[35,92]

Isomerization energies for $n = 4, 5$ DRAs are close to 0.7 eV but their peaks have high intensities in comparison with their corresponding hydrides. Meanwhile, the isomerization energy for NH_4^- is only 0.5 eV and the peak is relatively faint. Therefore, the experimental samples are far from equilibrium and kinetic products are available in the spectrum.

The photoelectron spectra contains additional peaks assigned to vibrational shifts and correlation final states. In this work, correlation final states occur when the Rydberg radical electron is excited to higher energy orbital and can be predicted by computational calculations of electron affinities of the closed–shell cations. Then, the excitation energies (EEs) of the Rydberg neutral radical are equal to the differences of the electron affinities.[101,102] Experimentally, these excitation energies can also be inferred from differences of VEDEs in PES.[88] For $n = 4, 5$, correlation states are observed in the spectrum and in Table 7.2 computational results show good agreement with experiments.[35,103,104] Because one experimental technique departs from the anion and the other departs from the neutral, the agreement between them and theory implies minor nuclear relaxation between the charged and neutral clusters.

The largest electron affinity is designated as EA_0 and correlates with the ground state of the Rydberg radical ($^2A_1$ or s–like). Figures 7.6 and 7.7 show Dyson orbitals for the electron affinities of the

Table 7.2: $N_nH^+_{3n+1}$ electron affinities and N_nH_{3n+1} excitation energies (eV)

n	EA_0	EA_1	EA_2	EEs–Theory	EE–Expt.[88]	EE–Expt.[103,104]
4	2.814	2.111	2.069	0.70, 0.75	0.83	0.81
5	2.570	1.988		0.58	0.70	0.71

Table 7.3: N_nH_{3n+1} excitation energies (eV)

l	n	Term	Energy	n	Term	Energy
s	4	$^2A_1$	0	5	$^2A_1$	0
p		^2E	0.703		$^2T_2$	0.582
		$^2A_1$	0.745			
d		$^2A_1$	1.368		$^2T_2$	1.200
		^2E	1.390		^2E	1.250
		^2E	1.464			
s		$^2A_1$	1.596		$^2A_1$	1.409
f		^2E	1.865		$^2T_1$	1.673
		$^2A_1$	1.921		$^2T_2$	1.757
		$^2A_2$	1.956		$^2A_1$	1.913
		^2E	2.143			
		$^2A_1$	2.156			
p		^2E	2.370		$^2T_2$	2.177
		$^2A_1$	2.373			
d		^2E	2.424		$^2T_2$	2.193
		$^2A_1$	2.547		^2E	2.200
		^2E	2.572			

closed–shell cations for n = 4 and 5, respectively. The Dyson orbitals for the first electron affinity of the cation and the first ionization energy of the anion are quite similar for both clusters. These Dyson orbitals have a semi-spherical shape with an approximate l quantum number of 0 (s–like) based in a hydrogenic characterization. For the second electron affinities of cations (EA_1), the Dyson orbitals have an approximate l quantum number of 1 (p–like) and for n = 4 there is a small energy difference of 0.05 eV between the p_z and the p_x, or degenerate p_y, orbitals. However for n = 5 all p–like states have the same energy. Table 7.3 displays excitation energies for n = 4 and 5 and their approximate l quantum numbers are based on a hydrogenic characterization of the Dyson orbitals. For both radicals, a pattern is observed: s, p, d, s, f, p and d.

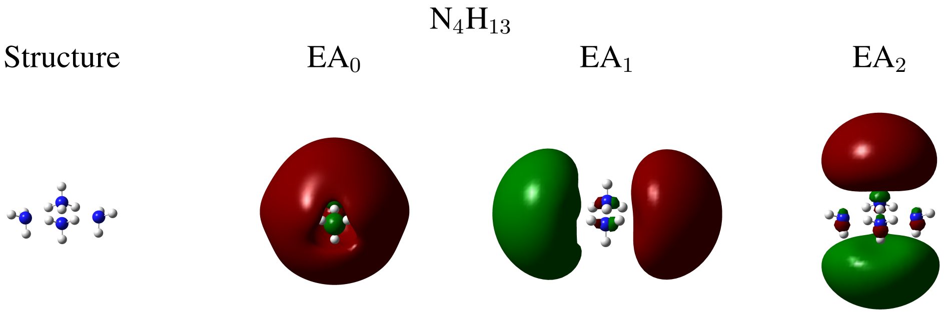

Figure 7.6: $N_4H_{13}^-$ structure and Dyson orbitals of electron attachment to cation

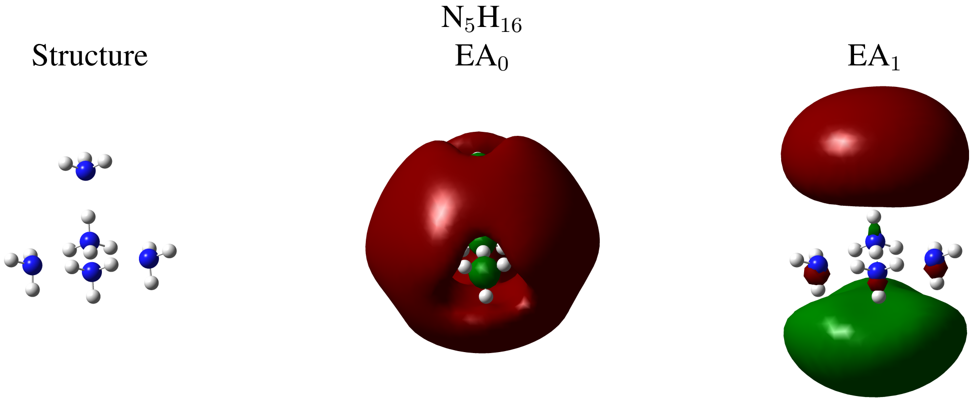

Figure 7.7: $N_5H_{16}^-$ structure and Dyson orbitals of electron attachment to cation

7.2 Double–Rydberg anions based on methylammmoniums, $(\mathrm{CH}_3)_n\mathrm{NH}_{4-n}^-$

Substitution of one or more hydrogen atoms by a methyl group in NH_4^- yields $(\mathrm{CH}_3)_n\mathrm{NH}_{4-n}^-$ clusters, for $n = 1, 2, 3, 4$. These clusters resemble protonated methyl amines and in their cationic forms are stable in aqueous solutions. Addition of one extra electron to these methylammoniums produces Rydberg neutral radicals. In this work, high quality calculations predict that the addition of two electrons to these methylammoniums would produce stable DRAs with VEDEs between 0.24 and 0.39 eV. In addition, Dyson orbitals obtained for these systems resemble Dyson orbitals obtained in the previous section.

Methodology

Structures of anions were optimized at the coupled–cluster singles and doubles (CCSD) level[93] with the 6-311++G(d,p) basis set[78,79,85] plus extra diffuse functions (exponents: H s 0.01080, N sp 0.01917). All frequencies were real. Electron binding energies were predicted with ΔCCSD(T)[64] and BDT1 EPT[5,94–96] using the augmented correlation consistent triple ζ basis–set[105–107] plus extra diffuse functions consisting of multiplying the most diffuse exponent by 0.3 of each angular momentum in all atoms (aug^2-cc-pVTZ). Brueckner–doubles coupled–cluster (BD)[97,98] calculations were performed with the oldfcbd and nosymm options.

All calculations were executed with the GDV version of Gaussian.[63]

Dyson orbitals of electron detachment from anions were plotted using Gaussview[99] from a cube file generated with an enhanced edge size in Molden.[100] Isovalues in the orbital plots are equal to 0.02 for $n = 1, 2$ and are equal to 0.01 for $n = 3, 4$.

Results

Predicted electron binding energies with both methods (ΔCCSD(T) and BDT1) are in good agreement with discrepancies lower than 0.025 eV, see Table 7.4. Dyson orbitals and optimized structures are shown in Figures 7.8–7.11. Anions with $n = 1$ and 4 have higher vertical electron binding energies (0.327 and 0.385 eV, respectively) and anions with $n = 2$ and 3 have lower binding energies (0.251 and 0.244 eV, respectively). The decrease of the binding energy by increasing the anion size have been seen also in the $\mathrm{N}_n\mathrm{H}_{3n+1}^-$ anions but the changes are less drastic that in this case. In addition, these methylammonium

Table 7.4: $(CH_3)_nNH_{4-n}^-$ predicted electron binding energies (eV)

n	DRA	Point group	BDT1[a]	ΔCCSD(T)[b]
1	$(CH_3)NH_3^-$	C_{3v}	0.350(0.84)	0.327
2	$(CH_3)_2NH_2^-$	C_{2v}	0.275(0.81)	0.251
3	$(CH_3)_3NH^-$	C_{3v}	0.278(0.77)	0.244
4	$(CH_3)_4N^-$	t_d	0.394(0.87)	0.385

[b] BDT1/aug^2-cc-pVTZ, PS values in parenthesis.

[c] ΔCCSD(T)/aug^2-cc-pVTZ.

$CH_3NH_3^-$

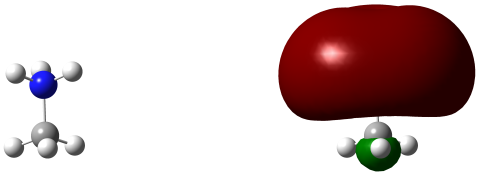

Figure 7.8: $CH_3NH_3^-$ Optimized structure (CCSD/6-311+^{2}+^{2}G(d,p)) and Dyson orbitals (isovalue = 0.02, HF/aug^2-cc-pVTZ)

DRAs have stronger correlation effects and different electronic states can be accessed complicating the accurate solution of these systems.

$(CH_3)_2NH_2^-$

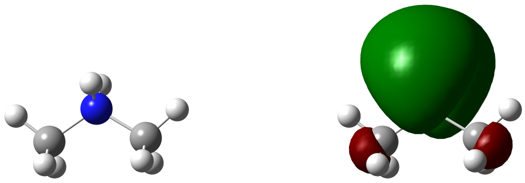

Figure 7.9: $(CH_3)_2NH_2^-$ Optimized structure (CCSD/6-311+^{2}+^{2}G(d,p)) and Dyson orbitals (isovalue = 0.02, HF/aug^2-cc-pVTZ)

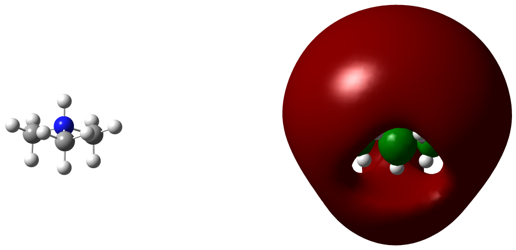

$(CH_3)_3NH^-$

Figure 7.10: $(CH_3)_3NH^-$ Optimized structure (CCSD/6-311$+^2+^2$G(d,p)) and Dyson orbitals (isovalue = 0.01, HF/aug^2-cc-pVTZ)

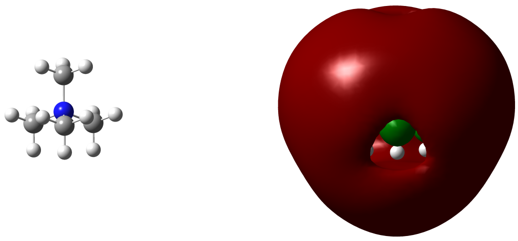

$(CH_3)_4N^-$

Figure 7.11: $(CH_3)_4N^-$ Optimized structure (CCSD/6-311$+^2+^2$G(d,p)) and Dyson orbitals (isovalue = 0.01, HF/aug^2-cc-pVTZ)

7.3 Double–Rydberg anions based on a protonated diamine, $NH_2(CH_3)_2NH_3^-$

An interesting system to work with is $NH_2(CH_3)_2NH_3^-$ because of the hydrogen bonding interaction between the nitrogen atoms. The global minimum calculated at the CCSD/6-311+^{2}+^{2}G(d,p) level (the basis set has extra diffuse functions with exponents: H s 0.01080, N sp 0.01917) is at 49.2 degrees in the dihedral angle between the N–C–C–N atoms, allowing the hydrogen bond to have a distance of 2.25 Å while negating the steric interactions by having a gauche configuration.

Methodology

The structure of the DRA $NH_2(CH_3)_2NH_3^-$ was optimized with the CCSD method and the 6-311+^{2}+^{2}G(d,p) basis–set. All frequencies were real. The vertical electron binding energy for the first ionization energy was predicted with ΔCCSD(T) and BDT1 using aug^2-cc-pVTZ. Brueckner–doubles coupled–cluster (BD) calculations were performed with the oldfcbd and nosymm options. Calculations were executed with the GDV version of Gaussian.[63]

The Dyson orbital for the first ionization energy was plotted using Gaussview[99] with 0.02 isovalue.

Results

The predicted electron binding energy is 0.311 and 0.299 eV with BDT1 and ΔCCSD(T), respectively. This result is similar to $(CH_3)_2NH_2^-$ and we seem to predict that the substitution of hydrogen for carbon decreases the binding energy. This can be due to the inductive effect of carbon to stabilize the cationic core. In general, a stable covalent cation has a delocalized charge in a large and polarizable structure, like a soft acid. Then, the respective DRA will be less bound.

Calculations performed with the CCSD/6-311+^{2}+^{2}G(d,p) give rotational barriers of 0.15 and 0.30 eV at 0 and 120 degrees in the dihedral angle. In addition, ΔCCSD results yield a decrease of 0.05 eV in the binding energy when the dihedral angle is close to 120 degrees instead of 49 while the binding energy increases by 0.02 eV when going close to zero degrees.

Table 7.5: $NH_2(CH_3)_2NH_3^-$ predicted electron binding energy (eV)

dih^a	BDT1[b]	ΔCCSD(T)[c]
49.2	0.311(0.794)	0.299

[a] Dihedral angle between NCCN atoms.

[b] BDT1/aug^2-cc-pVTZ,

PS values in parenthesis.

[c] ΔCCSD(T)/aug^2-cc-pVTZ.

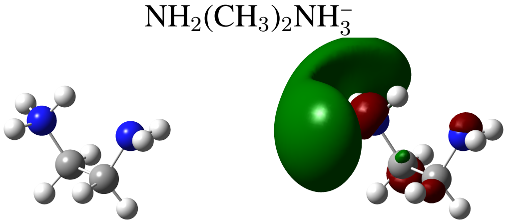

Figure 7.12: $NH_2(CH_3)_2NH_3^-$ Optimized structure (CCSD/6-311+^{2}+^{2}G(d,p)) and Dyson orbital (isovalue = 0.02, HF/aug^2-cc-pVTZ)

7.4 Double–Rydberg anions triplet states, $NH_4NH_3^-$ $NH_3CH_3^-$

In this section, triplet DRAs are predicted to exist for $NH_4NH_3^-$ and $NH_3CH_3^-$. High level calculations are used for geometry optimization and VEDEs prediction. Both structures have C_{3v} symmetry and both Rydberg electrons are in an a_1 orbital. For DRAs, triplet states require more diffuse functions than singlets to converge optimizations and VEDEs. Optimizations with quadruple augmentations are needed for $NH_4NH_3^-$. For $NH_3CH_3^-$, convergence of bonds and angles are obtained only with hextuple augmentations. Predicted VEDEs are 0.113 and 0.014 eV. for $NH_4NH_3^-$ and $NH_3CH_3^-$, respectively.

Methodology

The structures of the triplets DRAs were optimized with the CCSD method using the 6-311+^{4}+^{4}G(d,p) and 6-311+^{6}+^{6}G(d,p) basis–sets for the $NH_4NH_3^-$ and $NH_3CH_3^-$ clusters, respectively. All frequencies were real.

The vertical electron binding energy for the first ionization energy was predicted with the ΔCCSD(T) and P3+[108] methods using the aug^4-cc-pVTZ basis set. Calculations were executed with the G16 version of Gaussian.[63]

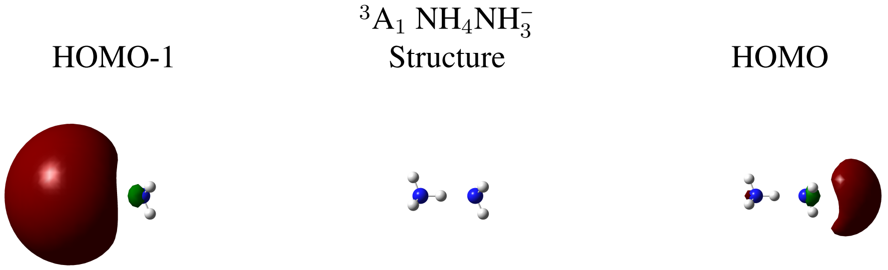

HOMO-1

$^3A_1$ $NH_4NH_3^-$
Structure

HOMO

Figure 7.13: $^3A_1$ $NH_4NH_3^-$ Optimized structure (CCSD/6-311+^{4}+^{4}G(d,p)) and Dyson orbitals (isovalue = 0.015, HF/aug^4-cc-pVTZ)

Optimizations and VEDEs were augmented until convergence of bond distances, angles and VEDEs was reached. The Dyson orbitals for the first ionization energy were plotted using Gaussview[99] using cube files generated with extended dimensions using Molden. The isovalues were 0.015 and 0.006 for $NH_4NH_3^-$ and $NH_3CH_3^-$, respectively.

Results

For the triplet DRA $NH_4NH_3^-$ ($^3A_1$), the structure is C_{3v} and the Rydberg electrons are localized in opposite sides of the anion. The HOMO is localized on the NH_3 side while the HOMO-1 is localized on the NH_4 side, see Figure 7.13. Labeling the NH_4 nitrogen as a and the NH_3 nitrogen as b, the distances N_a–H, N_a–H_{mid}, N_b–H and N_b–H_{mid} are 1.0323, 1.0656, 1.0211 and 1.7788 Å, respectively. The H_{mid}–N_a–H and H_{mid}–N_b–H angles are 111.14 and 113.54 degrees, respectively.

For the triplet DRA $NH_3CH_3^-$ ($^3A_1$), the structure is also C_{3v} and the Rydberg electrons are localized in opposite sides of the anion. The HOMO is localized in the CH_3 side while the HOMO-1 is localized in the NH_3 side, see Figure 7.14. The distances N–H, N–C, C–H are 1.0395, 1.5042 and 1.0905 Å, respectively. The C–N–H and N–C–H angles are 112.02 and 108.22 degrees, respectively.

The predicted VEDE for the triplet DRA $NH_4NH_3^-$ ($^3A_1$) is 0.113 eV at the ΔCCSD(T) level (0.148 eV at the P3+ level) with a relative energy of 0.310 eV with respect to the singlet $NH_4NH_3^-$ ($^1A_1$). Also, the predicted VEDE for the triplet DRA $NH_3CH_3^-$ ($^3A_1$) is 0.014 eV at the ΔCCSD(T) level (0.023 eV at the P3+ level) with a relative energy of 0.316 eV with respect to the singlet $NH_3CH_3^-$ ($^1A_1$). Therefore, this DRAs could be detected in PES experiments because high energy DRAs have been observed previously.[26,35,88]

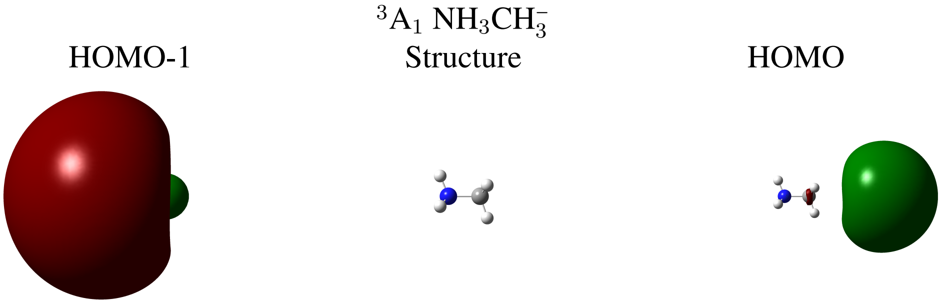

Figure 7.14: $^3A_1$ $NH_3CH_3^-$ Optimized structure (CCSD/6-311+^{6}+^{6}G(d,p)) and Dyson orbitals (isovalue = 0.006, HF/aug^4-cc-pVTZ)

7.5 Conclusions

This work first shows an excellent agreement between experimental results and the BDT1 electron propagator method for DRAs of the formula $N_nH_{3n+1}^-$ for the prediction of VEDEs. VEDEs for DRAs are between 0.47 and 0.43 eV. The minimum in energy for these clusters is the hydride coordinated to ammonia molecules and high energy hydrogen bonded DRAs and DRAs interacting with the dipole of ammonia molecules or clusters are also observed in the spectra. Then, calculations for methylic amines were performed with similar optimization techniques and now including comparisons between ΔCCSD(T) and BDT1. Lower VEDEs are obtained for these systems, 0.24 to 0.39 eV. Extra calculations in excited Rydberg neutral radicals and complexes with ammonia molecules could yield interesting results in the future. Good agreement between ΔCCSD(T) and BDT1 motivates the search for these DRAs experimentally. For $NH_2(CH_3)_2NH_3^-$, CCSD optimizations find a minimum when the dihedral angle between the N–C–C–N angle is 49.2 degrees. The predicted VEDE is 0.299 eV at the ΔCCSD level and in close agreement with BDT1. Change of the dihedral angle can either increase or decrease the VEDE. More calculations can be performed by double protonation and double reduction. This system is quite interesting because bonding and antibonding character might be found between the two Rydberg–like electrons. Finally, spherical DRAs like NH_4^- and $N_5H_{16}^-$ cannot have triplet DRAs because in order to do that they need to promote both electrons to p–like orbitals. However, systems like $NH_4NH_3^-$ and $NH_3CH_3^-$ have two similar a_1 orbitals localized on opposite sides of the molecule. Both triplet DRAs are bound and could be observed in PES experiments.

References

[1] J.-F. Li, M.-M. Li, H. Bai, Y.-Y. Sun, J.-L. Li, and B. Yin. “Probing the Properties of Polynuclear Superhalogens without Halogen Ligand via ab Initio Calculations: A Case Study on Double-Bridged [Mg2(CN)5]$^{-1}$ Anions”. *ChemPhysChem*, **16**:3652–3659, 2015.

[2] K. Kimura, S. Katsumata, Y. Achiba, T. Yamazaki, and S. Iwata. *Ionization energies, Ab initio assignments, and valence electronic structure for 200 molecules in Handbook of HeI Photoelectron Spectra of Fundamental Organic Compounds*. Japan Scientific Soc. Press, Tokyo, 1981.

[3] J. V. Ortiz. *The Electron Propagator Picture of Molecular Electronic Structure*, chapter 1, pages 1–61. World Scientific: Singapore, 1997.

[4] J. Linderberg and Y. Öhrn. *Propagators in quantum chemistry*. John Wiley & Sons, 2004.

[5] J. V. Ortiz. “Electron propagator theory: an approach to prediction and interpretation in quantum chemistry”. *WIREs Comput. Mol. Sci.*, **3**:123–142, 2013.

[6] M. Díaz-Tinoco and J. V. Ortiz. “Comment on ”Are polynuclear superhalogens without halogen atoms probable? A high-level ab initio case study on triple-bridged binuclear anions with cyanide ligands” [J. Chem. Phys. 140, 094301 (2014)]”. *J. Chem. Phys.*, **145**:147101, 2016.

[7] J. V. Ortiz. “A Nondiagonal, Renormalized Extension Of Partial Third–order Quasiparticle Theory: Comparisons For Closed–shell Ionization Energies”. *J. Chem. Phys.*, **108**:1008–1014, 1998.

[8] J. A. Pople, M. Head-Gordon, D. J. Fox, K. Raghavachari, and L. A. Curtiss. “Gaussian-1 theory: A general procedure for prediction of molecular energies”. *J. Chem. Phys.*, **90**:5622–29, 1989.

[9] L. A. Curtiss, C. Jones, G. W. Trucks, K. Raghavachari, and J. A. Pople. “Gaussian-1 theory of molecular energies for second-row compounds”. *J. Chem. Phys.*, **93**:2537–45, 1990.

[10] L. A. Curtiss, K. Raghavachari, G. W. Trucks, and J. A. Pople. “Gaussian-2 theory for molecular energies of first- and second-row compounds”. *J. Chem. Phys.*, **94**:7221–30, 1991.

[11] L. A. Curtiss, P. C. Redfern, K. Raghavachari, and J. A. Pople. “Assessment of Gaussian-2 and density functional theories for the computation of ionization potentials and electron affinities”. *J. Chem. Phys.*, **109**:42–55, 1998.

[12] L. A. Curtiss, K. Raghavachari, P. C. Redfern, V. Rassolov, and J. A. Pople. “Gaussian-3 (G3) theory for molecules containing first and second-row atoms”. *J. Chem. Phys.*, **109**:7764–76, 1998.

[13] L. A. Curtiss, P. C. Redfern, and K. Raghavachari. “Gaussian-4 theory”. *J. Chem. Phys.*, **126**: 084108, 2007.

[14] J. M. L. Martin and G. de Oliveira. “Towards standard methods for benchmark quality ab initio thermochemistry–W1 and W2 theory”. *J. Chem. Phys.*, **111**:1843–1856, 1999.

[15] S. Parthiban and J. M. L. Martin. “Assessment of W1 and W2 theories for the computation of electron affinities, ionization potentials, heats of formation, and proton affinities”. *J. Chem. Phys.*, **114**:6014–6029, 2001.

[16] A. Tajti, P. G. Szalay, A. G. Császár, M. Kállay, J. Gauss, E. F. Valeev, B. A. Flowers, J. Vázquez, and J. F. Stanton. “Heat: High accuracy extrapolated ab initio thermochemistry”. *J. Chem. Phys.*, **121**:11599–11613, 2004.

[17] N. J. DeYonker, T. R. Cundari, and A. K. Wilson. “The correlation consistent composite approach (ccCA): An alternative to the Gaussian-n methods”. *J. Chem. Phys.*, **124**:114104, 2006.

[18] D. Feller. “The use of systematic sequences of wave functions for estimating the complete basis set, full configuration interaction limit in water”. *J. Chem. Phys.*, **98**:7059–7071, 1993.

[19] T. Helgaker, W. Klopper, H. Koch, and J. Noga. “Basis-set convergence of correlated calculations on water”. *J. Chem. Phys.*, **106**:9639–9646, 1997.

[20] H. H. Corzo, A. Galano, O. Dolgounitcheva, V. G. Zakrzewski, and J. V. Ortiz. “NR2 and P3+: Accurate, Efficient Electron-Propagator Methods for Calculating Valence, Vertical Ionization Energies of Closed-Shell Molecules”. *J. Phys. Chem. A*, **119**:8813–8821, 2015.

[21] M. Díaz-Tinoco, O. Dolgounitcheva, V. G. Zakrzewski, and J. V. Ortiz. “Composite electron propagator methods for calculating ionization energies”. *J. Chem. Phys.*, **144**:224110, 2016.

[22] A. M. Velasco, C. Lavín, O. Dolgounitcheva, and J. V. Ortiz. “Excitation energies, photoionization cross sections, and asymmetry parameters of the methyl and silyl radicals”. *J. Chem. Phys.*, **141**:074308, 2014.

[23] A. M. Velasco, C. Lavín, M. Díaz-Tinoco, and J. V. Ortiz. “CaH Rydberg series, oscillator strengths and photoionization cross sections from Molecular Quantum Defect and Dyson Orbital theories”. *J. Quant. Spectrosc. Radiat. Transf.*, **187**:161 – 166, 2017.

[24] H. H. Corzo, A. M. Velasco, C. Lavín, and J. V. Ortiz. “MgH Rydberg series: Transition energies from electron propagator theory and oscillator strengths from the molecular quantum defect orbital method”. *J. Quant. Spectrosc. Radiat. Transf.*, **206**:323 – 327, 2018.

[25] A. N. Alexandrova, A. I. Boldyrev, H.-J. Zhai, and L.-S. Wang. “All-boron aromatic clusters as potential new inorganic ligands and building blocks in chemistry”. *Coordin. Chem. Rev.*, **250**: 2811 – 2866, 2006.

[26] J. T. Snodgrass, J. V. Coe, C. B. Freidhoff, K. M. McHugh, and K. H. Bowen. “Photodetachment spectroscopy of cluster anions. Photoelectron spectroscopy of $H^{-}(NH_3)_1$, $H^{-}(NH_3)_2$ and the tetrahedral isomer of NH_4^-”. *Faraday Discuss. Chem. Soc.*, **86**:241–256, 1988.

[27] J. V. Ortiz. “Vertical and adiabatic ionization energies of NH_4^- isomers via electron propagator theory and many body perturbation theory calculations with large basis sets”. *J. Chem. Phys.*, **87**: 3557–3562, 1987.

[28] M. Díaz-Tinoco, H. H. Corzo, and J. V. Ortiz. “Electron Propagator Methods for Vertical Electron Detachment Energies of Anions: Benchmarks and Case Studies”. *J. Chem. Theory Comput.*, **14**: 5881–5895, 2018.

[29] M. J. Frisch, G. W. Trucks, H. B. Schlegel, G. E. Scuseria, M. A. Robb, J. R. Cheeseman, G. Scalmani, V. Barone, G. A. Petersson, H. Nakatsuji, X. Li, M. Caricato, A. V. Marenich, J. Bloino, B. G. Janesko, R. Gomperts, B. Mennucci, H. P. Hratchian, J. V. Ortiz, A. F. Izmaylov, J. L. Sonnenberg, D. Williams-Young, F. Ding, F. Lipparini, F. Egidi, J. Goings, B. Peng, A. Petrone,

T. Henderson, D. Ranasinghe, V. G. Zakrzewski, J. Gao, N. Rega, G. Zheng, W. Liang, M. Hada, M. Ehara, K. Toyota, R. Fukuda, J. Hasegawa, M. Ishida, T. Nakajima, Y. Honda, O. Kitao, H. Nakai, T. Vreven, K. Throssell, J. A. Montgomery, Jr., J. E. Peralta, F. Ogliaro, M. J. Bearpark, J. J. Heyd, E. N. Brothers, K. N. Kudin, V. N. Staroverov, T. A. Keith, R. Kobayashi, J. Normand, K. Raghavachari, A. P. Rendell, J. C. Burant, S. S. Iyengar, J. Tomasi, M. Cossi, J. M. Millam, M. Klene, C. Adamo, R. Cammi, J. W. Ochterski, R. L. Martin, K. Morokuma, O. Farkas, J. B. Foresman, and D. J. Fox. “Gaussian16 Revision B.01”, 2016. Gaussian Inc. Wallingford CT.

[30] M. Díaz-Tinoco and J. V. Ortiz. “Comment on “Is the regulation of the electronic properties of organic molecules by polynuclear superhalogens more effective than that by mononuclear superhalogens? A high-level ab initio case study” by M.-M. Li, J.-F. Li, H.-C. Bai, Y.-Y. Sun, J.-L. Li and B. Yin, Phys. Chem. Chem. Phys., 2015, 17, 20338”. *Phys. Chem. Chem. Phys.*, **18**: 15456–15457, 2016.

[31] M. Díaz-Tinoco and J. V. Ortiz. “Comment on: “Probing the Properties of Polynuclear Superhalogens without Halogen Ligand via ab Initio Calculations: A Case Study on Double–Bridged $[Mg_2(CN)_5]^{-1}$ Anions” by Li et al.”. *ChemPhysChem.*, **17**:2945–2946, 2016.

[32] G. L. Gustev and A. I. Boldyrev. “DVM-Xα calculations on the ionization potentials of MX_{k+1}^- complex anions and the electron affinities of MX_{k+1} “superhalogens””. *Chem. Phys.*, **56**:277–283, 1981.

[33] X.-B. Wang, C.-F. Ding, L.-S. Wang, A. I. Boldyrev, and J. Simons. “First Experimental Photoelectron Spectra of Superhalogens and their Theoretical Interpretations”. *J. Chem. Phys.*, **110**: 4763–4771, 1999.

[34] M. Díaz-Tinoco and J. V. Ortiz. “Carborane superhalide bases and their conjugate Brønsted-Lowry Superacids: Electron binding energies and Dyson orbitals”. *Chem. Phys.*, **521**:77–84, 2019.

[35] S.-J. Xu, J. M. Nilles, J. H. Hendricks, S. A. Lyapustina, and K. H. Bowen. “Double Rydberg anions: Photoelectron spectroscopy of NH_4^-, $N_2H_7^-$, $N_3H_{10}^-$, $N_4H_{13}^-$, and $N_5H_{16}^-$”. *J. Chem. Phys.*, **117**:5742–5747, 2002.

[36] J. V. Ortiz. "A double Rydberg anion with a hydrogen bond and a solvated double Rydberg anion: Interpretation of the photoelectron spectrum of $N_2H_7^-$". *J. Chem. Phys.*, **117**:5748–5756, 2002.

[37] J. Schirmer, L. S. Cederbaum, and O. Walter. "New approach to the one– particle Green's function for finite Fermi systems". *Phys. Rev. A*, **28**:1237–1259, 1983.

[38] D. M. McQuarrie and J. D. Simon. *Physical chemistry a molecular approach*. University Science Books, Sausalito, California, 1997.

[39] C. D. Sherrill. "The Born–Oppenheimer approximation", 2005. URL `http://vergil.chemistry.gatech.edu/notes/bo/`.

[40] A. Szabo and N. S. Ostlund. *Modern quantum chemistry: introduction to advanced electronic structure theory*. Dover Publications, New York, 1996.

[41] D. R. Hartree. "The wave mechanics of an atom with a non–Coulomb central field. Part I. Theory and methods". *Proc. Camb. Phil. Soc.*, **24**:89–110, 1928.

[42] D. R. Hartree. "The wave mechanics of an atom with a non–Coulomb central field. Part II. Some results and discussion". *Proc. Camb. Phil. Soc.*, **24**:111–132, 1928.

[43] J. A. Gaunt. "A theory of Hartree's atomic fields". *Proc. Camb. Phil. Soc.*, **24**:328–342, 1928.

[44] V. A. Fock. "Näherungsmethode zur lösung des quantenmechanischen mehrkörperproblems". *Z. Phys. A.*, **61**:126–148, 1930.

[45] H. H. Corzo and J. V. Ortiz. "Electron propagator theory: Foundations and predictions". In *Adv. Quantum Chem.*, volume 74, pages 267–298. Elsevier, 2017.

[46] L. S. Cederbaum and W. Domcke. "Theoretical aspects of ionization potentials and photoelectron spectroscopy: a green's function approach". In *Adv. Chem. Phys.*, volume 36, pages 205–344. John Wiley & Sons, Inc., 1977.

[47] Y. Öhrn and G. Born. "Molecular electron propagator theory and calculations". In P.-O. Löwdin, editor, *Adv. Quantum Chem.*, volume 13, pages 1–88. Academic Press, 1981.

[48] W. von Niessen, J. Schirmer, and L. S. Cederbaum. "Computational methods for the one-particle Green's function". *Comput. Phys. Rep.*, **1**:57–125, 1984.

[49] J. V. Ortiz. “Toward an exact one-electron picture of chemical bonding”. In P.-O. Löwdin, editor, *Adv. Quantum Chem.*, volume 35, pages 33–52. Academic Press, 1999.

[50] P. Jørgensen and J. Simons. *Second quantization-based methods in quantum chemistry, 1st ed.* Academic, New York, NY, 1981.

[51] J. Simons. “Equations of motion theory for electron affinities”. *Collect. Czech Chem. Commun.*, **70**:579–604, 2005.

[52] M. F. Herman, K. F. Freed, and D. L. Yeager. “Analysis and evaluation of ionization potentials, electron affinities, and excitation energies by the equations of motion–Green’s function method”. In *Adv. Chem. Phys.*, pages 1–69. John Wiley & Sons, Inc., 1981.

[53] B. T. Pickup and O. Goscinski. “Direct calculation of ionization energies”. *Mol. Phys.*, **26**: 1013–1035, 1973.

[54] O. Goscinski and B. Lukman. “Moment-conserving decoupling of Green functions via Pade approximants”. *Chem. Phys. Lett.*, **7**:573–576, 1970.

[55] P.-O. Löwdin. “Studies in perturbation theory. X. Lower bounds to energy eigenvalues in perturbation–theory ground state”. *Phys. Rev.*, **139**:A357–A372, 1965.

[56] C. Møller and M. S. Pleßet. “Note on an approximation treatment for many-electron systems”. *Phys. Rev.*, **46**:618–622, 1934.

[57] K. A. Brueckner. “Two-Body Forces and Nuclear Saturation. III. Details of the Structure of the Nucleus”. *Phys. Rev.*, **97**:1353–1366, 1955.

[58] J. Goldstone. “Derivation of the Brueckner many-body theory”. *Proc. Roy. Soc. Lond. A*, **239**: 267–279, 1957.

[59] R. D. Mattuck. *A Guide to Feynman Diagrams in the Many Body Problem.* McGraw-Hill: New York., 1967.

[60] H. P. Kelly. “Correlation Effects in Atoms”. *Phys. Rev.*, **131**:684–699, 1963.

[61] C. Bloch and J. Horowitz. “Sur la determination des premiers etats d’un systeme de fermions dans le cas degenere”. *Nucl. Phys.*, **8**:91–105, 1958.

[62] B. H. Brandow. “Linked–Cluster Expansions for the Nuclear Many–Body Problem”. *Rev. Mod. Phys.*, **39**:771–828, 1967.

[63] M. J. Frisch, G. W. Trucks, H. B. Schlegel, G. E. Scuseria, M. A. Robb, J. R. Cheeseman, G. Scalmani, V. Barone, G. A. Petersson, H. Nakatsuji, X. Li, M. Caricato, A. V. Marenich, J. Bloino, B. G. Janesko, R. Gomperts, B. Mennucci, H. P. Hratchian, J. V. Ortiz, A. F. Izmaylov, J. L. Sonnenberg, D. Williams-Young, F. Ding, F. Lipparini, F. Egidi, J. Goings, B. Peng, A. Petrone, T. Henderson, D. Ranasinghe, V. G. Zakrzewski, J. Gao, N. Rega, G. Zheng, W. Liang, M. Hada, M. Ehara, K. Toyota, R. Fukuda, J. Hasegawa, M. Ishida, T. Nakajima, Y. Honda, O. Kitao, H. Nakai, T. Vreven, K. Throssell, J. A. Montgomery, J. E. Peralta, Jr., F. Ogliaro, M. J. Bearpark, J. J. Heyd, E. N. Brothers, K. N. Kudin, V. N. Staroverov, T. A. Keith, R. Kobayashi, J. Normand, K. Raghavachari, A. P. Rendell, J. C. Burant, S. S. Iyengar, J. Tomasi, M. Cossi, J. M. Millam, M. Klene, C. Adamo, R. Cammi, J. W. Ochterski, R. L. Martin, K. Morokuma, O. Farkas, J. B. Foresman, and D. J. Fox. “Gaussian development version, Revision I.11”, 2016. Gaussian Inc. Wallingford CT.

[64] K. Raghavachari, G. W. Trucks, J. A. Pople, and M. Head-Gordon. “A fifth-order perturbation comparison of electron correlation theories”. *Chem. Phys. Lett.*, **157**:479–483, 1989.

[65] M. M. Meyer, X.-B. Wang, C. A. Reed, L.-S. Wang, and S. R. Kass. “Investigating the Weak to Evaluate the Strong: An Experimental Determination of the Electron Binding Energy of Carborane Anions and the Gas phase Acidity of Carborane Acids”. *J. Am. Chem. Soc.*, **131**:18050–18051, 2009.

[66] M. Buehl, P. v. R. Schleyer, Z. Havlas, D. Hnyk, and S. Hermanek. “On the origin of the antipodal effect in closo-heteroboranes”. *Inorg. Chem.*, **30**:3107–3111, 1991.

[67] M. Díaz-Tinoco, J. Romero, J. V. Ortiz, A. Reyes, and R. Flores-Moreno. “A generalized any-particle propagator theory: Prediction of proton affinities and acidity properties with the proton propagator”. *J. Chem. Phys.*, **138**:194108, 2013.

[68] F. A. Cotton. “Proposed nomenclature for olefin-metal and other organometallic complexes”. *J. Am. Chem. Soc.*, **90**:6230–6232, 1968.

[69] T. Ichino, S. W. Wren, K. M. Vogelhuber, A. J. Gianola, W. C. Lineberger, and J. F. Stanton. "The vibronic level structure of the cyclopentadienyl radical". *J. Chem. Phys.*, **129**:084310, 2008.

[70] A. Velian and C. C. Cummins. " Synthesis and characterization of $P_2N_3^-$: An aromatic ion composed of phosphorus and nitrogen ". *Science*, **348**:1001–1004, 2015.

[71] G.-L. Hou, B. Chen, W. J. Transue, D. A. Hrovat, C. C. Cummins, W. T. Borden, and X.-B. Wang. "Negative ion photoelectron spectroscopy of $P_2N_3^-$: electron affinity and electronic structures of P_2N_3". *Chem. Sci.*, **7**:4667–4675, 2016.

[72] Y. Jin, A. Perera, and R. J. Bartlett. "Spectroscopic analysis of diphosphatriazolate anion ($P_2N_3^-$) by coupled-cluster methods as a step toward N_5^-". *Chem. Phys. Lett.*, **640**:68–71, 2015.

[73] G. L. Gutsev and A. I. Boldyrev. "The theoretical investigation of the electron affinity of chemical compounds". *Adv. Chem. Phys.*, **61**:169–221, 1985.

[74] G. L. Gutsev, C. A. Weatherford, L. E. Johnson, and P. Jena. "Structure and properties of the aluminum borates $Al(BO_2)_n$ and $Al(BO_2)_n^-$, (n = 1–4)". *J. Comput. Chem.*, **33**:416–424, 2012.

[75] M.-M. Li, J.-F. Li, H. Bai, Y.-Y. Sun, J.-L. Li, and B. Yin. "Is the regulation of the electronic properties of organic molecules by polynuclear superhalogens more effective than that by mononuclear superhalogens? a high-level ab initio case study". *Phys. Chem. Chem. Phys.*, **17**:20338–20346, 2015.

[76] V. G. Zakrzewski, J. V. Ortiz, J. A. Nichols, D. Heryadi, D. L. Yeager, and J. T. Golab. "Comparison of perturbative and multiconfigurational electron propagator methods". *Int. J. Quantum Chem.*, **60**:29–36, 1996.

[77] M. J. Frisch, G. W. Trucks, H. B. Schlegel, G. E. Scuseria, M. A. Robb, J. R. Cheeseman, G. Scalmani, V. Barone, B. Mennucci, G. A. Petersson, H. Nakatsuji, M. Caricato, X. Li, H. P. Hratchian, A. F. Izmaylov, J. Bloino, G. Zheng, J. L. Sonnenberg, M. Hada, M. Ehara, K. Toyota, R. Fukuda, J. Hasegawa, M. Ishida, T. Nakajima, Y. Honda, O. Kitao, H. Nakai, T. Vreven, J. J. A. Montgomery, J. E. Peralta, F. Ogliaro, M. Bearpark, J. J. Heyd, E. Brothers, K. N. Kudin, V. N. Staroverov, R. Kobayashi, J. Normand, K. Raghavachari, A. Rendell, J. C. Burant, S. S. Iyengar, J. Tomasi, M. Cossi, N. Rega, J. M. Millam, M. Klene, J. E. Knox, J. B. Cross, V. Bakken,

C. Adamo, J. Jaramillo, R. Gomperts, R. E. Stratmann, O. Yazyev, A. J. Austin, R. Cammi, C. Pomelli, J. W. Ochterski, R. L. Martin, K. Morokuma, V. G. Zakrzewski, G. A. Voth, P. Salvador, J. J. Dannenberg, S. Dapprich, A. D. Daniels, O. Farkas, J. B. Foresman, J. V. Ortiz, J. Cioslowski, and D. J. Fox. “Gaussian09 Revision D.01”, 2009. Gaussian Inc. Wallingford CT 2009.

[78] K. Raghavachari, J. S. Binkley, R. Seeger, and J. A. Pople. “Self–Consistent Molecular Orbital Methods. 20. Basis set for correlated wave–functions”. *J. Chem. Phys.*, **72**:650–654, 1980.

[79] T. Clark, J. Chandrasekhar, G. W. Spitznagel, and P. v. R. Schleyer. “Efficient diffuse function–augmented basis–sets for anion calculations. 3. The 3-21+G basis set for 1st–row elements, Li–F”. *J. Comp. Chem.*, **4**:294–301, 1983.

[80] A. Schaefer, H. Horn, and R. Ahlrichs. “Fully optimized contracted Gaussian-basis sets for atoms Li to Kr”. *J. Chem. Phys.*, **97**:2571–2577, 1992.

[81] A. Schaefer, C. Huber, and R. Ahlrichs. “Fully optimized contracted Gaussian-basis sets of triple zeta valence quality for atoms Li to Kr”. *J. Chem. Phys.*, **100**:5829–5835, 1994.

[82] F. Weigend and R. Ahlrichs. “Balanced basis sets of split valence, triple zeta valence and quadruple zeta valence quality for H to Rn: Design and assessment of accuracy”. *Phys. Chem. Chem. Phys.*, **7**:3297–3305, 2005.

[83] B. Yin, T. Li, J.-F. Li, Y. Yu, J.-L. Li, Z.-Y. Wen, and Z.-Y. Jiang. “Are polynuclear superhalogens without halogen atoms probable? A high-level ab initio case study on triple-bridged binuclear anions with cyanide ligands”. *J. Chem. Phys.*, **140**:094301, 2014.

[84] L. S. Cederbaum. “One–body Green’s function for atoms and molecules: theory and application”. *J. Phys. B.*, **8**:290–303, 1975.

[85] M. J. Frisch, J. A. Pople, and J. S. Binkley. “Self–Consistent Molecular Orbital Methods. 25. Supplementary Functions for Gaussian Basis Sets”. *J. Chem. Phys.*, **80**:3265–3269, 1984.

[86] T. J. Lee and P. R. Taylor. “A diagnostic for determining the quality of single-reference electron correlation methods”. *Int. J. Quantum Chem.*, **S23**:199–207, 1989.

[87] G. Herzberg and J. T. Hougen. "Spectra of the ammonium radical: The Schuster band of ND_4". *J. Mol. Spectrosc.*, **97**:430–440, 1983.

[88] D. Radisic, S. T. Stokes, and K. H. Bowen. "Two new double Rydberg anions plus access to excited states of neutral Rydberg radicals via anion photoelectron spectroscopy". *J. Chem. Phys.*, **123**:011101, 2005.

[89] M. Gutowski, J. Simons, R. Hernandez, and H. L. Taylor. ""Double-Rydberg" molecular anions". *J. Phys. Chem.*, **92**:6179–6182, 1988.

[90] N. Matsunaga and M. S. Gordon. "A Theoretical Study of NH_4^- and PH_4^-". *J. Phys. Chem.*, **99**: 12773–12780, 1995.

[91] Q. Hu, H. Song, C. J. Johnson, J. Li, H. Guo, and R. E. Continetti. "Imaging a multidimensional multichannel potential energy surface: Photodetachment of $H^-(NH_3)$ and NH_4^-". *J. Chem. Phys.*, **144**:244311, 2016.

[92] M. Díaz-Tinoco and J. V. Ortiz. "Double–Rydberg Anions: Electron Binding Energies and Dyson Orbitals of $N_nH_{3n+1}^-$". *J. Chem. Phys.*, accepted.

[93] G. D. Purvis and R. J. Bartlett. "A full coupled-cluster singles and doubles model – the inclusion of disconnected triples". *J. Chem. Phys.*, **76**:1910–1918, 1982.

[94] J. V. Ortiz. "Electron detachment energies of closed-shell anions calculated with a renormalized electron propagator". *Chem. Phys. Lett.*, **296**:494–498, 1998.

[95] J. V. Ortiz. "Single-reference electron propagator calculations on vertical ionization energies of ozone". *Chem. Phys. Lett.*, **297**:193–199, 1998.

[96] J. V. Ortiz. "Chapter four - interpreting bonding and spectra with correlated, one-electron concepts from electron propagator theory". In D. A. Dixon, editor, *Ann. Rep. Comput. Chem.*, volume 13, pages 139–182. Elsevier, 2017.

[97] R. A. Chiles and C. E. Dykstra. "An electron pair operator approach to coupled cluster wave functions. Application to diatomic hydrogen, diatomic beryllium, and diatomic magnesium and comparison with CEPA methods". *J. Chem. Phys.*, **74**:4544–56, 1981.

[98] N. C. Handy, J. A. Pople, M. Head-Gordon, K. Raghavachari, and G. W. Trucks. “Size-consistent brueckner theory limited to double substitutions”. *Chem. Phys. Lett.*, **164**:185–92, 1989.

[99] R. Dennington, T. A. Keith, and J. M. Millam. “Gaussview Version 6”, 2016. Semichem Inc. Shawnee Mission KS.

[100] G. Schaftenaar and J. H. Noordik. “Molden: a pre– and post–processing program for molecular and electronic structures”. *J. Comput. Aided Mol. Des.*, **14**:123–134, 2000.

[101] A. M. Velasco, C. Lavín, M. Díaz-Tinoco, and J. V. Ortiz. “CaH Rydberg series, oscillator strengths and photoionization cross sections from Molecular Quantum Defect and Dyson Orbital theories”. *J. Quant. Spectrosc. Ra.*, **187**:161–166, 2017.

[102] H. H. Corzo, A. M. Velasco, C. Lavín, and J. V. Ortiz. “MgH Rydberg series: Transition energies from electron propagator theory and oscillator strengths from the molecular quantum defect orbital method”. *J. Quant. Spectrosc. Ra.*, **206**:323–327, 2018.

[103] S. Nonose, T. Taguchi, K. Mizuma, and K. Fuke. “Electronic spectra of solvated NH4 radicals $NH_4(NH_3)_n$ for n = 1 - 6”. *Eur. Phys. J. D*, **9**:309–311, 1999.

[104] S. Nonose, T. Taguchi, F. Chen, S. Iwata, and K. Fuke. “Electronic Spectra and Structures of Solvated NH_4 Radicals, $NH_4(NH_3)_n$ (n = 1–8)”. *J. Phys. Chem. A*, **106**:5242–5248, 2002.

[105] T. H. Dunning Jr. “Gaussian basis sets for use in correlated molecular calculations. I. The atoms boron through neon and hydrogen”. *J. Chem. Phys.*, **90**:1007–1023, 1989.

[106] R. A. Kendall, T. H. Dunning Jr., and R. J. Harrison. “Electron affinities of the first-row atoms revisited. Systematic basis sets and wave functions”. *J. Chem. Phys.*, **96**:6796–6806, 1992.

[107] D. E. Woon and T. H. Dunning Jr. “Gaussian-basis sets for use in correlated molecular calculations. 3. The atoms aluminum through argon”. *J. Chem. Phys.*, **98**:1358–1371, 1993.

[108] J. V. Ortiz. “Renormalized Self-Energy for Calculating the Electron Binding Energies of Closed-Shell Molecules and Anions”. *Int. J. Quantum Chem.*, **105**:803–808, 2005.

Appendix A

Fourth order electron propagator Brandow (Feynman) diagrams.

This appendix shows all fourth order diagrams and their respective equations. These diagrams were implemented in a diagonal approximation and for this reason q was substituted for p in each equation. First, section A.1 displays all 72 constant diagrams for fourth order electron propagator. Secondly, section A.2 displays all 120 U–type diagrams and their corresponding equations. In addition, eight more equations are shown corresponding to the algebraic reduction of pseudo–f_7 into f_3–type diagrams. Thirdly, section A.3 displays all 48 V–type diagrams and their corresponding equations. In addition, eight more equations are shown corresponding to the algebraic reduction of pseudo–f_7 into f_3–type diagrams. Finally, section A.4 displays all 60 W–type diagrams and their corresponding equations. These type of diagrams don't have pseudo–f_7 diagrams.

A.1 Constant fourth–order diagrams

$$dc011 = 0.50 \sum_{a,b,c,d,i,j,k} \frac{\langle bd||ik\rangle\langle pc||pj\rangle\langle ak||bd\rangle\langle ij||ac\rangle}{(\epsilon_i+\epsilon_k-\epsilon_b-\epsilon_d)(\epsilon_i+\epsilon_j+\epsilon_k-\epsilon_b-\epsilon_c-\epsilon_d)(\epsilon_i+\epsilon_j-\epsilon_a-\epsilon_c)} \tag{A.1}$$

$$dc012 = -0.25 \sum_{a,b,c,d,i,j,k} \frac{\langle bd||jk\rangle\langle pa||pi\rangle\langle ic||bd\rangle\langle jk||ac\rangle}{(\epsilon_j+\epsilon_k-\epsilon_b-\epsilon_d)(\epsilon_i+\epsilon_j+\epsilon_k-\epsilon_a-\epsilon_b-\epsilon_d)(\epsilon_j+\epsilon_k-\epsilon_a-\epsilon_c)} \tag{A.2}$$

$$dc016 = -1.00 \sum_{a,b,c,d,i,j,k} \frac{\langle bd||jk\rangle\langle pa||pi\rangle\langle jc||ad\rangle\langle ik||bc\rangle}{(\epsilon_j+\epsilon_k-\epsilon_b-\epsilon_d)(\epsilon_i+\epsilon_j+\epsilon_k-\epsilon_a-\epsilon_b-\epsilon_d)(\epsilon_i+\epsilon_k-\epsilon_b-\epsilon_c)} \tag{A.3}$$

$$dc017 = 0.50 \sum_{a,b,c,d,i,j,k} \frac{\langle bd||ik\rangle\langle pc||pj\rangle\langle aj||bc\rangle\langle ik||ad\rangle}{(\epsilon_i+\epsilon_k-\epsilon_b-\epsilon_d)(\epsilon_i+\epsilon_j+\epsilon_k-\epsilon_b-\epsilon_c-\epsilon_d)(\epsilon_i+\epsilon_k-\epsilon_a-\epsilon_d)} \tag{A.4}$$

$$dc018 = -0.50 \sum_{a,b,c,i,j,k,l} \frac{\langle ac||jl\rangle\langle pb||pk\rangle\langle jl||ic\rangle\langle ik||ab\rangle}{(\epsilon_j+\epsilon_l-\epsilon_a-\epsilon_c)(\epsilon_j+\epsilon_k+\epsilon_l-\epsilon_a-\epsilon_b-\epsilon_c)(\epsilon_i+\epsilon_k-\epsilon_a-\epsilon_b)} \tag{A.5}$$

$$dc019 = 1.00 \sum_{a,b,c,i,j,k,l} \frac{\langle bc||jl\rangle\langle pa||pi\rangle\langle il||bk\rangle\langle jk||ac\rangle}{(\epsilon_j+\epsilon_l-\epsilon_b-\epsilon_c)(\epsilon_i+\epsilon_j+\epsilon_l-\epsilon_a-\epsilon_b-\epsilon_c)(\epsilon_j+\epsilon_k-\epsilon_a-\epsilon_c)} \tag{A.6}$$

$$dc022 = 0.25 \sum_{a,b,c,i,j,k,l} \frac{\langle bc||jl\rangle\langle pa||pi\rangle\langle jl||ak\rangle\langle ik||bc\rangle}{(\epsilon_j+\epsilon_l-\epsilon_b-\epsilon_c)(\epsilon_i+\epsilon_j+\epsilon_l-\epsilon_a-\epsilon_b-\epsilon_c)(\epsilon_i+\epsilon_k-\epsilon_b-\epsilon_c)} \tag{A.7}$$

$$dc024 = -0.50 \sum_{a,b,c,i,j,k,l} \frac{\langle ac||jl\rangle\langle pb||pk\rangle\langle jk||ib\rangle\langle il||ac\rangle}{(\epsilon_j+\epsilon_l-\epsilon_a-\epsilon_c)(\epsilon_j+\epsilon_k+\epsilon_l-\epsilon_a-\epsilon_b-\epsilon_c)(\epsilon_i+\epsilon_l-\epsilon_a-\epsilon_c)} \tag{A.8}$$

$$dc033 = 0.50 \sum_{a,b,c,d,i,j,k} \frac{\langle bc||ij\rangle\langle ad||bk\rangle\langle pj||pc\rangle\langle ik||ad\rangle}{(\epsilon_i+\epsilon_j-\epsilon_b-\epsilon_c)(\epsilon_i+\epsilon_j+\epsilon_k-\epsilon_a-\epsilon_c-\epsilon_d)(\epsilon_i+\epsilon_k-\epsilon_a-\epsilon_d)} \tag{A.9}$$

$$dc034 = -0.25 \sum_{a,b,c,d,i,j,k} \frac{\langle bd||jk\rangle\langle ac||id\rangle\langle pi||pb\rangle\langle jk||ac\rangle}{(\epsilon_j+\epsilon_k-\epsilon_b-\epsilon_d)(\epsilon_i+\epsilon_j+\epsilon_k-\epsilon_a-\epsilon_b-\epsilon_c)(\epsilon_j+\epsilon_k-\epsilon_a-\epsilon_c)} \tag{A.10}$$

$$dc039 = -1.00 \sum_{a,b,c,d,i,j,k} \frac{\langle bd||jk\rangle\langle ac||id\rangle\langle pj||pa\rangle\langle ik||bc\rangle}{(\epsilon_j+\epsilon_k-\epsilon_b-\epsilon_d)(\epsilon_i+\epsilon_j+\epsilon_k-\epsilon_a-\epsilon_b-\epsilon_c)(\epsilon_i+\epsilon_k-\epsilon_b-\epsilon_c)} \tag{A.11}$$

$$dc040 = 0.50 \sum_{a,b,c,d,i,j,k} \frac{\langle bd||ik\rangle\langle ac||bj\rangle\langle pj||pc\rangle\langle ik||ad\rangle}{(\epsilon_i+\epsilon_k-\epsilon_b-\epsilon_d)(\epsilon_i+\epsilon_j+\epsilon_k-\epsilon_a-\epsilon_c-\epsilon_d)(\epsilon_i+\epsilon_k-\epsilon_a-\epsilon_d)} \tag{A.12}$$

$$dc042 = -0.50 \sum_{a,b,c,i,j,k,l} \frac{\langle ab||jk\rangle\langle jc||il\rangle\langle pk||pb\rangle\langle il||ac\rangle}{(\epsilon_j+\epsilon_k-\epsilon_a-\epsilon_b)(\epsilon_i+\epsilon_k+\epsilon_l-\epsilon_a-\epsilon_b-\epsilon_c)(\epsilon_i+\epsilon_l-\epsilon_a-\epsilon_c)} \tag{A.13}$$

$$dc043 = 1.00 \sum_{a,b,c,i,j,k,l} \frac{\langle bc||jl\rangle\langle al||ik\rangle\langle pi||pb\rangle\langle jk||ac\rangle}{(\epsilon_j+\epsilon_l-\epsilon_b-\epsilon_c)(\epsilon_i+\epsilon_j+\epsilon_k-\epsilon_a-\epsilon_b-\epsilon_c)(\epsilon_j+\epsilon_k-\epsilon_a-\epsilon_c)} \tag{A.14}$$

$$dc045 = 0.25 \sum_{a,b,c,i,j,k,l} \frac{\langle bc||jl\rangle\langle al||ik\rangle\langle pj||pa\rangle\langle ik||bc\rangle}{(\epsilon_j+\epsilon_l-\epsilon_b-\epsilon_c)(\epsilon_i+\epsilon_j+\epsilon_k-\epsilon_a-\epsilon_b-\epsilon_c)(\epsilon_i+\epsilon_k-\epsilon_b-\epsilon_c)} \tag{A.15}$$

$$dc046 = -0.50 \sum_{a,b,c,i,j,k,l} \frac{\langle ac||jl\rangle\langle jb||ik\rangle\langle pk||pb\rangle\langle il||ac\rangle}{(\epsilon_j+\epsilon_l-\epsilon_a-\epsilon_c)(\epsilon_i+\epsilon_k+\epsilon_l-\epsilon_a-\epsilon_b-\epsilon_c)(\epsilon_i+\epsilon_l-\epsilon_a-\epsilon_c)} \tag{A.16}$$

$$dc004 = -1.00 \sum_{a,b,c,d,i,j,k} \frac{\langle pb\|pj\rangle\langle ad\|ik\rangle\langle ic\|bd\rangle\langle jk\|ac\rangle}{(\epsilon_j - \epsilon_b)(\epsilon_i + \epsilon_j + \epsilon_k - \epsilon_a - \epsilon_b - \epsilon_d)(\epsilon_j + \epsilon_k - \epsilon_a - \epsilon_c)} \tag{A.17}$$

$$dc007 = -0.50 \sum_{a,b,c,i,j,k,l} \frac{\langle pb\|pk\rangle\langle ac\|jl\rangle\langle jk\|ib\rangle\langle il\|ac\rangle}{(\epsilon_k - \epsilon_b)(\epsilon_j + \epsilon_k + \epsilon_l - \epsilon_a - \epsilon_b - \epsilon_c)(\epsilon_i + \epsilon_l - \epsilon_a - \epsilon_c)} \tag{A.18}$$

$$dc010 = 0.25 \sum_{a,b,c,i,j,k,l} \frac{\langle pb\|pj\rangle\langle ac\|il\rangle\langle il\|bk\rangle\langle jk\|ac\rangle}{(\epsilon_j - \epsilon_b)(\epsilon_i + \epsilon_j + \epsilon_l - \epsilon_a - \epsilon_b - \epsilon_c)(\epsilon_j + \epsilon_k - \epsilon_a - \epsilon_c)} \tag{A.19}$$

$$dc023 = -0.25 \sum_{a,b,c,d,i,j,k} \frac{\langle pb\|pj\rangle\langle ad\|ik\rangle\langle jc\|ad\rangle\langle ik\|bc\rangle}{(\epsilon_j - \epsilon_b)(\epsilon_i + \epsilon_j + \epsilon_k - \epsilon_a - \epsilon_b - \epsilon_d)(\epsilon_i + \epsilon_k - \epsilon_b - \epsilon_c)} \tag{A.20}$$

$$dc025 = 0.50 \sum_{a,b,c,d,i,j,k} \frac{\langle pc\|pj\rangle\langle bd\|ik\rangle\langle ak\|bd\rangle\langle ij\|ac\rangle}{(\epsilon_j - \epsilon_c)(\epsilon_i + \epsilon_j + \epsilon_k - \epsilon_b - \epsilon_c - \epsilon_d)(\epsilon_i + \epsilon_j - \epsilon_a - \epsilon_c)} \tag{A.21}$$

$$dc026 = 1.00 \sum_{a,b,c,i,j,k,l} \frac{\langle pb\|pj\rangle\langle ac\|il\rangle\langle jl\|ak\rangle\langle ik\|bc\rangle}{(\epsilon_j - \epsilon_b)(\epsilon_i + \epsilon_j + \epsilon_l - \epsilon_a - \epsilon_b - \epsilon_c)(\epsilon_i + \epsilon_k - \epsilon_b - \epsilon_c)} \tag{A.22}$$

$$dc027 = -0.50 \sum_{a,b,c,i,j,k,l} \frac{\langle pb\|pk\rangle\langle ac\|jl\rangle\langle jl\|ic\rangle\langle ik\|ab\rangle}{(\epsilon_k - \epsilon_b)(\epsilon_j + \epsilon_k + \epsilon_l - \epsilon_a - \epsilon_b - \epsilon_c)(\epsilon_i + \epsilon_k - \epsilon_a - \epsilon_b)} \tag{A.23}$$

$$dc072 = 0.50 \sum_{a,b,c,d,i,j,k} \frac{\langle pc\|pj\rangle\langle bd\|ik\rangle\langle aj\|bc\rangle\langle ik\|ad\rangle}{(\epsilon_j - \epsilon_c)(\epsilon_i + \epsilon_j + \epsilon_k - \epsilon_b - \epsilon_c - \epsilon_d)(\epsilon_i + \epsilon_k - \epsilon_a - \epsilon_d)} \tag{A.24}$$

$$dc055 = 0.50 \sum_{a,b,c,d,i,j,k} \frac{\langle bd\|ik\rangle\langle ac\|bj\rangle\langle ik\|ad\rangle\langle pj\|pc\rangle}{(\epsilon_i + \epsilon_k - \epsilon_b - \epsilon_d)(\epsilon_i + \epsilon_j + \epsilon_k - \epsilon_a - \epsilon_c - \epsilon_d)(\epsilon_j - \epsilon_c)} \tag{A.25}$$

$$dc056 = -1.00 \sum_{a,b,c,d,i,j,k} \frac{\langle bd\|jk\rangle\langle ac\|id\rangle\langle ik\|bc\rangle\langle pj\|pa\rangle}{(\epsilon_j + \epsilon_k - \epsilon_b - \epsilon_d)(\epsilon_i + \epsilon_j + \epsilon_k - \epsilon_a - \epsilon_b - \epsilon_c)(\epsilon_j - \epsilon_a)} \tag{A.26}$$

$$dc058 = -0.25 \sum_{a,b,c,d,i,j,k} \frac{\langle bd\|jk\rangle\langle ac\|id\rangle\langle jk\|ac\rangle\langle pi\|pb\rangle}{(\epsilon_j + \epsilon_k - \epsilon_b - \epsilon_d)(\epsilon_i + \epsilon_j + \epsilon_k - \epsilon_a - \epsilon_b - \epsilon_c)(\epsilon_i - \epsilon_b)} \tag{A.27}$$

$$dc059 = 0.50 \sum_{a,b,c,d,i,j,k} \frac{\langle bc\|ij\rangle\langle ad\|bk\rangle\langle ik\|ad\rangle\langle pj\|pc\rangle}{(\epsilon_i + \epsilon_j - \epsilon_b - \epsilon_c)(\epsilon_i + \epsilon_j + \epsilon_k - \epsilon_a - \epsilon_c - \epsilon_d)(\epsilon_j - \epsilon_c)} \tag{A.28}$$

$$dc061 = -0.50 \sum_{a,b,c,i,j,k,l} \frac{\langle ac\|jl\rangle\langle jb\|ik\rangle\langle il\|ac\rangle\langle pk\|pb\rangle}{(\epsilon_j + \epsilon_l - \epsilon_a - \epsilon_c)(\epsilon_i + \epsilon_k + \epsilon_l - \epsilon_a - \epsilon_b - \epsilon_c)(\epsilon_k - \epsilon_b)} \tag{A.29}$$

$$dc062 = 0.25 \sum_{a,b,c,i,j,k,l} \frac{\langle bc\|jl\rangle\langle al\|ik\rangle\langle ik\|bc\rangle\langle pj\|pa\rangle}{(\epsilon_j + \epsilon_l - \epsilon_b - \epsilon_c)(\epsilon_i + \epsilon_j + \epsilon_k - \epsilon_a - \epsilon_b - \epsilon_c)(\epsilon_j - \epsilon_a)} \tag{A.30}$$

$$dc064 = 1.00 \sum_{a,b,c,i,j,k,l} \frac{\langle bc\|jl\rangle\langle al\|ik\rangle\langle jk\|ac\rangle\langle pi\|pb\rangle}{(\epsilon_j + \epsilon_l - \epsilon_b - \epsilon_c)(\epsilon_i + \epsilon_j + \epsilon_k - \epsilon_a - \epsilon_b - \epsilon_c)(\epsilon_i - \epsilon_b)} \tag{A.31}$$

$$dc065 = -0.50 \sum_{a,b,c,i,j,k,l} \frac{\langle ab\|jk\rangle\langle jc\|il\rangle\langle il\|ac\rangle\langle pk\|pb\rangle}{(\epsilon_j + \epsilon_k - \epsilon_a - \epsilon_b)(\epsilon_i + \epsilon_k + \epsilon_l - \epsilon_a - \epsilon_b - \epsilon_c)(\epsilon_k - \epsilon_b)} \tag{A.32}$$

$$dc002 = 0.25 \sum_{a,b,c,d,e,i,j} \frac{\langle ce||ij\rangle\langle pb||pc\rangle\langle ad||be\rangle\langle ij||ad\rangle}{(\epsilon_i + \epsilon_j - \epsilon_c - \epsilon_e)(\epsilon_i + \epsilon_j - \epsilon_b - \epsilon_e)(\epsilon_i + \epsilon_j - \epsilon_a - \epsilon_d)} \tag{A.33}$$

$$dc003 = -1.00 \sum_{a,b,c,d,i,j,k} \frac{\langle bd||jk\rangle\langle pa||pb\rangle\langle jc||id\rangle\langle ik||ac\rangle}{(\epsilon_j + \epsilon_k - \epsilon_b - \epsilon_d)(\epsilon_j + \epsilon_k - \epsilon_a - \epsilon_d)(\epsilon_i + \epsilon_k - \epsilon_a - \epsilon_c)} \tag{A.34}$$

$$dc006 = -1.00 \sum_{a,b,c,d,i,j,k} \frac{\langle cd||ik\rangle\langle pb||pc\rangle\langle ak||bj\rangle\langle ij||ad\rangle}{(\epsilon_i + \epsilon_k - \epsilon_c - \epsilon_d)(\epsilon_i + \epsilon_k - \epsilon_b - \epsilon_d)(\epsilon_i + \epsilon_j - \epsilon_a - \epsilon_d)} \tag{A.35}$$

$$dc008 = 0.25 \sum_{a,b,c,i,j,k,l} \frac{\langle bc||jl\rangle\langle pa||pb\rangle\langle jl||ik\rangle\langle ik||ac\rangle}{(\epsilon_j + \epsilon_l - \epsilon_b - \epsilon_c)(\epsilon_j + \epsilon_l - \epsilon_a - \epsilon_c)(\epsilon_i + \epsilon_k - \epsilon_a - \epsilon_c)} \tag{A.36}$$

$$dc009 = -0.25 \sum_{a,b,c,d,i,j,k} \frac{\langle bd||jk\rangle\langle pj||pi\rangle\langle ac||bd\rangle\langle ik||ac\rangle}{(\epsilon_j + \epsilon_k - \epsilon_b - \epsilon_d)(\epsilon_i + \epsilon_k - \epsilon_b - \epsilon_d)(\epsilon_i + \epsilon_k - \epsilon_a - \epsilon_c)} \tag{A.37}$$

$$dc014 = 1.00 \sum_{a,b,c,i,j,k,l} \frac{\langle bc||jl\rangle\langle pj||pi\rangle\langle al||bk\rangle\langle ik||ac\rangle}{(\epsilon_j + \epsilon_l - \epsilon_b - \epsilon_c)(\epsilon_i + \epsilon_l - \epsilon_b - \epsilon_c)(\epsilon_i + \epsilon_k - \epsilon_a - \epsilon_c)} \tag{A.38}$$

$$dc015 = 1.00 \sum_{a,b,c,i,j,k,l} \frac{\langle ac||kl\rangle\langle pk||pi\rangle\langle ib||jc\rangle\langle jl||ab\rangle}{(\epsilon_k + \epsilon_l - \epsilon_a - \epsilon_c)(\epsilon_i + \epsilon_l - \epsilon_a - \epsilon_c)(\epsilon_j + \epsilon_l - \epsilon_a - \epsilon_b)} \tag{A.39}$$

$$dc021 = -0.25 \sum_{a,b,i,j,k,l,m} \frac{\langle ab||km\rangle\langle pk||pi\rangle\langle im||jl\rangle\langle jl||ab\rangle}{(\epsilon_k + \epsilon_m - \epsilon_a - \epsilon_b)(\epsilon_i + \epsilon_m - \epsilon_a - \epsilon_b)(\epsilon_j + \epsilon_l - \epsilon_a - \epsilon_b)} \tag{A.40}$$

$$dc029 = 0.25 \sum_{a,b,c,d,e,i,j} \frac{\langle ce||ij\rangle\langle bd||ce\rangle\langle pa||pb\rangle\langle ij||ad\rangle}{(\epsilon_i + \epsilon_j - \epsilon_c - \epsilon_e)(\epsilon_i + \epsilon_j - \epsilon_b - \epsilon_d)(\epsilon_i + \epsilon_j - \epsilon_a - \epsilon_d)} \tag{A.41}$$

$$dc031 = -0.25 \sum_{a,b,c,d,i,j,k} \frac{\langle bd||jk\rangle\langle ac||bd\rangle\langle pj||pi\rangle\langle ik||ac\rangle}{(\epsilon_j + \epsilon_k - \epsilon_b - \epsilon_d)(\epsilon_j + \epsilon_k - \epsilon_a - \epsilon_c)(\epsilon_i + \epsilon_k - \epsilon_a - \epsilon_c)} \tag{A.42}$$

$$dc032 = -1.00 \sum_{a,b,c,d,i,j,k} \frac{\langle bd||jk\rangle\langle jc||id\rangle\langle pa||pb\rangle\langle ik||ac\rangle}{(\epsilon_j + \epsilon_k - \epsilon_b - \epsilon_d)(\epsilon_i + \epsilon_k - \epsilon_b - \epsilon_c)(\epsilon_i + \epsilon_k - \epsilon_a - \epsilon_c)} \tag{A.43}$$

$$dc036 = -1.00 \sum_{a,b,c,d,i,j,k} \frac{\langle cd||ik\rangle\langle bk||cj\rangle\langle pa||pb\rangle\langle ij||ad\rangle}{(\epsilon_i + \epsilon_k - \epsilon_c - \epsilon_d)(\epsilon_i + \epsilon_j - \epsilon_b - \epsilon_d)(\epsilon_i + \epsilon_j - \epsilon_a - \epsilon_d)} \tag{A.44}$$

$$dc037 = 1.00 \sum_{a,b,c,i,j,k,l} \frac{\langle bc||jl\rangle\langle al||bk\rangle\langle pj||pi\rangle\langle ik||ac\rangle}{(\epsilon_j + \epsilon_l - \epsilon_b - \epsilon_c)(\epsilon_j + \epsilon_k - \epsilon_a - \epsilon_c)(\epsilon_i + \epsilon_k - \epsilon_a - \epsilon_c)} \tag{A.45}$$

$$dc038 = 1.00 \sum_{a,b,c,i,j,k,l} \frac{\langle ac||kl\rangle\langle kb||ic\rangle\langle pi||pj\rangle\langle jl||ab\rangle}{(\epsilon_k + \epsilon_l - \epsilon_a - \epsilon_c)(\epsilon_i + \epsilon_l - \epsilon_a - \epsilon_b)(\epsilon_j + \epsilon_l - \epsilon_a - \epsilon_b)} \tag{A.46}$$

$$dc041 = 0.25 \sum_{a,b,c,i,j,k,l} \frac{\langle bc||jl\rangle\langle jl||ik\rangle\langle pa||pb\rangle\langle ik||ac\rangle}{(\epsilon_j + \epsilon_l - \epsilon_b - \epsilon_c)(\epsilon_i + \epsilon_k - \epsilon_b - \epsilon_c)(\epsilon_i + \epsilon_k - \epsilon_a - \epsilon_c)} \tag{A.47}$$

$$dc044 = -0.25 \sum_{a,b,i,j,k,l,m} \frac{\langle ab||km\rangle\langle km||il\rangle\langle pi||pj\rangle\langle jl||ab\rangle}{(\epsilon_k + \epsilon_m - \epsilon_a - \epsilon_b)(\epsilon_i + \epsilon_l - \epsilon_a - \epsilon_b)(\epsilon_j + \epsilon_l - \epsilon_a - \epsilon_b)} \tag{A.48}$$

$$dc013 = 1.00 \sum_{a,b,c,i,j,k,l} \frac{\langle pa||pk\rangle\langle kc||il\rangle\langle ib||jc\rangle\langle jl||ab\rangle}{(\epsilon_k - \epsilon_a)(\epsilon_i + \epsilon_l - \epsilon_a - \epsilon_c)(\epsilon_j + \epsilon_l - \epsilon_a - \epsilon_b)} \tag{A.49}$$

$$dc020 = -0.25 \sum_{a,b,i,j,k,l,m} \frac{\langle pa||pk\rangle\langle kb||im\rangle\langle im||jl\rangle\langle jl||ab\rangle}{(\epsilon_k - \epsilon_a)(\epsilon_i + \epsilon_m - \epsilon_a - \epsilon_b)(\epsilon_j + \epsilon_l - \epsilon_a - \epsilon_b)} \tag{A.50}$$

$$dc066 = 0.25 \sum_{a,b,c,d,e,i,j} \frac{\langle pc||pi\rangle\langle be||cj\rangle\langle ad||be\rangle\langle ij||ad\rangle}{(\epsilon_i - \epsilon_c)(\epsilon_i + \epsilon_j - \epsilon_b - \epsilon_e)(\epsilon_i + \epsilon_j - \epsilon_a - \epsilon_d)} \tag{A.51}$$

$$dc067 = -1.00 \sum_{a,b,c,d,i,j,k} \frac{\langle pb||pj\rangle\langle ad||bk\rangle\langle jc||id\rangle\langle ik||ac\rangle}{(\epsilon_j - \epsilon_b)(\epsilon_j + \epsilon_k - \epsilon_a - \epsilon_d)(\epsilon_i + \epsilon_k - \epsilon_a - \epsilon_c)} \tag{A.52}$$

$$dc068 = -1.00 \sum_{a,b,c,d,i,j,k} \frac{\langle pc||pi\rangle\langle bd||ck\rangle\langle ak||bj\rangle\langle ij||ad\rangle}{(\epsilon_i - \epsilon_c)(\epsilon_i + \epsilon_k - \epsilon_b - \epsilon_d)(\epsilon_i + \epsilon_j - \epsilon_a - \epsilon_d)} \tag{A.53}$$

$$dc069 = 0.25 \sum_{a,b,c,i,j,k,l} \frac{\langle pb||pj\rangle\langle ac||bl\rangle\langle jl||ik\rangle\langle ik||ac\rangle}{(\epsilon_j - \epsilon_b)(\epsilon_j + \epsilon_l - \epsilon_a - \epsilon_c)(\epsilon_i + \epsilon_k - \epsilon_a - \epsilon_c)} \tag{A.54}$$

$$dc070 = -0.25 \sum_{a,b,c,d,i,j,k} \frac{\langle pb||pj\rangle\langle jd||ik\rangle\langle ac||bd\rangle\langle ik||ac\rangle}{(\epsilon_j - \epsilon_b)(\epsilon_i + \epsilon_k - \epsilon_b - \epsilon_d)(\epsilon_i + \epsilon_k - \epsilon_a - \epsilon_c)} \tag{A.55}$$

$$dc071 = 1.00 \sum_{a,b,c,i,j,k,l} \frac{\langle pb||pj\rangle\langle jc||il\rangle\langle al||bk\rangle\langle ik||ac\rangle}{(\epsilon_j - \epsilon_b)(\epsilon_i + \epsilon_l - \epsilon_b - \epsilon_c)(\epsilon_i + \epsilon_k - \epsilon_a - \epsilon_c)} \tag{A.56}$$

$$dc048 = 0.25 \sum_{a,b,c,d,e,i,j} \frac{\langle ce||ij\rangle\langle bd||ce\rangle\langle aj||bd\rangle\langle pi||pa\rangle}{(\epsilon_i + \epsilon_j - \epsilon_c - \epsilon_e)(\epsilon_i + \epsilon_j - \epsilon_b - \epsilon_d)(\epsilon_i - \epsilon_a)} \tag{A.57}$$

$$dc049 = -0.25 \sum_{a,b,c,d,i,j,k} \frac{\langle bd||jk\rangle\langle ac||bd\rangle\langle jk||ic\rangle\langle pi||pa\rangle}{(\epsilon_j + \epsilon_k - \epsilon_b - \epsilon_d)(\epsilon_j + \epsilon_k - \epsilon_a - \epsilon_c)(\epsilon_i - \epsilon_a)} \tag{A.58}$$

$$dc051 = -1.00 \sum_{a,b,c,d,i,j,k} \frac{\langle bd||jk\rangle\langle jc||id\rangle\langle ak||bc\rangle\langle pi||pa\rangle}{(\epsilon_j + \epsilon_k - \epsilon_b - \epsilon_d)(\epsilon_i + \epsilon_k - \epsilon_b - \epsilon_c)(\epsilon_i - \epsilon_a)} \tag{A.59}$$

$$dc052 = -1.00 \sum_{a,b,c,d,i,j,k} \frac{\langle cd||ik\rangle\langle bk||cj\rangle\langle aj||bd\rangle\langle pi||pa\rangle}{(\epsilon_i + \epsilon_k - \epsilon_c - \epsilon_d)(\epsilon_i + \epsilon_j - \epsilon_b - \epsilon_d)(\epsilon_i - \epsilon_a)} \tag{A.60}$$

$$dc053 = 1.00 \sum_{a,b,c,i,j,k,l} \frac{\langle bc||jl\rangle\langle al||bk\rangle\langle jk||ic\rangle\langle pi||pa\rangle}{(\epsilon_j + \epsilon_l - \epsilon_b - \epsilon_c)(\epsilon_j + \epsilon_k - \epsilon_a - \epsilon_c)(\epsilon_i - \epsilon_a)} \tag{A.61}$$

$$dc057 = 1.00 \sum_{a,b,c,i,j,k,l} \frac{\langle ac||kl\rangle\langle kb||ic\rangle\langle il||jb\rangle\langle pj||pa\rangle}{(\epsilon_k + \epsilon_l - \epsilon_a - \epsilon_c)(\epsilon_i + \epsilon_l - \epsilon_a - \epsilon_b)(\epsilon_j - \epsilon_a)} \tag{A.62}$$

$$dc060 = 0.25 \sum_{a,b,c,i,j,k,l} \frac{\langle bc||jl\rangle\langle jl||ik\rangle\langle ak||bc\rangle\langle pi||pa\rangle}{(\epsilon_j + \epsilon_l - \epsilon_b - \epsilon_c)(\epsilon_i + \epsilon_k - \epsilon_b - \epsilon_c)(\epsilon_i - \epsilon_a)} \tag{A.63}$$

$$dc063 = -0.25 \sum_{a,b,i,j,k,l,m} \frac{\langle ab||km\rangle\langle km||il\rangle\langle il||jb\rangle\langle pj||pa\rangle}{(\epsilon_k + \epsilon_m - \epsilon_a - \epsilon_b)(\epsilon_i + \epsilon_l - \epsilon_a - \epsilon_b)(\epsilon_j - \epsilon_a)} \tag{A.64}$$

$$dc001 = \ \ 0.50 \sum_{a,b,c,d,i,j,k} \frac{\langle bc||ij\rangle\langle pj||pc\rangle\langle ad||bk\rangle\langle ik||ad\rangle}{(\epsilon_i + \epsilon_j - \epsilon_b - \epsilon_c)(\epsilon_i - \epsilon_b)(\epsilon_i + \epsilon_k - \epsilon_a - \epsilon_d)} \tag{A.65}$$

$$dc005 = -0.50 \sum_{a,b,c,i,j,k,l} \frac{\langle ab||jk\rangle\langle pk||pb\rangle\langle jc||il\rangle\langle il||ac\rangle}{(\epsilon_j + \epsilon_k - \epsilon_a - \epsilon_b)(\epsilon_j - \epsilon_a)(\epsilon_i + \epsilon_l - \epsilon_a - \epsilon_c)} \tag{A.66}$$

$$dc028 = \ \ 0.50 \sum_{a,b,c,d,i,j,k} \frac{\langle bd||ik\rangle\langle ak||bd\rangle\langle pc||pj\rangle\langle ij||ac\rangle}{(\epsilon_i + \epsilon_k - \epsilon_b - \epsilon_d)(\epsilon_i - \epsilon_a)(\epsilon_i + \epsilon_j - \epsilon_a - \epsilon_c)} \tag{A.67}$$

$$dc035 = -0.50 \sum_{a,b,c,i,j,k,l} \frac{\langle ac||jl\rangle\langle jl||ic\rangle\langle pb||pk\rangle\langle ik||ab\rangle}{(\epsilon_j + \epsilon_l - \epsilon_a - \epsilon_c)(\epsilon_i - \epsilon_a)(\epsilon_i + \epsilon_k - \epsilon_a - \epsilon_b)} \tag{A.68}$$

$$dc030 = \ \ 0.50 \sum_{a,b,c,d,i,j,k} \frac{\langle pc||pj\rangle\langle bj||ic\rangle\langle ad||bk\rangle\langle ik||ad\rangle}{(\epsilon_j - \epsilon_c)(\epsilon_i - \epsilon_b)(\epsilon_i + \epsilon_k - \epsilon_a - \epsilon_d)} \tag{A.69}$$

$$dc054 = -0.50 \sum_{a,b,c,i,j,k,l} \frac{\langle pb||pk\rangle\langle ak||jb\rangle\langle jc||il\rangle\langle il||ac\rangle}{(\epsilon_k - \epsilon_b)(\epsilon_j - \epsilon_a)(\epsilon_i + \epsilon_l - \epsilon_a - \epsilon_c)} \tag{A.70}$$

$$dc047 = \ \ 0.50 \sum_{a,b,c,d,i,j,k} \frac{\langle bd||ik\rangle\langle ak||bd\rangle\langle ic||aj\rangle\langle pj||pc\rangle}{(\epsilon_i + \epsilon_k - \epsilon_b - \epsilon_d)(\epsilon_i - \epsilon_a)(\epsilon_j - \epsilon_c)} \tag{A.71}$$

$$dc050 = -0.50 \sum_{a,b,c,i,j,k,l} \frac{\langle ac||jl\rangle\langle jl||ic\rangle\langle ib||ak\rangle\langle pk||pb\rangle}{(\epsilon_j + \epsilon_l - \epsilon_a - \epsilon_c)(\epsilon_i - \epsilon_a)(\epsilon_k - \epsilon_b)} \tag{A.72}$$

Figure A.1: Fourth order constant diagrams

$dc011$

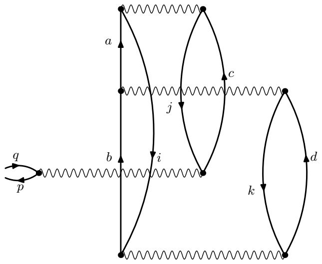

$dc012$

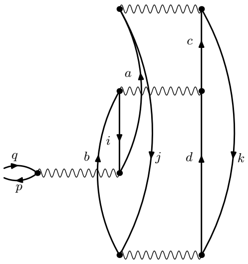

$dc016$

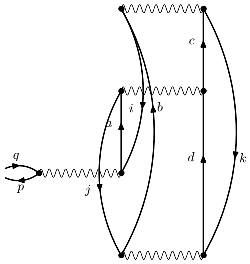

$dc017$

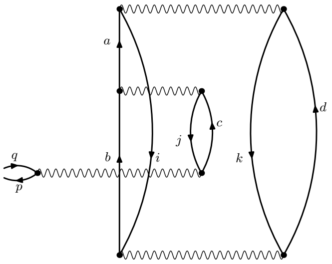

$dc018$

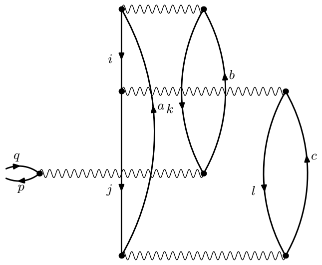

$dc019$

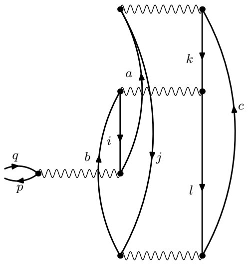

$dc022$

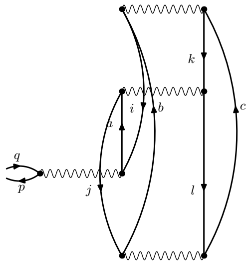

$dc024$

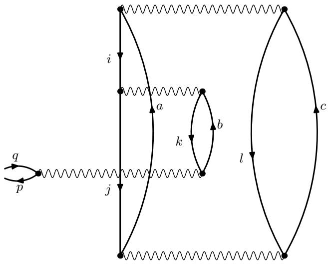

$dc033$

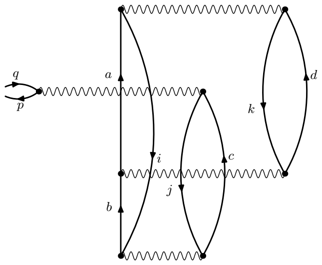

$dc034$

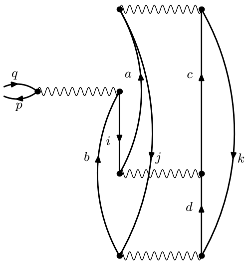

$dc039$

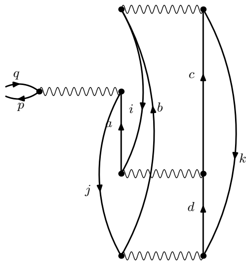

$dc040$

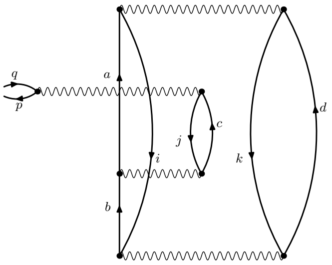

$dc042$

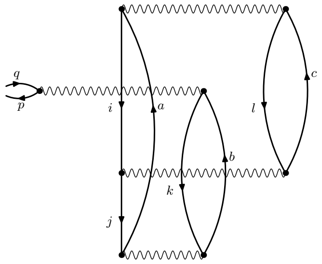

$dc043$

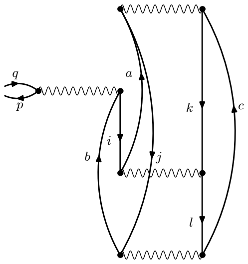

$dc045$

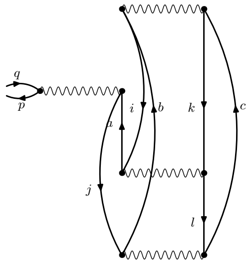

$dc046$

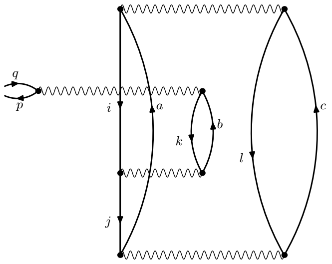

Figure A.2: Fourth order constant diagrams

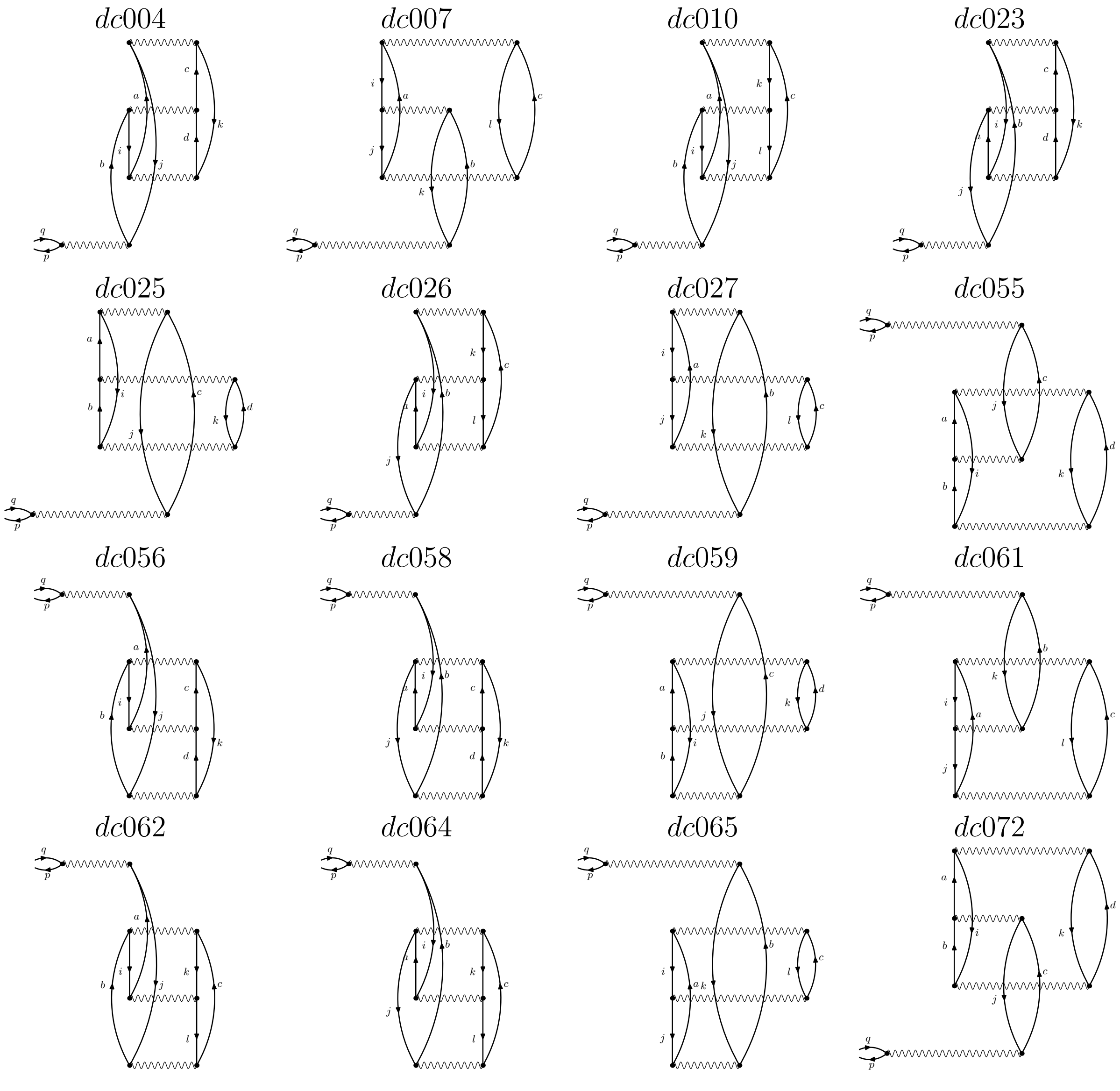
$dc004$ $dc007$ $dc010$ $dc023$

$dc025$ $dc026$ $dc027$ $dc055$

$dc056$ $dc058$ $dc059$ $dc061$

$dc062$ $dc064$ $dc065$ $dc072$

Figure A.3: Fourth order constant diagrams

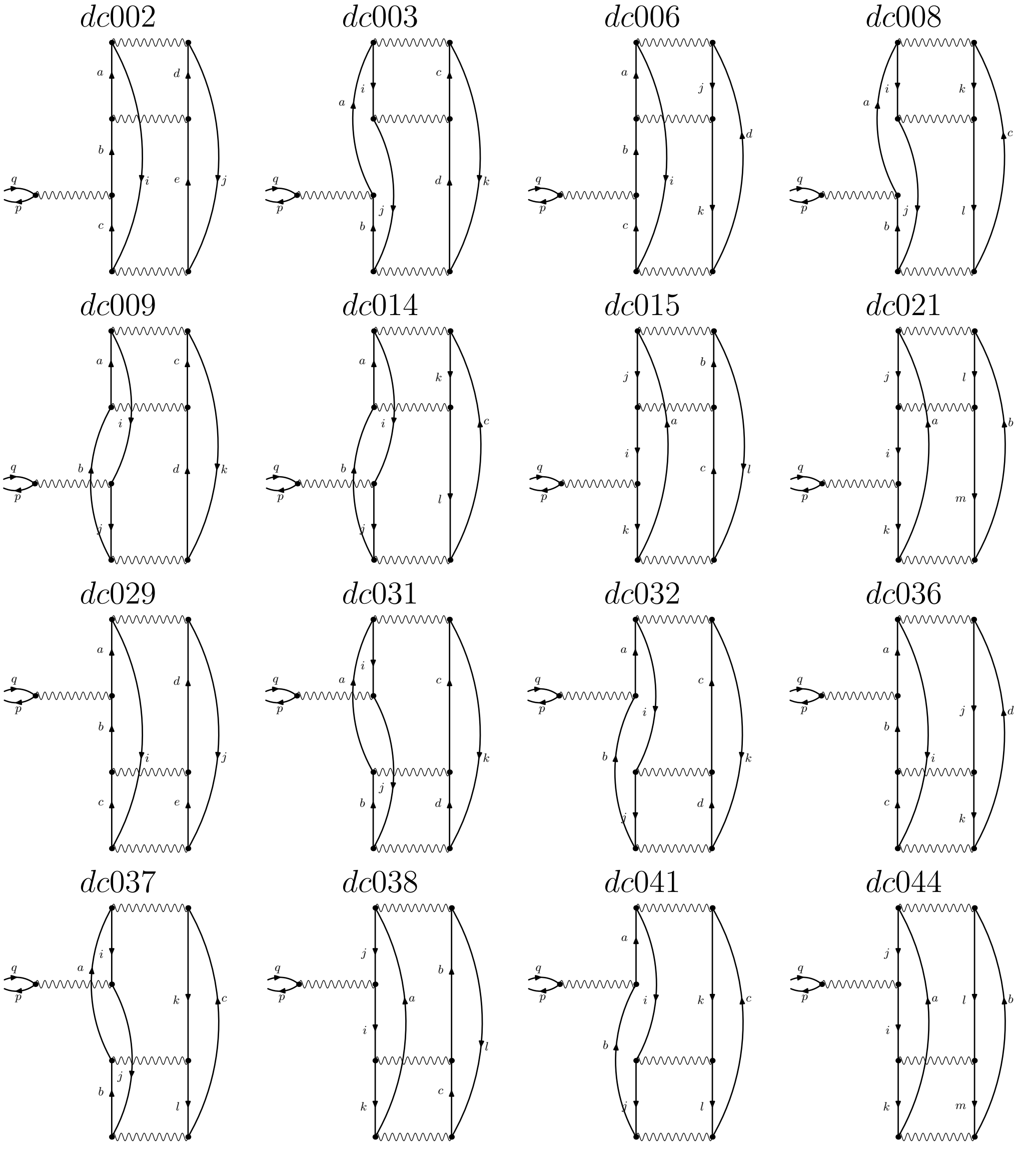

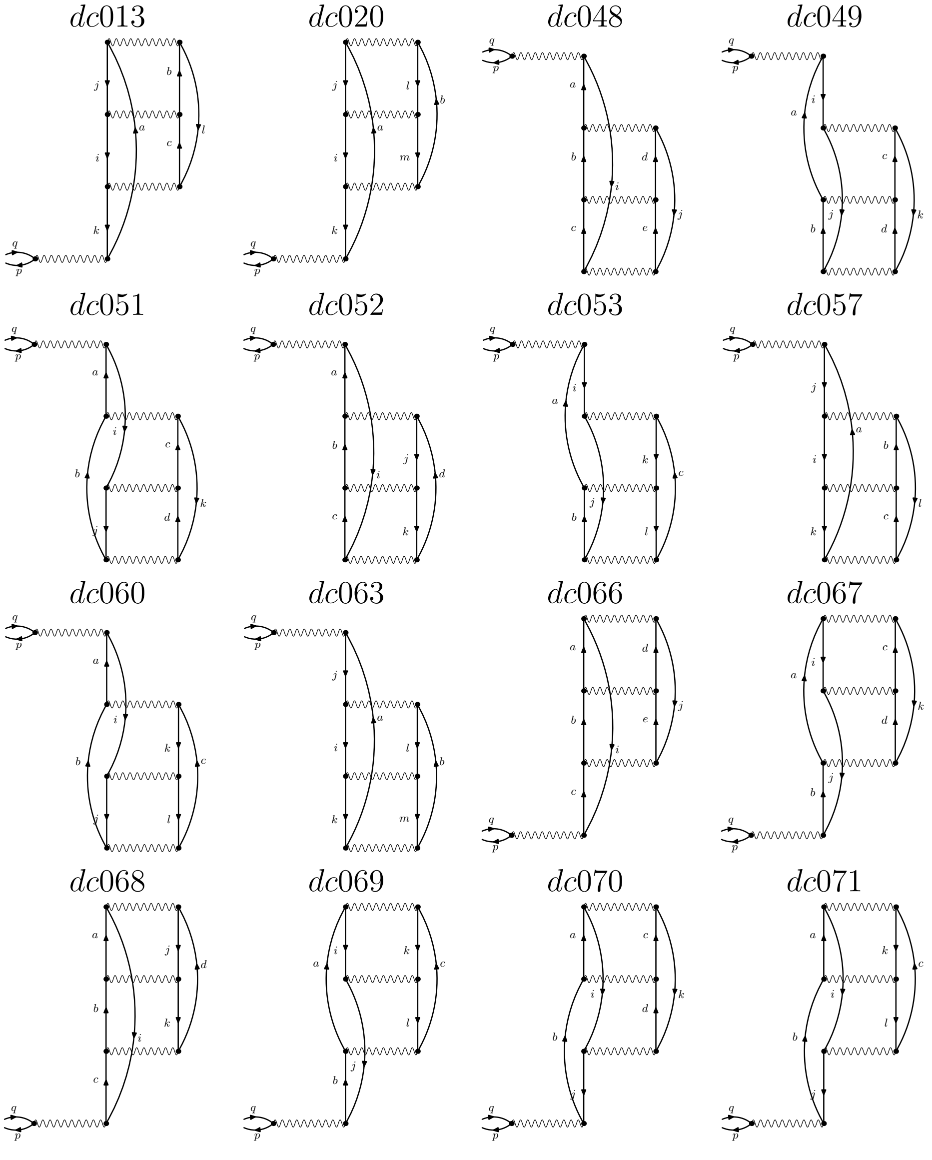

Figure A.4: Fourth order constant diagrams

Figure A.5: Fourth order constant diagrams

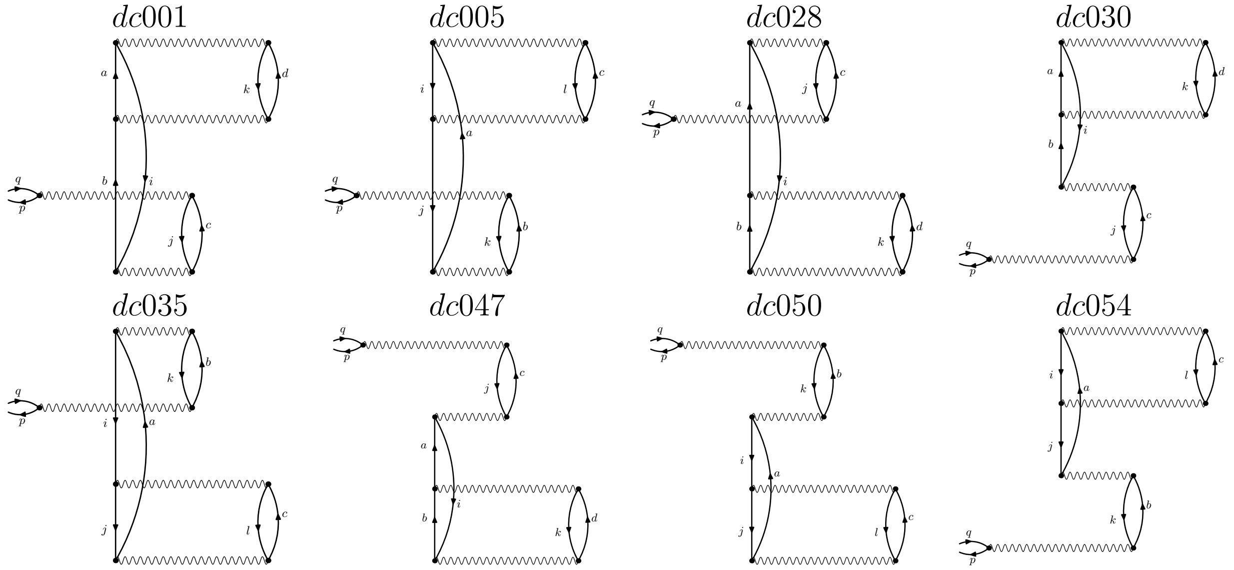

$dc001$ $dc005$ $dc028$ $dc030$

$dc035$ $dc047$ $dc050$ $dc054$

A.2 Type–U fourth–order diagrams

$$du101a = 1.000 \sum_{a,b,c,d,i,j,k} \frac{\langle cd||pk\rangle\langle bk||ci\rangle\langle ai||bj\rangle\langle pj||ad\rangle}{(E+\epsilon_k-\epsilon_c-\epsilon_d)(E+\epsilon_i-\epsilon_b-\epsilon_d)(E+\epsilon_j-\epsilon_a-\epsilon_d)} \tag{A.73}$$

$$du102a = 1.000 \sum_{a,b,c,d,i,j,k} \frac{\langle bd||pk\rangle\langle ac||ij\rangle\langle ik||bc\rangle\langle pj||ad\rangle}{(E+\epsilon_k-\epsilon_b-\epsilon_d)(E+\epsilon_i+\epsilon_j+\epsilon_k-\epsilon_a-\epsilon_b-\epsilon_c-\epsilon_d)(E+\epsilon_j-\epsilon_a-\epsilon_d)} \tag{A.74}$$

$$du103a = 1.000 \sum_{a,b,c,d,i,j,k} \frac{\langle bd||pk\rangle\langle ak||bj\rangle\langle pc||id\rangle\langle ij||ac\rangle}{(E+\epsilon_k-\epsilon_b-\epsilon_d)(E+\epsilon_j-\epsilon_a-\epsilon_d)(\epsilon_i+\epsilon_j-\epsilon_a-\epsilon_c)} \tag{A.75}$$

$$du104a = 1.000 \sum_{a,b,c,d,i,j,k} \frac{\langle bd||ik\rangle\langle ic||pd\rangle\langle ak||bj\rangle\langle pj||ac\rangle}{(\epsilon_i+\epsilon_k-\epsilon_b-\epsilon_d)(E+\epsilon_k-\epsilon_b-\epsilon_c)(E+\epsilon_j-\epsilon_a-\epsilon_c)} \tag{A.76}$$

$$du105a = 1.000 \sum_{a,b,c,d,i,j,k} \frac{\langle bd||pk\rangle\langle ac||ij\rangle\langle pj||ad\rangle\langle ik||bc\rangle}{(E+\epsilon_k-\epsilon_b-\epsilon_d)(E+\epsilon_i+\epsilon_j+\epsilon_k-\epsilon_a-\epsilon_b-\epsilon_c-\epsilon_d)(\epsilon_i+\epsilon_k-\epsilon_b-\epsilon_c)} \tag{A.77}$$

$$du106a = 1.000 \sum_{a,b,c,d,i,j,k} \frac{\langle ad||ik\rangle\langle bc||pj\rangle\langle ij||bd\rangle\langle pk||ac\rangle}{(\epsilon_i+\epsilon_k-\epsilon_a-\epsilon_d)(E+\epsilon_i+\epsilon_j+\epsilon_k-\epsilon_a-\epsilon_b-\epsilon_c-\epsilon_d)(E+\epsilon_k-\epsilon_a-\epsilon_c)} \tag{A.78}$$

$$du107a = 1.000 \sum_{a,b,c,d,i,j,k} \frac{\langle bd||ik\rangle\langle ak||bj\rangle\langle ic||pd\rangle\langle pj||ac\rangle}{(\epsilon_i+\epsilon_k-\epsilon_b-\epsilon_d)(\epsilon_i+\epsilon_j-\epsilon_a-\epsilon_d)(E+\epsilon_j-\epsilon_a-\epsilon_c)} \tag{A.79}$$

$$du108a = 1.000 \sum_{a,b,c,d,i,j,k} \frac{\langle bd||pk\rangle\langle pc||id\rangle\langle ak||bj\rangle\langle ij||ac\rangle}{(E+\epsilon_k-\epsilon_b-\epsilon_d)(\epsilon_i+\epsilon_k-\epsilon_b-\epsilon_c)(\epsilon_i+\epsilon_j-\epsilon_a-\epsilon_c)} \tag{A.80}$$

$$du109a = 1.000 \sum_{a,b,c,d,i,j,k} \frac{\langle ad||ik\rangle\langle ic||jd\rangle\langle jb||pc\rangle\langle pk||ab\rangle}{(\epsilon_i+\epsilon_k-\epsilon_a-\epsilon_d)(\epsilon_j+\epsilon_k-\epsilon_a-\epsilon_c)(E+\epsilon_k-\epsilon_a-\epsilon_b)} \tag{A.81}$$

$$du110a = 1.000 \sum_{a,b,c,d,i,j,k} \frac{\langle ad||pk\rangle\langle pc||id\rangle\langle ib||jc\rangle\langle jk||ab\rangle}{(E+\epsilon_k-\epsilon_a-\epsilon_d)(\epsilon_i+\epsilon_k-\epsilon_a-\epsilon_c)(\epsilon_j+\epsilon_k-\epsilon_a-\epsilon_b)} \tag{A.82}$$

$$du111a = 1.000 \sum_{a,b,c,d,i,j,k} \frac{\langle ad||jk\rangle\langle jc||pd\rangle\langle pb||ic\rangle\langle ik||ab\rangle}{(\epsilon_j+\epsilon_k-\epsilon_a-\epsilon_d)(E+\epsilon_k-\epsilon_a-\epsilon_c)(\epsilon_i+\epsilon_k-\epsilon_a-\epsilon_b)} \tag{A.83}$$

$$du112a = 1.000 \sum_{a,b,c,d,i,j,k} \frac{\langle ad||ik\rangle\langle bc||pj\rangle\langle pk||ac\rangle\langle ij||bd\rangle}{(\epsilon_i+\epsilon_k-\epsilon_a-\epsilon_d)(E+\epsilon_i+\epsilon_j+\epsilon_k-\epsilon_a-\epsilon_b-\epsilon_c-\epsilon_d)(\epsilon_i+\epsilon_j-\epsilon_b-\epsilon_d)} \tag{A.84}$$

$$du101b = -1.000 \sum_{a,b,c,i,j,k,l} \frac{\langle pc||il\rangle\langle ib||jc\rangle\langle ja||kb\rangle\langle kl||pa\rangle}{(\epsilon_i + \epsilon_l - E - \epsilon_c)(\epsilon_j + \epsilon_l - E - \epsilon_b)(\epsilon_k + \epsilon_l - E - \epsilon_a)} \tag{A.85}$$

$$du102b = -1.000 \sum_{a,b,c,i,j,k,l} \frac{\langle pc||il\rangle\langle ab||jk\rangle\langle ik||ac\rangle\langle jl||pb\rangle}{(\epsilon_i + \epsilon_l - E - \epsilon_c)(\epsilon_i + \epsilon_j + \epsilon_k + \epsilon_l - E - \epsilon_a - \epsilon_b - \epsilon_c)(\epsilon_j + \epsilon_l - E - \epsilon_b)} \tag{A.86}$$

$$du103b = -1.000 \sum_{a,b,c,i,j,k,l} \frac{\langle ac||il\rangle\langle pl||ak\rangle\langle ib||jc\rangle\langle jk||pb\rangle}{(\epsilon_i + \epsilon_l - \epsilon_a - \epsilon_c)(\epsilon_i + \epsilon_k - E - \epsilon_c)(\epsilon_j + \epsilon_k - E - \epsilon_b)} \tag{A.87}$$

$$du104b = -1.000 \sum_{a,b,c,i,j,k,l} \frac{\langle pc||il\rangle\langle ib||jc\rangle\langle al||pk\rangle\langle jk||ab\rangle}{(\epsilon_i + \epsilon_l - E - \epsilon_c)(\epsilon_j + \epsilon_l - E - \epsilon_b)(\epsilon_j + \epsilon_k - \epsilon_a - \epsilon_b)} \tag{A.88}$$

$$du105b = -1.000 \sum_{a,b,c,i,j,k,l} \frac{\langle ac||jl\rangle\langle pb||ik\rangle\langle il||ab\rangle\langle jk||pc\rangle}{(\epsilon_j + \epsilon_l - \epsilon_a - \epsilon_c)(\epsilon_i + \epsilon_j + \epsilon_k + \epsilon_l - E - \epsilon_a - \epsilon_b - \epsilon_c)(\epsilon_j + \epsilon_k - E - \epsilon_c)} \tag{A.89}$$

$$du106b = -1.000 \sum_{a,b,c,i,j,k,l} \frac{\langle pc||il\rangle\langle ab||jk\rangle\langle jl||pb\rangle\langle ik||ac\rangle}{(\epsilon_i + \epsilon_l - E - \epsilon_c)(\epsilon_i + \epsilon_j + \epsilon_k + \epsilon_l - E - \epsilon_a - \epsilon_b - \epsilon_c)(\epsilon_i + \epsilon_k - \epsilon_a - \epsilon_c)} \tag{A.90}$$

$$du107b = -1.000 \sum_{a,b,c,i,j,k,l} \frac{\langle pc||il\rangle\langle al||pk\rangle\langle ib||jc\rangle\langle jk||ab\rangle}{(\epsilon_i + \epsilon_l - E - \epsilon_c)(\epsilon_i + \epsilon_k - \epsilon_a - \epsilon_c)(\epsilon_j + \epsilon_k - \epsilon_a - \epsilon_b)} \tag{A.91}$$

$$du108b = -1.000 \sum_{a,b,c,i,j,k,l} \frac{\langle ac||il\rangle\langle ib||jc\rangle\langle pl||ak\rangle\langle jk||pb\rangle}{(\epsilon_i + \epsilon_l - \epsilon_a - \epsilon_c)(\epsilon_j + \epsilon_l - \epsilon_a - \epsilon_b)(\epsilon_j + \epsilon_k - E - \epsilon_b)} \tag{A.92}$$

$$du109b = -1.000 \sum_{a,b,c,i,j,k,l} \frac{\langle pc||il\rangle\langle bl||pj\rangle\langle aj||bk\rangle\langle ik||ac\rangle}{(\epsilon_i + \epsilon_l - E - \epsilon_c)(\epsilon_i + \epsilon_j - \epsilon_b - \epsilon_c)(\epsilon_i + \epsilon_k - \epsilon_a - \epsilon_c)} \tag{A.93}$$

$$du110b = -1.000 \sum_{a,b,c,i,j,k,l} \frac{\langle bc||il\rangle\langle al||bj\rangle\langle pj||ak\rangle\langle ik||pc\rangle}{(\epsilon_i + \epsilon_l - \epsilon_b - \epsilon_c)(\epsilon_i + \epsilon_j - \epsilon_a - \epsilon_c)(\epsilon_i + \epsilon_k - E - \epsilon_c)} \tag{A.94}$$

$$du111b = -1.000 \sum_{a,b,c,i,j,k,l} \frac{\langle ac||il\rangle\langle pl||aj\rangle\langle bj||pk\rangle\langle ik||bc\rangle}{(\epsilon_i + \epsilon_l - \epsilon_a - \epsilon_c)(\epsilon_i + \epsilon_j - E - \epsilon_c)(\epsilon_i + \epsilon_k - \epsilon_b - \epsilon_c)} \tag{A.95}$$

$$du112b = -1.000 \sum_{a,b,c,i,j,k,l} \frac{\langle ac||jl\rangle\langle pb||ik\rangle\langle jk||pc\rangle\langle il||ab\rangle}{(\epsilon_j + \epsilon_l - \epsilon_a - \epsilon_c)(\epsilon_i + \epsilon_j + \epsilon_k + \epsilon_l - E - \epsilon_a - \epsilon_b - \epsilon_c)(\epsilon_i + \epsilon_l - \epsilon_a - \epsilon_b)} \tag{A.96}$$

$$du121a = 1.000 \sum_{a,b,c,d,i,j,k} \frac{\langle pj||ad\rangle\langle ac||ij\rangle\langle ik||bc\rangle\langle bd||pk\rangle}{(E+\epsilon_k-\epsilon_b-\epsilon_d)(E+\epsilon_j-\epsilon_a-\epsilon_d)(\epsilon_i+\epsilon_k-\epsilon_b-\epsilon_c)} \tag{A.97}$$

$$du123a = 1.000 \sum_{a,b,c,d,i,j,k} \frac{\langle pj||ad\rangle\langle ac||ij\rangle\langle ik||bc\rangle\langle bd||pk\rangle}{(E+\epsilon_k-\epsilon_b-\epsilon_d)(\epsilon_i+\epsilon_k-\epsilon_b-\epsilon_c)(\epsilon_i+\epsilon_j-\epsilon_a-\epsilon_c)} \tag{A.98}$$

$$du121b = -1.000 \sum_{a,b,c,i,j,k,l} \frac{\langle pc||il\rangle\langle ik||ac\rangle\langle ab||jk\rangle\langle jl||pb\rangle}{(\epsilon_i+\epsilon_l-E-\epsilon_c)(\epsilon_j+\epsilon_l-E-\epsilon_b)(\epsilon_j+\epsilon_k-\epsilon_a-\epsilon_b)} \tag{A.99}$$

$$du123b = -1.000 \sum_{a,b,c,i,j,k,l} \frac{\langle pc||il\rangle\langle ik||ac\rangle\langle ab||jk\rangle\langle jl||pb\rangle}{(\epsilon_i+\epsilon_l-E-\epsilon_c)(\epsilon_j+\epsilon_k-\epsilon_a-\epsilon_b)(\epsilon_i+\epsilon_k-\epsilon_a-\epsilon_c)} \tag{A.100}$$

$$du201a = 0.125 \sum_{a,b,c,d,e,f,i} \frac{\langle cf||pi\rangle\langle be||cf\rangle\langle ad||be\rangle\langle pi||ad\rangle}{(E+\epsilon_i-\epsilon_c-\epsilon_f)(E+\epsilon_i-\epsilon_b-\epsilon_e)(E+\epsilon_i-\epsilon_a-\epsilon_d)} \tag{A.101}$$

$$du202a = 0.125 \sum_{a,b,c,d,i,j,k} \frac{\langle bd||pk\rangle\langle ac||ij\rangle\langle ij||bd\rangle\langle pk||ac\rangle}{(E+\epsilon_k-\epsilon_b-\epsilon_d)(E+\epsilon_i+\epsilon_j+\epsilon_k-\epsilon_a-\epsilon_b-\epsilon_c-\epsilon_d)(E+\epsilon_k-\epsilon_a-\epsilon_c)} \tag{A.102}$$

$$du203a = 0.125 \sum_{a,b,c,d,i,j,k} \frac{\langle bd||pk\rangle\langle ac||bd\rangle\langle pk||ij\rangle\langle ij||ac\rangle}{(E+\epsilon_k-\epsilon_b-\epsilon_d)(E+\epsilon_k-\epsilon_a-\epsilon_c)(\epsilon_i+\epsilon_j-\epsilon_a-\epsilon_c)} \tag{A.103}$$

$$du204a = 0.125 \sum_{a,b,c,d,i,j,k} \frac{\langle bd||ik\rangle\langle ik||pj\rangle\langle ac||bd\rangle\langle pj||ac\rangle}{(\epsilon_i+\epsilon_k-\epsilon_b-\epsilon_d)(E+\epsilon_j-\epsilon_b-\epsilon_d)(E+\epsilon_j-\epsilon_a-\epsilon_c)} \tag{A.104}$$

$$du205a = 0.125 \sum_{a,b,c,d,i,j,k} \frac{\langle bd||pk\rangle\langle ac||ij\rangle\langle pk||ac\rangle\langle ij||bd\rangle}{(E+\epsilon_k-\epsilon_b-\epsilon_d)(E+\epsilon_i+\epsilon_j+\epsilon_k-\epsilon_a-\epsilon_b-\epsilon_c-\epsilon_d)(\epsilon_i+\epsilon_j-\epsilon_b-\epsilon_d)} \tag{A.105}$$

$$du206a = 0.125 \sum_{a,b,c,d,i,j,k} \frac{\langle ad||ik\rangle\langle bc||pj\rangle\langle ik||bc\rangle\langle pj||ad\rangle}{(\epsilon_i+\epsilon_k-\epsilon_a-\epsilon_d)(E+\epsilon_i+\epsilon_j+\epsilon_k-\epsilon_a-\epsilon_b-\epsilon_c-\epsilon_d)(E+\epsilon_j-\epsilon_a-\epsilon_d)} \tag{A.106}$$

$$du207a = 0.125 \sum_{a,b,c,d,i,j,k} \frac{\langle bd||ik\rangle\langle ac||bd\rangle\langle ik||pj\rangle\langle pj||ac\rangle}{(\epsilon_i+\epsilon_k-\epsilon_b-\epsilon_d)(\epsilon_i+\epsilon_k-\epsilon_a-\epsilon_c)(E+\epsilon_j-\epsilon_a-\epsilon_c)} \tag{A.107}$$

$$du208a = 0.125 \sum_{a,b,c,d,i,j,k} \frac{\langle bd||pk\rangle\langle pk||ij\rangle\langle ac||bd\rangle\langle ij||ac\rangle}{(E+\epsilon_k-\epsilon_b-\epsilon_d)(\epsilon_i+\epsilon_j-\epsilon_b-\epsilon_d)(\epsilon_i+\epsilon_j-\epsilon_a-\epsilon_c)} \tag{A.108}$$

$$du209a = 0.125 \sum_{a,b,i,j,k,l,m} \frac{\langle ab||im\rangle\langle im||jk\rangle\langle jk||pl\rangle\langle pl||ab\rangle}{(\epsilon_i+\epsilon_m-\epsilon_a-\epsilon_b)(\epsilon_j+\epsilon_k-\epsilon_a-\epsilon_b)(E+\epsilon_l-\epsilon_a-\epsilon_b)} \tag{A.109}$$

$$du210a = 0.125 \sum_{a,b,i,j,k,l,m} \frac{\langle ab||pm\rangle\langle pm||ik\rangle\langle ik||jl\rangle\langle jl||ab\rangle}{(E+\epsilon_m-\epsilon_a-\epsilon_b)(\epsilon_i+\epsilon_k-\epsilon_a-\epsilon_b)(\epsilon_j+\epsilon_l-\epsilon_a-\epsilon_b)} \tag{A.110}$$

$$du211a = 0.125 \sum_{a,b,i,j,k,l,m} \frac{\langle ab||jm\rangle\langle jm||pk\rangle\langle pk||il\rangle\langle il||ab\rangle}{(\epsilon_j+\epsilon_m-\epsilon_a-\epsilon_b)(E+\epsilon_k-\epsilon_a-\epsilon_b)(\epsilon_i+\epsilon_l-\epsilon_a-\epsilon_b)} \tag{A.111}$$

$$du212a = 0.125 \sum_{a,b,c,d,i,j,k} \frac{\langle ad||ik\rangle\langle bc||pj\rangle\langle pj||ad\rangle\langle ik||bc\rangle}{(\epsilon_i+\epsilon_k-\epsilon_a-\epsilon_d)(E+\epsilon_i+\epsilon_j+\epsilon_k-\epsilon_a-\epsilon_b-\epsilon_c-\epsilon_d)(\epsilon_i+\epsilon_k-\epsilon_b-\epsilon_c)} \tag{A.112}$$

$$du201b = -0.125 \sum_{a,i,j,k,l,m,n} \frac{\langle pa||in\rangle\langle in||jl\rangle\langle jl||km\rangle\langle km||pa\rangle}{(\epsilon_i + \epsilon_n - E - \epsilon_a)(\epsilon_j + \epsilon_l - E - \epsilon_a)(\epsilon_k + \epsilon_m - E - \epsilon_a)} \tag{A.113}$$

$$du202b = -0.125 \sum_{a,b,c,i,j,k,l} \frac{\langle pc||il\rangle\langle ab||jk\rangle\langle il||ab\rangle\langle jk||pc\rangle}{(\epsilon_i + \epsilon_l - E - \epsilon_c)(\epsilon_i + \epsilon_j + \epsilon_k + \epsilon_l - E - \epsilon_a - \epsilon_b - \epsilon_c)(\epsilon_j + \epsilon_k - E - \epsilon_c)} \tag{A.114}$$

$$du203b = -0.125 \sum_{a,b,c,i,j,k,l} \frac{\langle ac||il\rangle\langle pb||ac\rangle\langle il||jk\rangle\langle jk||pb\rangle}{(\epsilon_i + \epsilon_l - \epsilon_a - \epsilon_c)(\epsilon_i + \epsilon_l - E - \epsilon_b)(\epsilon_j + \epsilon_k - E - \epsilon_b)} \tag{A.115}$$

$$du204b = -0.125 \sum_{a,b,c,i,j,k,l} \frac{\langle pc||il\rangle\langle il||jk\rangle\langle ab||pc\rangle\langle jk||ab\rangle}{(\epsilon_i + \epsilon_l - E - \epsilon_c)(\epsilon_j + \epsilon_k - E - \epsilon_c)(\epsilon_j + \epsilon_k - \epsilon_a - \epsilon_b)} \tag{A.116}$$

$$du205b = -0.125 \sum_{a,b,c,i,j,k,l} \frac{\langle ac||jl\rangle\langle pb||ik\rangle\langle ik||ac\rangle\langle jl||pb\rangle}{(\epsilon_j + \epsilon_l - \epsilon_a - \epsilon_c)(\epsilon_i + \epsilon_j + \epsilon_k + \epsilon_l - E - \epsilon_a - \epsilon_b - \epsilon_c)(\epsilon_j + \epsilon_l - E - \epsilon_b)} \tag{A.117}$$

$$du206b = -0.125 \sum_{a,b,c,i,j,k,l} \frac{\langle pc||il\rangle\langle ab||jk\rangle\langle jk||pc\rangle\langle il||ab\rangle}{(\epsilon_i + \epsilon_l - E - \epsilon_c)(\epsilon_i + \epsilon_j + \epsilon_k + \epsilon_l - E - \epsilon_a - \epsilon_b - \epsilon_c)(\epsilon_i + \epsilon_l - \epsilon_a - \epsilon_b)} \tag{A.118}$$

$$du207b = -0.125 \sum_{a,b,c,i,j,k,l} \frac{\langle pc||il\rangle\langle ab||pc\rangle\langle il||jk\rangle\langle jk||ab\rangle}{(\epsilon_i + \epsilon_l - E - \epsilon_c)(\epsilon_i + \epsilon_l - \epsilon_a - \epsilon_b)(\epsilon_j + \epsilon_k - \epsilon_a - \epsilon_b)} \tag{A.119}$$

$$du208b = -0.125 \sum_{a,b,c,i,j,k,l} \frac{\langle ac||il\rangle\langle il||jk\rangle\langle pb||ac\rangle\langle jk||pb\rangle}{(\epsilon_i + \epsilon_l - \epsilon_a - \epsilon_c)(\epsilon_j + \epsilon_k - \epsilon_a - \epsilon_c)(\epsilon_j + \epsilon_k - E - \epsilon_b)} \tag{A.120}$$

$$du209b = -0.125 \sum_{a,b,c,d,e,i,j} \frac{\langle pe||ij\rangle\langle bd||pe\rangle\langle ac||bd\rangle\langle ij||ac\rangle}{(\epsilon_i + \epsilon_j - E - \epsilon_e)(\epsilon_i + \epsilon_j - \epsilon_b - \epsilon_d)(\epsilon_i + \epsilon_j - \epsilon_a - \epsilon_c)} \tag{A.121}$$

$$du210b = -0.125 \sum_{a,b,c,d,e,i,j} \frac{\langle be||ij\rangle\langle ad||be\rangle\langle pc||ad\rangle\langle ij||pc\rangle}{(\epsilon_i + \epsilon_j - \epsilon_b - \epsilon_e)(\epsilon_i + \epsilon_j - \epsilon_a - \epsilon_d)(\epsilon_i + \epsilon_j - E - \epsilon_c)} \tag{A.122}$$

$$du211b = -0.125 \sum_{a,b,c,d,e,i,j} \frac{\langle ae||ij\rangle\langle pd||ae\rangle\langle bc||pd\rangle\langle ij||bc\rangle}{(\epsilon_i + \epsilon_j - \epsilon_a - \epsilon_e)(\epsilon_i + \epsilon_j - E - \epsilon_d)(\epsilon_i + \epsilon_j - \epsilon_b - \epsilon_c)} \tag{A.123}$$

$$du212b = -0.125 \sum_{a,b,c,i,j,k,l} \frac{\langle ac||jl\rangle\langle pb||ik\rangle\langle jl||pb\rangle\langle ik||ac\rangle}{(\epsilon_j + \epsilon_l - \epsilon_a - \epsilon_c)(\epsilon_i + \epsilon_j + \epsilon_k + \epsilon_l - E - \epsilon_a - \epsilon_b - \epsilon_c)(\epsilon_i + \epsilon_k - \epsilon_a - \epsilon_c)} \tag{A.124}$$

$$du221a = 0.125 \sum_{a,b,c,d,i,j,k} \frac{\langle bd||pk\rangle\langle ac||ij\rangle\langle ij||bd\rangle\langle pk||ac\rangle}{(E + \epsilon_k - \epsilon_b - \epsilon_d)(E + \epsilon_k - \epsilon_a - \epsilon_c)(\epsilon_i + \epsilon_j - \epsilon_b - \epsilon_d)} \tag{A.125}$$

$$du223a = 0.125 \sum_{a,b,c,d,i,j,k} \frac{\langle bd||pk\rangle\langle ac||ij\rangle\langle ij||bd\rangle\langle pk||ac\rangle}{(E + \epsilon_k - \epsilon_b - \epsilon_d)(\epsilon_i + \epsilon_j - \epsilon_b - \epsilon_d)(\epsilon_i + \epsilon_j - \epsilon_a - \epsilon_c)} \tag{A.126}$$

$$du221b = -0.125 \sum_{a,b,c,i,j,k,l} \frac{\langle pc||il\rangle\langle ab||jk\rangle\langle il||ab\rangle\langle jk||pc\rangle}{(\epsilon_i + \epsilon_l - E - \epsilon_c)(\epsilon_j + \epsilon_k - E - \epsilon_c)(\epsilon_i + \epsilon_l - \epsilon_a - \epsilon_b)} \tag{A.127}$$

$$du223b = -0.125 \sum_{a,b,c,i,j,k,l} \frac{\langle pc||il\rangle\langle ab||jk\rangle\langle il||ab\rangle\langle jk||pc\rangle}{(\epsilon_i + \epsilon_l - E - \epsilon_c)(\epsilon_i + \epsilon_l - \epsilon_a - \epsilon_b)(\epsilon_j + \epsilon_k - \epsilon_a - \epsilon_b)} \tag{A.128}$$

$$du301a = -0.500 \sum_{a,b,c,d,e,i,j} \frac{\langle ce||pj\rangle\langle bd||ce\rangle\langle aj||bi\rangle\langle pi||ad\rangle}{(E+\epsilon_j-\epsilon_c-\epsilon_e)(E+\epsilon_j-\epsilon_b-\epsilon_d)(E+\epsilon_i-\epsilon_a-\epsilon_d)} \tag{A.129}$$

$$du302a = 0.500 \sum_{a,b,c,d,i,j,k} \frac{\langle bd||pk\rangle\langle ak||ij\rangle\langle ic||bd\rangle\langle pj||ac\rangle}{(E+\epsilon_k-\epsilon_b-\epsilon_d)(E+\epsilon_i+\epsilon_j-\epsilon_a-\epsilon_b-\epsilon_d)(E+\epsilon_j-\epsilon_a-\epsilon_c)} \tag{A.130}$$

$$du303a = -0.500 \sum_{a,b,c,d,e,i,j} \frac{\langle be||pj\rangle\langle ad||be\rangle\langle pc||id\rangle\langle ij||ac\rangle}{(E+\epsilon_j-\epsilon_b-\epsilon_e)(E+\epsilon_j-\epsilon_a-\epsilon_d)(\epsilon_i+\epsilon_j-\epsilon_a-\epsilon_c)} \tag{A.131}$$

$$du304a = -0.500 \sum_{a,b,c,i,j,k,l} \frac{\langle bc||il\rangle\langle il||pj\rangle\langle aj||bk\rangle\langle pk||ac\rangle}{(\epsilon_i+\epsilon_l-\epsilon_b-\epsilon_c)(E+\epsilon_j-\epsilon_b-\epsilon_c)(E+\epsilon_k-\epsilon_a-\epsilon_c)} \tag{A.132}$$

$$du305a = -0.500 \sum_{a,b,c,i,j,k,l} \frac{\langle bc||pl\rangle\langle al||ij\rangle\langle pj||ak\rangle\langle ik||bc\rangle}{(E+\epsilon_l-\epsilon_b-\epsilon_c)(E+\epsilon_i+\epsilon_j-\epsilon_a-\epsilon_b-\epsilon_c)(\epsilon_i+\epsilon_k-\epsilon_b-\epsilon_c)} \tag{A.133}$$

$$du306a = -0.500 \sum_{a,b,c,d,e,i,j} \frac{\langle ae||ij\rangle\langle bd||pe\rangle\langle ic||bd\rangle\langle pj||ac\rangle}{(\epsilon_i+\epsilon_j-\epsilon_a-\epsilon_e)(E+\epsilon_i+\epsilon_j-\epsilon_a-\epsilon_b-\epsilon_d)(E+\epsilon_j-\epsilon_a-\epsilon_c)} \tag{A.134}$$

$$du307a = 0.500 \sum_{a,b,c,d,i,j,k} \frac{\langle bd||ik\rangle\langle ac||bj\rangle\langle ik||pc\rangle\langle pj||ad\rangle}{(\epsilon_i+\epsilon_k-\epsilon_b-\epsilon_d)(\epsilon_i+\epsilon_j+\epsilon_k-\epsilon_a-\epsilon_c-\epsilon_d)(E+\epsilon_j-\epsilon_a-\epsilon_d)} \tag{A.135}$$

$$du308a = 0.500 \sum_{a,b,c,d,i,j,k} \frac{\langle bd||pk\rangle\langle pc||ij\rangle\langle aj||bd\rangle\langle ik||ac\rangle}{(E+\epsilon_k-\epsilon_b-\epsilon_d)(\epsilon_i+\epsilon_j+\epsilon_k-\epsilon_b-\epsilon_c-\epsilon_d)(\epsilon_i+\epsilon_k-\epsilon_a-\epsilon_c)} \tag{A.136}$$

$$du309a = -0.500 \sum_{a,b,c,i,j,k,l} \frac{\langle ac||il\rangle\langle ib||jk\rangle\langle jk||pc\rangle\langle pl||ab\rangle}{(\epsilon_i+\epsilon_l-\epsilon_a-\epsilon_c)(\epsilon_j+\epsilon_k+\epsilon_l-\epsilon_a-\epsilon_b-\epsilon_c)(E+\epsilon_l-\epsilon_a-\epsilon_b)} \tag{A.137}$$

$$du310a = -0.500 \sum_{a,b,c,i,j,k,l} \frac{\langle ac||pl\rangle\langle pb||ik\rangle\langle il||jb\rangle\langle jk||ac\rangle}{(E+\epsilon_l-\epsilon_a-\epsilon_c)(\epsilon_i+\epsilon_k+\epsilon_l-\epsilon_a-\epsilon_b-\epsilon_c)(\epsilon_j+\epsilon_k-\epsilon_a-\epsilon_c)} \tag{A.138}$$

$$du311a = -0.500 \sum_{a,b,c,i,j,k,l} \frac{\langle ac||jl\rangle\langle jl||pk\rangle\langle pb||ic\rangle\langle ik||ab\rangle}{(\epsilon_j+\epsilon_l-\epsilon_a-\epsilon_c)(E+\epsilon_k-\epsilon_a-\epsilon_c)(\epsilon_i+\epsilon_k-\epsilon_a-\epsilon_b)} \tag{A.139}$$

$$du312a = 0.500 \sum_{a,b,c,d,i,j,k} \frac{\langle ad||ik\rangle\langle bc||pd\rangle\langle pk||aj\rangle\langle ij||bc\rangle}{(\epsilon_i+\epsilon_k-\epsilon_a-\epsilon_d)(E+\epsilon_i+\epsilon_k-\epsilon_a-\epsilon_b-\epsilon_c)(\epsilon_i+\epsilon_j-\epsilon_b-\epsilon_c)} \tag{A.140}$$

$$du301b = 0.500 \sum_{a,b,i,j,k,l,m} \frac{\langle pb||im\rangle\langle ia||jb\rangle\langle jm||kl\rangle\langle kl||pa\rangle}{(\epsilon_i+\epsilon_m-E-\epsilon_b)(\epsilon_j+\epsilon_m-E-\epsilon_a)(\epsilon_k+\epsilon_l-E-\epsilon_a)} \tag{A.141}$$

$$du302b = -0.500 \sum_{a,b,c,i,j,k,l} \frac{\langle pc||il\rangle\langle al||jk\rangle\langle ib||ac\rangle\langle jk||pb\rangle}{(\epsilon_i+\epsilon_l-E-\epsilon_c)(\epsilon_i+\epsilon_j+\epsilon_k-E-\epsilon_a-\epsilon_c)(\epsilon_j+\epsilon_k-E-\epsilon_b)} \tag{A.142}$$

$$du303b = 0.500 \sum_{a,b,i,j,k,l,m} \frac{\langle ab||im\rangle\langle pm||ak\rangle\langle ik||jl\rangle\langle jl||pb\rangle}{(\epsilon_i+\epsilon_m-\epsilon_a-\epsilon_b)(\epsilon_i+\epsilon_k-E-\epsilon_b)(\epsilon_j+\epsilon_l-E-\epsilon_b)} \tag{A.143}$$

$$du304b = 0.500 \sum_{a,b,c,d,i,j,k} \frac{\langle pd||ik\rangle\langle ic||jd\rangle\langle ab||pc\rangle\langle jk||ab\rangle}{(\epsilon_i+\epsilon_k-E-\epsilon_d)(\epsilon_j+\epsilon_k-E-\epsilon_c)(\epsilon_j+\epsilon_k-\epsilon_a-\epsilon_b)} \tag{A.144}$$

$$du305b = 0.500 \sum_{a,b,c,d,i,j,k} \frac{\langle ad||jk\rangle\langle pc||id\rangle\langle ib||ac\rangle\langle jk||pb\rangle}{(\epsilon_j+\epsilon_k-\epsilon_a-\epsilon_d)(\epsilon_i+\epsilon_j+\epsilon_k-E-\epsilon_a-\epsilon_c)(\epsilon_j+\epsilon_k-E-\epsilon_b)} \tag{A.145}$$

$$du306b = 0.500 \sum_{a,b,i,j,k,l,m} \frac{\langle pb||im\rangle\langle am||jk\rangle\langle jk||pl\rangle\langle il||ab\rangle}{(\epsilon_i+\epsilon_m-E-\epsilon_b)(\epsilon_i+\epsilon_j+\epsilon_k-E-\epsilon_a-\epsilon_b)(\epsilon_i+\epsilon_l-\epsilon_a-\epsilon_b)} \tag{A.146}$$

$$du307b = -0.500 \sum_{a,b,c,i,j,k,l} \frac{\langle pc||il\rangle\langle ab||pk\rangle\langle ik||jc\rangle\langle jl||ab\rangle}{(\epsilon_i+\epsilon_l-E-\epsilon_c)(\epsilon_i+\epsilon_k+\epsilon_l-\epsilon_a-\epsilon_b-\epsilon_c)(\epsilon_j+\epsilon_l-\epsilon_a-\epsilon_b)} \tag{A.147}$$

$$du308b = -0.500 \sum_{a,b,c,i,j,k,l} \frac{\langle ac||il\rangle\langle ib||jk\rangle\langle pl||ab\rangle\langle jk||pc\rangle}{(\epsilon_i+\epsilon_l-\epsilon_a-\epsilon_c)(\epsilon_j+\epsilon_k+\epsilon_l-\epsilon_a-\epsilon_b-\epsilon_c)(\epsilon_j+\epsilon_k-E-\epsilon_c)} \tag{A.148}$$

$$du309b = 0.500 \sum_{a,b,c,d,i,j,k} \frac{\langle pd||ik\rangle\langle bc||pj\rangle\langle ak||bc\rangle\langle ij||ad\rangle}{(\epsilon_i+\epsilon_k-E-\epsilon_d)(\epsilon_i+\epsilon_j+\epsilon_k-\epsilon_b-\epsilon_c-\epsilon_d)(\epsilon_i+\epsilon_j-\epsilon_a-\epsilon_d)} \tag{A.149}$$

$$du310b = 0.500 \sum_{a,b,c,d,i,j,k} \frac{\langle bd||ik\rangle\langle ac||bj\rangle\langle pj||ad\rangle\langle ik||pc\rangle}{(\epsilon_i+\epsilon_k-\epsilon_b-\epsilon_d)(\epsilon_i+\epsilon_j+\epsilon_k-\epsilon_a-\epsilon_c-\epsilon_d)(\epsilon_i+\epsilon_k-E-\epsilon_c)} \tag{A.150}$$

$$du311b = 0.500 \sum_{a,b,c,d,i,j,k} \frac{\langle ad||ik\rangle\langle pk||aj\rangle\langle bc||pd\rangle\langle ij||bc\rangle}{(\epsilon_i+\epsilon_k-\epsilon_a-\epsilon_d)(\epsilon_i+\epsilon_j-E-\epsilon_d)(\epsilon_i+\epsilon_j-\epsilon_b-\epsilon_c)} \tag{A.151}$$

$$du312b = -0.500 \sum_{a,b,c,i,j,k,l} \frac{\langle ac||jl\rangle\langle pb||ic\rangle\langle jl||pk\rangle\langle ik||ab\rangle}{(\epsilon_j+\epsilon_l-\epsilon_a-\epsilon_c)(\epsilon_i+\epsilon_j+\epsilon_l-E-\epsilon_a-\epsilon_b)(\epsilon_i+\epsilon_k-\epsilon_a-\epsilon_b)} \tag{A.152}$$

$$du401a = -0.500 \sum_{a,b,c,d,e,i,j} \frac{\langle ce||pj\rangle\langle bj||ci\rangle\langle ad||be\rangle\langle pi||ad\rangle}{(E+\epsilon_j-\epsilon_c-\epsilon_e)(E+\epsilon_i-\epsilon_b-\epsilon_e)(E+\epsilon_i-\epsilon_a-\epsilon_d)} \tag{A.153}$$

$$du402a = 0.500 \sum_{a,b,c,d,i,j,k} \frac{\langle bd||pk\rangle\langle ac||id\rangle\langle ik||bj\rangle\langle pj||ac\rangle}{(E+\epsilon_k-\epsilon_b-\epsilon_d)(E+\epsilon_i+\epsilon_k-\epsilon_a-\epsilon_b-\epsilon_c)(E+\epsilon_j-\epsilon_a-\epsilon_c)} \tag{A.154}$$

$$du403a = -0.500 \sum_{a,b,c,i,j,k,l} \frac{\langle bc||pl\rangle\langle al||bj\rangle\langle pj||ik\rangle\langle ik||ac\rangle}{(E+\epsilon_l-\epsilon_b-\epsilon_c)(E+\epsilon_j-\epsilon_a-\epsilon_c)(\epsilon_i+\epsilon_k-\epsilon_a-\epsilon_c)} \tag{A.155}$$

$$du404a = -0.500 \sum_{a,b,c,d,e,i,j} \frac{\langle be||ij\rangle\langle id||pe\rangle\langle ac||bd\rangle\langle pj||ac\rangle}{(\epsilon_i+\epsilon_j-\epsilon_b-\epsilon_e)(E+\epsilon_j-\epsilon_b-\epsilon_d)(E+\epsilon_j-\epsilon_a-\epsilon_c)} \tag{A.156}$$

$$du405a = -0.500 \sum_{a,b,c,d,e,i,j} \frac{\langle be||pj\rangle\langle ad||ie\rangle\langle pc||ad\rangle\langle ij||bc\rangle}{(E+\epsilon_j-\epsilon_b-\epsilon_e)(E+\epsilon_i+\epsilon_j-\epsilon_a-\epsilon_b-\epsilon_d)(\epsilon_i+\epsilon_j-\epsilon_b-\epsilon_c)} \tag{A.157}$$

$$du406a = -0.500 \sum_{a,b,c,i,j,k,l} \frac{\langle ac||il\rangle\langle bl||pj\rangle\langle ij||bk\rangle\langle pk||ac\rangle}{(\epsilon_i+\epsilon_l-\epsilon_a-\epsilon_c)(E+\epsilon_i+\epsilon_j-\epsilon_a-\epsilon_b-\epsilon_c)(E+\epsilon_k-\epsilon_a-\epsilon_c)} \tag{A.158}$$

$$du407a = 0.500 \sum_{a,b,c,d,i,j,k} \frac{\langle bd||ik\rangle\langle ac||bj\rangle\langle ij||pd\rangle\langle pk||ac\rangle}{(\epsilon_i+\epsilon_k-\epsilon_b-\epsilon_d)(\epsilon_i+\epsilon_j+\epsilon_k-\epsilon_a-\epsilon_c-\epsilon_d)(E+\epsilon_k-\epsilon_a-\epsilon_c)} \tag{A.159}$$

$$du408a = 0.500 \sum_{a,b,c,d,i,j,k} \frac{\langle bd||pk\rangle\langle pc||ij\rangle\langle ak||bc\rangle\langle ij||ad\rangle}{(E+\epsilon_k-\epsilon_b-\epsilon_d)(\epsilon_i+\epsilon_j+\epsilon_k-\epsilon_b-\epsilon_c-\epsilon_d)(\epsilon_i+\epsilon_j-\epsilon_a-\epsilon_d)} \tag{A.160}$$

$$du409a = -0.500 \sum_{a,b,c,i,j,k,l} \frac{\langle ac||il\rangle\langle ib||jk\rangle\langle jl||pb\rangle\langle pk||ac\rangle}{(\epsilon_i+\epsilon_l-\epsilon_a-\epsilon_c)(\epsilon_j+\epsilon_k+\epsilon_l-\epsilon_a-\epsilon_b-\epsilon_c)(E+\epsilon_k-\epsilon_a-\epsilon_c)} \tag{A.161}$$

$$du410a = -0.500 \sum_{a,b,c,i,j,k,l} \frac{\langle ac||pl\rangle\langle pb||ik\rangle\langle ik||jc\rangle\langle jl||ab\rangle}{(E+\epsilon_l-\epsilon_a-\epsilon_c)(\epsilon_i+\epsilon_k+\epsilon_l-\epsilon_a-\epsilon_b-\epsilon_c)(\epsilon_j+\epsilon_l-\epsilon_a-\epsilon_b)} \tag{A.162}$$

$$du411a = -0.500 \sum_{a,b,c,i,j,k,l} \frac{\langle ac||jl\rangle\langle jb||pc\rangle\langle pl||ik\rangle\langle ik||ab\rangle}{(\epsilon_j+\epsilon_l-\epsilon_a-\epsilon_c)(E+\epsilon_l-\epsilon_a-\epsilon_b)(\epsilon_i+\epsilon_k-\epsilon_a-\epsilon_b)} \tag{A.163}$$

$$du412a = 0.500 \sum_{a,b,c,d,i,j,k} \frac{\langle ad||ik\rangle\langle bk||pj\rangle\langle pc||ad\rangle\langle ij||bc\rangle}{(\epsilon_i+\epsilon_k-\epsilon_a-\epsilon_d)(E+\epsilon_i+\epsilon_j-\epsilon_a-\epsilon_b-\epsilon_d)(\epsilon_i+\epsilon_j-\epsilon_b-\epsilon_c)} \tag{A.164}$$

$$du401b = 0.500 \sum_{a,b,i,j,k,l,m} \frac{\langle pb||im\rangle\langle im||jl\rangle\langle ja||kb\rangle\langle kl||pa\rangle}{(\epsilon_i + \epsilon_m - E - \epsilon_b)(\epsilon_j + \epsilon_l - E - \epsilon_b)(\epsilon_k + \epsilon_l - E - \epsilon_a)} \tag{A.165}$$

$$du402b = -0.500 \sum_{a,b,c,i,j,k,l} \frac{\langle pc||il\rangle\langle ab||jc\rangle\langle il||ak\rangle\langle jk||pb\rangle}{(\epsilon_i + \epsilon_l - E - \epsilon_c)(\epsilon_i + \epsilon_j + \epsilon_l - E - \epsilon_a - \epsilon_b)(\epsilon_j + \epsilon_k - E - \epsilon_b)} \tag{A.166}$$

$$du403b = 0.500 \sum_{a,b,c,d,i,j,k} \frac{\langle ad||ik\rangle\langle pc||ad\rangle\langle ib||jc\rangle\langle jk||pb\rangle}{(\epsilon_i + \epsilon_k - \epsilon_a - \epsilon_d)(\epsilon_i + \epsilon_k - E - \epsilon_c)(\epsilon_j + \epsilon_k - E - \epsilon_b)} \tag{A.167}$$

$$du404b = 0.500 \sum_{a,b,i,j,k,l,m} \frac{\langle pb||im\rangle\langle im||jk\rangle\langle ak||pl\rangle\langle jl||ab\rangle}{(\epsilon_i + \epsilon_m - E - \epsilon_b)(\epsilon_j + \epsilon_k - E - \epsilon_b)(\epsilon_j + \epsilon_l - \epsilon_a - \epsilon_b)} \tag{A.168}$$

$$du405b = 0.500 \sum_{a,b,i,j,k,l,m} \frac{\langle ab||jm\rangle\langle pm||ik\rangle\langle ik||al\rangle\langle jl||pb\rangle}{(\epsilon_j + \epsilon_m - \epsilon_a - \epsilon_b)(\epsilon_i + \epsilon_j + \epsilon_k - E - \epsilon_a - \epsilon_b)(\epsilon_j + \epsilon_l - E - \epsilon_b)} \tag{A.169}$$

$$du406b = 0.500 \sum_{a,b,c,d,i,j,k} \frac{\langle pd||ik\rangle\langle ac||jd\rangle\langle jb||pc\rangle\langle ik||ab\rangle}{(\epsilon_i + \epsilon_k - E - \epsilon_d)(\epsilon_i + \epsilon_j + \epsilon_k - E - \epsilon_a - \epsilon_c)(\epsilon_i + \epsilon_k - \epsilon_a - \epsilon_b)} \tag{A.170}$$

$$du407b = -0.500 \sum_{a,b,c,i,j,k,l} \frac{\langle pc||il\rangle\langle ab||pk\rangle\langle il||jb\rangle\langle jk||ac\rangle}{(\epsilon_i + \epsilon_l - E - \epsilon_c)(\epsilon_i + \epsilon_k + \epsilon_l - \epsilon_a - \epsilon_b - \epsilon_c)(\epsilon_j + \epsilon_k - \epsilon_a - \epsilon_c)} \tag{A.171}$$

$$du408b = -0.500 \sum_{a,b,c,i,j,k,l} \frac{\langle ac||il\rangle\langle ib||jk\rangle\langle pk||ac\rangle\langle jl||pb\rangle}{(\epsilon_i + \epsilon_l - \epsilon_a - \epsilon_c)(\epsilon_j + \epsilon_k + \epsilon_l - \epsilon_a - \epsilon_b - \epsilon_c)(\epsilon_j + \epsilon_l - E - \epsilon_b)} \tag{A.172}$$

$$du409b = 0.500 \sum_{a,b,c,d,i,j,k} \frac{\langle pd||ik\rangle\langle bc||pj\rangle\langle aj||bd\rangle\langle ik||ac\rangle}{(\epsilon_i + \epsilon_k - E - \epsilon_d)(\epsilon_i + \epsilon_j + \epsilon_k - \epsilon_b - \epsilon_c - \epsilon_d)(\epsilon_i + \epsilon_k - \epsilon_a - \epsilon_c)} \tag{A.173}$$

$$du410b = 0.500 \sum_{a,b,c,d,i,j,k} \frac{\langle bd||ik\rangle\langle ac||bj\rangle\langle pk||ac\rangle\langle ij||pd\rangle}{(\epsilon_i + \epsilon_k - \epsilon_b - \epsilon_d)(\epsilon_i + \epsilon_j + \epsilon_k - \epsilon_a - \epsilon_c - \epsilon_d)(\epsilon_i + \epsilon_j - E - \epsilon_d)} \tag{A.174}$$

$$du411b = 0.500 \sum_{a,b,c,d,i,j,k} \frac{\langle ad||ik\rangle\langle pc||ad\rangle\langle bk||pj\rangle\langle ij||bc\rangle}{(\epsilon_i + \epsilon_k - \epsilon_a - \epsilon_d)(\epsilon_i + \epsilon_k - E - \epsilon_c)(\epsilon_i + \epsilon_j - \epsilon_b - \epsilon_c)} \tag{A.175}$$

$$du412b = -0.500 \sum_{a,b,c,i,j,k,l} \frac{\langle ac||jl\rangle\langle pl||ik\rangle\langle jb||pc\rangle\langle ik||ab\rangle}{(\epsilon_j + \epsilon_l - \epsilon_a - \epsilon_c)(\epsilon_i + \epsilon_j + \epsilon_k - E - \epsilon_a - \epsilon_c)(\epsilon_i + \epsilon_k - \epsilon_a - \epsilon_b)} \tag{A.176}$$

$$du501a = -1.000 \sum_{a,b,c,d,i,j,k} \frac{\langle bc||pj\rangle\langle aj||bi\rangle\langle id||ck\rangle\langle pk||ad\rangle}{(E+\epsilon_j-\epsilon_b-\epsilon_c)(E+\epsilon_i-\epsilon_a-\epsilon_c)(E+\epsilon_k-\epsilon_a-\epsilon_d)} \tag{A.177}$$

$$du502a = 1.000 \sum_{a,b,c,d,e,i,j} \frac{\langle cd||pi\rangle\langle be||cj\rangle\langle ai||bd\rangle\langle pj||ae\rangle}{(E+\epsilon_i-\epsilon_c-\epsilon_d)(E+\epsilon_i+\epsilon_j-\epsilon_b-\epsilon_d-\epsilon_e)(E+\epsilon_j-\epsilon_a-\epsilon_e)} \tag{A.178}$$

$$du503a = -1.000 \sum_{a,b,c,d,i,j,k} \frac{\langle bc||pj\rangle\langle aj||bi\rangle\langle pd||ak\rangle\langle ik||cd\rangle}{(E+\epsilon_j-\epsilon_b-\epsilon_c)(E+\epsilon_i-\epsilon_a-\epsilon_c)(\epsilon_i+\epsilon_k-\epsilon_c-\epsilon_d)} \tag{A.179}$$

$$du504a = -1.000 \sum_{a,b,c,d,i,j,k} \frac{\langle ac||ij\rangle\langle ib||pc\rangle\langle jd||bk\rangle\langle pk||ad\rangle}{(\epsilon_i+\epsilon_j-\epsilon_a-\epsilon_c)(E+\epsilon_j-\epsilon_a-\epsilon_b)(E+\epsilon_k-\epsilon_a-\epsilon_d)} \tag{A.180}$$

$$du505a = -1.000 \sum_{a,b,c,d,i,j,k} \frac{\langle bc||pj\rangle\langle ad||bk\rangle\langle pk||id\rangle\langle ij||ac\rangle}{(E+\epsilon_j-\epsilon_b-\epsilon_c)(E+\epsilon_j+\epsilon_k-\epsilon_a-\epsilon_c-\epsilon_d)(\epsilon_i+\epsilon_j-\epsilon_a-\epsilon_c)} \tag{A.181}$$

$$du506a = -1.000 \sum_{a,b,c,d,i,j,k} \frac{\langle bc||ij\rangle\langle id||pk\rangle\langle ak||bd\rangle\langle pj||ac\rangle}{(\epsilon_i+\epsilon_j-\epsilon_b-\epsilon_c)(E+\epsilon_j+\epsilon_k-\epsilon_b-\epsilon_c-\epsilon_d)(E+\epsilon_j-\epsilon_a-\epsilon_c)} \tag{A.182}$$

$$du507a = 1.000 \sum_{a,b,c,i,j,k,l} \frac{\langle ab||ik\rangle\langle ic||jl\rangle\langle jk||pb\rangle\langle pl||ac\rangle}{(\epsilon_i+\epsilon_k-\epsilon_a-\epsilon_b)(\epsilon_j+\epsilon_k+\epsilon_l-\epsilon_a-\epsilon_b-\epsilon_c)(E+\epsilon_l-\epsilon_a-\epsilon_c)} \tag{A.183}$$

$$du508a = 1.000 \sum_{a,b,c,i,j,k,l} \frac{\langle ab||pk\rangle\langle pc||il\rangle\langle ik||jb\rangle\langle jl||ac\rangle}{(E+\epsilon_k-\epsilon_a-\epsilon_b)(\epsilon_i+\epsilon_k+\epsilon_l-\epsilon_a-\epsilon_b-\epsilon_c)(\epsilon_j+\epsilon_l-\epsilon_a-\epsilon_c)} \tag{A.184}$$

$$du509a = -1.000 \sum_{a,b,c,d,i,j,k} \frac{\langle bc||ij\rangle\langle ad||bk\rangle\langle ik||pd\rangle\langle pj||ac\rangle}{(\epsilon_i+\epsilon_j-\epsilon_b-\epsilon_c)(\epsilon_i+\epsilon_j+\epsilon_k-\epsilon_a-\epsilon_c-\epsilon_d)(E+\epsilon_j-\epsilon_a-\epsilon_c)} \tag{A.185}$$

$$du510a = -1.000 \sum_{a,b,c,d,i,j,k} \frac{\langle bc||pj\rangle\langle pd||ik\rangle\langle ak||bd\rangle\langle ij||ac\rangle}{(E+\epsilon_j-\epsilon_b-\epsilon_c)(\epsilon_i+\epsilon_j+\epsilon_k-\epsilon_b-\epsilon_c-\epsilon_d)(\epsilon_i+\epsilon_j-\epsilon_a-\epsilon_c)} \tag{A.186}$$

$$du511a = -1.000 \sum_{a,b,c,d,i,j,k} \frac{\langle ac||ij\rangle\langle ib||pc\rangle\langle pd||ak\rangle\langle jk||bd\rangle}{(\epsilon_i+\epsilon_j-\epsilon_a-\epsilon_c)(E+\epsilon_j-\epsilon_a-\epsilon_b)(\epsilon_j+\epsilon_k-\epsilon_b-\epsilon_d)} \tag{A.187}$$

$$du512a = 1.000 \sum_{a,b,c,i,j,k,l} \frac{\langle ab||jk\rangle\langle jc||pl\rangle\langle pk||ib\rangle\langle il||ac\rangle}{(\epsilon_j+\epsilon_k-\epsilon_a-\epsilon_b)(E+\epsilon_k+\epsilon_l-\epsilon_a-\epsilon_b-\epsilon_c)(\epsilon_i+\epsilon_l-\epsilon_a-\epsilon_c)} \tag{A.188}$$

$$du501b = 1.000 \sum_{a,b,c,i,j,k,l} \frac{\langle pb||ik\rangle\langle ia||jb\rangle\langle kc||al\rangle\langle jl||pc\rangle}{(\epsilon_i + \epsilon_k - E - \epsilon_b)(\epsilon_j + \epsilon_k - E - \epsilon_a)(\epsilon_j + \epsilon_l - E - \epsilon_c)} \tag{A.189}$$

$$du502b = -1.000 \sum_{a,b,i,j,k,l,m} \frac{\langle pa||il\rangle\langle ib||jm\rangle\langle jl||ka\rangle\langle km||pb\rangle}{(\epsilon_i + \epsilon_l - E - \epsilon_a)(\epsilon_j + \epsilon_l + \epsilon_m - E - \epsilon_a - \epsilon_b)(\epsilon_k + \epsilon_m - E - \epsilon_b)} \tag{A.190}$$

$$du503b = 1.000 \sum_{a,b,c,i,j,k,l} \frac{\langle ab||ik\rangle\langle pk||aj\rangle\langle jc||bl\rangle\langle il||pc\rangle}{(\epsilon_i + \epsilon_k - \epsilon_a - \epsilon_b)(\epsilon_i + \epsilon_j - E - \epsilon_b)(\epsilon_i + \epsilon_l - E - \epsilon_c)} \tag{A.191}$$

$$du504b = 1.000 \sum_{a,b,c,i,j,k,l} \frac{\langle pb||ik\rangle\langle ia||jb\rangle\langle jc||pl\rangle\langle kl||ac\rangle}{(\epsilon_i + \epsilon_k - E - \epsilon_b)(\epsilon_j + \epsilon_k - E - \epsilon_a)(\epsilon_k + \epsilon_l - \epsilon_a - \epsilon_c)} \tag{A.192}$$

$$du505b = 1.000 \sum_{a,b,c,i,j,k,l} \frac{\langle ab||ik\rangle\langle pc||al\rangle\langle il||jc\rangle\langle jk||pb\rangle}{(\epsilon_i + \epsilon_k - \epsilon_a - \epsilon_b)(\epsilon_i + \epsilon_k + \epsilon_l - E - \epsilon_b - \epsilon_c)(\epsilon_j + \epsilon_k - E - \epsilon_b)} \tag{A.193}$$

$$du506b = 1.000 \sum_{a,b,c,i,j,k,l} \frac{\langle pb||ik\rangle\langle ic||jl\rangle\langle al||pc\rangle\langle jk||ab\rangle}{(\epsilon_i + \epsilon_k - E - \epsilon_b)(\epsilon_j + \epsilon_k + \epsilon_l - E - \epsilon_b - \epsilon_c)(\epsilon_j + \epsilon_k - \epsilon_a - \epsilon_b)} \tag{A.194}$$

$$du507b = -1.000 \sum_{a,b,c,d,i,j,k} \frac{\langle pc||ij\rangle\langle bd||pk\rangle\langle aj||bc\rangle\langle ik||ad\rangle}{(\epsilon_i + \epsilon_j - E - \epsilon_c)(\epsilon_i + \epsilon_j + \epsilon_k - \epsilon_b - \epsilon_c - \epsilon_d)(\epsilon_i + \epsilon_k - \epsilon_a - \epsilon_d)} \tag{A.195}$$

$$du508b = -1.000 \sum_{a,b,c,d,i,j,k} \frac{\langle bc||ij\rangle\langle ad||bk\rangle\langle pj||ac\rangle\langle ik||pd\rangle}{(\epsilon_i + \epsilon_j - \epsilon_b - \epsilon_c)(\epsilon_i + \epsilon_j + \epsilon_k - \epsilon_a - \epsilon_c - \epsilon_d)(\epsilon_i + \epsilon_k - E - \epsilon_d)} \tag{A.196}$$

$$du509b = 1.000 \sum_{a,b,c,i,j,k,l} \frac{\langle pb||ik\rangle\langle ac||pl\rangle\langle il||jc\rangle\langle jk||ab\rangle}{(\epsilon_i + \epsilon_k - E - \epsilon_b)(\epsilon_i + \epsilon_k + \epsilon_l - \epsilon_a - \epsilon_b - \epsilon_c)(\epsilon_j + \epsilon_k - \epsilon_a - \epsilon_b)} \tag{A.197}$$

$$du510b = 1.000 \sum_{a,b,c,i,j,k,l} \frac{\langle ab||ik\rangle\langle ic||jl\rangle\langle pl||ac\rangle\langle jk||pb\rangle}{(\epsilon_i + \epsilon_k - \epsilon_a - \epsilon_b)(\epsilon_j + \epsilon_k + \epsilon_l - \epsilon_a - \epsilon_b - \epsilon_c)(\epsilon_j + \epsilon_k - E - \epsilon_b)} \tag{A.198}$$

$$du511b = 1.000 \sum_{a,b,c,i,j,k,l} \frac{\langle ab||ik\rangle\langle pk||aj\rangle\langle ic||pl\rangle\langle jl||bc\rangle}{(\epsilon_i + \epsilon_k - \epsilon_a - \epsilon_b)(\epsilon_i + \epsilon_j - E - \epsilon_b)(\epsilon_j + \epsilon_l - \epsilon_b - \epsilon_c)} \tag{A.199}$$

$$du512b = -1.000 \sum_{a,b,c,d,i,j,k} \frac{\langle ac||ij\rangle\langle pd||ak\rangle\langle bj||pc\rangle\langle ik||bd\rangle}{(\epsilon_i + \epsilon_j - \epsilon_a - \epsilon_c)(\epsilon_i + \epsilon_j + \epsilon_k - E - \epsilon_c - \epsilon_d)(\epsilon_i + \epsilon_k - \epsilon_b - \epsilon_d)} \tag{A.200}$$

Figure A.6: Fourth order diagrams

$du101a$

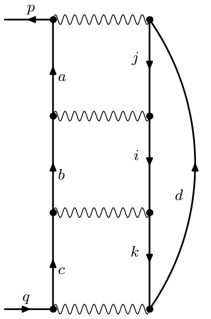

$du102a$

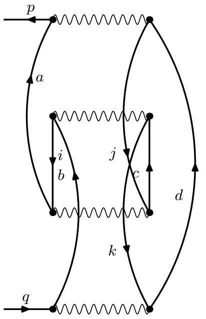

$du103a$

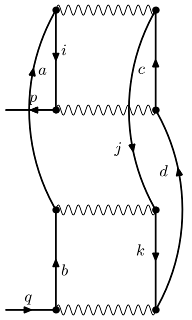

$du104a$

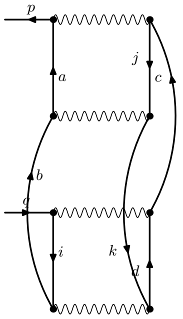

$du105a$

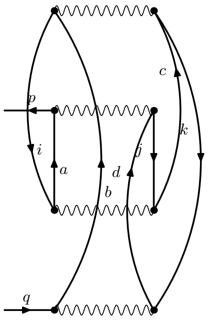

$du106a$

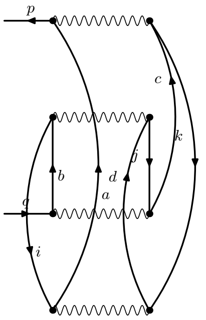

$du107a$

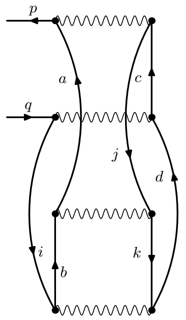

$du108a$

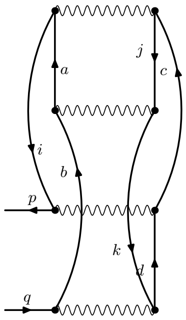

$du109a$

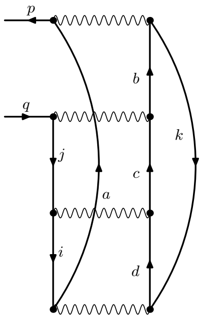

$du110a$

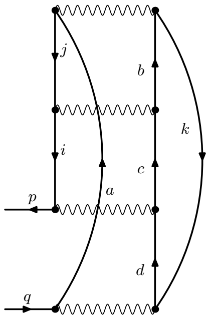

$du111a$

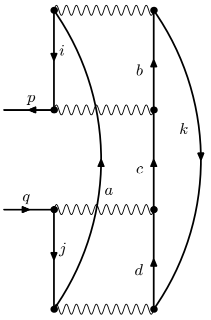

$du112a$

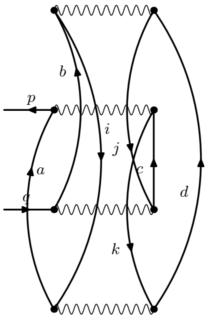

Figure A.7: Fourth order diagrams

$du201a$

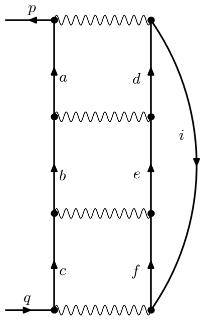

$du202a$

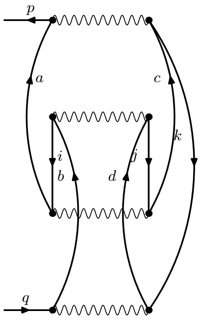

$du203a$

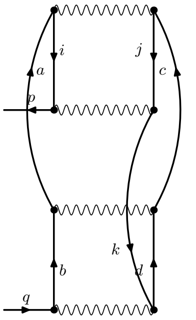

$du204a$

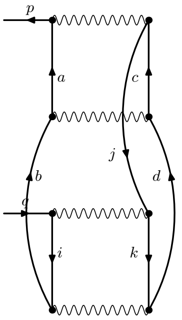

$du205a$

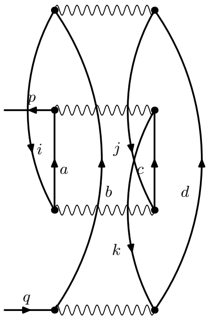

$du206a$

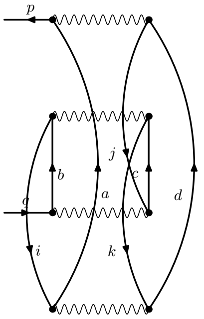

$du207a$

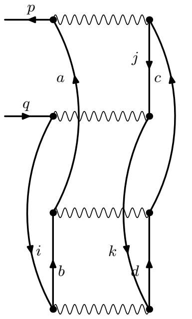

$du208a$

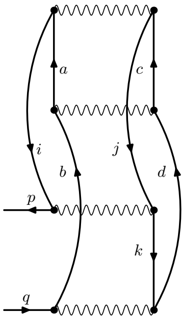

$du209a$

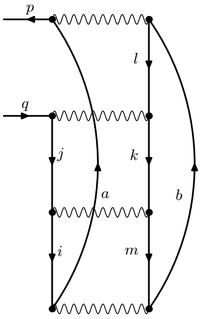

$du210a$

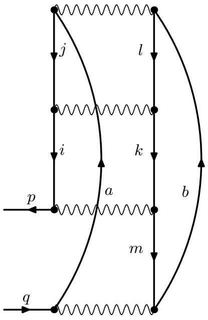

$du211a$

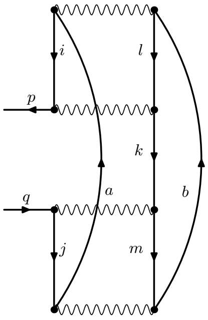

$du212a$

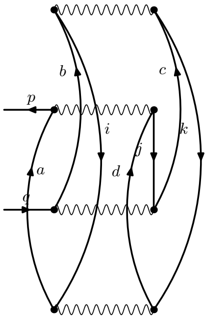

Figure A.8: Fourth order diagrams

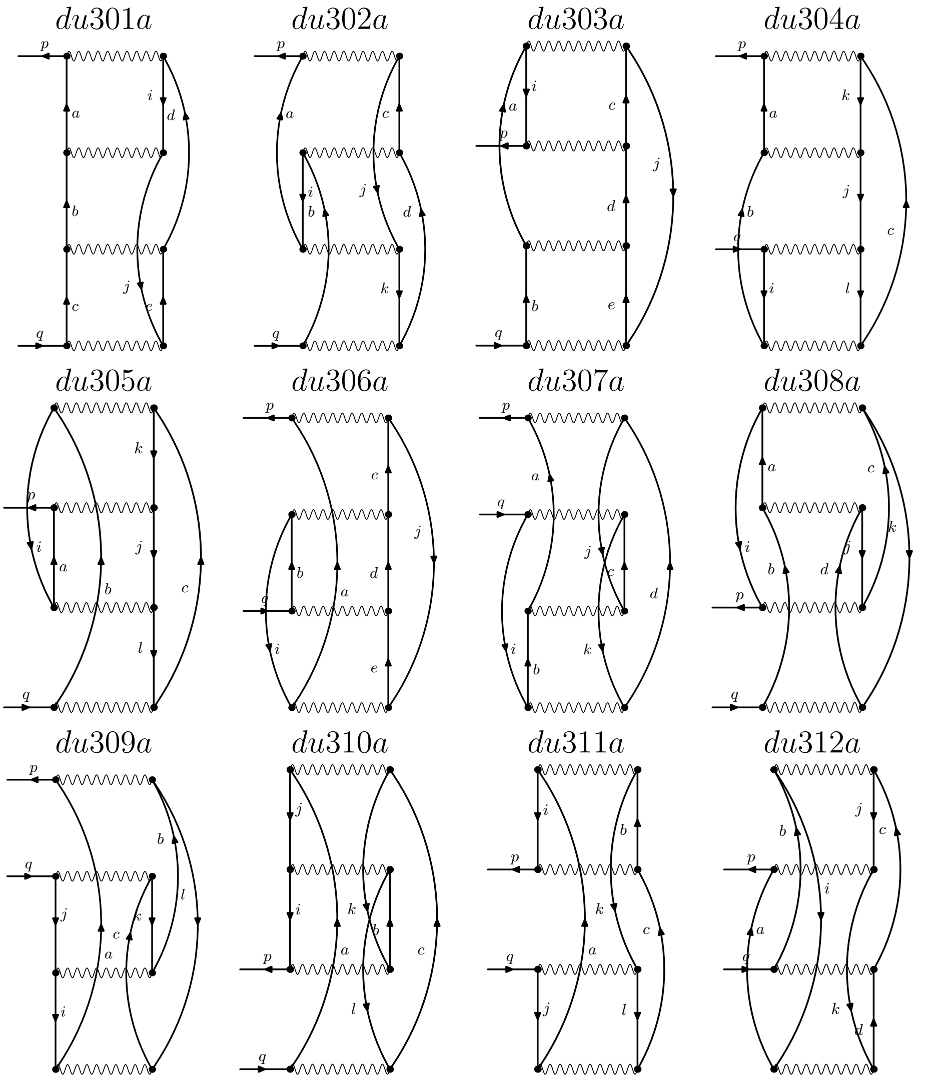

$du301a$ $du302a$ $du303a$ $du304a$

$du305a$ $du306a$ $du307a$ $du308a$

$du309a$ $du310a$ $du311a$ $du312a$

Figure A.9: Fourth order diagrams

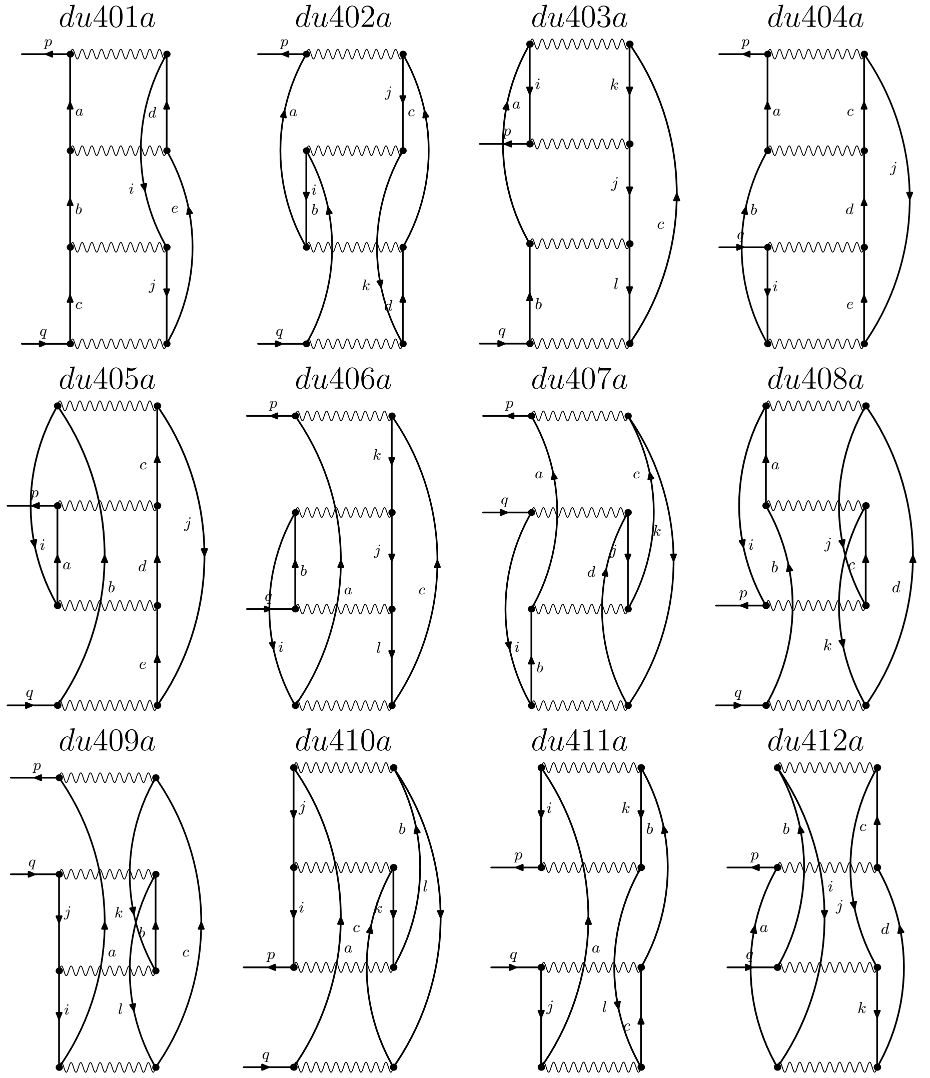

$du401a$ $du402a$ $du403a$ $du404a$

$du405a$ $du406a$ $du407a$ $du408a$

$du409a$ $du410a$ $du411a$ $du412a$

Figure A.10: Fourth order diagrams

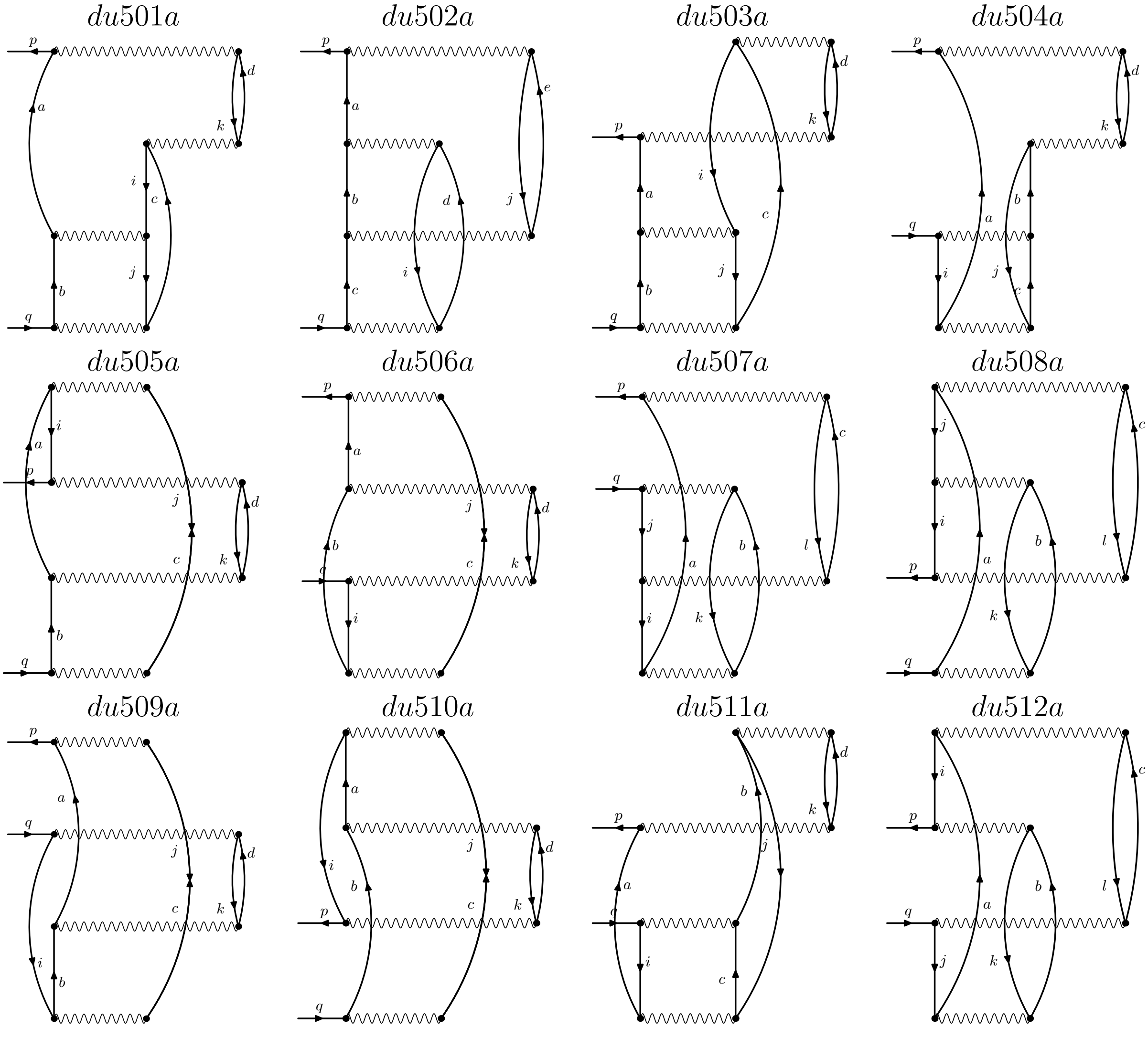
$du501a$ $du502a$ $du503a$ $du504a$

$du505a$ $du506a$ $du507a$ $du508a$

$du509a$ $du510a$ $du511a$ $du512a$

Figure A.11: Fourth order diagrams

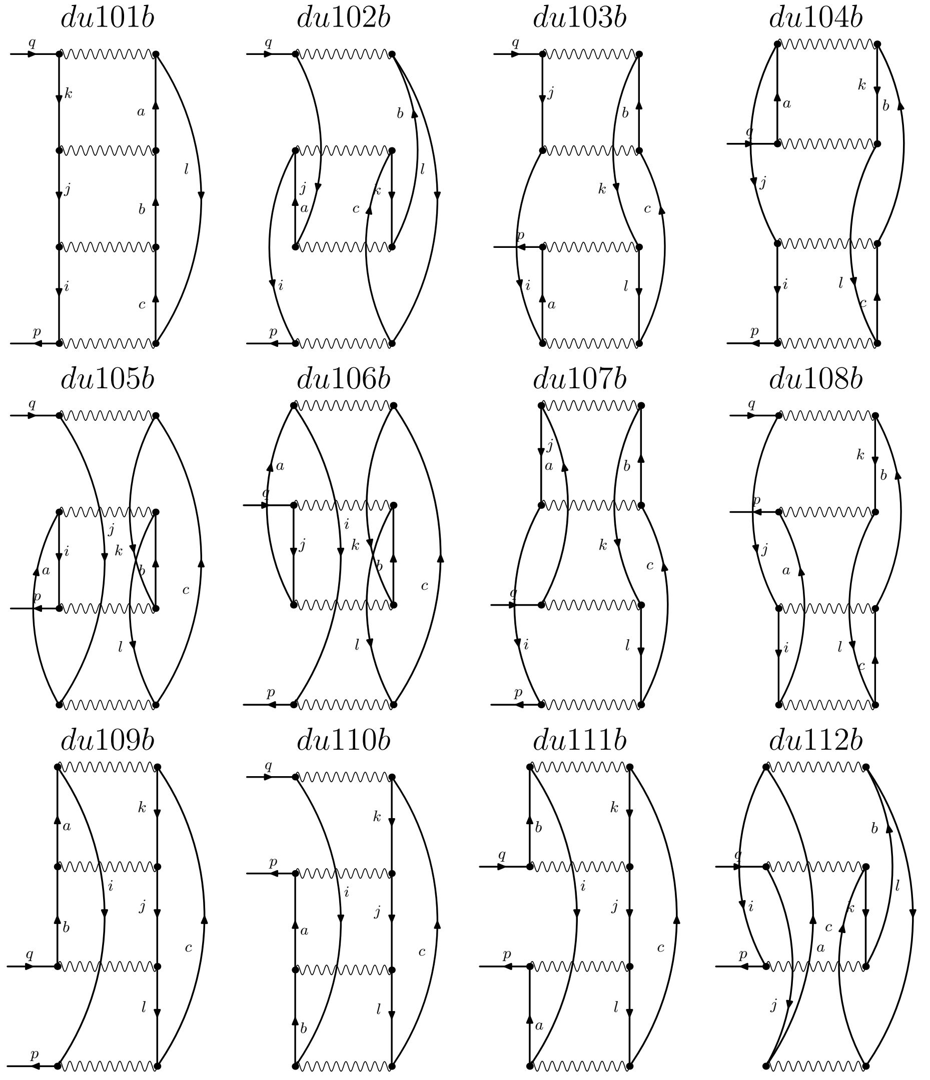

$du101b$ $du102b$ $du103b$ $du104b$

$du105b$ $du106b$ $du107b$ $du108b$

$du109b$ $du110b$ $du111b$ $du112b$

Figure A.12: Fourth order diagrams

$du201b$

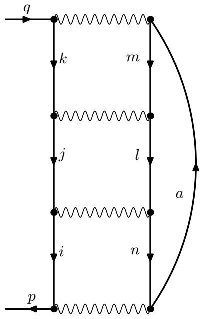

$du202b$

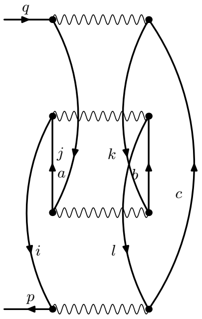

$du203b$

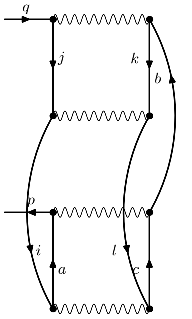

$du204b$

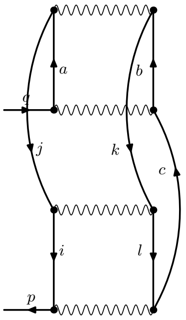

$du205b$

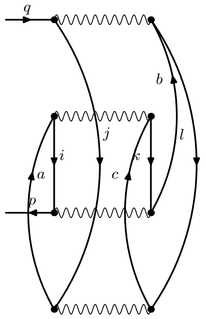

$du206b$

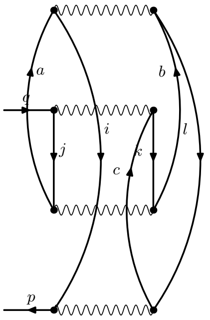

$du207b$

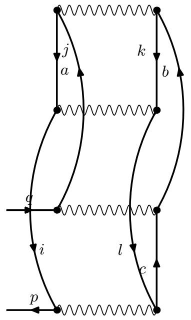

$du208b$

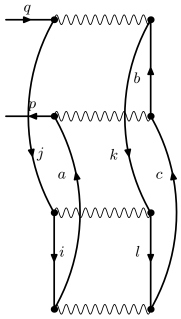

$du209b$

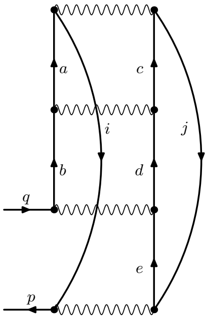

$du210b$

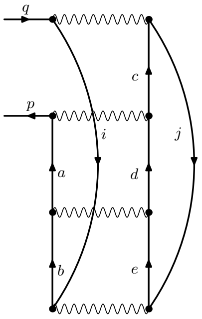

$du211b$

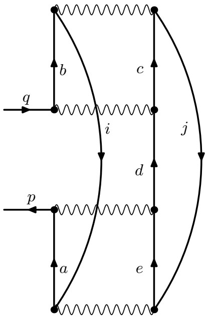

$du212b$

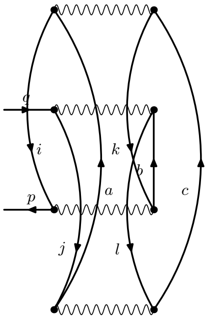

Figure A.13: Fourth order diagrams

$du301b$

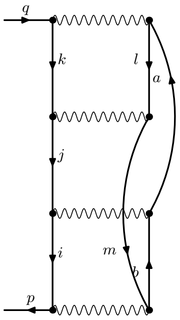

$du302b$

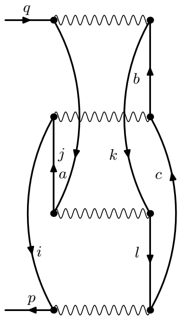

$du303b$

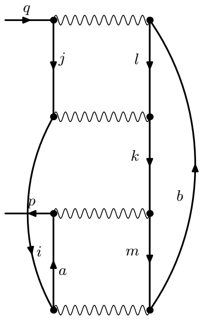

$du304b$

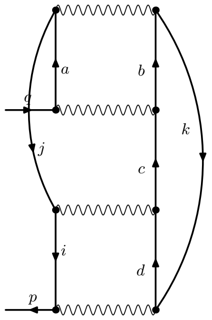

$du305b$

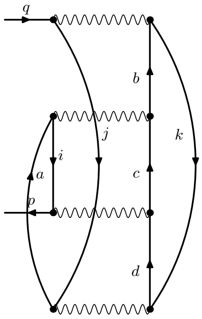

$du306b$

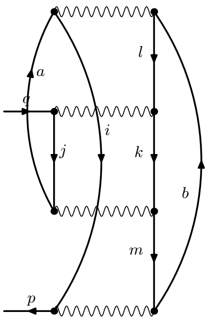

$du307b$

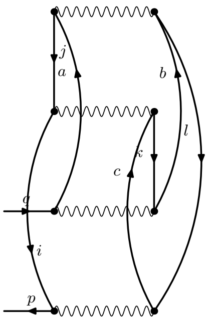

$du308b$

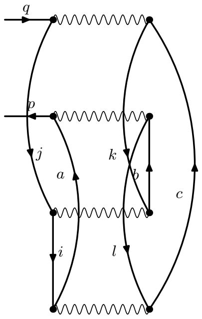

$du309b$

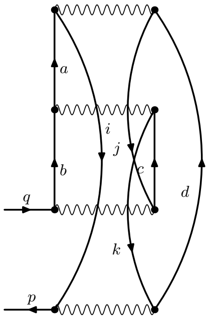

$du310b$

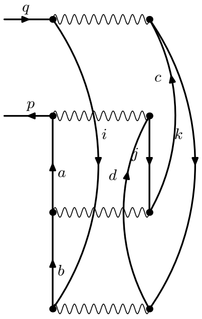

$du311b$

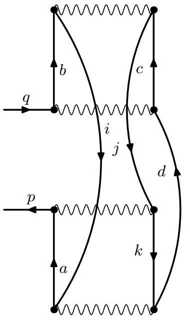

$du312b$

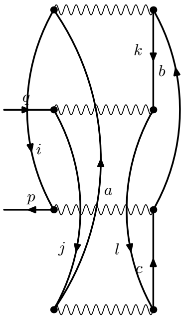

Figure A.14: Fourth order diagrams

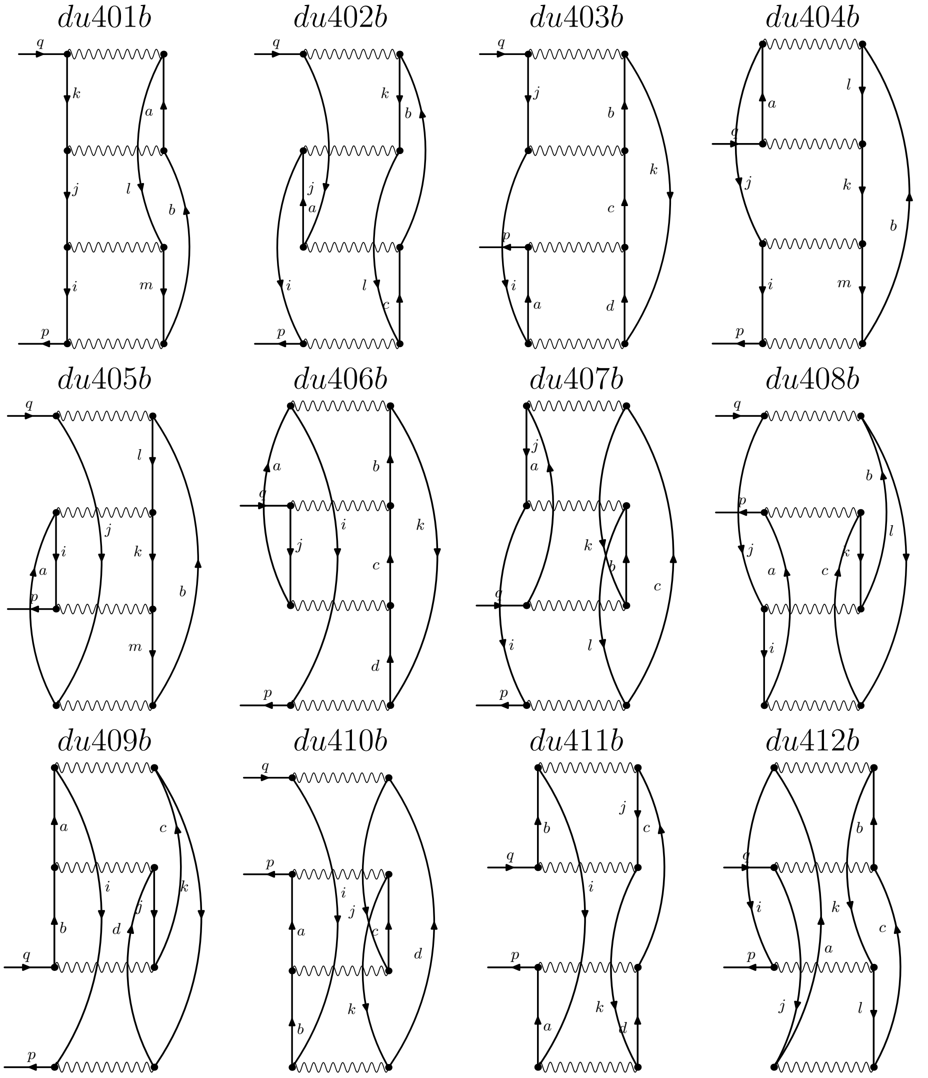

Figure A.15: Fourth order diagrams

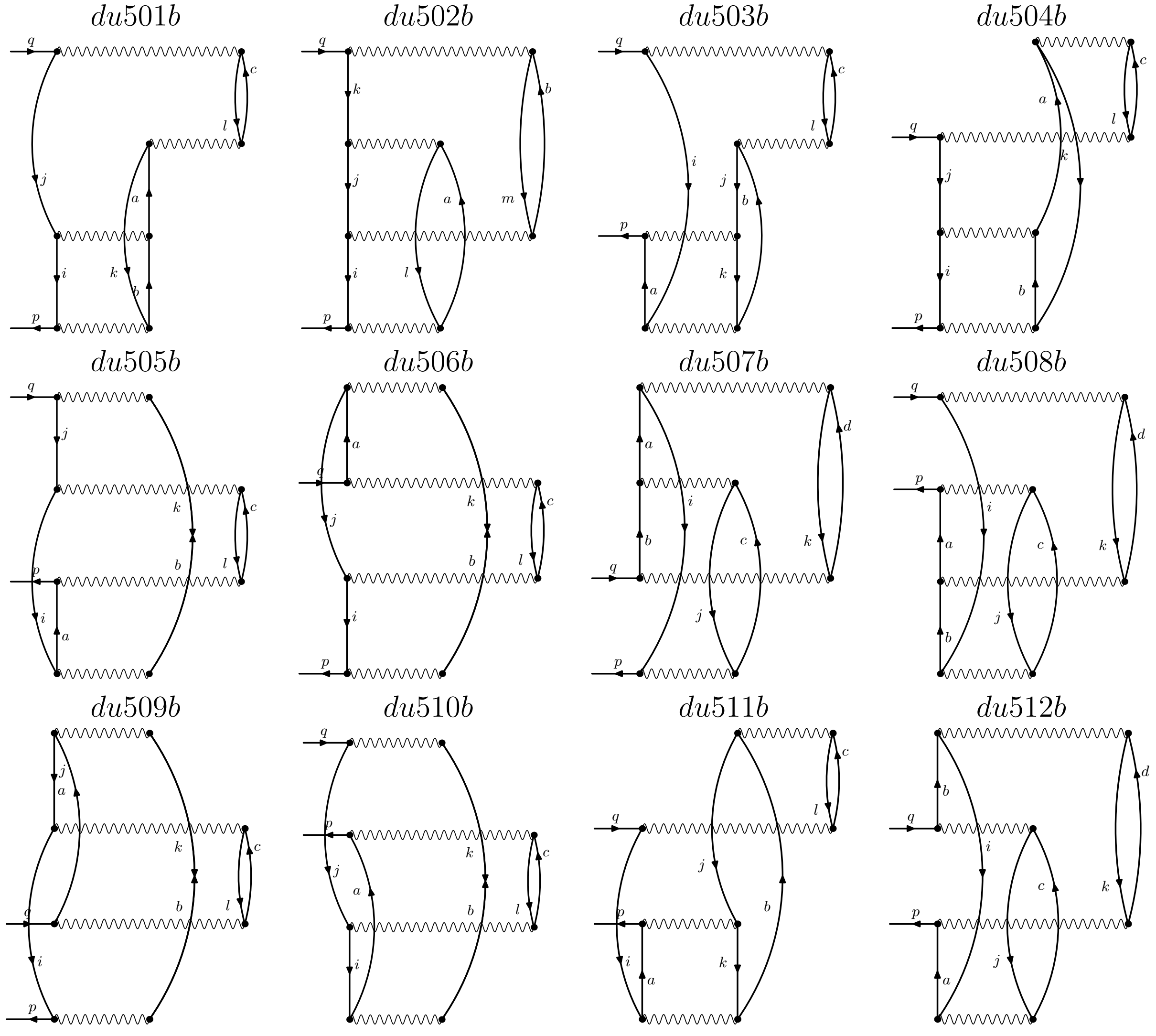

$du501b$ $du502b$ $du503b$ $du504b$

$du505b$ $du506b$ $du507b$ $du508b$

$du509b$ $du510b$ $du511b$ $du512b$

A.3 Type–V fourth–order diagrams

$$dv101a = 0.250 \sum_{a,b,c,i,j,k,l} \frac{\langle ab||pk\rangle\langle kc||il\rangle\langle il||jc\rangle\langle pj||ab\rangle}{(E+\epsilon_k-\epsilon_a-\epsilon_b)(E+\epsilon_i+\epsilon_l-\epsilon_a-\epsilon_b-\epsilon_c)(E+\epsilon_j-\epsilon_a-\epsilon_b)} \tag{A.201}$$

$$dv102a = -0.250 \sum_{a,b,c,d,i,j,k} \frac{\langle ac||pj\rangle\langle bd||ik\rangle\langle jk||bd\rangle\langle pi||ac\rangle}{(E+\epsilon_j-\epsilon_a-\epsilon_c)(E+\epsilon_i+\epsilon_j+\epsilon_k-\epsilon_a-\epsilon_b-\epsilon_c-\epsilon_d)(E+\epsilon_i-\epsilon_a-\epsilon_c)} \tag{A.202}$$

$$dv103a = -0.250 \sum_{a,b,c,d,i,j,k} \frac{\langle ac||pj\rangle\langle jd||ik\rangle\langle pb||ac\rangle\langle ik||bd\rangle}{(E+\epsilon_j-\epsilon_a-\epsilon_c)(E+\epsilon_i+\epsilon_k-\epsilon_a-\epsilon_c-\epsilon_d)(\epsilon_i+\epsilon_k-\epsilon_b-\epsilon_d)} \tag{A.203}$$

$$dv104a = -0.250 \sum_{a,b,c,d,i,j,k} \frac{\langle cd||jk\rangle\langle ab||pc\rangle\langle jk||id\rangle\langle pi||ab\rangle}{(\epsilon_j+\epsilon_k-\epsilon_c-\epsilon_d)(E+\epsilon_j+\epsilon_k-\epsilon_a-\epsilon_b-\epsilon_d)(E+\epsilon_i-\epsilon_a-\epsilon_b)} \tag{A.204}$$

$$dv105a = -0.250 \sum_{a,b,c,d,i,j,k} \frac{\langle ac||pj\rangle\langle bd||ik\rangle\langle pi||ac\rangle\langle jk||bd\rangle}{(E+\epsilon_j-\epsilon_a-\epsilon_c)(E+\epsilon_i+\epsilon_j+\epsilon_k-\epsilon_a-\epsilon_b-\epsilon_c-\epsilon_d)(\epsilon_j+\epsilon_k-\epsilon_b-\epsilon_d)} \tag{A.205}$$

$$dv106a = -0.250 \sum_{a,b,c,d,i,j,k} \frac{\langle cd||jk\rangle\langle ab||pi\rangle\langle ik||cd\rangle\langle pj||ab\rangle}{(\epsilon_j+\epsilon_k-\epsilon_c-\epsilon_d)(E+\epsilon_i+\epsilon_j+\epsilon_k-\epsilon_a-\epsilon_b-\epsilon_c-\epsilon_d)(E+\epsilon_j-\epsilon_a-\epsilon_b)} \tag{A.206}$$

$$dv107a = -0.250 \sum_{a,b,c,d,i,j,k} \frac{\langle cd||jk\rangle\langle jk||id\rangle\langle ab||pc\rangle\langle pi||ab\rangle}{(\epsilon_j+\epsilon_k-\epsilon_c-\epsilon_d)(\epsilon_i-\epsilon_c)(E+\epsilon_i-\epsilon_a-\epsilon_b)} \tag{A.207}$$

$$dv108a = -0.250 \sum_{a,b,c,d,i,j,k} \frac{\langle ac||pj\rangle\langle pb||ac\rangle\langle jd||ik\rangle\langle ik||bd\rangle}{(E+\epsilon_j-\epsilon_a-\epsilon_c)(\epsilon_j-\epsilon_b)(\epsilon_i+\epsilon_k-\epsilon_b-\epsilon_d)} \tag{A.208}$$

$$dv109a = 0.250 \sum_{a,b,c,d,e,i,j} \frac{\langle de||ij\rangle\langle cj||de\rangle\langle ab||pc\rangle\langle pi||ab\rangle}{(\epsilon_i+\epsilon_j-\epsilon_d-\epsilon_e)(\epsilon_i-\epsilon_c)(E+\epsilon_i-\epsilon_a-\epsilon_b)} \tag{A.209}$$

$$dv110a = 0.250 \sum_{a,b,c,d,e,i,j} \frac{\langle ad||pi\rangle\langle pc||ad\rangle\langle be||cj\rangle\langle ij||be\rangle}{(E+\epsilon_i-\epsilon_a-\epsilon_d)(\epsilon_i-\epsilon_c)(\epsilon_i+\epsilon_j-\epsilon_b-\epsilon_e)} \tag{A.210}$$

$$dv111a = 0.250 \sum_{a,b,c,d,e,i,j} \frac{\langle de||ij\rangle\langle ac||pd\rangle\langle pb||ac\rangle\langle ij||be\rangle}{(\epsilon_i+\epsilon_j-\epsilon_d-\epsilon_e)(E+\epsilon_i+\epsilon_j-\epsilon_a-\epsilon_c-\epsilon_e)(\epsilon_i+\epsilon_j-\epsilon_b-\epsilon_e)} \tag{A.211}$$

$$dv112a = -0.250 \sum_{a,b,c,d,i,j,k} \frac{\langle cd||jk\rangle\langle ab||pi\rangle\langle pj||ab\rangle\langle ik||cd\rangle}{(\epsilon_j+\epsilon_k-\epsilon_c-\epsilon_d)(E+\epsilon_i+\epsilon_j+\epsilon_k-\epsilon_a-\epsilon_b-\epsilon_c-\epsilon_d)(\epsilon_i+\epsilon_k-\epsilon_c-\epsilon_d)} \tag{A.212}$$

$$dv201a = 0.500 \sum_{a,b,c,d,e,i,j} \frac{\langle cd||pi\rangle\langle be||cj\rangle\langle aj||be\rangle\langle pi||ad\rangle}{(E+\epsilon_i-\epsilon_c-\epsilon_d)(E+\epsilon_i+\epsilon_j-\epsilon_b-\epsilon_d-\epsilon_e)(E+\epsilon_i-\epsilon_a-\epsilon_d)} \tag{A.213}$$

$$dv202a = -0.500 \sum_{a,b,c,d,i,j,k} \frac{\langle bc||pj\rangle\langle ad||ik\rangle\langle ik||bd\rangle\langle pj||ac\rangle}{(E+\epsilon_j-\epsilon_b-\epsilon_c)(E+\epsilon_i+\epsilon_j+\epsilon_k-\epsilon_a-\epsilon_b-\epsilon_c-\epsilon_d)(E+\epsilon_j-\epsilon_a-\epsilon_c)} \tag{A.214}$$

$$dv203a = -0.500 \sum_{a,b,c,d,i,j,k} \frac{\langle bc||pj\rangle\langle ad||bk\rangle\langle pj||ic\rangle\langle ik||ad\rangle}{(E+\epsilon_j-\epsilon_b-\epsilon_c)(E+\epsilon_j+\epsilon_k-\epsilon_a-\epsilon_c-\epsilon_d)(\epsilon_i+\epsilon_k-\epsilon_a-\epsilon_d)} \tag{A.215}$$

$$dv204a = -0.500 \sum_{a,b,c,d,i,j,k} \frac{\langle bc||ij\rangle\langle id||pk\rangle\langle aj||bc\rangle\langle pk||ad\rangle}{(\epsilon_i+\epsilon_j-\epsilon_b-\epsilon_c)(E+\epsilon_j+\epsilon_k-\epsilon_b-\epsilon_c-\epsilon_d)(E+\epsilon_k-\epsilon_a-\epsilon_d)} \tag{A.216}$$

$$dv205a = -0.500 \sum_{a,b,c,d,i,j,k} \frac{\langle bc||pj\rangle\langle ad||ik\rangle\langle pj||ac\rangle\langle ik||bd\rangle}{(E+\epsilon_j-\epsilon_b-\epsilon_c)(E+\epsilon_i+\epsilon_j+\epsilon_k-\epsilon_a-\epsilon_b-\epsilon_c-\epsilon_d)(\epsilon_i+\epsilon_k-\epsilon_b-\epsilon_d)} \tag{A.217}$$

$$dv206a = -0.500 \sum_{a,b,c,d,i,j,k} \frac{\langle ac||ij\rangle\langle bd||pk\rangle\langle ij||bc\rangle\langle pk||ad\rangle}{(\epsilon_i+\epsilon_j-\epsilon_a-\epsilon_c)(E+\epsilon_i+\epsilon_j+\epsilon_k-\epsilon_a-\epsilon_b-\epsilon_c-\epsilon_d)(E+\epsilon_k-\epsilon_a-\epsilon_d)} \tag{A.218}$$

$$dv207a = -0.500 \sum_{a,b,c,d,i,j,k} \frac{\langle cd||jk\rangle\langle bk||cd\rangle\langle aj||pi\rangle\langle pi||ab\rangle}{(\epsilon_j+\epsilon_k-\epsilon_c-\epsilon_d)(\epsilon_j-\epsilon_b)(E+\epsilon_i-\epsilon_a-\epsilon_b)} \tag{A.219}$$

$$dv208a = -0.500 \sum_{a,b,c,d,i,j,k} \frac{\langle ac||pj\rangle\langle pj||ai\rangle\langle bd||ck\rangle\langle ik||bd\rangle}{(E+\epsilon_j-\epsilon_a-\epsilon_c)(\epsilon_i-\epsilon_c)(\epsilon_i+\epsilon_k-\epsilon_b-\epsilon_d)} \tag{A.220}$$

$$dv209a = 0.500 \sum_{a,b,c,i,j,k,l} \frac{\langle bc||kl\rangle\langle kl||ic\rangle\langle ai||pj\rangle\langle pj||ab\rangle}{(\epsilon_k+\epsilon_l-\epsilon_b-\epsilon_c)(\epsilon_i-\epsilon_b)(E+\epsilon_j-\epsilon_a-\epsilon_b)} \tag{A.221}$$

$$dv210a = 0.500 \sum_{a,b,c,i,j,k,l} \frac{\langle ab||pk\rangle\langle pk||ai\rangle\langle ic||jl\rangle\langle jl||bc\rangle}{(E+\epsilon_k-\epsilon_a-\epsilon_b)(\epsilon_i-\epsilon_b)(\epsilon_j+\epsilon_l-\epsilon_b-\epsilon_c)} \tag{A.222}$$

$$dv211a = 0.500 \sum_{a,b,c,i,j,k,l} \frac{\langle ab||jk\rangle\langle jc||pl\rangle\langle pl||ic\rangle\langle ik||ab\rangle}{(\epsilon_j+\epsilon_k-\epsilon_a-\epsilon_b)(E+\epsilon_k+\epsilon_l-\epsilon_a-\epsilon_b-\epsilon_c)(\epsilon_i+\epsilon_k-\epsilon_a-\epsilon_b)} \tag{A.223}$$

$$dv212a = -0.500 \sum_{a,b,c,d,i,j,k} \frac{\langle ac||ij\rangle\langle bd||pk\rangle\langle pk||ad\rangle\langle ij||bc\rangle}{(\epsilon_i+\epsilon_j-\epsilon_a-\epsilon_c)(E+\epsilon_i+\epsilon_j+\epsilon_k-\epsilon_a-\epsilon_b-\epsilon_c-\epsilon_d)(\epsilon_i+\epsilon_j-\epsilon_b-\epsilon_c)} \tag{A.224}$$

$$dv101b = -0.250 \sum_{a,b,c,d,i,j,k} \frac{\langle pc\|ij\rangle\langle bd\|ck\rangle\langle ak\|bd\rangle\langle ij\|pa\rangle}{(\epsilon_i + \epsilon_j - E - \epsilon_c)(\epsilon_i + \epsilon_j + \epsilon_k - E - \epsilon_b - \epsilon_d)(\epsilon_i + \epsilon_j - E - \epsilon_a)} \tag{A.225}$$

$$dv102b = 0.250 \sum_{a,b,c,i,j,k,l} \frac{\langle pb\|ik\rangle\langle ac\|jl\rangle\langle jl\|bc\rangle\langle ik\|pa\rangle}{(\epsilon_i + \epsilon_k - E - \epsilon_b)(\epsilon_i + \epsilon_j + \epsilon_k + \epsilon_l - E - \epsilon_a - \epsilon_b - \epsilon_c)(\epsilon_i + \epsilon_k - E - \epsilon_a)} \tag{A.226}$$

$$dv103b = 0.250 \sum_{a,b,c,i,j,k,l} \frac{\langle bc\|kl\rangle\langle pk\|ij\rangle\langle al\|bc\rangle\langle ij\|pa\rangle}{(\epsilon_k + \epsilon_l - \epsilon_b - \epsilon_c)(\epsilon_i + \epsilon_j + \epsilon_l - E - \epsilon_b - \epsilon_c)(\epsilon_i + \epsilon_j - E - \epsilon_a)} \tag{A.227}$$

$$dv104b = 0.250 \sum_{a,b,c,i,j,k,l} \frac{\langle pb\|ik\rangle\langle ac\|bl\rangle\langle ik\|pj\rangle\langle jl\|ac\rangle}{(\epsilon_i + \epsilon_k - E - \epsilon_b)(\epsilon_i + \epsilon_k + \epsilon_l - E - \epsilon_a - \epsilon_c)(\epsilon_j + \epsilon_l - \epsilon_a - \epsilon_c)} \tag{A.228}$$

$$dv105b = 0.250 \sum_{a,b,c,i,j,k,l} \frac{\langle bc\|kl\rangle\langle pa\|ij\rangle\langle kl\|ac\rangle\langle ij\|pb\rangle}{(\epsilon_k + \epsilon_l - \epsilon_b - \epsilon_c)(\epsilon_i + \epsilon_j + \epsilon_k + \epsilon_l - E - \epsilon_a - \epsilon_b - \epsilon_c)(\epsilon_i + \epsilon_j - E - \epsilon_b)} \tag{A.229}$$

$$dv106b = 0.250 \sum_{a,b,c,i,j,k,l} \frac{\langle pb\|ik\rangle\langle ac\|jl\rangle\langle ik\|pa\rangle\langle jl\|bc\rangle}{(\epsilon_i + \epsilon_k - E - \epsilon_b)(\epsilon_i + \epsilon_j + \epsilon_k + \epsilon_l - E - \epsilon_a - \epsilon_b - \epsilon_c)(\epsilon_j + \epsilon_l - \epsilon_b - \epsilon_c)} \tag{A.230}$$

$$dv107b = 0.250 \sum_{a,b,c,i,j,k,l} \frac{\langle pb\|ik\rangle\langle ik\|pj\rangle\langle ac\|bl\rangle\langle jl\|ac\rangle}{(\epsilon_i + \epsilon_k - E - \epsilon_b)(\epsilon_j - \epsilon_b)(\epsilon_j + \epsilon_l - \epsilon_a - \epsilon_c)} \tag{A.231}$$

$$dv108b = 0.250 \sum_{a,b,c,i,j,k,l} \frac{\langle bc\|kl\rangle\langle al\|bc\rangle\langle pk\|ij\rangle\langle ij\|pa\rangle}{(\epsilon_k + \epsilon_l - \epsilon_b - \epsilon_c)(\epsilon_k - \epsilon_a)(\epsilon_i + \epsilon_j - E - \epsilon_a)} \tag{A.232}$$

$$dv109b = -0.250 \sum_{a,b,i,j,k,l,m} \frac{\langle pa\|il\rangle\langle il\|pj\rangle\langle jb\|km\rangle\langle km\|ab\rangle}{(\epsilon_i + \epsilon_l - E - \epsilon_a)(\epsilon_j - \epsilon_a)(\epsilon_k + \epsilon_m - \epsilon_a - \epsilon_b)} \tag{A.233}$$

$$dv110b = -0.250 \sum_{a,b,i,j,k,l,m} \frac{\langle ab\|lm\rangle\langle lm\|jb\rangle\langle pj\|ik\rangle\langle ik\|pa\rangle}{(\epsilon_l + \epsilon_m - \epsilon_a - \epsilon_b)(\epsilon_j - \epsilon_a)(\epsilon_i + \epsilon_k - E - \epsilon_a)} \tag{A.234}$$

$$dv111b = -0.250 \sum_{a,b,i,j,k,l,m} \frac{\langle ab\|lm\rangle\langle pl\|ij\rangle\langle ij\|pk\rangle\langle km\|ab\rangle}{(\epsilon_l + \epsilon_m - \epsilon_a - \epsilon_b)(\epsilon_i + \epsilon_j + \epsilon_m - E - \epsilon_a - \epsilon_b)(\epsilon_k + \epsilon_m - \epsilon_a - \epsilon_b)} \tag{A.235}$$

$$dv112b = 0.250 \sum_{a,b,c,i,j,k,l} \frac{\langle bc\|kl\rangle\langle pa\|ij\rangle\langle ij\|pb\rangle\langle kl\|ac\rangle}{(\epsilon_k + \epsilon_l - \epsilon_b - \epsilon_c)(\epsilon_i + \epsilon_j + \epsilon_k + \epsilon_l - E - \epsilon_a - \epsilon_b - \epsilon_c)(\epsilon_k + \epsilon_l - \epsilon_a - \epsilon_c)} \tag{A.236}$$

$$dv201b = -0.500 \sum_{a,b,i,j,k,l,m} \frac{\langle pa||il\rangle\langle ib||jm\rangle\langle jm||kb\rangle\langle kl||pa\rangle}{(\epsilon_i + \epsilon_l - E - \epsilon_a)(\epsilon_j + \epsilon_l + \epsilon_m - E - \epsilon_a - \epsilon_b)(\epsilon_k + \epsilon_l - E - \epsilon_a)} \tag{A.237}$$

$$dv202b = 0.500 \sum_{a,b,c,i,j,k,l} \frac{\langle pb||ik\rangle\langle ac||jl\rangle\langle il||ac\rangle\langle jk||pb\rangle}{(\epsilon_i + \epsilon_k - E - \epsilon_b)(\epsilon_i + \epsilon_j + \epsilon_k + \epsilon_l - E - \epsilon_a - \epsilon_b - \epsilon_c)(\epsilon_j + \epsilon_k - E - \epsilon_b)} \tag{A.238}$$

$$dv203b = 0.500 \sum_{a,b,c,i,j,k,l} \frac{\langle ab||ik\rangle\langle pc||al\rangle\langle ik||jb\rangle\langle jl||pc\rangle}{(\epsilon_i + \epsilon_k - \epsilon_a - \epsilon_b)(\epsilon_i + \epsilon_k + \epsilon_l - E - \epsilon_b - \epsilon_c)(\epsilon_j + \epsilon_l - E - \epsilon_c)} \tag{A.239}$$

$$dv204b = 0.500 \sum_{a,b,c,i,j,k,l} \frac{\langle pb||ik\rangle\langle ic||jl\rangle\langle ak||pb\rangle\langle jl||ac\rangle}{(\epsilon_i + \epsilon_k - E - \epsilon_b)(\epsilon_j + \epsilon_k + \epsilon_l - E - \epsilon_b - \epsilon_c)(\epsilon_j + \epsilon_l - \epsilon_a - \epsilon_c)} \tag{A.240}$$

$$dv205b = 0.500 \sum_{a,b,c,i,j,k,l} \frac{\langle ab||jk\rangle\langle pc||il\rangle\langle ik||ab\rangle\langle jl||pc\rangle}{(\epsilon_j + \epsilon_k - \epsilon_a - \epsilon_b)(\epsilon_i + \epsilon_j + \epsilon_k + \epsilon_l - E - \epsilon_a - \epsilon_b - \epsilon_c)(\epsilon_j + \epsilon_l - E - \epsilon_c)} \tag{A.241}$$

$$dv206b = 0.500 \sum_{a,b,c,i,j,k,l} \frac{\langle pb||ik\rangle\langle ac||jl\rangle\langle jk||pb\rangle\langle il||ac\rangle}{(\epsilon_i + \epsilon_k - E - \epsilon_b)(\epsilon_i + \epsilon_j + \epsilon_k + \epsilon_l - E - \epsilon_a - \epsilon_b - \epsilon_c)(\epsilon_i + \epsilon_l - \epsilon_a - \epsilon_c)} \tag{A.242}$$

$$dv207b = 0.500 \sum_{a,b,c,i,j,k,l} \frac{\langle pb||ik\rangle\langle ia||pb\rangle\langle kc||jl\rangle\langle jl||ac\rangle}{(\epsilon_i + \epsilon_k - E - \epsilon_b)(\epsilon_k - \epsilon_a)(\epsilon_j + \epsilon_l - \epsilon_a - \epsilon_c)} \tag{A.243}$$

$$dv208b = 0.500 \sum_{a,b,c,i,j,k,l} \frac{\langle bc||kl\rangle\langle kl||jc\rangle\langle pa||ib\rangle\langle ij||pa\rangle}{(\epsilon_k + \epsilon_l - \epsilon_b - \epsilon_c)(\epsilon_j - \epsilon_b)(\epsilon_i + \epsilon_j - E - \epsilon_a)} \tag{A.244}$$

$$dv209b = -0.500 \sum_{a,b,c,d,i,j,k} \frac{\langle pc||ij\rangle\langle ib||pc\rangle\langle ad||bk\rangle\langle jk||ad\rangle}{(\epsilon_i + \epsilon_j - E - \epsilon_c)(\epsilon_j - \epsilon_b)(\epsilon_j + \epsilon_k - \epsilon_a - \epsilon_d)} \tag{A.245}$$

$$dv210b = -0.500 \sum_{a,b,c,d,i,j,k} \frac{\langle cd||jk\rangle\langle bk||cd\rangle\langle pa||ib\rangle\langle ij||pa\rangle}{(\epsilon_j + \epsilon_k - \epsilon_c - \epsilon_d)(\epsilon_j - \epsilon_b)(\epsilon_i + \epsilon_j - E - \epsilon_a)} \tag{A.246}$$

$$dv211b = -0.500 \sum_{a,b,c,d,i,j,k} \frac{\langle ac||ij\rangle\langle pd||ak\rangle\langle bk||pd\rangle\langle ij||bc\rangle}{(\epsilon_i + \epsilon_j - \epsilon_a - \epsilon_c)(\epsilon_i + \epsilon_j + \epsilon_k - E - \epsilon_c - \epsilon_d)(\epsilon_i + \epsilon_j - \epsilon_b - \epsilon_c)} \tag{A.247}$$

$$dv212b = 0.500 \sum_{a,b,c,i,j,k,l} \frac{\langle ab||jk\rangle\langle pc||il\rangle\langle jl||pc\rangle\langle ik||ab\rangle}{(\epsilon_j + \epsilon_k - \epsilon_a - \epsilon_b)(\epsilon_i + \epsilon_j + \epsilon_k + \epsilon_l - E - \epsilon_a - \epsilon_b - \epsilon_c)(\epsilon_i + \epsilon_k - \epsilon_a - \epsilon_b)} \tag{A.248}$$

$$dv121a = -0.250 \sum_{a,b,c,d,i,j,k} \frac{\langle pi||ac\rangle\langle bd||ik\rangle\langle jk||bd\rangle\langle ac||pj\rangle}{(E+\epsilon_j-\epsilon_a-\epsilon_c)(E+\epsilon_i-\epsilon_a-\epsilon_c)(\epsilon_j+\epsilon_k-\epsilon_b-\epsilon_d)} \tag{A.249}$$

$$dv123a = -0.250 \sum_{a,b,c,d,i,j,k} \frac{\langle pi||ac\rangle\langle bd||ik\rangle\langle jk||bd\rangle\langle ac||pj\rangle}{(E+\epsilon_j-\epsilon_a-\epsilon_c)(\epsilon_j+\epsilon_k-\epsilon_b-\epsilon_d)(\epsilon_i+\epsilon_k-\epsilon_b-\epsilon_d)} \tag{A.250}$$

$$dv121b = 0.250 \sum_{a,b,c,i,j,k,l} \frac{\langle pa||ij\rangle\langle kl||ac\rangle\langle bc||kl\rangle\langle ij||pb\rangle}{(\epsilon_i+\epsilon_j-E-\epsilon_a)(\epsilon_i+\epsilon_j-E-\epsilon_b)(\epsilon_k+\epsilon_l-\epsilon_b-\epsilon_c)} \tag{A.251}$$

$$dv123b = 0.250 \sum_{a,b,c,i,j,k,l} \frac{\langle pa||ij\rangle\langle kl||ac\rangle\langle bc||kl\rangle\langle ij||pb\rangle}{(\epsilon_i+\epsilon_j-E-\epsilon_a)(\epsilon_k+\epsilon_l-\epsilon_b-\epsilon_c)(\epsilon_k+\epsilon_l-\epsilon_a-\epsilon_c)} \tag{A.252}$$

$$dv221a = -0.500 \sum_{a,b,c,d,i,j,k} \frac{\langle pj||ac\rangle\langle ad||ik\rangle\langle ik||bd\rangle\langle bc||pj\rangle}{(E+\epsilon_j-\epsilon_b-\epsilon_c)(E+\epsilon_j-\epsilon_a-\epsilon_c)(\epsilon_i+\epsilon_k-\epsilon_b-\epsilon_d)} \tag{A.253}$$

$$dv223a = -0.500 \sum_{a,b,c,d,i,j,k} \frac{\langle pj||ac\rangle\langle ad||ik\rangle\langle ik||bd\rangle\langle bc||pj\rangle}{(E+\epsilon_j-\epsilon_b-\epsilon_c)(\epsilon_i+\epsilon_k-\epsilon_b-\epsilon_d)(\epsilon_i+\epsilon_k-\epsilon_a-\epsilon_d)} \tag{A.254}$$

$$dv221b = 0.500 \sum_{a,b,c,i,j,k,l} \frac{\langle pc||il\rangle\langle ik||ab\rangle\langle ab||jk\rangle\langle jl||pc\rangle}{(\epsilon_i+\epsilon_l-E-\epsilon_c)(\epsilon_j+\epsilon_l-E-\epsilon_c)(\epsilon_j+\epsilon_k-\epsilon_a-\epsilon_b)} \tag{A.255}$$

$$dv223b = 0.500 \sum_{a,b,c,i,j,k,l} \frac{\langle pc||il\rangle\langle ik||ab\rangle\langle ab||jk\rangle\langle jl||pc\rangle}{(\epsilon_i+\epsilon_l-E-\epsilon_c)(\epsilon_j+\epsilon_k-\epsilon_a-\epsilon_b)(\epsilon_i+\epsilon_k-\epsilon_a-\epsilon_b)} \tag{A.256}$$

Figure A.16: Fourth order diagrams

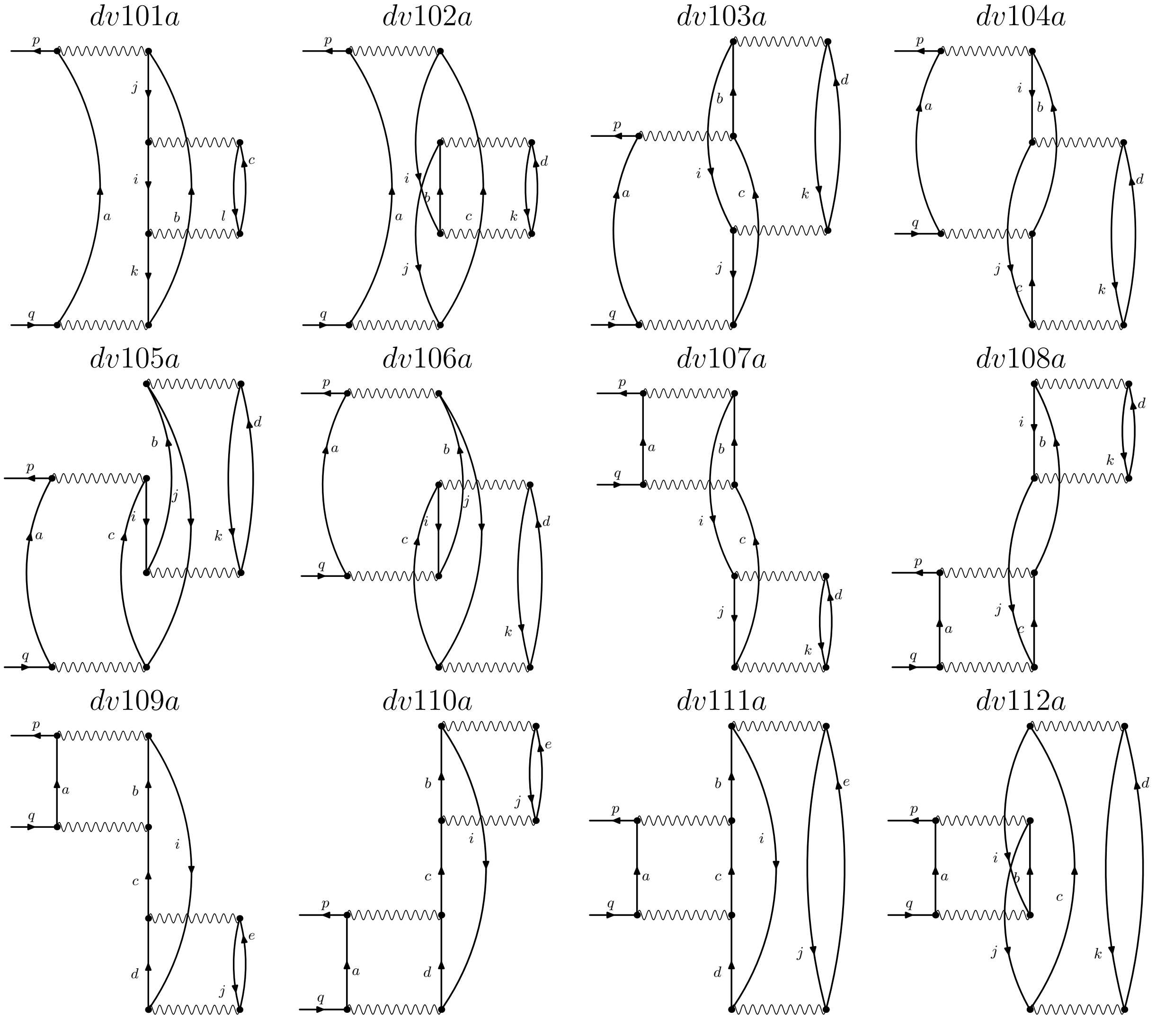
$dv101a$ $dv102a$ $dv103a$ $dv104a$

$dv105a$ $dv106a$ $dv107a$ $dv108a$

$dv109a$ $dv110a$ $dv111a$ $dv112a$

Figure A.17: Fourth order diagrams

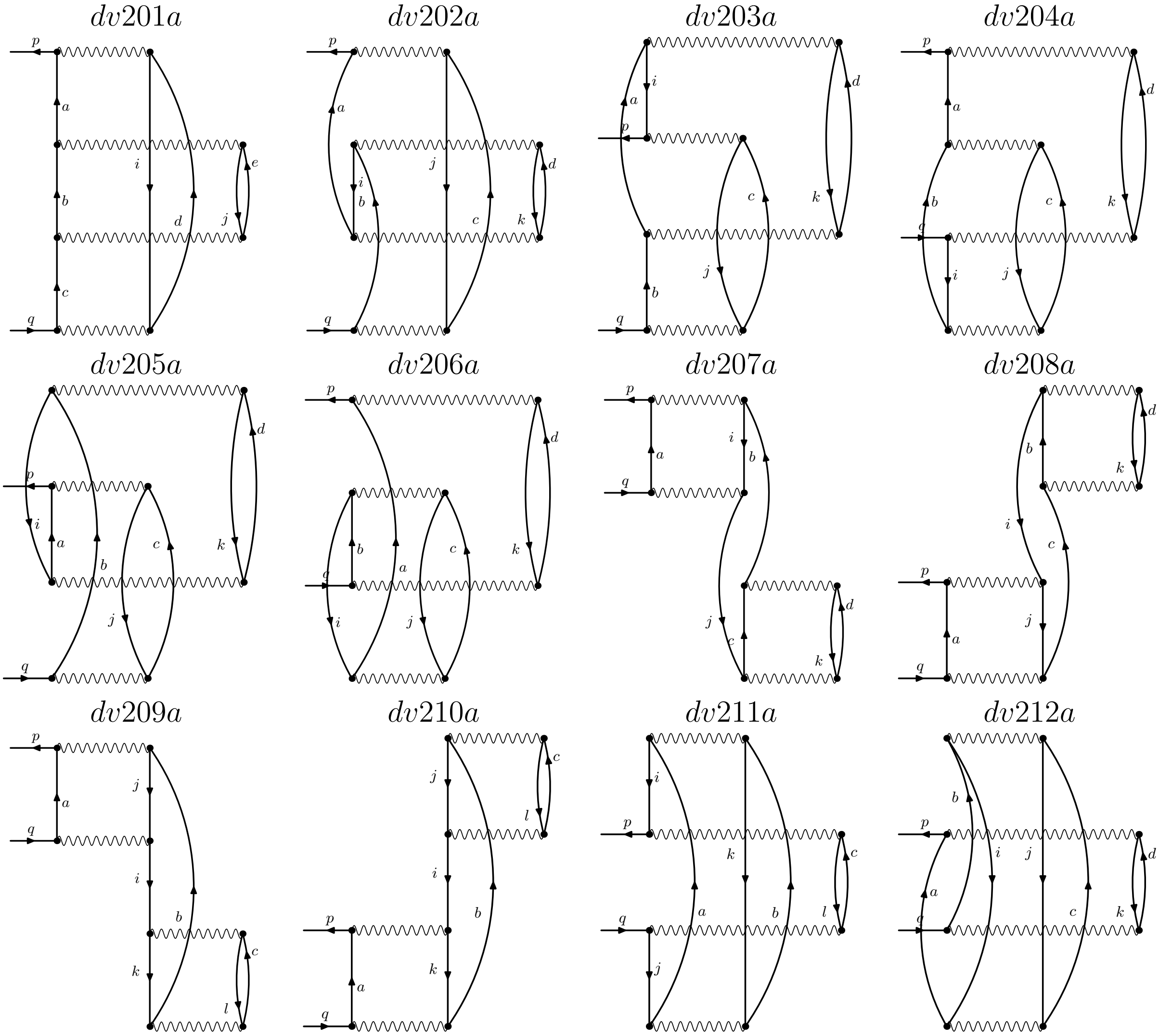

$dv201a$ $dv202a$ $dv203a$ $dv204a$

$dv205a$ $dv206a$ $dv207a$ $dv208a$

$dv209a$ $dv210a$ $dv211a$ $dv212a$

Figure A.18: Fourth order diagrams

$dv101b$

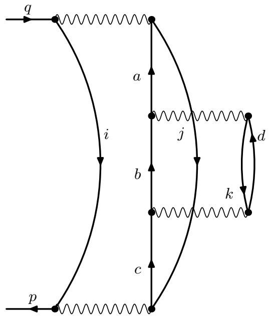

$dv102b$

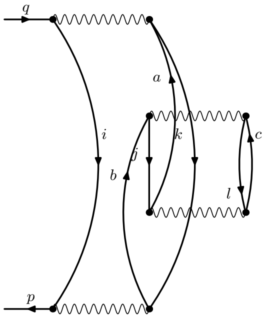

$dv103b$

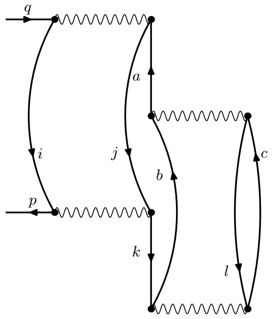

$dv104b$

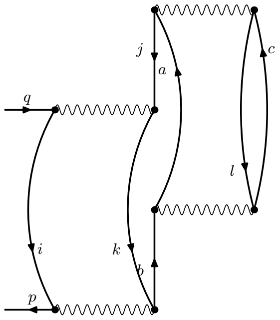

$dv105b$

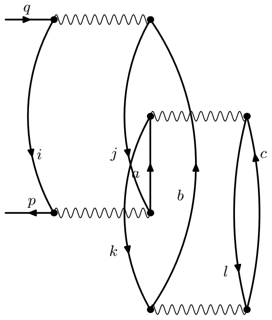

$dv106b$

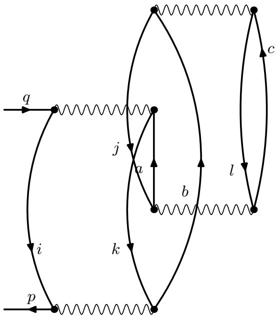

$dv107b$

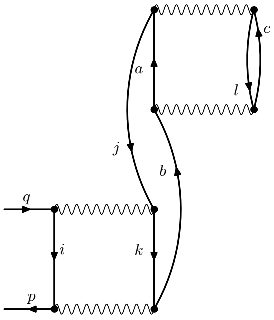

$dv108b$

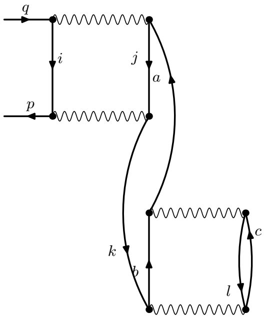

$dv109b$

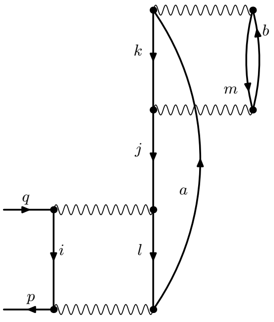

$dv110b$

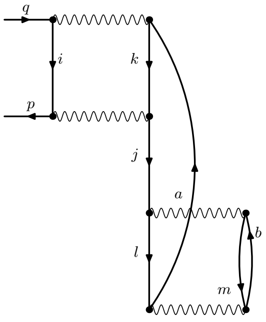

$dv111b$

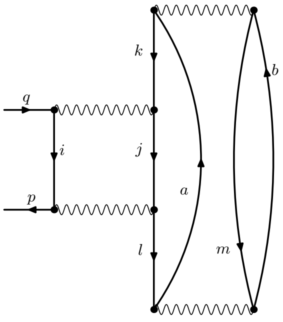

$dv112b$

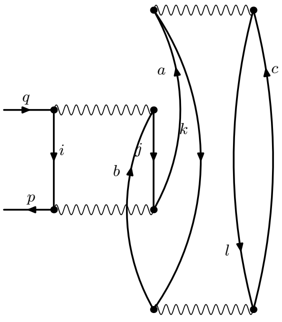

Figure A.19: Fourth order diagrams

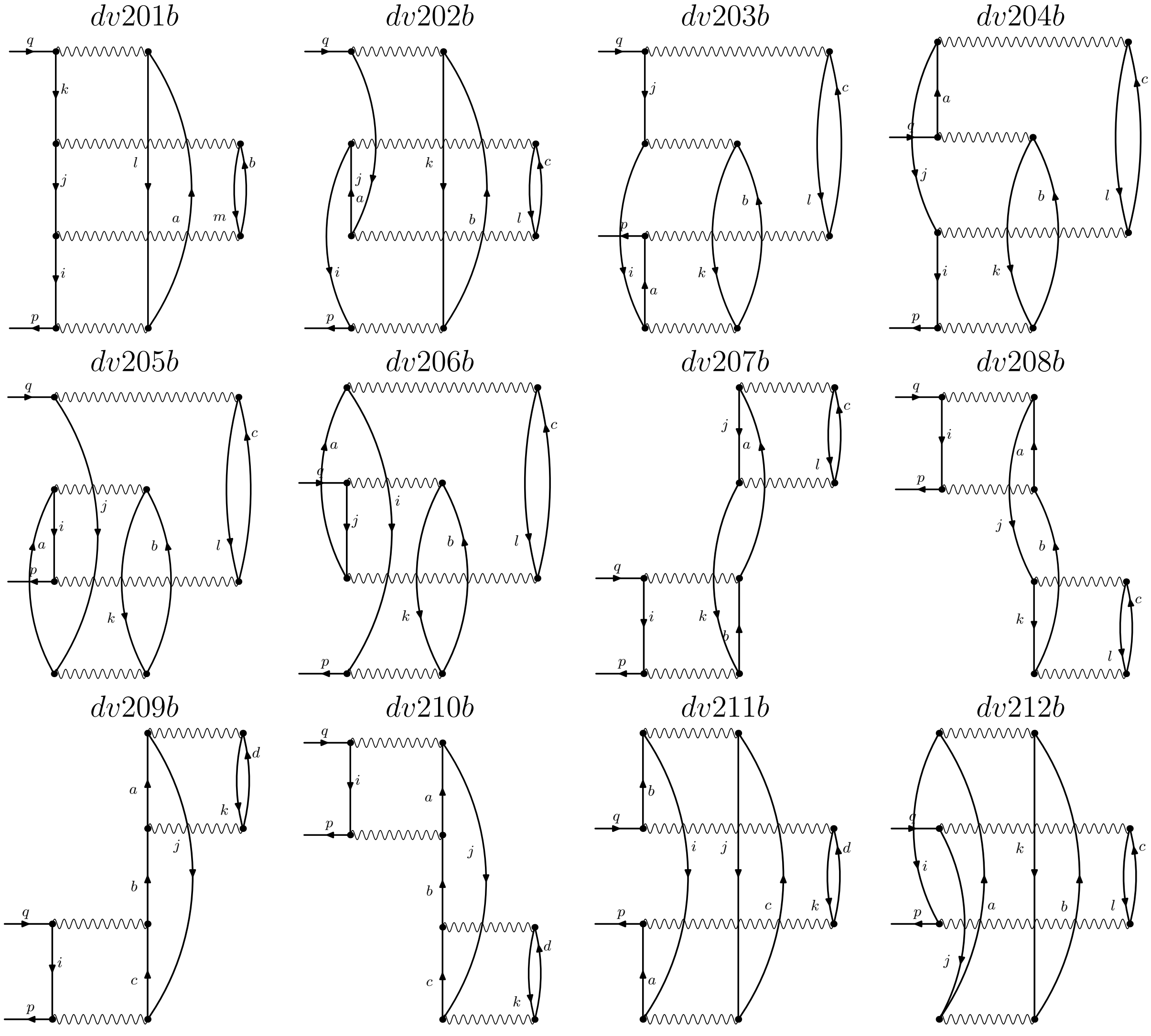
$dv201b$ $dv202b$ $dv203b$ $dv204b$

$dv205b$ $dv206b$ $dv207b$ $dv208b$

$dv209b$ $dv210b$ $dv211b$ $dv212b$

A.4 Type–W fourth–order diagrams

$$dw101a = -1.000 \sum_{a,b,c,d,e,i,j} \frac{\langle ce||pj\rangle\langle bd||ci\rangle\langle ai||be\rangle\langle pj||ad\rangle}{(E+\epsilon_j-\epsilon_c-\epsilon_e)(E+\epsilon_i+\epsilon_j-\epsilon_b-\epsilon_d-\epsilon_e)(E+\epsilon_j-\epsilon_a-\epsilon_d)} \tag{A.257}$$

$$dw103a = 1.000 \sum_{a,b,c,d,i,j,k} \frac{\langle bd||pk\rangle\langle ac||bj\rangle\langle pk||ic\rangle\langle ij||ad\rangle}{(E+\epsilon_k-\epsilon_b-\epsilon_d)(E+\epsilon_j+\epsilon_k-\epsilon_a-\epsilon_c-\epsilon_d)(\epsilon_i+\epsilon_j-\epsilon_a-\epsilon_d)} \tag{A.258}$$

$$dw104a = 1.000 \sum_{a,b,c,d,i,j,k} \frac{\langle bd||ik\rangle\langle ic||pj\rangle\langle ak||bc\rangle\langle pj||ad\rangle}{(\epsilon_i+\epsilon_k-\epsilon_b-\epsilon_d)(E+\epsilon_j+\epsilon_k-\epsilon_b-\epsilon_c-\epsilon_d)(E+\epsilon_j-\epsilon_a-\epsilon_d)} \tag{A.259}$$

$$dw107a = -1.000 \sum_{a,b,c,i,j,k,l} \frac{\langle bc||il\rangle\langle al||bj\rangle\langle ij||pk\rangle\langle pk||ac\rangle}{(\epsilon_i+\epsilon_l-\epsilon_b-\epsilon_c)(\epsilon_i+\epsilon_j-\epsilon_a-\epsilon_c)(E+\epsilon_k-\epsilon_a-\epsilon_c)} \tag{A.260}$$

$$dw108a = -1.000 \sum_{a,b,c,i,j,k,l} \frac{\langle bc||pl\rangle\langle pl||ij\rangle\langle aj||bk\rangle\langle ik||ac\rangle}{(E+\epsilon_l-\epsilon_b-\epsilon_c)(\epsilon_i+\epsilon_j-\epsilon_b-\epsilon_c)(\epsilon_i+\epsilon_k-\epsilon_a-\epsilon_c)} \tag{A.261}$$

$$dw111a = -1.000 \sum_{a,b,c,i,j,k,l} \frac{\langle ac||jl\rangle\langle jb||pk\rangle\langle pk||ic\rangle\langle il||ab\rangle}{(\epsilon_j+\epsilon_l-\epsilon_a-\epsilon_c)(E+\epsilon_k+\epsilon_l-\epsilon_a-\epsilon_b-\epsilon_c)(\epsilon_i+\epsilon_l-\epsilon_a-\epsilon_b)} \tag{A.262}$$

$$dw201a = -1.000 \sum_{a,b,c,d,i,j,k} \frac{\langle bc||pj\rangle\langle ad||bk\rangle\langle jk||id\rangle\langle pi||ac\rangle}{(E+\epsilon_j-\epsilon_b-\epsilon_c)(E+\epsilon_j+\epsilon_k-\epsilon_a-\epsilon_c-\epsilon_d)(E+\epsilon_i-\epsilon_a-\epsilon_c)} \tag{A.263}$$

$$dw202a = -1.000 \sum_{a,b,c,d,i,j,k} \frac{\langle bc||pj\rangle\langle jd||ik\rangle\langle ak||bd\rangle\langle pi||ac\rangle}{(E+\epsilon_j-\epsilon_b-\epsilon_c)(E+\epsilon_i+\epsilon_k-\epsilon_b-\epsilon_c-\epsilon_d)(E+\epsilon_i-\epsilon_a-\epsilon_c)} \tag{A.264}$$

$$dw203a = 1.000 \sum_{a,b,c,d,e,i,j} \frac{\langle bd||pi\rangle\langle ae||bj\rangle\langle pc||ad\rangle\langle ij||ce\rangle}{(E+\epsilon_i-\epsilon_b-\epsilon_d)(E+\epsilon_i+\epsilon_j-\epsilon_a-\epsilon_d-\epsilon_e)(\epsilon_i+\epsilon_j-\epsilon_c-\epsilon_e)} \tag{A.265}$$

$$dw204a = 1.000 \sum_{a,b,c,i,j,k,l} \frac{\langle ac||il\rangle\langle ib||pk\rangle\langle kl||jc\rangle\langle pj||ab\rangle}{(\epsilon_i+\epsilon_l-\epsilon_a-\epsilon_c)(E+\epsilon_k+\epsilon_l-\epsilon_a-\epsilon_b-\epsilon_c)(E+\epsilon_j-\epsilon_a-\epsilon_b)} \tag{A.266}$$

$$dw205a = 1.000 \sum_{a,b,c,i,j,k,l} \frac{\langle ab||pk\rangle\langle kc||jl\rangle\langle pj||ib\rangle\langle il||ac\rangle}{(E+\epsilon_k-\epsilon_a-\epsilon_b)(E+\epsilon_j+\epsilon_l-\epsilon_a-\epsilon_b-\epsilon_c)(\epsilon_i+\epsilon_l-\epsilon_a-\epsilon_c)} \tag{A.267}$$

$$dw206a = 1.000 \sum_{a,b,c,d,e,i,j} \frac{\langle de||ij\rangle\langle bc||pd\rangle\langle aj||be\rangle\langle pi||ac\rangle}{(\epsilon_i+\epsilon_j-\epsilon_d-\epsilon_e)(E+\epsilon_i+\epsilon_j-\epsilon_b-\epsilon_c-\epsilon_e)(E+\epsilon_i-\epsilon_a-\epsilon_c)} \tag{A.268}$$

$$dw207a = -1.000 \sum_{a,b,c,d,i,j,k} \frac{\langle ad||ik\rangle\langle ck||jd\rangle\langle ib||pc\rangle\langle pj||ab\rangle}{(\epsilon_i+\epsilon_k-\epsilon_a-\epsilon_d)(\epsilon_i+\epsilon_j-\epsilon_a-\epsilon_c)(E+\epsilon_j-\epsilon_a-\epsilon_b)} \tag{A.269}$$

$$dw208a = -1.000 \sum_{a,b,c,d,i,j,k} \frac{\langle ac||pj\rangle\langle pb||ic\rangle\langle id||ak\rangle\langle jk||bd\rangle}{(E+\epsilon_j-\epsilon_a-\epsilon_c)(\epsilon_i+\epsilon_j-\epsilon_a-\epsilon_b)(\epsilon_j+\epsilon_k-\epsilon_b-\epsilon_d)} \tag{A.270}$$

$$dw209a = -1.000 \sum_{a,b,c,d,i,j,k} \frac{\langle cd||jk\rangle\langle ak||id\rangle\langle ib||pc\rangle\langle pj||ab\rangle}{(\epsilon_j+\epsilon_k-\epsilon_c-\epsilon_d)(\epsilon_i+\epsilon_j-\epsilon_a-\epsilon_c)(E+\epsilon_j-\epsilon_a-\epsilon_b)} \tag{A.271}$$

$$dw210a = -1.000 \sum_{a,b,c,d,i,j,k} \frac{\langle ac||pj\rangle\langle pb||ic\rangle\langle jd||bk\rangle\langle ik||ad\rangle}{(E+\epsilon_j-\epsilon_a-\epsilon_c)(\epsilon_i+\epsilon_j-\epsilon_a-\epsilon_b)(\epsilon_i+\epsilon_k-\epsilon_a-\epsilon_d)} \tag{A.272}$$

$$dw211a = -1.000 \sum_{a,b,c,d,i,j,k} \frac{\langle ad||ik\rangle\langle ic||pj\rangle\langle pb||ac\rangle\langle jk||bd\rangle}{(\epsilon_i+\epsilon_k-\epsilon_a-\epsilon_d)(E+\epsilon_j+\epsilon_k-\epsilon_a-\epsilon_c-\epsilon_d)(\epsilon_j+\epsilon_k-\epsilon_b-\epsilon_d)} \tag{A.273}$$

$$dw212a = -1.000 \sum_{a,b,c,d,i,j,k} \frac{\langle cd||jk\rangle\langle ab||pc\rangle\langle pj||ib\rangle\langle ik||ad\rangle}{(\epsilon_j+\epsilon_k-\epsilon_c-\epsilon_d)(E+\epsilon_j+\epsilon_k-\epsilon_a-\epsilon_b-\epsilon_d)(\epsilon_i+\epsilon_k-\epsilon_a-\epsilon_d)} \tag{A.274}$$

$$dw301a = -0.500 \sum_{a,b,c,i,j,k,l} \frac{\langle bc||pl\rangle\langle al||ij\rangle\langle ij||bk\rangle\langle pk||ac\rangle}{(E+\epsilon_l-\epsilon_b-\epsilon_c)(E+\epsilon_i+\epsilon_j-\epsilon_a-\epsilon_b-\epsilon_c)(E+\epsilon_k-\epsilon_a-\epsilon_c)} \tag{A.275}$$

$$dw302a = -0.500 \sum_{a,b,c,d,e,i,j} \frac{\langle ce||pj\rangle\langle bd||ci\rangle\langle aj||bd\rangle\langle pi||ae\rangle}{(E+\epsilon_j-\epsilon_c-\epsilon_e)(E+\epsilon_i+\epsilon_j-\epsilon_b-\epsilon_d-\epsilon_e)(E+\epsilon_i-\epsilon_a-\epsilon_e)} \tag{A.276}$$

$$dw303a = 0.500 \sum_{a,b,c,d,i,j,k} \frac{\langle bd||pk\rangle\langle ak||ij\rangle\langle pc||ad\rangle\langle ij||bc\rangle}{(E+\epsilon_k-\epsilon_b-\epsilon_d)(E+\epsilon_i+\epsilon_j-\epsilon_a-\epsilon_b-\epsilon_d)(\epsilon_i+\epsilon_j-\epsilon_b-\epsilon_c)} \tag{A.277}$$

$$dw304a = 0.500 \sum_{a,b,c,d,i,j,k} \frac{\langle ad||ik\rangle\langle bc||pd\rangle\langle ik||bj\rangle\langle pj||ac\rangle}{(\epsilon_i+\epsilon_k-\epsilon_a-\epsilon_d)(E+\epsilon_i+\epsilon_k-\epsilon_a-\epsilon_b-\epsilon_c)(E+\epsilon_j-\epsilon_a-\epsilon_c)} \tag{A.278}$$

$$dw305a = 0.500 \sum_{a,b,c,d,i,j,k} \frac{\langle bd||pk\rangle\langle ac||bj\rangle\langle pj||id\rangle\langle ik||ac\rangle}{(E+\epsilon_k-\epsilon_b-\epsilon_d)(E+\epsilon_j+\epsilon_k-\epsilon_a-\epsilon_c-\epsilon_d)(\epsilon_i+\epsilon_k-\epsilon_a-\epsilon_c)} \tag{A.279}$$

$$dw306a = 0.500 \sum_{a,b,c,d,i,j,k} \frac{\langle bd||ik\rangle\langle ic||pj\rangle\langle aj||bd\rangle\langle pk||ac\rangle}{(\epsilon_i+\epsilon_k-\epsilon_b-\epsilon_d)(E+\epsilon_j+\epsilon_k-\epsilon_b-\epsilon_c-\epsilon_d)(E+\epsilon_k-\epsilon_a-\epsilon_c)} \tag{A.280}$$

$$dw307a = -0.500 \sum_{a,b,c,i,j,k,l} \frac{\langle ac||il\rangle\langle il||jk\rangle\langle jb||pc\rangle\langle pk||ab\rangle}{(\epsilon_i+\epsilon_l-\epsilon_a-\epsilon_c)(\epsilon_j+\epsilon_k-\epsilon_a-\epsilon_c)(E+\epsilon_k-\epsilon_a-\epsilon_b)} \tag{A.281}$$

$$dw308a = -0.500 \sum_{a,b,c,i,j,k,l} \frac{\langle ac||pl\rangle\langle pb||ic\rangle\langle il||jk\rangle\langle jk||ab\rangle}{(E+\epsilon_l-\epsilon_a-\epsilon_c)(\epsilon_i+\epsilon_l-\epsilon_a-\epsilon_b)(\epsilon_j+\epsilon_k-\epsilon_a-\epsilon_b)} \tag{A.282}$$

$$dw309a = -0.500 \sum_{a,b,c,d,e,i,j} \frac{\langle be||ij\rangle\langle ad||be\rangle\langle ic||pd\rangle\langle pj||ac\rangle}{(\epsilon_i+\epsilon_j-\epsilon_b-\epsilon_e)(\epsilon_i+\epsilon_j-\epsilon_a-\epsilon_d)(E+\epsilon_j-\epsilon_a-\epsilon_c)} \tag{A.283}$$

$$dw310a = -0.500 \sum_{a,b,c,d,e,i,j} \frac{\langle be||pj\rangle\langle pd||ie\rangle\langle ac||bd\rangle\langle ij||ac\rangle}{(E+\epsilon_j-\epsilon_b-\epsilon_e)(\epsilon_i+\epsilon_j-\epsilon_b-\epsilon_d)(\epsilon_i+\epsilon_j-\epsilon_a-\epsilon_c)} \tag{A.284}$$

$$dw311a = -0.500 \sum_{a,b,c,d,e,i,j} \frac{\langle ae||ij\rangle\langle bd||pe\rangle\langle pc||ad\rangle\langle ij||bc\rangle}{(\epsilon_i+\epsilon_j-\epsilon_a-\epsilon_e)(E+\epsilon_i+\epsilon_j-\epsilon_a-\epsilon_b-\epsilon_d)(\epsilon_i+\epsilon_j-\epsilon_b-\epsilon_c)} \tag{A.285}$$

$$dw312a = -0.500 \sum_{a,b,c,i,j,k,l} \frac{\langle ac||jl\rangle\langle jb||pk\rangle\langle pl||ib\rangle\langle ik||ac\rangle}{(\epsilon_j+\epsilon_l-\epsilon_a-\epsilon_c)(E+\epsilon_k+\epsilon_l-\epsilon_a-\epsilon_b-\epsilon_c)(\epsilon_i+\epsilon_k-\epsilon_a-\epsilon_c)} \tag{A.286}$$

$$dw101b = 1.000 \sum_{a,b,i,j,k,l,m} \frac{\langle pb||im\rangle\langle am||jk\rangle\langle ik||al\rangle\langle jl||pb\rangle}{(\epsilon_i + \epsilon_m - E - \epsilon_b)(\epsilon_i + \epsilon_j + \epsilon_k - E - \epsilon_a - \epsilon_b)(\epsilon_j + \epsilon_l - E - \epsilon_b)} \tag{A.287}$$

$$dw103b = -1.000 \sum_{a,b,c,i,j,k,l} \frac{\langle ac||jl\rangle\langle pb||ic\rangle\langle il||ak\rangle\langle jk||pb\rangle}{(\epsilon_j + \epsilon_l - \epsilon_a - \epsilon_c)(\epsilon_i + \epsilon_j + \epsilon_l - E - \epsilon_a - \epsilon_b)(\epsilon_j + \epsilon_k - E - \epsilon_b)} \tag{A.288}$$

$$dw104b = -1.000 \sum_{a,b,c,i,j,k,l} \frac{\langle pc||il\rangle\langle al||jk\rangle\langle jb||pc\rangle\langle ik||ab\rangle}{(\epsilon_i + \epsilon_l - E - \epsilon_c)(\epsilon_i + \epsilon_j + \epsilon_k - E - \epsilon_a - \epsilon_c)(\epsilon_i + \epsilon_k - \epsilon_a - \epsilon_b)} \tag{A.289}$$

$$dw107b = 1.000 \sum_{a,b,c,d,i,j,k} \frac{\langle pd||ik\rangle\langle bc||pd\rangle\langle ak||bj\rangle\langle ij||ac\rangle}{(\epsilon_i + \epsilon_k - E - \epsilon_d)(\epsilon_i + \epsilon_k - \epsilon_b - \epsilon_c)(\epsilon_i + \epsilon_j - \epsilon_a - \epsilon_c)} \tag{A.290}$$

$$dw108b = 1.000 \sum_{a,b,c,d,i,j,k} \frac{\langle bd||ik\rangle\langle ak||bj\rangle\langle pc||ad\rangle\langle ij||pc\rangle}{(\epsilon_i + \epsilon_k - \epsilon_b - \epsilon_d)(\epsilon_i + \epsilon_j - \epsilon_a - \epsilon_d)(\epsilon_i + \epsilon_j - E - \epsilon_c)} \tag{A.291}$$

$$dw111b = 1.000 \sum_{a,b,c,d,i,j,k} \frac{\langle ad||jk\rangle\langle pc||id\rangle\langle jb||pc\rangle\langle ik||ab\rangle}{(\epsilon_j + \epsilon_k - \epsilon_a - \epsilon_d)(\epsilon_i + \epsilon_j + \epsilon_k - E - \epsilon_a - \epsilon_c)(\epsilon_i + \epsilon_k - \epsilon_a - \epsilon_b)} \tag{A.292}$$

$$dw201b = 1.000 \sum_{a,b,c,i,j,k,l} \frac{\langle pb||ik\rangle\langle ac||bl\rangle\langle il||jc\rangle\langle jk||pa\rangle}{(\epsilon_i + \epsilon_k - E - \epsilon_b)(\epsilon_i + \epsilon_k + \epsilon_l - E - \epsilon_a - \epsilon_c)(\epsilon_j + \epsilon_k - E - \epsilon_a)} \tag{A.293}$$

$$dw202b = 1.000 \sum_{a,b,c,i,j,k,l} \frac{\langle pb||ik\rangle\langle ic||jl\rangle\langle al||bc\rangle\langle jk||pa\rangle}{(\epsilon_i + \epsilon_k - E - \epsilon_b)(\epsilon_j + \epsilon_k + \epsilon_l - E - \epsilon_b - \epsilon_c)(\epsilon_j + \epsilon_k - E - \epsilon_a)} \tag{A.294}$$

$$dw203b = -1.000 \sum_{a,b,i,j,k,l,m} \frac{\langle ab||lm\rangle\langle pl||ik\rangle\langle im||jb\rangle\langle jk||pa\rangle}{(\epsilon_l + \epsilon_m - \epsilon_a - \epsilon_b)(\epsilon_i + \epsilon_k + \epsilon_m - E - \epsilon_a - \epsilon_b)(\epsilon_j + \epsilon_k - E - \epsilon_a)} \tag{A.295}$$

$$dw204b = -1.000 \sum_{a,b,c,d,i,j,k} \frac{\langle pc||ij\rangle\langle bd||ck\rangle\langle aj||pb\rangle\langle ik||ad\rangle}{(\epsilon_i + \epsilon_j - E - \epsilon_c)(\epsilon_i + \epsilon_j + \epsilon_k - E - \epsilon_b - \epsilon_d)(\epsilon_i + \epsilon_k - \epsilon_a - \epsilon_d)} \tag{A.296}$$

$$dw205b = -1.000 \sum_{a,b,c,d,i,j,k} \frac{\langle ad||ik\rangle\langle pc||aj\rangle\langle bk||cd\rangle\langle ij||pb\rangle}{(\epsilon_i + \epsilon_k - \epsilon_a - \epsilon_d)(\epsilon_i + \epsilon_j + \epsilon_k - E - \epsilon_c - \epsilon_d)(\epsilon_i + \epsilon_j - E - \epsilon_b)} \tag{A.297}$$

$$dw206b = -1.000 \sum_{a,b,i,j,k,l,m} \frac{\langle pa||il\rangle\langle ib||jm\rangle\langle jl||pk\rangle\langle km||ab\rangle}{(\epsilon_i + \epsilon_l - E - \epsilon_a)(\epsilon_j + \epsilon_l + \epsilon_m - E - \epsilon_a - \epsilon_b)(\epsilon_k + \epsilon_m - \epsilon_a - \epsilon_b)} \tag{A.298}$$

$$dw207b = 1.000 \sum_{a,b,c,i,j,k,l} \frac{\langle pb||ik\rangle\langle ak||pj\rangle\langle jc||bl\rangle\langle il||ac\rangle}{(\epsilon_i + \epsilon_k - E - \epsilon_b)(\epsilon_i + \epsilon_j - \epsilon_a - \epsilon_b)(\epsilon_i + \epsilon_l - \epsilon_a - \epsilon_c)} \tag{A.299}$$

$$dw208b = 1.000 \sum_{a,b,c,i,j,k,l} \frac{\langle bc||kl\rangle\langle al||ic\rangle\langle pk||aj\rangle\langle ij||pb\rangle}{(\epsilon_k + \epsilon_l - \epsilon_b - \epsilon_c)(\epsilon_i + \epsilon_k - \epsilon_a - \epsilon_b)(\epsilon_i + \epsilon_j - E - \epsilon_b)} \tag{A.300}$$

$$dw209b = 1.000 \sum_{a,b,c,i,j,k,l} \frac{\langle pb||ik\rangle\langle ak||pj\rangle\langle ic||al\rangle\langle jl||bc\rangle}{(\epsilon_i + \epsilon_k - E - \epsilon_b)(\epsilon_i + \epsilon_j - \epsilon_a - \epsilon_b)(\epsilon_j + \epsilon_l - \epsilon_b - \epsilon_c)} \tag{A.301}$$

$$dw210b = 1.000 \sum_{a,b,c,i,j,k,l} \frac{\langle ac||il\rangle\langle bl||kc\rangle\langle pk||aj\rangle\langle ij||pb\rangle}{(\epsilon_i + \epsilon_l - \epsilon_a - \epsilon_c)(\epsilon_i + \epsilon_k - \epsilon_a - \epsilon_b)(\epsilon_i + \epsilon_j - E - \epsilon_b)} \tag{A.302}$$

$$dw211b = 1.000 \sum_{a,b,c,i,j,k,l} \frac{\langle bc||kl\rangle\langle pk||ij\rangle\langle aj||pb\rangle\langle il||ac\rangle}{(\epsilon_k + \epsilon_l - \epsilon_b - \epsilon_c)(\epsilon_i + \epsilon_j + \epsilon_l - E - \epsilon_b - \epsilon_c)(\epsilon_i + \epsilon_l - \epsilon_a - \epsilon_c)} \tag{A.303}$$

$$dw212b = 1.000 \sum_{a,b,c,i,j,k,l} \frac{\langle ac||il\rangle\langle pb||ak\rangle\langle ik||pj\rangle\langle jl||bc\rangle}{(\epsilon_i + \epsilon_l - \epsilon_a - \epsilon_c)(\epsilon_i + \epsilon_k + \epsilon_l - E - \epsilon_b - \epsilon_c)(\epsilon_j + \epsilon_l - \epsilon_b - \epsilon_c)} \tag{A.304}$$

$$dw301b = 0.500 \sum_{a,b,c,d,i,j,k} \frac{\langle pd||ik\rangle\langle ac||jd\rangle\langle ib||ac\rangle\langle jk||pb\rangle}{(\epsilon_i + \epsilon_k - E - \epsilon_d)(\epsilon_i + \epsilon_j + \epsilon_k - E - \epsilon_a - \epsilon_c)(\epsilon_j + \epsilon_k - E - \epsilon_b)} \tag{A.305}$$

$$dw302b = 0.500 \sum_{a,b,i,j,k,l,m} \frac{\langle pb||im\rangle\langle ia||jl\rangle\langle jl||kb\rangle\langle km||pa\rangle}{(\epsilon_i + \epsilon_m - E - \epsilon_b)(\epsilon_j + \epsilon_l + \epsilon_m - E - \epsilon_a - \epsilon_b)(\epsilon_k + \epsilon_m - E - \epsilon_a)} \tag{A.306}$$

$$dw303b = -0.500 \sum_{a,b,c,i,j,k,l} \frac{\langle ac||jl\rangle\langle pl||ik\rangle\langle ib||ac\rangle\langle jk||pb\rangle}{(\epsilon_j + \epsilon_l - \epsilon_a - \epsilon_c)(\epsilon_i + \epsilon_j + \epsilon_k - E - \epsilon_a - \epsilon_c)(\epsilon_j + \epsilon_k - E - \epsilon_b)} \tag{A.307}$$

$$dw304b = -0.500 \sum_{a,b,c,i,j,k,l} \frac{\langle pc||il\rangle\langle ab||jc\rangle\langle jl||pk\rangle\langle ik||ab\rangle}{(\epsilon_i + \epsilon_l - E - \epsilon_c)(\epsilon_i + \epsilon_j + \epsilon_l - E - \epsilon_a - \epsilon_b)(\epsilon_i + \epsilon_k - \epsilon_a - \epsilon_b)} \tag{A.308}$$

$$dw305b = -0.500 \sum_{a,b,c,i,j,k,l} \frac{\langle ac||il\rangle\langle pb||ak\rangle\langle il||jb\rangle\langle jk||pc\rangle}{(\epsilon_i + \epsilon_l - \epsilon_a - \epsilon_c)(\epsilon_i + \epsilon_k + \epsilon_l - E - \epsilon_b - \epsilon_c)(\epsilon_j + \epsilon_k - E - \epsilon_c)} \tag{A.309}$$

$$dw306b = -0.500 \sum_{a,b,c,i,j,k,l} \frac{\langle pc||il\rangle\langle ib||jk\rangle\langle al||pb\rangle\langle jk||ac\rangle}{(\epsilon_i + \epsilon_l - E - \epsilon_c)(\epsilon_j + \epsilon_k + \epsilon_l - E - \epsilon_b - \epsilon_c)(\epsilon_j + \epsilon_k - \epsilon_a - \epsilon_c)} \tag{A.310}$$

$$dw307b = 0.500 \sum_{a,b,c,d,i,j,k} \frac{\langle pd||ik\rangle\langle bk||pj\rangle\langle ac||bd\rangle\langle ij||ac\rangle}{(\epsilon_i + \epsilon_k - E - \epsilon_d)(\epsilon_i + \epsilon_j - \epsilon_b - \epsilon_d)(\epsilon_i + \epsilon_j - \epsilon_a - \epsilon_c)} \tag{A.311}$$

$$dw308b = 0.500 \sum_{a,b,c,d,i,j,k} \frac{\langle bd||ik\rangle\langle ac||bd\rangle\langle pk||aj\rangle\langle ij||pc\rangle}{(\epsilon_i + \epsilon_k - \epsilon_b - \epsilon_d)(\epsilon_i + \epsilon_k - \epsilon_a - \epsilon_c)(\epsilon_i + \epsilon_j - E - \epsilon_c)} \tag{A.312}$$

$$dw309b = 0.500 \sum_{a,b,i,j,k,l,m} \frac{\langle pb||im\rangle\langle am||pk\rangle\langle ik||jl\rangle\langle jl||ab\rangle}{(\epsilon_i + \epsilon_m - E - \epsilon_b)(\epsilon_i + \epsilon_k - \epsilon_a - \epsilon_b)(\epsilon_j + \epsilon_l - \epsilon_a - \epsilon_b)} \tag{A.313}$$

$$dw310b = 0.500 \sum_{a,b,i,j,k,l,m} \frac{\langle ab||im\rangle\langle im||jk\rangle\langle pk||al\rangle\langle jl||pb\rangle}{(\epsilon_i + \epsilon_m - \epsilon_a - \epsilon_b)(\epsilon_j + \epsilon_k - \epsilon_a - \epsilon_b)(\epsilon_j + \epsilon_l - E - \epsilon_b)} \tag{A.314}$$

$$dw311b = 0.500 \sum_{a,b,i,j,k,l,m} \frac{\langle ab||jm\rangle\langle pm||ik\rangle\langle jk||pl\rangle\langle il||ab\rangle}{(\epsilon_j + \epsilon_m - \epsilon_a - \epsilon_b)(\epsilon_i + \epsilon_j + \epsilon_k - E - \epsilon_a - \epsilon_b)(\epsilon_i + \epsilon_l - \epsilon_a - \epsilon_b)} \tag{A.315}$$

$$dw312b = 0.500 \sum_{a,b,c,d,i,j,k} \frac{\langle ad||ik\rangle\langle pc||aj\rangle\langle bj||pd\rangle\langle ik||bc\rangle}{(\epsilon_i + \epsilon_k - \epsilon_a - \epsilon_d)(\epsilon_i + \epsilon_j + \epsilon_k - E - \epsilon_c - \epsilon_d)(\epsilon_i + \epsilon_k - \epsilon_b - \epsilon_c)} \tag{A.316}$$

Figure A.20: Fourth order diagrams

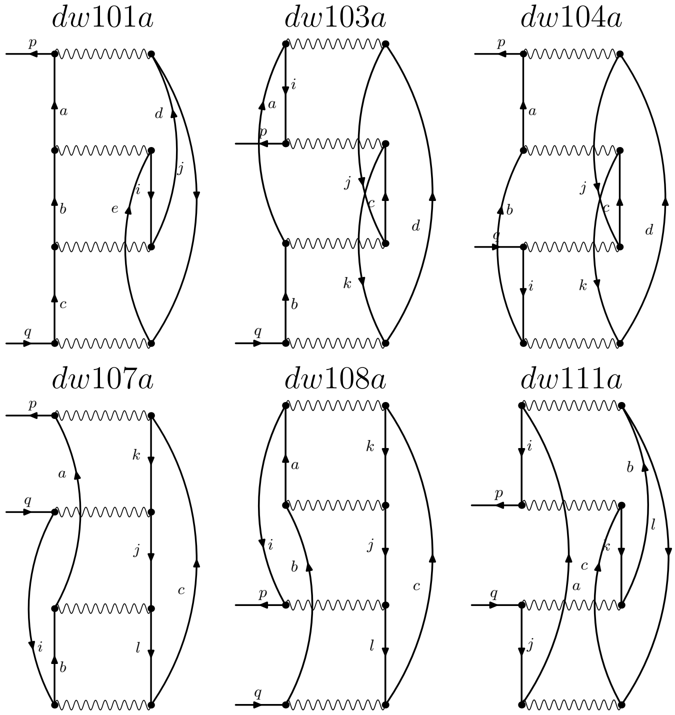

$dw101a$ $dw103a$ $dw104a$

$dw107a$ $dw108a$ $dw111a$

Figure A.21: Fourth order diagrams

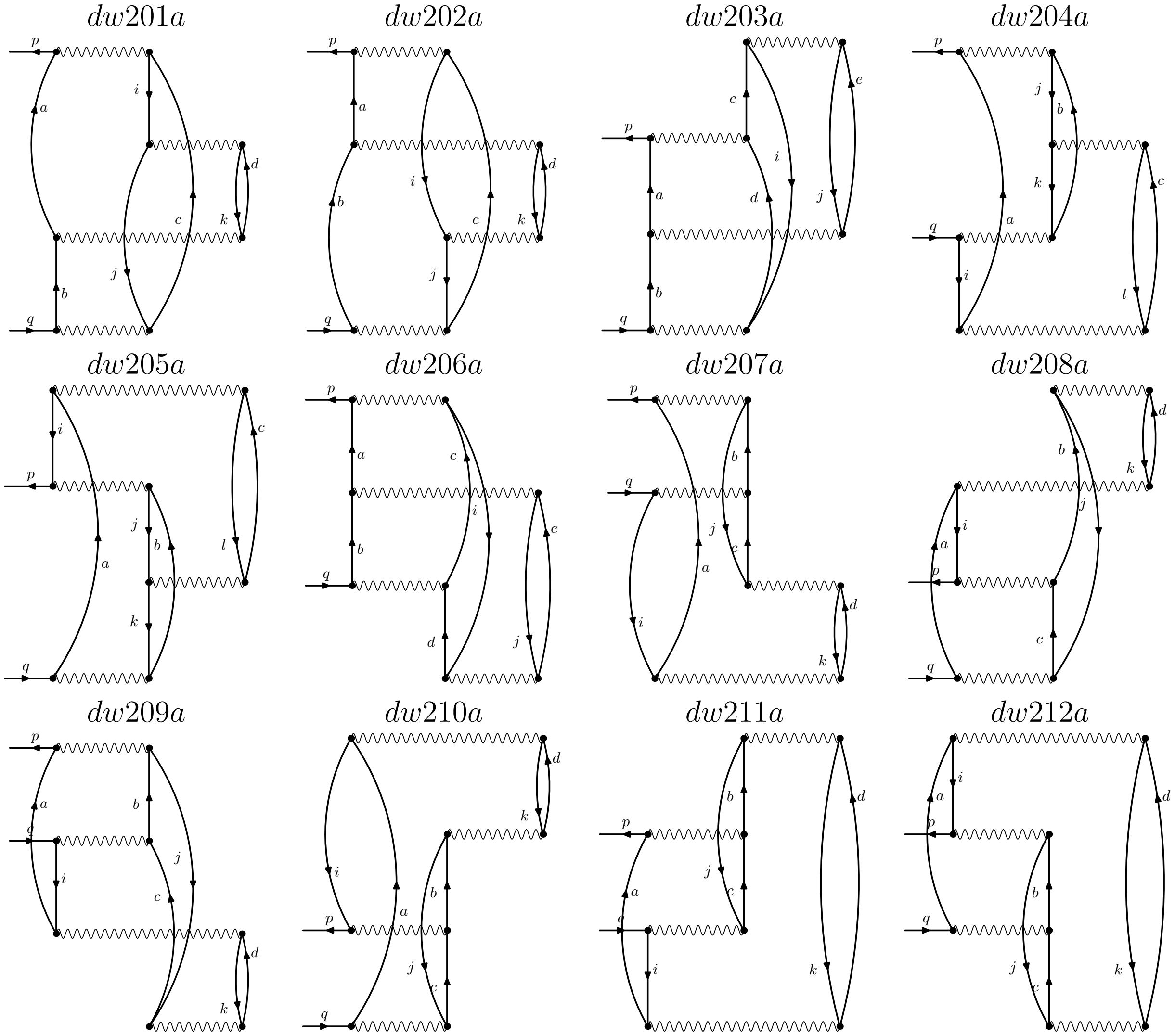

Figure A.22: Fourth order diagrams

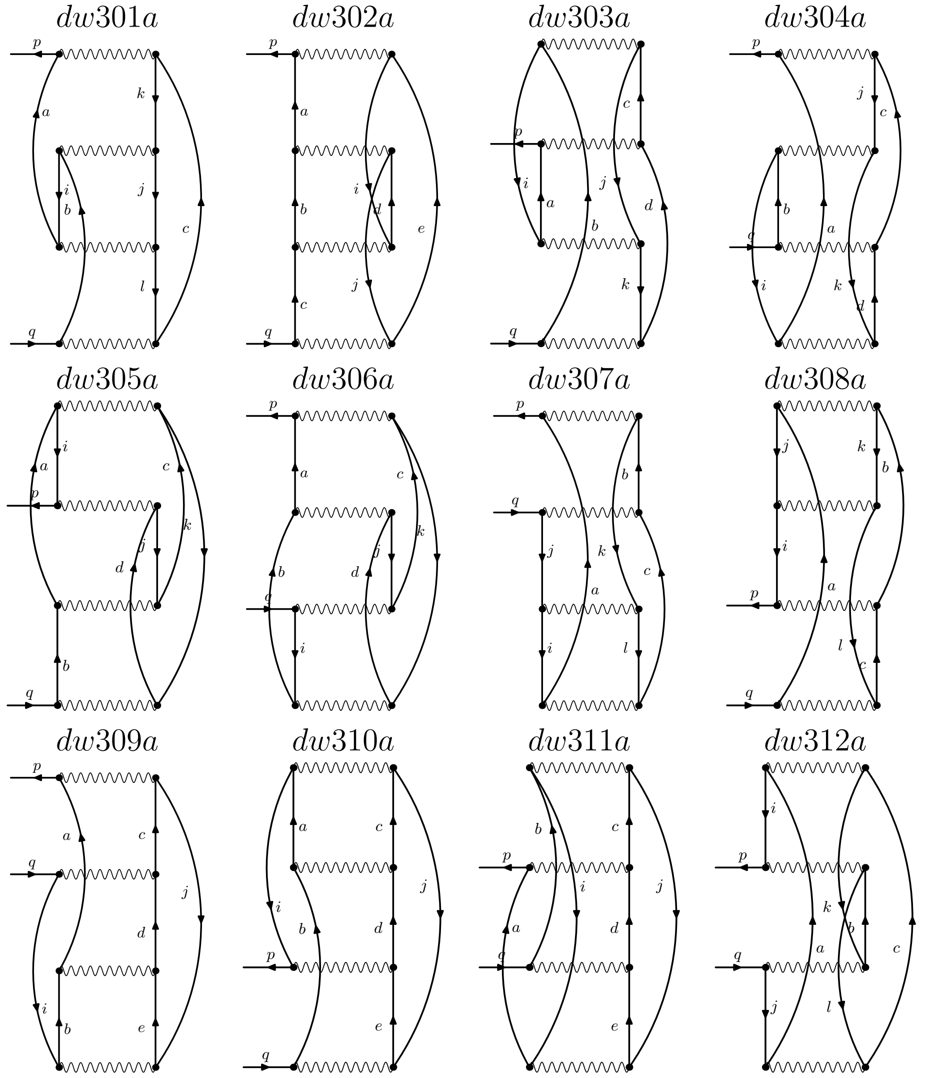

Figure A.23: Fourth order diagrams

$dw101b$ $dw103b$ $dw104b$

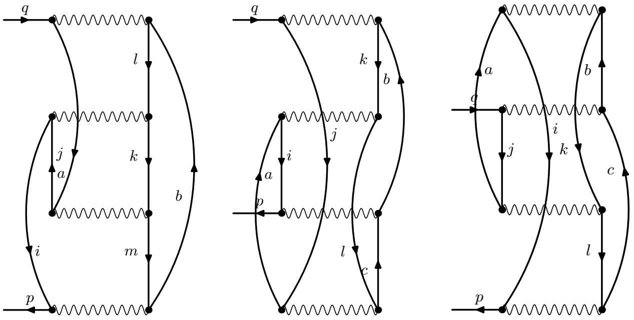

$dw107b$ $dw108b$ $dw111b$

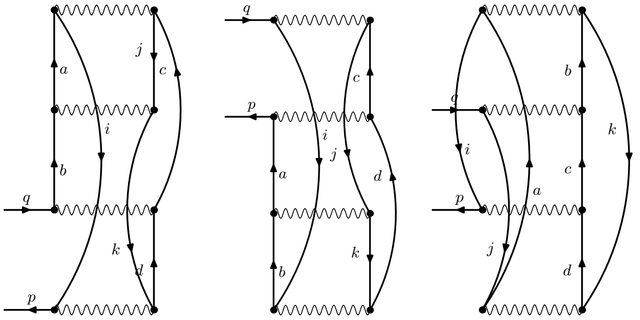

Figure A.24: Fourth order diagrams

$dw201b$

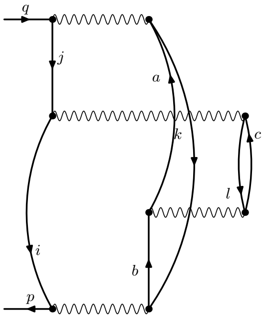

$dw202b$

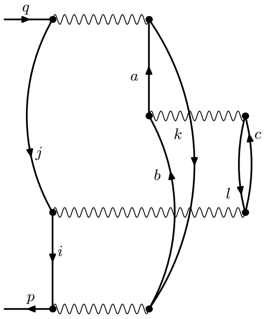

$dw203b$

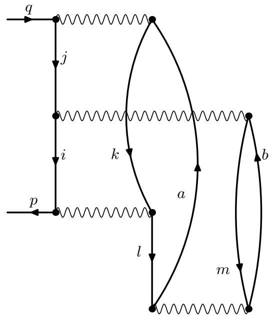

$dw204b$

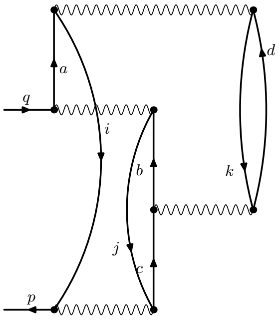

$dw205b$

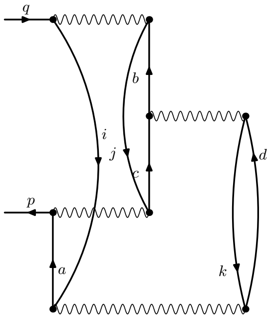

$dw206b$

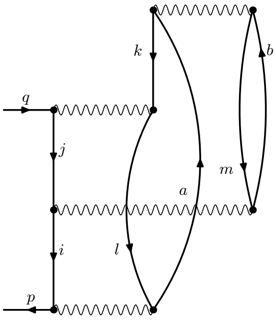

$dw207b$

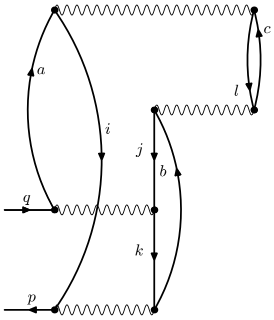

$dw208b$

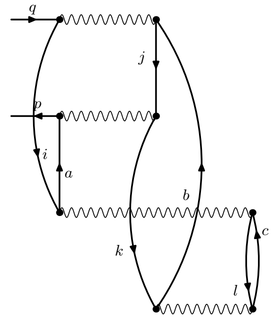

$dw209b$

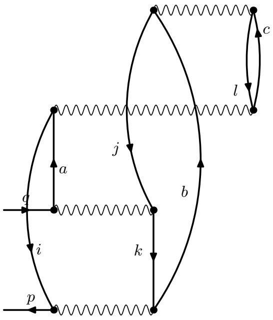

$dw210b$

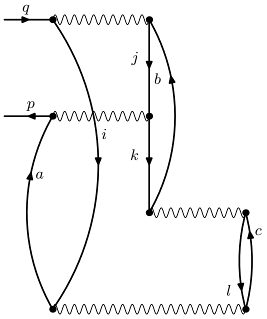

$dw211b$

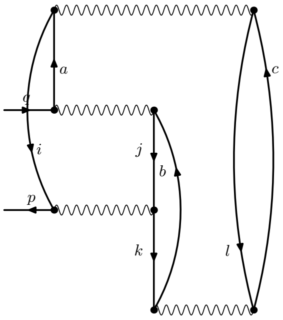

$dw212b$

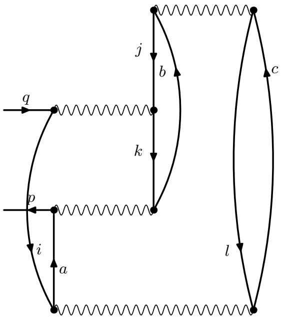

Figure A.25: Fourth order diagrams

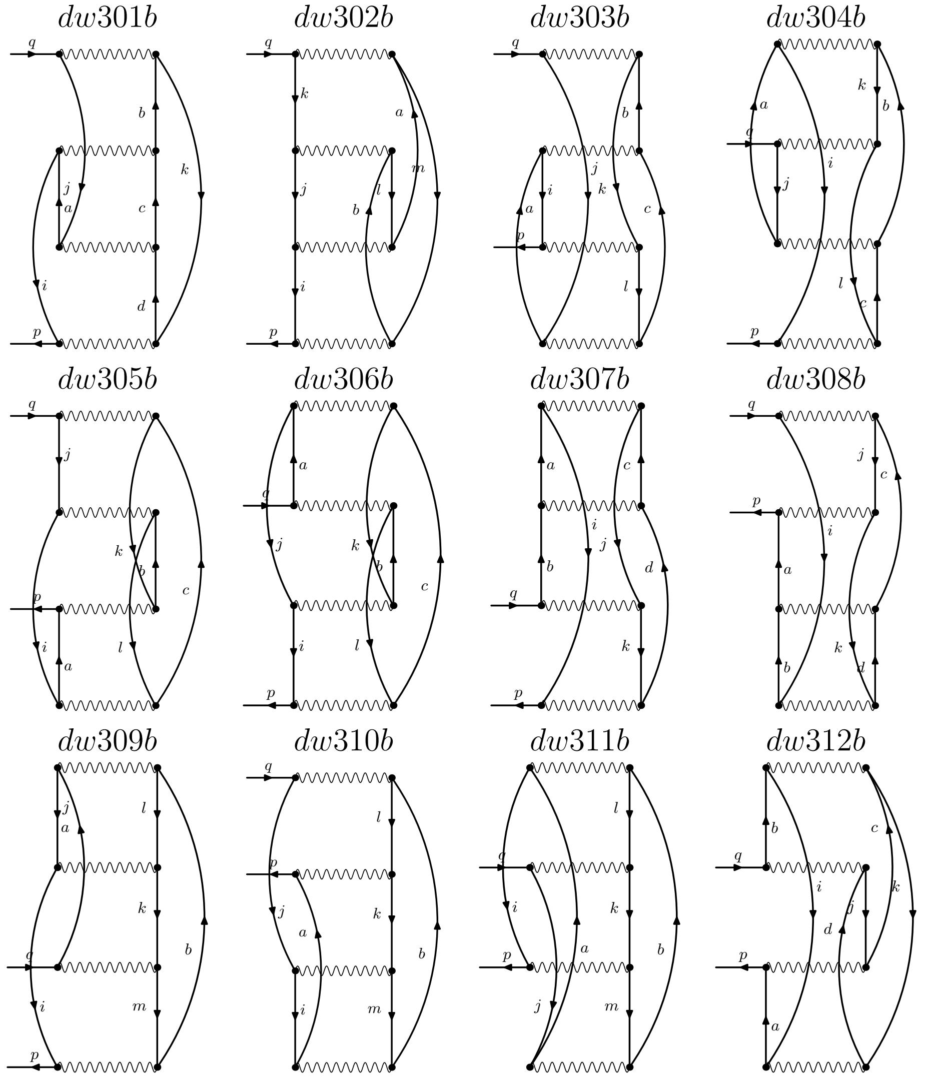

$dw301b$ $dw302b$ $dw303b$ $dw304b$

$dw305b$ $dw306b$ $dw307b$ $dw308b$

$dw309b$ $dw310b$ $dw311b$ $dw312b$